



City Research Online

City, University of London Institutional Repository

Citation: Higgins, Bethany (2022). Aspects of Measuring Dark Adaptation in People with Age-Related Macular Degeneration. (Unpublished Doctoral thesis, City, University of London)

This is the accepted version of the paper.

This version of the publication may differ from the final published version.

Permanent repository link: <https://openaccess.city.ac.uk/id/eprint/29827/>

Link to published version:

Copyright: City Research Online aims to make research outputs of City, University of London available to a wider audience. Copyright and Moral Rights remain with the author(s) and/or copyright holders. URLs from City Research Online may be freely distributed and linked to.

Reuse: Copies of full items can be used for personal research or study, educational, or not-for-profit purposes without prior permission or charge. Provided that the authors, title and full bibliographic details are credited, a hyperlink and/or URL is given for the original metadata page and the content is not changed in any way.

City Research Online:

<http://openaccess.city.ac.uk/>

publications@city.ac.uk

Aspects of Measuring Dark Adaptation in People with Age-Related Macular Degeneration

Bethany Elora Higgins

A Thesis submitted for the degree of
Doctor of Philosophy



Division of Optometry and Visual Sciences

School of Health Sciences

June 2022

To my Big Grandad

Thank you for all of your love and support. You would have been so proud of what I've accomplished, and I dedicate this thesis to you.

Table of Contents

1	Chapter 1; Introduction.....	1
1.1	General Introduction	1
1.2	Retina.....	2
1.2.1	Retinal Structure	2
1.2.2	Retinal Physiology	6
1.2.3	The Ageing Retina	8
1.3	Age-Related Macular Degeneration	9
1.3.1	Epidemiology	9
1.3.2	Pathogenesis	10
1.3.3	Risk Factors	13
1.4	Clinical Features of Age-Related Macular Degeneration	15
1.4.1	Drusen.....	15
1.4.2	Subretinal Drusenoid Deposits	16
1.4.3	Pigmentary Changes and Hyperreflective Foci	17
1.4.4	Geographic Atrophy.....	18
1.4.5	Choroidal Neovascularisation	19
1.5	Classification	20
1.5.1	Symptoms, Diagnosis and Treatment	22
1.6	Imaging the Retina with Age-Related Macular Degeneration	29
1.6.1	Digital Colour Fundus Photography and Age-Related Macular Degeneration.....	30
1.6.2	Optical Coherence Tomography and Age-Related Macular Degeneration.....	31
1.6.3	Optical Coherence Tomography versus Colour Fundus Photography	34
1.6.4	Other imaging modalities.....	35
1.7	Assessing Visual Function in Age-Related Macular Degeneration.....	36
1.7.1	Visual Acuity.....	36
1.7.2	Contrast Sensitivity	37
1.7.3	Microperimetry.....	40
1.7.4	Dark Adaptation	41
1.7.5	Other Measures of Visual Function.....	45
1.8	Dark Adaptation and Age-Related Macular Degeneration	46
1.8.1	An Overview.....	46
1.8.2	Metrics of Dark Adaptation in Age-Related Macular Degeneration	48
1.8.3	Dark Adaptation and Subretinal Drusenoid Deposits	50
1.8.4	Is Dark Adaptation a Potential Clinical Biomarker for Age-Related Macular Degeneration?	51
1.9	Rationale and Aims of PhD Thesis	52

2 Chapter 2; Are Current Methods of Measuring Dark Adaptation Effective in Detecting the Onset and Progression of Age-Related Macular Degeneration? A Systematic Literature Review.....	54
2.1 Introduction.....	54
2.2 Methods.....	55
2.3 Results	56
2.3.1 AdaptDx: Testing Procedures.....	57
2.3.2 AdaptDx: Diagnostic Precision, Repeatability and Longitudinal Studies.....	62
2.3.3 AdaptDx: Relationship with Other Measures	64
2.3.4 Other Adaptometers and Photostress Tests.....	67
2.4 Discussion	75
2.5 Conclusion	78
2.6 Update to Systematic Literature Review	78
2.6.1 Update on Testing Procedures.....	82
2.6.2 Update on Diagnostic Precision, Repeatability and Longitudinal Studies.....	82
2.6.3 Update on Relationship with Other Measures	83
3 Chapter 3; Optimising Assessment of Dark Adaptation Data Using Time-to-Event Analysis.....	84
3.1 Introduction.....	84
3.2 Methods.....	85
3.2.1 Participant Selection	85
3.2.2 Dark Adaptation Procedure	85
3.2.3 Time-to-event Analysis	86
3.2.4 Other Parametric Methods.....	88
3.2.5 Power Calculation	89
3.2.6 Web Application.....	90
3.3 Results	91
3.4 Discussion	95
3.5 Conclusion	98
4 Chapter 4; Assessment of a Classification Of Age-Related Macular Degeneration Severity from the Northern Ireland Sensory Aging Study Using a Measure of Dark Adaptation.....	100
4.1 Introduction.....	99
4.2 Methods.....	101
4.2.1 Brief Review of NISA Study Methodology.....	101
4.2.2 Statistical Analysis.....	103
4.3 Results	103
4.4 Discussion	108

4.5	Conclusion	113
5	Chapter 5; Properties of Measurements from Microperimetry and Dark Adaptation Assessment in People with Intermediate Age-Related Macular Degeneration.....	114
5.1	Introduction.....	114
5.2	Methods.....	116
5.3	Results	119
5.4	Discussion	126
5.5	Conclusions.....	128
6	Chapter 6; Overview of Findings and Future Work.....	130
6.1	Overview of findings.....	130
6.1.1	Research Summary	130
6.1.2	Systematic Literature Review Summary	130
6.1.3	Time-to-event Analysis and Rod-Intercept Time Data.....	131
6.1.4	Optical Coherence Tomography-based Classification of Age-Related Macular Degeneration Disease Severity.....	132
6.1.5	Test-retest variability and discrimination performance of the AdaptDx versus S-MAIA.....	132
6.2	Ideas for future work.....	133
6.3	Peer-reviewed manuscripts	135
6.4	Conference Abstracts	136
7	References.....	137
8	Supplemental Materials.....	167
8.1	Supplemental Tables	167
8.2	Supplemental Figures	245
8.3	Supplemental Methods	257

List of Tables

Table 1.1 Table comparing the Beckman (Ferris et al., 2013) and the AREDs (AREDS Research Group, 2001) classification systems, illustrating the potential differences between early and iAMD when using different classifications. Note: SDDs not mentioned. Table adapted from Miller, Bagheri and Vavvas (2017).	22
Table 1.2 Ongoing clinical trials, based on table from Cabral De Guimaraes et al. (2021).	28
Table 2. 1 Dark adaptation methodology adopted with the AdaptDx/AdaptRx.....	59
Table 2. 2 Table of studies that compared DA parameters to presence and severity of AMD.....	65
Table 2. 3 Table of procedures adopted by included studies that did not use the AdaptDx.....	69
Table 2. 4 Dark adaptation methodology adopted by the 16 studies published 2020-2022.....	79
Table 3.1 Clinical characteristics of all participants.	91
Table 3.2 Central estimates [95% CI] of RIT values (in minutes) with the three methods considered	92
Table 3.3 Sample size (to whole number) of each group required to reach 80% power at $\alpha=0.05$ with the three methods considered.....	94
Table 4.1 Summary statistics for demographic and visual function data stratified using Beckman classification.....	105
Table 4.2 Summary statistics for demographic and visual function data stratified using OCT classification.....	105
Table 5.1 Test-retest variability assessment results for AdaptDx (RIT[mins]) and S-MAIA (MMAT (dB) and SMAT (dB)) in people with iAMD.....	123

List of Figures

Figure 1.1 Diagram of the macula showing the fovea, parafovea and perifovea, with respective diameters in mm. Source: Author’s own.....	3
Figure 1.2 Cross-section of retina and photoreceptor mosaic. Inner limiting membrane (ILM), nerve fibre layer (NFL), ganglion cell layer (GCL), inner plexiform layer (IPL), inner nuclear layer (INL), outer plexiform layer (OPL), outer nuclear layer (ONL), outer limiting membrane (OLM), photoreceptor layer (PL), retinal pigment epithelium (RPE), Bruch’s membrane (BM), anterior part of the choroid (CHO). Image adapted from Harmening & Sincich, (2019).	4
Figure 1.3 Graph showing distribution of rods and cones across the retina. Image sourced from Osterberg, (1937); accessed from www.webvision.med.utah.edu/	5
Figure 1.4 Diagram of visual cycle showing phototransduction and the recycling of retinoids to enable rhodopsin regeneration. Sourced from Bavik et al., (2015).	8
Figure 1.5 Diagram illustrating one model of the differences between normal ageing versus AMD. Figure sourced from Zarbin (2004).	9
Figure 1.6 A severity grading system for SDDs proposed by Zweifel et al. (2010) shown in a diagram and OCT images. Stage 1 indicates SDDs appear as granular hyperreflective material between the RPE and the boundary between the inner and outer sections of the photoreceptor layer. Stage 2 indicates accumulations of material that visibly impact the boundary between the inner and outer sections of the photoreceptor layer. Stage 3 indicates when SDDs form a conical appearance and break through the inner and outer sections of the photoreceptor layer (Zweifel et al., 2010).	17
Figure 1.7 Colour fundus image from participant with early AMD from the Blue Mountains Eye Study, adapted from Lim et al. (2012). Panel A shows large drusen appearing as yellow spots. Panel B shows progression in both the size and area covered of the drusen five years later.	18
Figure 1.8 Figure sourced from Holz et al. (2014), illustrating a diagram of evolutionary changes in the macula as a function of GA.	19
Figure 1.9 A picture that is commonly used to describe the experience of someone with AMD with the left-hand side depicting ‘normal’ vision while the right depicts what vision with AMD is like, sourced from Taylor et al. (2018).	23
Figure 1.10 A colour fundus image showing medium and large soft drusen on the left and GA on the right. Note the visible choroidal vessels underlying the pale area of atrophy. Sourced from Kanagasingam et al. (2014).	31
Figure 1.11 Panel A features a diagram for time-domain OCT while panel B features a diagram of spectral-domain OCT. Sourced from Wang et al. (2022).	33
Figure 1.12 Images from a time-domain OCT (top-left), SD-OCT (top-right) and SS-OCT (bottom). Note the differences in resolution achieved the Fourier-domain OCT systems. Sourced from Bhende et al. (2018).	33
Figure 1.13 An OCT image (Cirrus HD-OCT; Carl Zeiss Meditec), showing a large druse, visible as a large dome RPE-elevation. Sourced from Keane et al. (2012).	34

Figure 1.14 A fluorescein angiogram image of a normal fundus in early venous phase, showing the fluoresceine dye beginning to fill the veins. Accessed from The University of Iowa.	35
Figure 1.15 A blue light short-wavelength FAF image of normal fundus. The arrow indicates an artefact from a vitreous opacity. Sourced from Bhagat (2021).	36
Figure 1.16 An ETDRS chart Image from National Eye Institute, National Institutes of Health.	37
Figure 1.17 CS functions of seven different age groups. Sourced from Schieber (1992).	38
Figure 1.18 Pelli-Robson CS chart. Sourced from Parede et al. (2013).	38
Figure 1.19 Image from MAIA microperimeter report. Green colour indicate normal values while red indicate abnormal. The dark green dots indicate participant fixation which was relatively unstable. Adapted from Estudillo et al. (2017).	41
Figure 1.20 Image of AdaptDx. Accessed from Maculogix (www.maculogix.com).....	42
Figure 1.21 Diagram of setting up for the AdaptDx testing procedure. Anticlockwise: A. Assessment must take place in scotopic conditions (with or without a period of pre adaptation, as discussed above). B. AdaptDx machine has a chinrest that participant is instructed to place their chin on and given the response button to press when they see the stimuli. C. Participant is instructed to fixate on the fixation cross. D. Examiner uses the red filter on the AdaptDx to reduce stray light and ensures the bleach will be given to the correct location on the retina. E. The AdaptDx produces a DA curve, indicating the RIT and fixation errors. Note: Images were taken under photopic conditions for ease of photography, the assessment is conducted in scotopic conditions. Source: Author’s own.	45
Figure 1.22 DA curves for a visually healthy eye exposed to five different bleaching intensities, plotted on a \log_{10} scale against time. Sourced from Hecht, Haig and Chase (1937).	48
Figure 1.23 A plot showing the DA functions for three people with AMD at different severity levels and one older healthy control. All participants have 20/25 VA or better. ARM 1 is >5 small drusen ($\leq 63\mu\text{m}$). ARM 2 is defined as ≥ 1 large drusen ($>63\mu\text{m}$), focal hyperpigmentation, or both. ARM 3 is drusen and CNV. Sourced from Owsley et al. (2001).	49
 Figure 2.1 Flowchart of study selection process.....	57
 Figure 3.1 The change in Log_{10} sensitivity for three control subjects and three patients with AMD is plotted in the top panel (filled dots) with the corresponding RIT values (vertical strokes) provided by the device. The horizontal dashed line represents the 3 log-step change in sensitivity used by the device to define the event (recovery from bleaching). The RIT time for each recovery “event” is used to build the survival curves (bottom panels). In this case, the vertical-coloured lines also identify the same RIT values recorded for the curves plotted in the top panels. Notice how each vertical line corresponds to a downward step change in the survival curve (in black). The same process is applied for all RIT values in the dataset to calculate the other step changes that make up the rest of the survival curve.....	87

Figure 3.2 Empirical curves for the original (top) and the transformed (bottom) data, scaled to illustrate RITs that surpass a cut off time. The vertical dashed line acts as a marker, representing this capping limit of 20 minutes. Note that the actual underlying distribution of RIT values is depicted in the figure, so no censoring is shown here. However, the survival model is fitted considering all values beyond 20 minutes as censored. For the scaled data, both the fitted survival curves from the mode (dashed curves) and the median values (vertical solid lines) were calculated from capped data. However, the time-to-event model fits the data well even beyond the cut off time. For the scaled AMD data, the time-to-event model correctly predicts a median value beyond the capping limit.....92

Figure 3.3 Power curves as a function of sample size for the three methods considered with and without capping for the scaled data. The power curves for the original data (not scaled) are identical to the scaled uncapped data and are therefore not reported (10,000 bootstrap simulations for each step in the sample size).....94

Figure 4.1 The 459 participants were graded by the Beckman classification (0-3) and the OCT classification (0-2). Section A. shows the participant cohorts in each class and Section B shows the agreement between the two classifications. For the participants with the greatest discordance between classifications (n=8 in OCT 0 and Beckman 3 and n=11 in OCT 2 and Beckman 0) a further check was completed of the grading by RH. Reasons for disagreement were confirmed to be due to the different imaging technologies used such as vitreous abnormalities on OCT looking like soft drusen on colour, small drusen visible on OCT but not on colour, and poorer quality images on colour in comparison to OCT masking subtle abnormalities on colour.104

Figure 4.2 Upper row: Kaplan-Meier curves illustrating the time taken for participant sensitivity to recover to a value of 5.0×10^{-3} scotopic cd/m^2 (3.0 log units of stimulus attenuation). This time taken is the RIT. The two plots show survival times for the control and AMD groups stratified by Beckman classification (left) and OCT classification (right). Bottom row: Age distribution for each classification. Visually, it seems like there is significant difference in OCT-classification in RIT, but after correction for age this is lost in earlier stages of AMD disease.106

Figure 4.3 Kaplan-Meier curves illustrating the time taken for participant sensitivity to recover to a value of 5.0×10^{-3} scotopic cd/m^2 (3.0 log units of stimulus attenuation). This time taken is the RIT. Survival curves shown for control group and AMD group stratified by OCT classification and SDD presence.....108

Figure 5.1 Flowchart of participant screening with iAMD. (In some cases, multiple reasons for removal were recorded for a participant. In this case, whatever reason that occurred first in the screening processes was reported here. For example, if a participant was recorded as having ‘DA outside tolerance’ (screening 1 exclusion) and recorded an unsuitable false-positive rate (screening 3 exclusion), the participant was removed based on the screening 1 exclusion.).....120

Figure 5.2 BA plots to show the test-retest agreement for the three metrics for participants with iAMD. (Note RIT data [B] has been transformed by $10 \cdot \log^{10}$ to mimic the logged output of the S-MAIA for better comparison).122

Figure 5.3 ROCs to show discrimination performance between the three measures' individual ability to separate people with iAMD from healthy controls and people with early AMD using baseline visit data.124

Figure 5.4 ROCs to compare discrimination performance between the measures' ability to separate people with iAMD from healthy controls and people with early AMD using baseline visit data. (Note the smaller sample sizes representing participants from each group that performed both tests plotted e.g. 24 participants with early AMD successfully performed both AdaptDx and scotopic S-MAIA testing.)125



COVID-19 Impact Statement

This statement is provided for the aid and benefit of future readers to summarise the impact of the COVID-19 pandemic on the scope, methodology, and research activity associated with this thesis. The academic standards for a research degree awarded by City, University of London and for which this thesis is submitted remain the same regardless of this context.

Title of the research project: *Aspects of Measuring Dark Adaptation in People with Age-Related Macular Degeneration*

1. Summary of how the research project, scope or methodology has been revised because of COVID-19 restrictions

Due to the pandemic, it was City, University of London's protocol to follow governmental guidelines and stop recruitment of participants and studies that would involve face-to-face procedures. As a result, the protocol and ethics application for the planned face-to-face research study for this thesis was postponed and eventually abandoned, along with any plan for data collection due to the uncertainty over the future. This was a monumental disappointment as it meant no data collection was featured in this body of work.

To adapt to the difficult circumstances we were thrust into and owing to the excellent networking of the supervisory team, collaborative relationships were built with other universities and multicenter studies. This led to access to a dataset similar to what was planned to be collected in-house at City, University of London. The stress in building hurried collaborating relationships with different projects and then to adapt the PhD thesis plan from scratch was a challenging experience.

2. Summary of how research activity and/or data collection was impacted because of COVID-19 restrictions, and how any initially planned activity would have fitted within the thesis narrative

The plan set out in the PhD Upgrade was to submit a protocol and ethics application to City, with plans to begin data collection in September 2020. The title was: *Exploring the Learning Effect in the Assessment of Dark Adaptation Using the AdaptDx*. The plan was to recruit students and conduct a dark adaptation testing procedure with them on two occasions, using the AdaptDx device. This would have involved face-to-face data collection. However, due to the pandemic this plan was halted.

3. Summary of actions or decisions taken to mitigate for the impact of data collection or research activity that was prevented by COVID-19

With the supervisory team's unwavering support, the thesis methodology was revised, and potential collaborators were contacted in the hunt for other AdaptDx data to use in this thesis. Happily, the MACUSTAR multicenter study committee were open to sharing their data with the expectation of a manuscript published in a peer-reviewed journal in return. Despite the added pressure to meet these expectations, the dataset helped form the final chapter in this thesis and enabled a full body of work to be drawn up on the topic of measuring dark adaptation.

4. Summary of how any planned work might have changed the thesis narrative, including new research questions that have arisen from adjusting the scope of the research project

It was very fortunate to source test-retest dark adaptation data from the MACUSTAR study as it still allowed this thesis to follow the original narrative of exploring assessment of dark adaptation using the AdaptDx. Another plan at the start of the PhD was to relate the measurement of dark adaptation to other surrogate measures of everyday visual function like visual search. Indeed, at the beginning of the PhD programme, I worked on a project that led to the first-authored publication: *Novel computer-based assessments of everyday visual function in people with age-related macular degeneration*, published in PLOS one in 2020. I submitted this to the Worshipful Company of Spectacle Makers and was awarded the Master's Medal 2021. It was decided that this work would not be part of this thesis narrative but the exercise served as an excellent introduction to my programme of studies.

Date of statement: 24/06/2022

Acknowledgements

I would like to express my sincere gratitude to my supervisors David Crabb, Alison Binns and Deanna Taylor. Their unwavering support throughout the pandemic enabled me to continue with my studies and helped me make this thesis what it is today. I am also very grateful for City, University of London for partly funding my research using the SHS Research Sustainability Fund and to David for supporting the remainder with various grants directly won by the Crabb Lab.

I must also thank Ruth Hogg for granting me access to NICOLA/NISA study data which enabled me to shape this body of work into the thesis that it is. The NICOLA/NISA studies were funded by the Atlantic Philanthropies, the Economic and Social Research Council, the UKCRC Centre of Excellence for Public Health Northern Ireland, the Centre for Ageing Research and Development in Ireland, the Office of the First Minister and Deputy First Minister, the Health and Social Care Research and Development Division of the Public Health Agency, the Wellcome Trust/Wolfson Foundation, Queen's University Belfast, the College of Optometrists, Diabetes UK, Macular Society, Guidedogs for the Blind, Thomas Pocklington Trust and the Belfast Association for the Blind. I have also benefitted from access to data from the MACUSTAR study and must thank all the consortium members for their tremendous help and support. MACUSTAR is funded by the Innovative Medicines Initiative 2 Joint Undertaking under grant agreement No 116076. This Joint Undertaking receives support from the European Union's Horizon 2020 research and innovation programme and EFPIA.

I would also like to thank my fellow Crabb Lab members for providing me with enormous support. Special thanks must be given to Deanna Taylor who has mentored me and helped shape me into the researcher I am today. I'd also like to express my gratitude to Giovanni Montesano, who has also served as a brilliant mentor and helped hone my statistical analysis and coding skills. Also thank you to Lee Jones and Jamie Enoch who have been wonderful to work with and have provided laughter and friendship that I will always cherish.

Finally, to my closest friends, Laura, Sarah, Shona and Fiona, thank you for your energy and enthusiasm that has kept me on track. To Lewis, thank you for loving me and supporting me each day, through the highs and the lows. Lastly to my family, Mum, Dad and Hannah, I am forever grateful for your love, understanding and support. Thank you for making this possible.

Declaration

The work contained in this thesis was completed by the candidate, Bethany Elora Higgins (BEH), under the supervision of Professor David Crabb, Dr Alison Binns, and Dr Deanna Taylor. It has not been submitted for any other degrees, either now or in the past. Where work contained within it has been previously published, this has been stated in the text. All sources of information have been acknowledged and references have been given. The University Librarian of City, University of London is permitted to allow the thesis to be copied in whole or in part without further reference to the author. This permission covers only single copies made for study purposes, subject to normal conditions of acknowledgement.

Abstract

In age-related macular degeneration (AMD) research, dark adaptation (DA) has been found to be a promising functional measurement and a potential biomarker for AMD onset and progression. The studies presented in this thesis aimed to better understand and improve upon how DA is assessed in people with AMD.

The first study was a systematic literature review which aimed to evaluate current methodology used to assess DA in people with AMD. Forty-eight eligible studies indicated overwhelming evidence of an association between impaired DA and AMD. Furthermore, there was evidence that the presence of structural abnormalities such as subretinal drusenoid deposits (SDD) are associated with prolongation of DA time. However, data on repeatability and reproducibility of DA measurement was sparse.

In the second study, time-to-event analysis was proposed to be a more statistically powerful method for analysing rod-mediated DA (RMDA) data in people with AMD (n=14) and controls (n=8) (measured by rod-intercept time [RIT; mins] using the AdaptDx [MacuLogix, Hummelstown, PA]). A series of calculations using these data indicated that sample sizes could potentially be reduced by between 40-53% by using the time-to-event analysis compared to a standard t-test of means.

The third study utilised a large multicentre dataset (n=459) from the Northern Ireland Sensory Aging study (NISA). The main aim was to assess differences in RMDA (RIT [mins]; AdaptDx) between different grades of AMD severity classified using a novel OCT-based grading system, compared to the current standard colour fundus photography (CFP) based system (Beckman classification). The second aim was to assess the association between SDD presence and RMDA at different AMD severity grades, using the OCT-based classification. It was concluded RMDA is delayed in eyes with a structural definition of intermediate AMD (iAMD) regardless of whether classified using a CFP or OCT-based criterion when age was correctly controlled for. SDD presence is associated with delays in RMDA within different AMD severity grades.

In the fourth study, data from the large multicentre MACUSTAR cross-sectional study (n=258) was used to assess the test-retest variability and discrimination performance of microperimetry metrics (S-MAIA [CenterVue, Padova, Italy]; mesopic and scotopic average thresholds [MMAT, SMAT; dB]) and RMDA (AdaptDx; RIT [mins]) in eyes with iAMD. MMAT, SMAT and RIT had adequate test-retest variability and are all moderately good at separating people defined as having iAMD from controls under a multi-centre setting (area under the ROC curve was 71% RIT, 68% MMAT and 69% SMAT). More people with iAMD were unable to provide valid AdaptDx data (n=64; 38%) when compared to data yielded from mesopic and scotopic microperimetry (n=39; 23% and n=36; 22%, respectively). Incomplete results and unreliable data using these tests of visual function need to be considered when designing trials using these technologies.

In conclusion, the results of this thesis highlight strengths of using RMDA as a measure of visual function in AMD. Conversely the results indicate some weakness in the current technology used to assess RMDA. Results from the studies presented in this thesis will be useful for those designing new trials where the intention is to use RMDA as a measure of visual function in AMD.

List of Abbreviations

AIC: Akaike Information Criterion	ELM: External limiting membrane
AREDS: Age-Related Eye Disease study	FAF: Fundus autofluorescence
AMD: Age-related macular degeneration (iAMD: intermediate AMD)	FU: Follow-up
ARM: Age-related maculopathy	GA: Geographic atrophy
ARMS2: Age-related maculopathy susceptibility-2	GLM: Generalised linear model
AUC: Area under the curve	HDF: Hyporeflective drusen cores
BCEA: Bivariate Contour Ellipse Area	HTRA1: HtrA Serine Peptidase 1
BA: Bland Altman	HVFP: Humphrey Visual Field Perimeter
BM: Bruch's membrane	HF: Hyperreflective foci
CAM: Classification of Atrophy Meeting	ICC: Intraclass correlation coefficient
CAREDS: Carotenoids in Age-Related Eye Disease study	ILM: Inner limiting membrane
CARMS: Clinical Age- Related Maculopathy Staging	INL: Inner nuclear layer
CASP: Critical Appraisal Skills Programme	iORA: Incomplete outer retinal atrophy
CFH: Complement factor H	IPL: Inner plexiform layer
CFP: Colour fundus photography	IQR: Interquartile range
cGMP: Cyclic guanosine monophosphate	IRHF: Intraretinal hyperreflective foci
CI: Confidence interval	iRORA: Incomplete RPE and outer retinal atrophy
CoR: Coefficient of repeatability	JBI: Joanna Briggs Institute
CNTF: Ciliary neurotrophic factor	LALES: Los Angeles Latino Eye study
CNV: Choroidal neovascularisation	LLQ: Low Luminance Questionnaire
cORA: Complete outer retinal atrophy	LoA: Limits of agreement
CS: Contrast sensitivity	LogMAR: Log minimum angle of resolution
DA: Dark Adaptation (RMDA: rod-mediated DA)	MAC: Membrane attack complex
dB: Decibels	Meta II: metarhodopsin II
DHA: Docosahexanoic acid	MDD-2: Macular Disease Detection Device
EDNA: Early Detection of Neovascular Age-Related Macular Degeneration	MDAC: Medmont Dark Adapted Chromatic perimeter
EMS: Eger macular stressometer	MMAT: Mesopic S-MAIA average threshold
EPA: Eicosapentaenoic acid	NEI-VFQ: National Eye Institute Visual Function Questionnaire
EQ-5D: EuroQol-5 Dimension Questionnaire	NHS: National Health Service
ERG: Electroretinograms	NISA: Northern Ireland Sensory Aging study
ETDRS: Early treatment in diabetic retinopathy study	NICE: National Institute for Health and Care Excellence

OCT: Optical coherence tomography (SD-OCT: Spectral domain OCT, SS-OCT: swept-source OCT, TD-OCT: Time domain OCT)

ONL: Outer nuclear layer

OPL: Outer plexiform layer

PCV: Polypoidal choroidal vasculopathy

PED: retinal pigment epithelial detachment

PL: Photoreceptor layer

PRL: Preferred retinal locus

PROM: Patient reported outcome measure

PSQI: Pittsburgh Sleep Quality Index

QoL: Quality of life

RCB: rod-cone-break

RCDA: Roland Consult Dark Adaptometer

RGCL: Retinal ganglion cell layer

RIT: Rod-intercept time

RR: Relative risk

RNFL: Retinal nerve fibre layer

ROC: Receiver operator characteristic

RPE: Retinal pigment epithelium

SD: Standard Deviation

SDC: smallest detectable change

SDD: Subretinal drusenoid deposits

SLO: Scanning Laser Ophthalmoscopy (AOSLO: adaptive optics SLO)

SMAT: Scotopic S-MAIA average threshold

SOP: Standard Operating Procedure

SST-1: Scotopic Sensitivity Tester-1

STARD: Standards for the Reporting of Diagnostic accuracy studies

TUDCA: Tauroursodeoxycholic acid

VA: Visual acuity (BCVA: Best corrected VA)

VEGF: Vascular endothelial growth factor (VEGF-A)

VFQ-48: Veterans Affairs Low Vision Visual Function Questionnaire

1 CHAPTER 1; INTRODUCTION

1.1 GENERAL INTRODUCTION

Age-related macular degeneration (AMD) is a leading cause of vision loss in the elderly population in the developed world (Bourne et al., 2014). AMD can progress from an early asymptomatic stage, into intermediate AMD (iAMD) and ultimately late-stage AMD with severe and often irreversible visual impairment (Lim et al., 2012). AMD prevalence is expected to increase exponentially due to progressively increasing ageing populations (Wong et al., 2014).

Age-related macular degeneration can be split into non-neovascular (dry or atrophic) AMD and neovascular (wet) AMD. Non-neovascular AMD associated with the death of the retinal pigment epithelium cells (RPE) and photoreceptors (rods and cones). There is no treatment for non-neovascular AMD as the disease mechanism is not completely understood (Fisher & Ferrington, 2018). However, structural and functional damage to the RPE is hypothesised to be integral to the onset and progression of early AMD (Ambati & Fowler, 2012; Fisher & Ferrington, 2018). The RPE plays an essential role in visual function, such as adaption to changes in ambient light intensity (Lamb & Pugh, 2004). Therefore, the rate of dark adaptation (DA) is a candidate biomarker for AMD diagnosis and disease progression (Jackson et al., 2005; Owsley, McGwin, et al., 2016; Owsley et al., 2007, 2014; Owsley, Clark and McGwin, 2017; Chen et al., 2019).

Dark adaptation is the recovery of visual sensitivity after a large proportion of visual pigment has been bleached by a high intensity light source (Owsley et al., 2007). The rate of DA is dependent on the rate of visual pigment regeneration in photoreceptors, which is also dependent on the functional integrity of the RPE (Lamb & Pugh, 2004). Hence, this process has been found to be delayed in people with early AMD and iAMD, before other abnormalities in other metrics of visual function are present (Dimitrov et al., 2008; Owsley et al., 2001; Ying et al., 2008).

Rod-mediated DA (RMDA) can be assessed using the AdaptDx (MacuLogix, Hummelstown, PA). The AdaptDX assesses the rod-intercept time (RIT), an estimate of the time duration for the rods to recover to an established criterion sensitivity (e.g. 5×10^{-3} cd/m² [3 logarithmic units]) after focal bleaching (Jackson & Edwards, 2008). The AdaptDX is commercially available and with the release of the portable and automated AdaptDX Pro (MacuLogix, Hummelstown, PA), the clinical use of the AdaptDx may increase. DA assessment must be better understood if clinicians are increasingly using DA metrics as a method to assess disease progression.

The studies described in this PhD thesis seek to better understand the strengths and limitations of DA assessment in AMD. For example, to provide a better understanding of the repeatability metrics of DA

assessment in people with AMD, its diagnostic capacity, and relationship to structural markers of AMD disease severity.

The following introductory chapter (Chapter 1) will introduce the reader to the concepts central to this thesis:

- I. We begin with an overview of the structure and physiology of the retina and associated ageing changes
- II. The next section will discuss AMD epidemiology, pathogenesis, followed by diagnosis, treatment, and overall management of people with AMD
- III. This will be followed by discussion of retinal imaging and functional assessment of AMD, concluded by a focus on DA assessment and the overall aims of the thesis

The thesis will then explore the following:

- I. The procedural methodology currently used for DA assessment in AMD and the current evidence regarding sensitivity to AMD onset and progression (Chapter 2)
- II. How to optimally analyse DA metrics in people with AMD (Chapter 3)
- III. The relationship between DA impairment and AMD severity using an OCT-based grading system (Chapter 4)
- IV. A comparison of the test-retest variability and diagnostic accuracy of DA and microperimetry assessments in people with AMD (Chapter 5)
- V. A summary of the body of work as a whole and additional ideas that might be considered subjects of future work (Chapter 6)

1.2 RETINA

1.2.1 Retinal Structure

The human retina consists of 10 layers of cells that work both together and independently to translate light into chemical energy (Hoon et al., 2014). Situated in the posterior of the eye, the retina is an outgrowth of the brain and marks the beginning of the visual system that terminates in the visual cortex (Mahabadi & Al Khalili, 2019). The retina is 30-40mm in diameter in total and at the centre is the optic disc, which forms the exit point of the optic nerve from the eye and is also the point from which blood vessels of the inner retinal circulation (the central retinal artery and vein) radiate (Kolb, 1995). Approximately 3.4 mm (11.8 degrees) temporal to the optic disc edge is the fovea, a circular landmark absent of vessels at the centre of the macula (Kolb, 2005). The macula is the central region of the retina specialised for high acuity vision, which extends ~3mm to either side of the centre of the

fovea (the foveola) and subtends a visual angle of $\sim 20^\circ$. The macula can be further divided into the parafovea, extending out from the foveola which in turn is circumscribed by the perifovea (Figure 1.1) (Kolb, 2005). The macula can also be described as the retinal region in which the retinal ganglion cell layer is greater than one cell thick. These definitions provide useful reference points for imaging assessment (Quinn et al., 2019).

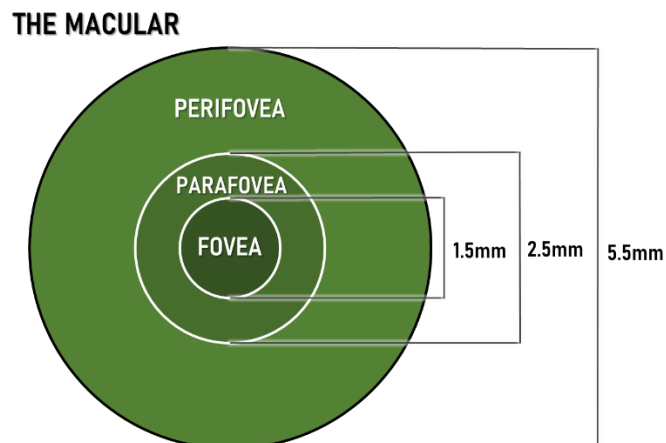


Figure 1.1 Diagram of the macula showing the fovea, parafovea and perifovea, with respective diameters in mm. Source: Author's own.

The retina is organised neatly into layers that can be divided into distinct sections, all playing a key role in transmitting light into visual output by forming a functional circuit (Mahabadi & Al Khalili, 2019). The retina features three cell categories: glial cells, neuronal cells and photoreceptor cells. These split into: retinal ganglion cells, bipolar cells, horizontal cells, amacrine cells, rods and cones. There are also further subtypes of these cells which form subsystems for specific visual processes (Joselevitch, 2008). For a thorough and accessible review of retinal cells, see Mahabadi and Al Khalili (2019).

From anterior to posterior, the strata constituting the retina are: the inner limiting membrane (ILM), retinal nerve fibre layer (RNFL), retinal ganglion cell layer (RGCL), inner plexiform layer (IPL), inner nuclear layer (INL), outer plexiform layer (OPL), outer nuclear layer (ONL), external limiting membrane (ELM), the photoreceptor layer (PL), and the RPE (See Figure 1.2). The ILM is formed of astrocytes and Müller cells and is the outermost layer of the retina, acting as a boundary between the retina and the vitreous body. The RNFL contains ganglion cell axons that travel to the optic nerve disc, carrying electrical signals from the retina into the brain. The RGCL consists of ganglion cells separated by Müller cells and displaced amacrine cells. The thickness of this layer varies and reaches up to ~ 10 cells thick in the macula (Remington, 2012). The IPL is a synaptic layer that contains the dendrites of the cells located in the inner nuclear layer. The inner nuclear layer comprises the cell bodies of the bipolar cells,

horizontal cells and amacrine cells. The OPL is another synaptic layer and connects the bipolar cells and photoreceptors. The ONL consists of the rod and cone cell bodies. The OLM is an epithelial layer that helps hold the structure of the retina. The PL is comprised of rod and cone outer segments is the site of phototransduction. Although the PL is the outermost neural layer of the retina, the underlying RPE is often considered to comprise the tenth layer of the retina (Harmening & Sincich, 2019; Mahabadi & Al Khalili, 2019; Remington, 2012). For further details, see section 8.1.1.1 and 8.1.2.1.

The outer segment of the photoreceptor layer is embedded in the RPE, a single layer of pigmented cells. Although the RPE is not strictly speaking part of the retina, it orchestrates vital functions in the visual cycle and the overall maintenance of the retina. These roles include absorbing excess photons to reduce intraocular light scatter (Tsacopoulos et al., 1998), photoreceptor renewal and phagocytic functions, and facilitation of photopigment regeneration (Lamb & Pugh, 2004). For further details on the RPE's involvement in the visual cycle, see section 1.1.2.1.

Bruch's membrane (BM) lies posterior to the RPE, separating the RPE from the choriocapillaris. Its main role is to act as a semi-permeable membrane controlling the movement of waste materials and metabolites between the RPE and the choroidal circulation. The retina requires a constant oxygen rich blood flow to function effectively and utilises oxygen more rapidly than any other tissue in the body (Anderson & Saltzman, 1964). A dual circulation to allow for this is unique to the retina, whereby the photoreceptor layer and macular region are served by the underlying choroidal blood supply, whilst the inner retinal layers are nourished by the central retinal artery and its tributaries (Kaur, 2008).

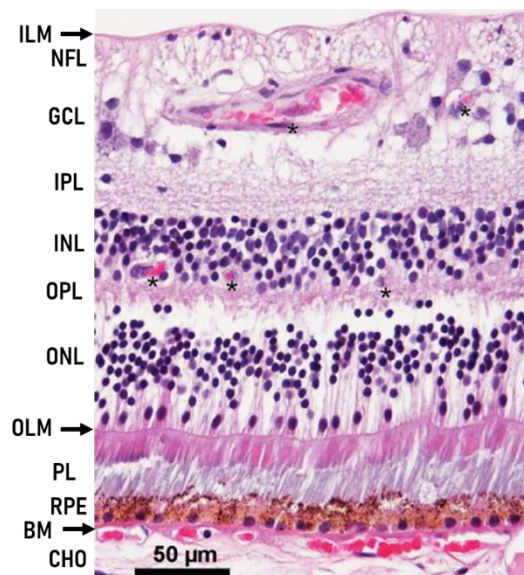


Figure 1.2 Cross-section of retina and photoreceptor mosaic. Inner limiting membrane (ILM), nerve fibre layer (NFL), ganglion cell layer (GCL), inner plexiform layer (IPL), inner nuclear layer (INL), outer plexiform layer (OPL), outer nuclear layer (ONL), outer limiting membrane (OLM), photoreceptor layer (PL), retinal pigment epithelium (RPE), Bruch's membrane (BM), anterior part of the choroid (CHO). Image adapted from Harmening & Sincich (2019).

1.2.1.1 Photoreceptors

Photoreceptors can be found across the entirety of the retina. The average, healthy human retina contains approximately 4.6 million cones and 92 million rods (Curcio et al., 1990). Rods are responsible for detecting visual stimuli in dim light conditions and are sensitive enough to detect a single photon (Rieke, 2000). Detection of visual stimuli in bright-lighting conditions (photopic) is conducted by cones (Jackson, Owsley and Curcio, 2002). Cones are less sensitive to light than rods but yield a higher temporal and spatial resolution, and the presence of three types of cone (L-, M- and S-cones) containing visual pigment with different spectral sensitivity curves enables colour vision (Kawamura & Tachibanaki, 2014). On the other hand, the rod system functions more slowly and has poorer contrast sensitivity (CS) and spatial acuity compared to the cone system. This is because improved sensitivity to low light levels is achieved by increased spatial and temporal summation in the rod system; that is to say that multiple rods link to one ganglion cell while only a single cone may converge on a single ganglion cell, and the rod system collates information over a longer time period (Kawamura & Tachibanaki, 2014).

Cone density is at its highest in the centre of the fovea and rapidly drops off with increasing eccentricity from the centre of the macula. Cone numbers are also higher in the nasal compared to temporal retina (Curcio et al., 1990). Despite rods outnumbering cones, the fovea is cone dominant. In contrast to cones, rod numbers rise as one moves from the fovea and dominate the parafovea. The highest number of rods can be located in the nasal and superior retina (Curcio et al., 1990) (See Figure 1.3). Both photoreceptor types feature an outer segment shaped like a stack of discs that contain photopigment (rhodopsin in rods; iodopsin in cones). These discs are closed in rods but are open in cones (Kawamura & Tachibanaki, 2014) and are the apparatus for phototransduction.

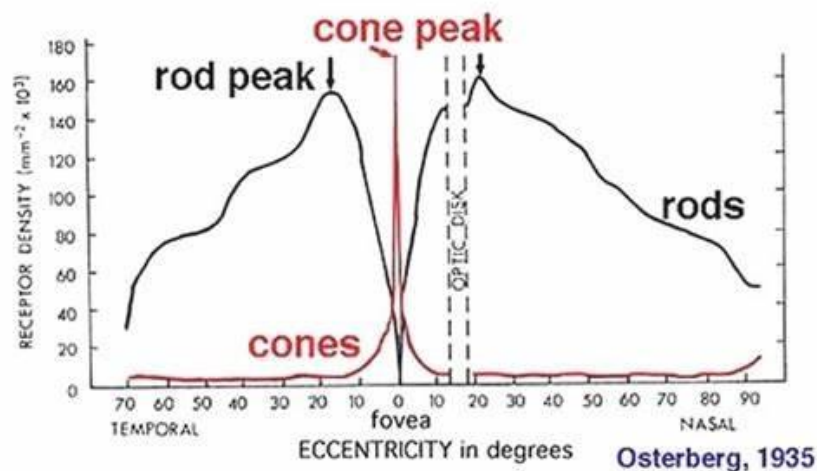


Figure 1.3 Graph showing distribution of rods and cones across the retina. Image sourced from Osterberg (1937); accessed from www.webvision.med.utah.edu/

1.2.1.2 Macular Pigment

Macular pigment refers to the yellow pigment that accumulates in the macula. It is composed of three dietary carotenoids: meso-zeaxanthin, lutein and zeaxanthin. Macular pigment can absorb 40–90 % of incident high-energy, short-wavelength visible light (460nm) and reduces blue-light scattering in the retina (Arunkumar et al., 2018). Out of the three carotenoids present lutein filters blue light more efficiently, attributed to the different organisation within the lipid bilayer (Sujak et al., 1999). Macular pigment cannot be synthesised by the body and must be ingested via green leafy vegetables and orange/yellow fruits and vegetables (Sommerburg et al., 1998).

1.2.2 Retinal Physiology

The retina must encode and transmit a wide range of stimulus magnitudes as efficiently as possible despite neural noise, metabolic needs and restrictions of response speed of cells associated with biological systems (Joselevitch, 2008). The nature of the signals received by the ganglion cells (e.g. locality, timing, strength, and whether they are inhibitory or excitatory (Wensel, 2012) communicates intricate information about the visual scene and how it is changing in real time. Joselevitch (2008) summarises three ways the retina has evolved to transmit information to the brain as rapidly as possible (Joselevitch, 2008). For example, the convergence of many photoreceptors to a single ganglion cell. However, there is a resultant trade-off with visual acuity (VA). A further strategy the retina has evolved is that photoreceptors feed into different, specialised pathways in order to transmit specific information (Zhang & Sejnowski, 1999). A final way the retina enables the transfer of as much visual information as possible is the heterogeneous distribution of photoreceptors. For example, the fovea has a structure dedicated to retaining a high level of spatial resolution by only consisting of photoreceptors (cones) that transmit to ganglion cells at a 1:1 ratio (Joselevitch, 2008).

The retina further enhances information transmission via two retinal visual pathways to the brain: the vertical and lateral pathways. The vertical pathway is the primary transmission pathway and consists a route from photoreceptor to bipolar cells to ganglion cells and onto the brain. The two lateral (or negative feedback) pathways are secondary routes and feature smaller circuits back to the photoreceptors via horizontal cells (Kamermans et al., 2001) and from amacrine cells to bipolar cells (Kaneko & Tachibana, 1987). These lateral pathways result in a post-synaptic voltage change that aid the vertical pathway. For a detailed review of retinal circuitry, see Joselevitch (2008).

1.2.2.1 The Visual Cycle

The visual cycle (also called Wald's visual cycle) is a chain of biochemical reactions that result in the conversion of a single photon into an electrical signal in the retina, and the regeneration of visual pigment to an unbleached state in which it is ready to absorb the next photon of light. The cycle was first described by George Wald who discovered vitamin A in the retina and described its involvement in the molecular basics of vision, winning him the Nobel Prize in 1967 (Wald, 1935, 1968). For simplicity and ultimate relevance to this thesis, phototransduction with rhodopsin will be described. It should be noted, however, that evidence now suggests that cone photoreceptors also have access to a different, intraretinal route for obtaining 11-cis retinal to enable a more rapid process of pigment regeneration (Mata et al., 2002)

A molecule of unbleached rhodopsin consists of 11-cis retinal covalently bound to a molecule of the protein opsin. Presence of 11-cis retinal 'locks' rhodopsin into an inactive state. The process of visual transduction starts when a photon is absorbed by the 11-cis retinal chromophore, causing it to photoisomerise into all-trans retinal. Rhodopsin is converted into metarhodopsin II (meta II) which binds to and activates the G-protein transducin. Following this, a biochemical cascade is triggered leading to the closure of cyclic guanosine monophosphate (cGMP)-sensitive cation channels. This causes the photoreceptor to become hyperpolarised, which acts as the first signal on the visual pathway to the brain (Figure 1.4). For a detailed review of the process of phototransduction, see Burns and Baylor (2001).

After photoisomerisation, all-trans retinal is reduced into all-trans retinol (also known as vitamin A) (See Figure 1.4). All-trans retinol returns to the RPE to be reverted into 11-cis retinal via esterification (Figure 1.4 step 1), isomerisation via the RPE-specific protein RPE65 (Figure 1.4 step 2) and finally oxidation (Figure 1.4 step 3). The molecule 11-cis retinal then returns to the photoreceptor outer segment, where it re-joins an opsin molecule to, once again, become rhodopsin (Figure 1.4 step 4). The series of biochemical reactions that facilitate this is called the retinoid cycle. For a review of the retinoid cycle, see landmark paper by Lamb and Pugh (2004). Until the photoreceptor has undergone the retinoid cycle, it cannot absorb another photon so cannot send any additional signals along the visual pathways. In this case, the photoreceptor is referred to as 'bleached'. Lamb and Pugh's (2004) model of pigment regeneration reasons that 11-cis retinal must pass through a 'resistive' barrier down a concentration gradient from the RPE to the photoreceptors. Therefore, the rate of visual regeneration is determined by the concentration of 11-cis retinal available and the rate at which 11-cis retinal is delivered to the bleached photoreceptors' outer segments. As a result, efficient visual pigment regeneration is heavily reliant upon the functionality of the RPE. Ocular pathologies that compromise the structure and enzymatic processes of the RPE are known to manifest in delayed rhodopsin regeneration (Fuchs et al., 1995; Thompson et al., 2000; Hartong, Berson and Dryja, 2006; Owsley, McGwin, et al., 2016). Photopigment regeneration obeys rate-limited kinetics which becomes

particularly apparent following substantial bleaching exposures. This forms the basis of DA (see section 1.6 for dedicated discussion of DA).

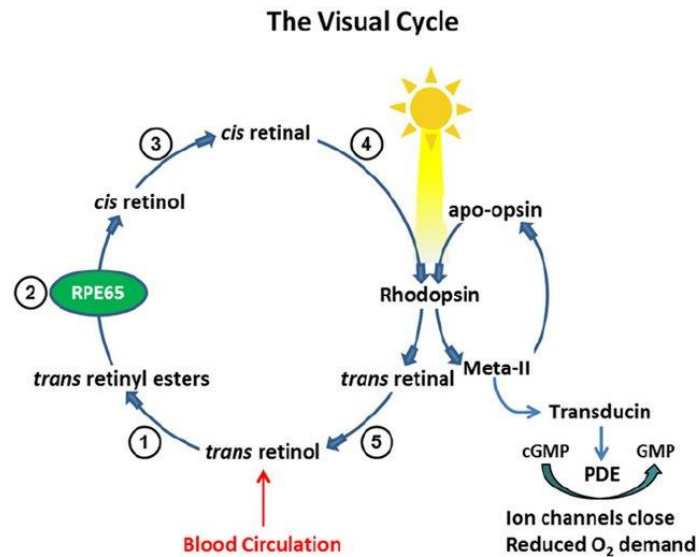


Figure 1.4 Diagram of visual cycle showing phototransduction and the recycling of retinoids to enable rhodopsin regeneration. Sourced from Bavik et al. (2015).

1.2.3 The Ageing Retina

As the retina ages, changes occur at a cellular level. Metabolic waste builds up in the RPE, the BM increases in thickness and becomes hydrophobic forming a barrier to transfer of materials between the RPE and choroidal circulation, pupillary miosis and changes in ocular media occur and permanent vascular changes are evident in the choroid such as choroidal thinning and reduced choroidal perfusion, to name a few (Sarks, 1976; Salvi, Akhtar and Currie, 2006; Curcio et al., 2011; Emeterio Nateras et al., 2014; Wakatsuki et al., 2015). This is a normal part of the ageing process. Virtually every measure of visual function evidences decline in older age, including but not limited to VA, visual field sensitivity, CS and DA (Salvi, Akhtar and Currie, 2006). There are a number of theories that may explain the ageing seen in the eye. For instance, the programmed theory (also called biological clock theory) postulates that bodies have a set time in the genetic code that stipulates when it is time for cells to die (Jin, 2010). Similarly, the evolutionary theory explains that our genetic code promotes cell senescence (where cells stop dividing) in later life once our period for procreation has ended (Hamilton, 1966). There is also the error theory (also called wear and tear theory) that believes cells are subjected to damage by excessive use or abuse over time first proposed by Dr August Weismann in a lecture in 1881 (Weismann, 2011). This links to the free radical theory of ageing, which proposes the cumulative

damage to cells arises from reactions involving free radicals (namely reactive oxygen intermediates) (Beatty et al., 2000). For a thorough review of the ageing retina, see Salvi, Akhtar and Currie (2006).

It is difficult to tease out the differences between age-related changes that occur naturally in the retina and age-related pathology (Marshall, 1987) such as AMD. Indeed, ageing changes are of course also present in eyes with AMD as the disease occurs in the elderly. Therefore, it is imperative to understand the variations between normal ageing of the retina (along with the RPE-BM-choriocapillaris complex) and AMD pathophysiology (Figure 1.5) (Zarbin, 2004). For a review of normal ageing versus AMD see Zarbin (2004).

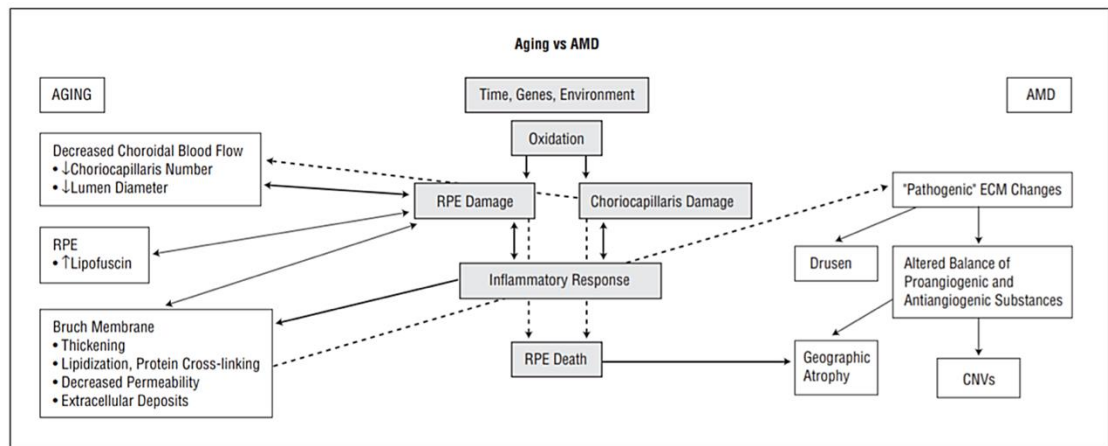


Figure 1.5 Diagram illustrating one model of the differences between normal ageing versus AMD. Figure sourced from Zarbin (2004).

1.3 AGE-RELATED MACULAR DEGENERATION

1.3.1 Epidemiology

Age-related macular degeneration is a leading cause of vision loss in the developed world globally, seen in 30% of elderly populations and is accountable for ~50% of sight impairment registrations in England and Wales (Quartilho et al., 2016). As previously stated, advanced AMD can be divided into two forms: non-neovascular (also known as non-exudative or 'dry') and neovascular (also known as exudative or 'wet'). Non-neovascular AMD accounts for 85-90% of all AMD cases while neovascular AMD accounts for 10-15% (Ambati & Fowler, 2012). Onset is after the age of 55 years, with increasing age associated with increasing incidence (Augood et al., 2006). This thesis will largely focus on the early and intermediate stages of AMD, where VA is often still near normal. Due to the ageing of populations in developed countries, the prevalence of AMD is expected to increase exponentially. By

the year 2040, it is estimated that there will be ~288 million cases (Wong et al., 2014). A systematic review and meta-analysis of 39 population-based studies of AMD by Wong et al. (2014) examined AMD prevalence in 129,664 European, Asian and African people (aged 30-97 years) with associated retinal imaging and standardised AMD severity grading. The analysis found the pooled prevalence of AMD in people aged 45-85 years to be 8.69% (95% confidence intervals [CI]; 4.26–17.40), with 8.01% of people diagnosed with early AMD (3.98–15.49) and 0.37% (0.18–0.77) diagnosed with late AMD. The review concluded that AMD will become a ‘substantial global burden’ (Wong et al., 2014). A later meta-analysis by Colijn et al. (2017) of prevalence data for 42080 people from European-based studies suggested a decreasing prevalence of late AMD and of visual impairment associated with neovascular AMD, likely due to healthier lifestyles and improved treatment options (see section 1.2.5 for details of AMD management and treatments). Yet, with an exponential increase of AMD still likely to occur due to the ageing demographic of the population, by 2040 the number of Europeans with more severe AMD is likely to reach 3.9-4.8 million (Colijn et al., 2017).

1.3.2 Pathogenesis

The pathogenesis of AMD is multifactorial, likely consisting of many environmental, genetic and metabolic interactions (Ambati & Fowler, 2012). Yet, the exact stages remain poorly understood. Despite the dichotomisation of neovascular and non-neovascular AMD in the literature (presence and lack of choroidal neovascularisation [CNV], respectively) there is an overlap in pathological mechanisms behind them. Neovascular AMD is not the main focus of this thesis but, briefly, CNV describes the abnormal proliferation of choroidal blood vessels that break through the BM into the sub-RPE and, in some cases, subretinal space. It is formed by a complex chain of molecular reactions, but it is believed unbalanced upregulation of vascular endothelial growth factor (VEGF) plays a role in its development (Campochiaro, 2004) (see section 1.3.4.5). Anti-VEGF treatment is an approved therapy for neovascular AMD and is born from understanding the pathological mechanisms behind CNV. In contrast, this therapy does not work for non-neovascular AMD, thus it is imperative to understand the unique mechanisms to the non-neovascular type of AMD to realise future treatments.

It is generally agreed that while AMD pathogenesis is multifactorial, the RPE appears as the ‘fulcrum’ of AMD pathogenesis, categorised by RPE dysfunction and degeneration (Ambati & Fowler, 2012). The RPE is complex and orchestrates vital functions in the retina, including (but not limited to) maintenance of the blood-retina barrier and facilitating the visual cycle. Progress in sequencing the deleterious and protective gene expressions in the RPE may reveal key molecular changes in the retina that drive AMD disease pathogenesis (Ambati & Fowler, 2012).

1.3.2.1 Oxidative Stress

One main candidate aetiology for AMD is oxidative stress. Oxidation simply refers to the removal of electrons. Free radicals are unstable atoms or molecules with an unpaired electron. Free radicals are a by-product of enzymatic processes and photochemical reactions such as those that occur in the retina, which can be increased by ageing, inflammation and cigarette smoking (Beatty et al., 2000). Reactive oxygen intermediates are a subset of free radicals that contain oxygen which occur frequently in the retina due in part to the high concentration of oxygen (Anderson & Saltzman, 1964). To become stable, free radicals engage in a cytotoxic oxidative cascade reaction by extracting electrons from nearby molecules such as carbohydrates, membrane lipids, proteins and nucleic acids. This leaves these molecules unstable and disrupts their functionality in the retina. The photoreceptor outer segment is rich in polyunsaturated fatty acids (namely Docosahexanoic acid [DHA], sourced solely from diet) which are vulnerable to lipid peroxidation (forming alkyl lipids) thus readily instigate cytotoxic oxidative cascade reactions. Lipid peroxidation results in loss of photoreceptor outer segment membrane function which impacts the visual cycle (Beatty et al., 2000). It is worth noting susceptibility for lipid peroxidation is positively associated with age (De La Paz & Anderson, 1992).

1.3.2.2 Photoreceptor outer segment phagocytosis

The RPE cells are responsible for the maintenance of the photoreceptors. As the photoreceptor outer segment undergoes constant renewal and forms new outer segment discs (Young, 1967), the RPE cells assist daily by removing the tip of the outer segments in a phagocytic process referred to as 'disk shedding' (Mazzoni, Safa and Finnemann, 2014). Despite changes to the membranes as a result of cytotoxic oxidative cascade reactions, the RPE cells continue to ingest these distal portions of the photoreceptors containing abnormal oxidised material. This process causes reactive oxygen intermediates and also lipofuscin to build-up within the RPE cells as they are unable to remove these products via the choroidal circulation (Beatty et al., 2000).

Lipofuscin is a chromophore mainly derived from digested photoreceptor tips, which is made up of lipid-protein material (Sparrow & Boulton, 2005). Lipofuscin accumulation (lipofuscinogenesis) in the RPE is considered to be an indicator of ageing and cellular senescence (Kennedy, Rakoczy and Constable, 1995). Higher lipofuscin concentration in the RPE is associated with age (Delori, Goger and Dorey, 2001). As a result of the accumulation of lipofuscin and other waste products, RPE function degrades and permeability of BM changes. The extrusion of waste materials from the RPE contributes to the formation of drusen and basal laminar and linear deposits (Beatty et al., 2000). Drusen are yellow, insoluble hydrophobic deposits that collect between the RPE and BM and are a characteristic phenotype of AMD (see section 1.3.4.1 for details).

1.3.2.3 Immune dysfunction

Another candidate aetiology for AMD pathogenesis is immune dysfunction. Among the different immune pathways, the complement system is the most widely agreed upon pathway associated with AMD (Ambati, Atkinson and Gelfand, 2013). For example, studies assessing genome-wide association has evidenced an overactive complement cascade occurs in AMD (Haines et al., 2005). There are certain variants of genes associated with complement pathway (complement factor H [CFH] etc) associated with increased risk of AMD (see section 1.3.2.3) In predisposed individuals, the presence of abnormal material as a result of oxidative stress and impaired RPE cells (inflammatory signals) can activate an immune response (Ambati, Atkinson and Gelfand, 2013). The inflammatory cells of the retina are called microglia and their responsiveness to inflammatory markers decreases with age (Xu et al., 2008). In AMD, microglia presence increases in the subretinal space which exacerbates macular degeneration (Xu, Chen and Forrester, 2009).

Molecular examination of enzymes within RPE cells identified low levels of DICER1 in people with non-neovascular AMD (Ambati et al., 2003). Cells deficient in DICER1 lead to activation of inflammatory proteins which results in RPE cell death (Tarallo et al., 2012). Furthermore, molecular and histological assessment of drusen reveals materials including classic acute phase reactants and complement cascade components responsible for complement system inactivation (Mullins et al., 2000). Presence of these products that are upregulated during an immune response has led to the proposal that complement cascade-related events are associated with drusen formation (Hageman et al., 2001). It has also been evidenced that increased levels of systemic inflammatory markers are associated with progression of AMD (Seddon et al., 2005).

1.3.2.4 Genetics

Evidence suggests an association between certain genetic variants and the development of AMD. Thirty-four genetic loci including 52 gene variants have been linked to AMD incidence (Fritsche et al., 2016). For example, genotyping studies have determined a link between certain variants of the CFH gene on chromosome 1 (Edwards et al., 2005), age-related maculopathy susceptibility-2 (ARMS2) (Seddon et al., 2003; Weeks et al., 2000) PLEKHA1 gene and hypothetical gene LOC387715 on chromosome 10 (region q26) with an increased risk of AMD (Jakobsdottir et al., 2005). The role of CFH in the body is to suppress the complement pathway. Thus, certain variants in the CFH results in an augmented inflammatory response. Another gene of note in AMD pathology is the VEGF-A gene (vascular endothelial growth factor A); the allele rs4711751 on 6p12 has also been associated with AMD susceptibility (Yu et al., 2011). VEGF-A encodes a heparin-binding protein and is a growth factor specific to endothelium cells (Ferrara et al., 2006). It is an essential factor of pathological angiogenesis and of CNV, which characterises the neovascular AMD as well as other diseases such as proliferative

diabetic retinopathy and diabetic macular oedema (Zampros et al., 2012), The RPE plays a key role in regulating VEGF levels and secretion has been identified to be increased by hypoxia (lack of oxygen as a result of reduced choroidal blood flow) which induces an inflammatory response in RPE cells (Arjamaa et al., 2017; Feigl, 2009).

1.3.3 Risk Factors

Major non-modifiable risk factors frequently associated with AMD are age and family history (Chakravarthy et al., 2010; Klein et al., 2004). For an overview of the risk factors associated with AMD in 113,780 people, see meta-analysis by Chakravarthy et al. (2010). Age is the most prominent and unambiguous risk factor for AMD, with every study on AMD illustrating this association (Klein, Klein and Linton, 1992; Klein et al., 2004; Chakravarthy et al., 2010). For example, Klein, Klein and Linton (1992) reported the prevalence of age-related maculopathy (ARM) phenotypes in 4926 white participants (aged 43-86 years) who participated in the Beaver Dam Eye Study. The authors found participants aged ≥ 75 years had a significantly higher number of ARM phenotypes detected ($p < 0.01$) than those aged ≤ 54 years. These phenotypes included drusen $\geq 125 \mu\text{m}$ in size (24.0% and 1.9%, respectively), soft indistinct drusen (23.0% and 2.1 %, respectively), retinal pigment abnormalities (26.6% and 7.3%, respectively), CNV (5.2% and 0.1%, respectively), and GA (2.0%, 0%, respectively) (Klein, Klein and Linton, 1992). Varma et al. (2004) reported the prevalence of early AMD and late-stage AMD (both neovascular and GA) in 6357 Latino participants (aged ≥ 40 years; mean [standard deviation; SD] 54.6 [10.7] years) in the Los Angeles Latino Eye Study (LALES). The data indicated that prevalence of early AMD increased from 6.2% in those aged 40-49 years to 29.7% in those aged ≥ 80 years, while prevalence of advanced AMD increased from 0% to 8.5%, respectively, Overall, the authors concluded that prevalence of early AMD and advanced AMD lesions increased with age ($p < 0.0001$) (Varma et al., 2004). Note, both these epidemiological studies used versions of the Wisconsin Age-Related Maculopathy Grading System (Klein et al., 1991) to grade fundus images and report monocular AMD disease.

Familial factors are also linked to the development and resultant severity of AMD (Klaver et al., 1998; Klein et al., 2001). The Beaver Dam Study assessed presence of AMD-related lesions and identified the likelihood (via odds ratio) of presence of AMD-related lesions in a younger sibling five years later if an older sibling had these lesions at baseline. The authors found an increased likelihood (1.82 [95% CI: 0.91, 3.66]) of a younger sibling developing soft drusen and RPE depigmentation (8.18 [95% CI: 3.34, 20.08]) over a five year period if an older sibling had it at baseline (Klein et al., 2001). Similarly, Maller et al. (2006) reported that siblings of an individual with AMD have a three-to-six-fold higher recurrence ratio risk than those of the general population

There is no great surprise considering the familial risk factor associated with AMD that genetics plays a role in AMD (see section 1.3.2.4). Yet, the precise interaction between genes and other environmental factors is not yet determined. For example, variants of the CFH, HtrA Serine Peptidase 1 (HTRA1) and ARMS2 genes have been shown to have strong links with AMD (Haddad et al., 2006; Chen, Bedell and Zhang, 2010). For a full review of genetics and AMD, see Schwartz et al., (2016).

Another non-modifiable risk factor is ethnicity. The systematic review by Wong et al (2014) (see section 1.3.1) determined a higher prevalence of AMD in Europeans in Europe and North America compared to Asians and Africans (Wong et al., 2014). The LALES study reported that participants with Native American ancestry were 15-times more likely to develop GA compared to participant who identified as Latinos. More recently, AMD incidence was assessed in four ethnic groups (white, black, Hispanic and Chinese) in 3811 participants (aged 46–86 years) from the Multi-Ethnic Study of Atherosclerosis study (Fisher et al., 2016). The authors reported the highest incidence of early and late AMD was in white participants (5.3% and 4.1%, respectively) and lowest in black participants (1.6% and 0.4%, respectively). Furthermore, black participants had 70% lower risk of developing early AMD than white participants (Fisher et al., 2016).

Despite evidence from a large population-based study suggesting that women are at higher risk of developing AMD compared to men (Klein, Klein and Linton, 1992), the systematic literature review by Wong and team did not report gender to be a risk factor of AMD (Wong et al., 2014). Similarly, Chakravarthy et al. (2010) reviewed six studies that examined gender as a risk factor for AMD and concluded that the literature suggests gender is not a risk factor, the odds ratio equalling approximately 1 across all six studies featured in the meta-analysis (2 cross-sectional studies, 2 case-control studies and 2 prospective studies).

Modifiable risk factors have also been associated with AMD. The most documented example by far is cigarette smoking (Klein et al., 1993; Christen et al., 1996; Smith, Mitchell and Leeder, 1996; Ardourel, 2000; Chen et al., 2011). Chen et al. (2011) reported that in a cohort of 1884 (unrelated, white) participants, current cigarette smokers are approximately four-times more likely to develop AMD compared to non-smokers (Chen et al., 2011). In Chakravarthy et al. (2010) meta-analyses, data from 16 studies that examined smoking were reviewed and authors concluded smoking to be a risk factor for AMD (current smokers versus participants who have never smoked), with an average odds ratio of 1.78 (95% CI 1.52-2.09) from the case-control studies and 3.58 (95% CI 2.68-4.79) from the cross-sectional studies. For example, McCarty et al. (2001) found current smokers were between two-to-four times more likely to develop AMD than non-smokers of the same age.

Another example of a modifiable risk factor is diet. For example, there is evidence to suggest that diets high in polyunsaturated fats may be a risk factor for AMD. The association between dietary fat intake and AMD was assessed in the Carotenoids in Age-Related Eye Disease Study (CAREDS) (Parekh et al., 2009). Parekh et al. (2009) found a two-times higher prevalence of iAMD in high vs low quintiles in

women (aged 50-79 years) that consumed polyunsaturated fatty acids such as omega-6 and omega-3. Jiang et al. (2021) conducted a meta-analysis to assess the literature on the association between omega-3 polyunsaturated fatty acids such as those found in oily fish and risk of AMD. The authors found a significant association between the consumption of omega-3 polyunsaturated fatty acids with 14% lower risk of early AMD (relative risk [RR]: 0.86, CI; 0.77, 0.96) and 29% (RR: 0.71, CI; 0.55, 0.91) lower risk of late AMD, respectively. There is also evidence that an increased intake of dietary carotenoids can reduce risk of AMD progression. The Eye Disease Case-Control Study Group compared 350 people with late AMD with 520 age-matched, control participants to investigate the association between dietary intake of carotenoids and subsequent risk for AMD and found increased intake of spinach and collard greens (high in lutein and zeaxanthin) was strongly linked to reduced AMD risk (42% risk reduction between the highest and lowest quintile) (Seddon et al., 1994).

As oxidative damage is suspected to be linked to the pathogenesis of AMD, research into antioxidant supplements has been conducted. The large randomised controlled Age-Related Eye Disease (AREDS) trial investigated the ability of high concentration antioxidant vitamins A, C, E and zinc to slow the progression of AMD. It was found that risk of progression from intermediate to advanced AMD was reduced by 25% over five years in people receiving the supplement vs. a placebo (AREDS Research Group et al., 2001). The subsequent AREDS 2 trial found no increased effect from adding carotenoids or omega-3 fatty acids to the supplement, but did demonstrate that beta carotene could be replaced by lutein and zeaxanthin, reducing the risk of negative outcomes in smokers.

Sunlight exposure has also been investigated as a potential modifiable risk factor for AMD. This association follows evidence that ultra-violet or blue light results in RPE impairment (Grimm et al., 2001; Hafezi et al., 1997; Youn et al., 2011). However, there is conflicting evidence that sunlight can be considered a risk factor for AMD. On the one hand, a systematic literature review and meta-analysis by Sui et al. (2013) reviewed epidemiological literature examining this association and concluded 12 studies found an increasing risk of AMD associated with greater sunlight exposure, with a pooled OR was 1.379 (95% CI 1.091,1.745). However, five years later this conclusion was disputed by a meta-analysis by Zhou et al. (2018), who did not find a statistically significant association between AMD risk and greater sunlight exposure. The authors account the differences between the findings to be due to limitations of the former review and meta-analysis.

1.4 CLINICAL FEATURES OF AGE-RELATED MACULAR DEGENERATION

1.4.1 Drusen

Drusen are yellow, insoluble hydrophobic deposits that collect between the RPE and BM. Analysis of the composition of drusen has revealed they consist of proteins (apolipoproteins), lipids (cholesterol),

amyloid, complement factors, carbohydrates and other trace materials (Mullins et al., 2000; Zhang and Sivaprasad, 2021). There are two main phenotypes: soft and hard drusen. Hard drusen (sometimes called drupelets) are small (<63 µm in size), well defined, and consist of hyaline material (Sarks, 1976). Small hard drusen naturally occur in visually healthy retinas and are considered part of normal ageing changes (Ferris et al., 2013; Wu et al., 2021), although the presence of multiple hard drusen is considered a risk factor for AMD onset (Klein et al., 2002). Soft drusen are larger with an irregular shape, and may be distinct or indistinct in appearance, or may coalesce to form confluent drusen. Soft drusen are widely considered the hallmark sign of AMD (when they are found in people >55 years). See section 1.2.2 for details of drusenogenesis in AMD.

As AMD becomes more severe, drusen may increase in number, in size or both and, perhaps surprisingly, in some cases drusen regress before progression to advanced disease (Glaser et al., 2013). The presence of large drusen is considered to be a risk factor for AMD progression (Ferris et al., 2005). See section 1.3 to read more about how these clinical manifestations appear on different modes of imaging.

1.4.2 Subretinal Drusenoid Deposits

Subretinal drusenoid deposits (SDDs), also referred to as ‘pseudodrusen’ or ‘reticular pseudodrusen’, are accretions of material located internal to the RPE (Spaide, Ooto and Curcio, 2018) best seen on optical coherence tomography (OCT) and short wavelength / infra-red imaging rather than standard colour fundus photography (CFP) (Zweifel et al., 2010) (for further details, see section 1.3.1). There is currently no consensus on the correct term (Sivaprasad et al., 2016; Wu et al., 2021), but for ease ‘SDDs’ will be used throughout this thesis.

Like hard drusen, SDDs are found in eyes with AMD (Curcio et al., 2013) but can also be found in healthy retinas (Gabrielle et al., 2019). Furthermore, SDDs contain similar proteins to soft drusen but differ in lipid content (Spaide, Ooto and Curcio, 2018). SDDs were first described in 1990 as “*les pseudo-drusen visibles en lumière bleue*” as they were best seen by via blue light channel funduscopy (Mimoun, Soubrane and Coscas, 1990). It wasn’t until multimodal imaging techniques were used that they were revealed to be lesions distinct from soft drusen and occurred in sub-retinal space, hence the term SDD was encouraged as more apt (Zweifel et al., 2010).

Zweifel et al. (2010) proposed a severity grading system for SDDs, ranging from stage 1 (SDDs appear as granular hyperreflective material between the RPE and the boundary between the inner and outer sections of the photoreceptors layer) to stage 3 (SDDs form a conical appearance and break through the inner and outer sections of the photoreceptors layer) (See Figure 1.6). Querques et al. (2012) later confirmed the dynamism of SDDs and that ‘stage 4’ finds the lesions reabsorb into the retinal layers.

Subretinal drusenoid deposit presence is considered a risk factor for atrophy and CNV (Finger et al., 2014; Hogg, 2014) and has been linked with a two-times increased likelihood of late stage AMD development in the fellow eye of neovascular AMD (Pumariega et al., 2011). SDDs are fast becoming a topic of research interest in the literature (Zweifel et al., 2010; Pumariega et al., 2011; Hogg, 2014; Flamendorf et al., 2015; Laíns et al., 2017; Spaide, Ooto and Curcio, 2018; Chen et al., 2019; Gabrielle et al., 2019; Wu et al., 2021). For details on the relationship between SDDs and DA, see section 1.5). For a thorough review of SDDs, see Hogg (2014), Sivaprasad et al. (2016) and Wu et al. (2021).

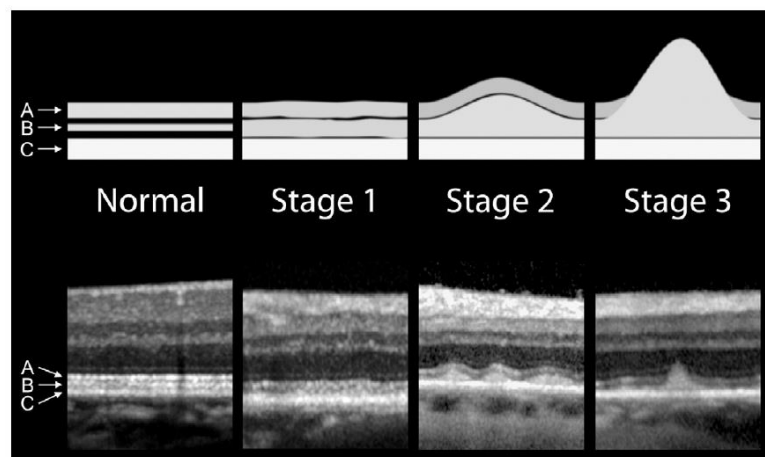


Figure 1.6 A severity grading system for SDDs proposed by Zweifel et al. (2010) shown in a diagram and OCT images. Stage 1 indicates SDDs appear as granular hyperreflective material between the RPE and the boundary between the inner and outer sections of the photoreceptor layer. Stage 2 indicates accumulations of material that visibly impact the boundary between the inner and outer sections of the photoreceptor layer. Stage 3 indicates when SDDs form a conical appearance and break through the inner and outer sections of the photoreceptor layer (Zweifel et al., 2010).

1.4.3 Pigmentary Changes and Hyperreflective Foci

Focal pigmentary changes are a hallmark of progressing AMD, evidencing RPE atrophy. Via fundus imaging, areas of the macula (and sometimes peripheral regions) will appear mottled, showing hyperpigmentation and hypopigmentation. The presence of focal pigmentary changes is a known risk factor for progression of AMD (Ferris et al., 2005). As AMD progresses, further demarcated areas of depigmentation will be evident. See Figure 1.7 and section 1.5 for further details on imaging. Other morphological changes tend to accompany pigmentary changes, such as drusen presence. For example, hyperpigmentation on fundus photographs has been evidenced to show significant spatial alignment with hyperreflective foci seen on OCT overlying drusen (Khanifar et al., 2008) and may reflect similar pathology. Hyperreflective foci are likely due to disruption of the RPE (Folgar et al., 2012). Some studies have found participants with pigmentary abnormalities and soft drusen perform worse on measures of visual function (e.g. short-wavelength cone thresholds and sensitivity to 14-Hz

flicker (Dimitrov et al., 2012) and shape discrimination hyperacuity tests (Schneck et al., 2021)) compared to eyes with just drusen.

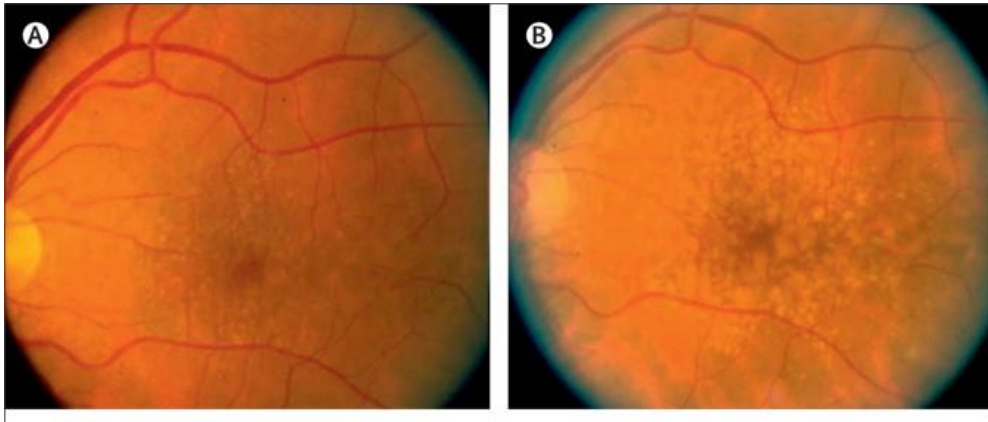


Figure 1.7 Colour fundus image from participant with early AMD from the Blue Mountains Eye Study, adapted from Lim et al. (2012). Panel A shows large drusen appearing as yellow spots. Panel B shows progression in both the size and area covered of the drusen five years later.

1.4.4 Geographic Atrophy

Geographic atrophy (GA) consists of retinal cell degradation that progresses slowly, mainly in rod-dominant regions (parafoveal) before eventually spreading to the fovea. This is also termed as late stage non-neovascular AMD. Lesions of GA are associated with scotomas (blind spots). Progression rates of scotomal regions vary widely among patients, as indicated by longitudinal studies (Brinkmann et al., 2010). For example, in the Beaver Dam Eye Study, the overall increase in GA was 6.4 mm² over five years (Klein et al., 2008). While GA can result in significant visual function deficits in reading, night vision, and DA, and produce dense, irreversible scotomas in the visual field, the initial decline in VA may be relatively minor if the fovea is spared (Holz et al., 2014). On colour imaging, GA appears as a clearly demarcated area, where choroidal vessels may be visible as the RPE and choriocapillaris may have atrophied. Unfortunately, defining the edges of atrophy is difficult on CFP. As OCT has a higher resolution, a novel classification system of GA in AMD that considers microstructural changes has been suggested by the Classification of Atrophy Meetings (CAM) group (Sadda et al., 2018). This classification consists of: iRORA (incomplete RPE and outer retinal atrophy), cRORA (complete RPE and outer retinal atrophy), iORA (incomplete outer retinal atrophy) and cORA (complete outer retinal atrophy). However, in practice there is evidence to suggest cRORA is difficult to repeatably diagnose and training is required before it is implemented into clinical practice (Chandra, Rasheed, et al., 2022). See Figure 1.8 and section 1.5 for further details on imaging.

Evolution of geographic atrophy

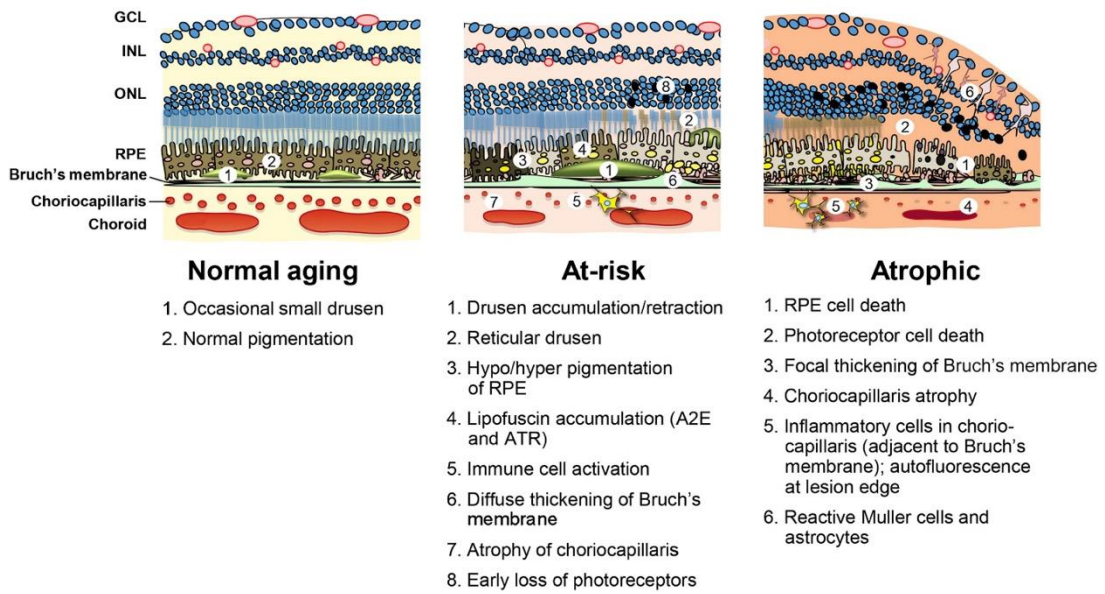


Figure 1.8 Figure sourced from Holz et al. (2014), illustrating a diagram of evolutionary changes in the macula as a function of GA.

1.4.5 Choroidal Neovascularisation

Choroidal neovascularisation is the manifestation of neovascular AMD and is one of the leading causes of irreversible severe loss of vision among the elderly. CNV is not the subject of this thesis, which focusses upon non-neovascular AMD. Briefly, CNV is characterised by blood vessels that push through the BM into subretinal (type 1 CNV) or sub-RPE space (type 2 CNV) (Yonekawa & Kim, 2014). It is formed by a complex chain of molecular reactions, but it is believed unbalanced upregulation of VEGF plays a role in its development (Kwak et al., 2000). Typical indicators of CNV include haemorrhages, intra or subretinal fluid, pigment epithelial detachment (PED), with the end stage of untreated disease being disciform scar formation (Wong et al., 2022). Type 1 CNV generally manifests as PED, whereby the RPE dissociates from the inner part of the BM. There are different forms of PED, including fibrovascular, drusenoid, and serous. The former is associated with CNV (Wong et al., 2022). The gold standard for imaging and diagnosing CNV is fluorescein angiography. See section 1.5.4 for further details.

Polypoidal choroidal vasculopathy (PCV) is a subtype of CNV commonly seen in the Asian population. A recent multimodal imaging study by Corvi et al. (2022) compared 128 Asian to 122 Caucasian eyes with PCV and suggested the pathophysiology of PCV could depend on ethnicity which may account for the variation in disease phenotypes (Corvi et al., 2022). It is characterized by the presence of multiple polyps in choroidal circulation and is different in its epidemiology, pathogenesis and response to

therapy to neovascular AMD. For a review of PCV and current management strategies, refer to Palkar and Khetan (2019).

1.5 CLASSIFICATION

Naturally, a consistent framework that describes clinical phenotypes of AMD is essential for the assessment of novel treatments as they edge closer to approval and to ensure necessary cost effectiveness of expensive clinical trials (see section 1.5.1). Not only is it essential for clinicians to share the same terminology for clinical phenotypes and to share the same idea of their clinical significance, but a standardised classification of AMD is required to facilitate effective comparisons across research studies of people with AMD (Ferris et al., 2013). There are a number of classifications and severity scales that have been developed and are based on grading CFP images and focus on drusen presence/size/number and RPE changes to determine the extent of the disease. Generally, disease severity is split into 'early' stage AMD whereby eyes have drusen above a set threshold number/size, 'intermediate' stage AMD whereby eyes have focal pigmentary disturbances with or without drusen and 'late' stage AMD which indicates GA or CNV. However, herein lies a substantial issue. Terms such as 'early' AMD or 'intermediate' AMD may mean entirely different things depending on the classification system utilised. To illustrate how this may look, see Table 1.1 for comparisons of AREDS and Beckman classification systems.

Examples of current severity classifications of AMD include the Beckman classification (Ferris et al., 2013), international classification system (Bird et al., 1995), Wisconsin classification system (Klein et al., 1991), Rotterdam staging system (Van Leeuwen et al., 2003), National Institute for Health and Excellence (NICE) grading system (NICE Recommendations for Age-Related Macular Degeneration NG82, 2018) and the AREDS classification (AREDS Research Group, 2001) all of which utilise CFP as they originate from epidemiological studies (Bird et al., 1995; Klein et al., 1991; Saßmannshausen et al., 2018; Thee et al., 2020). As the Beckman classification is used throughout this thesis, this system will be focused on.

The Beckman classification was devised using a modified Delphi process featuring 26 AMD experts, one neuro-ophthalmologist, two committee chairmen, and one methodologist. Each member of the panel rated current AMD gradings and stated their agreement and/or disagreement via a 9-item scale. A review was held to discuss the results and to determine the necessary elements of a classification until consensus was met. As a result, the Beckman Initiative for Macular Research Classification Committee published a consensus paper in 2013 (Ferris et al., 2013). In summary, it was agreed fundus lesions would be used to assess AMD severity, with drusen $<63\mu\text{m}$ (or drupelets) being a sign of early ageing changes, $<63\text{--}\leq 125\mu\text{m}$ drusen and no pigment changes considered as early AMD, $\leq 125\mu\text{m}$ drusen and/or pigment changes was categorised as iAMD and signs of CNV or GA was a sign of late

AMD. See Table 1.1 for details of the Beckman classification. The committee's aim for uniformity was seen as final, yet a wide array of classifications are still used in research to this day.

The use of a variety of different classification systems makes comparing data from epidemiological studies difficult (and in some cases impossible) (Brandl et al., 2018). Differences across classifications of AMD are partly due to their unique aims. For example, the Beckman classification was developed so that the stages (presence of different sized drusen and/or RPE abnormalities) reflected risk of progression to late-stage AMD and resulting vision loss (Ferris et al., 2013).

Pertinent to this thesis, current classifications of AMD that rely on CFP do not feature SDDs. For example, the AREDS and Wisconsin classification systems misclassify them as severe soft drusen while the Beckman classification negates them entirely (Spaide, 2018). This is unfortunate as there is evidence that SDDs are associated with increased likelihood of progression to later stage AMD (Hogg, 2014). As part of this programme of research, SDDs will be incorporated into a novel classification of AMD severity using OCT (see Chapter 4).

While the Beckman classification was designed to only require clinical examination or fundus photography to assign a scale of severity to ensure ease of adoption, it is ultimately hindered by the limitations of CFP. For example, CFP is more hampered by media opacities than other, newer modalities such as OCT. See section 1.6 of details of CFP and section 1.6.3. for a comparison between CFP and OCT. Recent advances in imaging technologies provide a deeper examination of AMD disease severity and it is now possible to improve upon current severity grading scales in determining stages of AMD. Indeed, as mentioned earlier (section 1.4.4) an international team of retinal experts have formed the CAM group and are working towards a consensus on the terminology and framework for defining atrophy based specifically on OCT imaging (Sadda et al., 2018). As a result of the introduction of new imaging technologies, it is now considered good practice to utilise multimodal imaging strategies to classify phenotypes of AMD to capture more changes than achieved by CFP alone. It is thought that the future of classification of AMD will rely upon OCT alongside artificial intelligence to automatically segment each layer of the retina to assess atrophy. Therefore, it is imperative that OCT-based classifications of AMD are explored (see Chapter 4).

Table 1.1 Table comparing the Beckman (Ferris et al., 2013) and the AREDs (AREDS Research Group, 2001) classification systems, illustrating the potential differences between early and iAMD when using different classifications. Note: SDDs not mentioned. Table adapted from Miller, Bagheri and Vavvas (2017).

Stage description	Beckman classification	AREDs classification
No drusen/pigment changes	No disease	No disease
≤63µm drusen	Normal Ageing	No disease or Early AMD
<63-≤125µm drusen and no pigment changes	Early AMD	Early AMD or iAMD
≤125µm drusen and/or pigment changes	iAMD	iAMD
GA or CNV	Late AMD	Late AMD

1.5.1 Symptoms, Diagnosis and Treatment

Classic symptoms of AMD include blurred vision, metamorphopsia (where straight lines appear distorted), scotomas (missing areas of the visual field) (Jager, Mieler and Miller, 2009), difficulty with activities at night or low illumination (like reading, mobility or driving) (Owsley, McGwin, Scilley et al., 2006) and issues with adapting from dark to light illumination levels, i.e., DA (the focus of this thesis). DA relies upon the biological mechanisms featured in visual cycle (see section 1.1.2.1) and influences the capacity of the visual system to adjust to light level changes, which can have a significant impact on an individual's ability to perform daily activities where light levels suddenly change e.g., turning on a bedside lamp in the middle of the night and struggling to see to get to the bathroom (Yazdanie et al., 2017). Impairment of night vision in people with AMD is likely a result of degeneration and loss of rod photoreceptors (Curcio, Medeiros and Millican, 1996). Despite one of the common symptoms reported by people with AMD is nyctalopia or 'night blindness' and devices becoming clinically available like the AdaptDx, DA is not routinely assessed in clinic in the UK. For further details about assessing DA in people with AMD, see section 1.8.

These aforementioned symptoms are characteristic of later stage AMD while less is known of symptoms experienced by people with early and iAMD. Indeed, Huang et al. (2013) found evidence that the majority of people with ocular pathology including AMD were unaware of their condition. Taylor et al. (2018) conducted an investigation into self-reported perceptions of visual impairment in people with AMD. The most frequently reported descriptions of visual experience were: 'blur', 'missing' and 'distortion'. Furthermore, the majority of participants rejected a commonly used image depicting what people with AMD 'see' as not accurately reflecting their experience (see Figure 1.9). Not only does this study indicate the requirement to update currently used imagery of visual

impairment in AMD, but also highlights the diverse ways in which visual impairment associated with AMD can manifest.



Figure 1.9 A picture that is commonly used to describe the experience of someone with AMD sourced from Taylor et al. (2018).

Age-related macular degeneration is usually detected by optometrists or ophthalmologists during routine examination. This often involves a dilated exam where the fundus is examined for signs of AMD-related changes using binocular indirect or direct ophthalmoscopic examination and CFP. Further investigative techniques such as OCT imaging are also now widely used (see sections 1.3 and 1.4 for more details on the assessment of retinal structure and function in AMD). However, early stages of AMD can be difficult to differentiate from normal ageing changes, even by seasoned ophthalmic professionals, as demonstrated by Neely et al. (2017).

An Amsler chart is also used to assess for the presence of metamorphopsia and scotomas, which may be indicative of the onset of advanced disease. However, Crossland and Rubin (2007) have found Amsler charts to have a high false negative rate, with a sensitivity level of less than 50% in detecting people with advanced AMD, speculated to be due to the perceptual completion phenomenon or poor administration of the test (Crossland & Rubin, 2007). More recently, the Early Detection of Neovascular Age-Related Macular Degeneration (EDNA) three year multicentre study also found the Amsler test to have poor sensitivity and specificity in a UK population, with a preference suggested instead for OCT imaging for optimum clinical practice (Sivaprasad et al., 2021). Despite this, the chart remains simple, cost-effective and easily understood by patients and clinicians alike, meaning its use will likely continue.

The main focus of clinicians is to monitor non-neovascular AMD for any changes in visual impairment that may indicate progression into neovascular AMD. This is important, as early detection and treatment of neovascular AMD is key to the success of the treatment (Schwartz & Loewenstein, 2015). As AMD is a long-term chronic disease, repeated testing and monitoring is required of patients which is burdensome, which may lead to lack of adherence and subsequent loss of VA if treatment is implemented at a late stage (Holz, Schmitz-Valckenberg and Fleckenstein, 2014). Furthermore,

diagnosis for people with non-neovascular AMD is stressful and impacts patient quality of life (QoL) (Taylor et al., 2019).

Lifestyle advice should be offered to people diagnosed with early stages of AMD such as dietary advice and offer support options available to quit smoking (a known risk factor for AMD progression and incidence) (Mares and Moeller, 2006; Bott, Huntjens and Binns, 2018). Examples of evidence-backed dietary advice include, increasing intake of green leafy vegetables high in lutein and zeaxanthin (such as spinach and collard greens), yellow/orange fruit and vegetables (such as yellow peppers) (Ma et al., 2016) and eating eggs and oily fish rich in omega-3 (SanGiovanni et al., 2007; Chakravarthy, Williams and Group, 2013; Chew et al., 2013; Chandra, McKibbin, et al., 2022). This is to increase the macular pigment and fatty acids found in photoreceptors impacted by the pathogenesis of AMD (Wilson et al., 2021) (see section 1.3.2). People with iAMD and people with unilateral advanced AMD may be advised to take vitamin supplements based on the AREDS trial formulas (AREDS Research Group et al., 2001; Chew et al., 2013) (see section 1.4.1.2 for further details). Unfortunately, medical treatment options are currently only available for late-stage diagnosis of CNV (see section 1.2.5.1). There is no current treatment available for non-neovascular AMD and effects of GA cannot be reversed.

1.5.1.1 Current Treatments for Neovascular Age-Related Macular Degeneration

None of the current treatments available can 'cure' wet AMD but help in reducing and delaying vision loss. It is generally accepted that upregulation of the growth factor VEGF-A in response to chronic inflammation and outer retinal hypoxia plays a key role in the development of CNV via angiogenesis (Campochiaro, 2004). VEGF was first isolated by Senger et al. (1983) as a factor secreted by tumours that increased vascular permeability

Anti-VEGF treatment employs drugs that block VEGF from binding its receptors thus preventing the promotion of proliferation of vascular endothelial cells. Anti-VEGF drugs which have been shown to be effective in the treatment of neovascular AMD include ranibizumab (Lucentis), bevacizumab (Avastin), brolucizumab (Beovu) and aflibercept (Eylea) which are delivered via intravitreal injections (Rosenfeld, Rich and Lalwani, 2006; Heier et al., 2012; Maguire et al., 2016; Clearkin et al., 2019; Dugel et al., 2020). Ranibizumab is a humanized antibody fragment that targets VEGF-A (like brolucizumab and bevacizumab) and was approved as a treatment for wet AMD in 2006 after its success in the ANCHOR (Brown et al., 2009) and MARINA (Rosenfeld et al., 2006) clinical trials with both evidencing improvement in participant VA. Phase III clinical trials evidenced ranibizumab stabilised vision in >90% of participants with neovascular AMD (Rosenfeld, Rich and Lalwani, 2006). Aflibercept is a recombinant fusion protein that contains components of VEGF receptors and the immunoglobulin G1, and acts as a decoy receptor for all VEGF-A isoforms and placental growth factor (Heier et al., 2012). In the United Kingdom, ranibizumab, brolucizumab and aflibercept are currently approved for use by the NICE (NICE Technology Appraisal Guidance TA155, 2008; TA294, 2013; TA672, 2021) whilst

bevacizumab has been shown to be effective but is only used off-label for treatment. Anti-VEGF drugs are administered on a monthly basis for a three-month loading phase and then at regular intervals thereafter for as long as positive treatment effects continue to be noted. Most hospitals currently use a treat and extend protocol whereby the patients are given an intravitreal injection at every hospital visit but will have an increased period between visits if their condition appears to be stable (Li et al., 2020). As AMD is a chronic eye disease, this anti-VEGF treatment protocol may continue over a long period of time, resulting in a high burden on patients and National Health Service (NHS) resources. However, prior to the widespread treatment using anti VEGF drugs, neovascular AMD was responsible for 80-90% of blindness caused by AMD, despite only accounting for 10% of AMD cases (Ambati & Fowler, 2012). Since anti-VEGF drugs became available, approximately 50% of cases of severe sight impairment in England attributable to AMD are caused by GA (Bunce et al., 2015). Hence, anti-VEGF drugs have had a major impact on the number of people with neovascular AMD who progress to severe visual loss (Ferris, Fine and Hyman, 1984; Bunce et al., 2015). For a review of current and upcoming anti-VEGF therapies, see Khanna et al. (2019).

1.5.1.2 Potential Treatments for Non-neovascular Age-Related Macular Degeneration

While no treatments for non-neovascular AMD are available presently, there are clinical trials investigating AMD prevention, halting AMD progression or restoring lost vision (Cabral De Guimaraes et al., 2021). Cabral de Guimaraes et al. (2021) summarised the avenues currently being explored as: (i) antioxidant treatments, (ii) drugs that inhibit the complement cascade (part of the immune system that enhances antibodies), (iii) neuroprotective agents, (iv) visual cycle inhibitors, (v) gene therapies and (vi) cell-based therapies (See Table 1.2).

With respect to antioxidant treatments, the aim has largely been to slow progression from early AMD to the sight threatening later stages of the disease. For example, the large phase III double blind randomised controlled clinical trial, AREDS (NCT00000145) examined the impact of antioxidant supplements on disease progression in 3640 people with early/intermediate or unilateral advanced AMD followed up for 5 years. It concluded that daily high doses of β -carotene, vitamin C, vitamin E and zinc (AREDS Research Group et al., 2001) reduced likelihood of progression to late-stage AMD from iAMD by around 25%. However, the following AREDS study (AREDS2; NCT00345176) found supplements of lutein and zeaxanthin or DHA and eicosapentaenoic acid (EPA) (or a combination of both) did not further reduce progression to late-stage AMD, (Chew et al., 2013). However, AREDS2 results did indicate that the beta-carotene present in the original formulation could be replaced by lutein and zeaxanthin without reducing the effectiveness of the intervention (Chew et al., 2012). This is important as beta carotene has been shown to increase the risk of lung cancer in smokers (Goralczyk, 2009).

More recent trials have attempted to find treatments for GA rather than aiming to delay progression to advanced disease. For example, the complement cascade inhibitor drug lampalizumab inhibits complement factor D (or adipsin) which plays a critical catalytic role in the alternative complement pathway (Barratt & Weitz, 2021; Cabral De Guimaraes et al., 2021). Two of the largest phase III trials on GA to date (CHROMA; NCT02247479 and SPECTRI; NCT02247531) investigated the safety and efficacy of intravitreal lampalizumab injections (10mg) on the progression of GA in 906 and 925 (respectively) people with bilateral advanced non-neovascular AMD. However, no meaningful difference was found in reducing GA progression versus sham injections (Holz et al., 2018). Another drug currently under investigation that targets the complement pathway is Avacincaptad pegol, an anti-C5 aptamer which aims to reduce upregulation of inflammatory markers and the formation of membrane attack complex (MAC). A phase II/III randomised controlled trial (GATHER1; NCT02686658) in 286 people with GA evidenced a reduction in rate of GA growth and a second confirmatory phase III trial (GATHER2) is currently underway (Jaffe et al., 2021). Other drugs of note that target the complement cascade include Pegcetacoplan (Liao et al., 2020) (currently undergoing investigation in DERBY (NCT03525600) and OAKS (NCT0355613) phase III studies) and Risuteganib (Shaw et al., 2020)

Other promising avenues of GA treatment research includes neuroprotective agents. Neuroprotection refers to the recovery or regeneration of the nervous system. Example drugs include antiapoptotic agents like tauroursodeoxycholic acid (TUDCA) found naturally in bile which have antioxidant activity (Oveson et al., 2011) and growth factors such as ciliary neurotrophic factor (CNTF) (Kauper et al., 2012; Sieving et al., 2006). Another treatment modality being explored is visual cycle inhibitors as modifying elements of the disadvantaged visual cycle may ease progression of the disease. Key drugs include emixustat hydrochloride (Rosenfeld et al., 2018), fenretinide (Mata et al., 2013) and deuterated vitamin A, a modified form of vitamin A (Kaufman, Ma and Washington, 2011). Gene therapy intervention is another area of research into arresting GA spread, with a focus on deregulating the complement cascade such as reducing MAC formation (Kumar-Singh, 2019). Lastly, cell-based therapies also offer an option for the treatment for GA. For example, there have been two phase I and II trials assessing the tolerability and safety of RPE transplantation in people with GA and advanced non-neovascular AMD. RPE cells sourced from stem cells were delivered following surgery to a small cohort of nine participants and no adverse events related to the transplanted tissue arose in the 22 month follow-up (FU), while adverse events were experienced related to the surgery itself and immunosuppression (Schwartz et al., 2015). It was concluded that transplanted RPE cells may improve visual function in the short term in participants with severe vision loss (Kashani et al., 2018) but further study in a larger cohort would be needed.

Overall, due to the several pathogenic pathways associated with AMD, finding a treatment for non-neovascular AMD poses a therapeutic challenge (Cabral De Guimaraes et al., 2021). As Volz and Pauly (2015) eloquently conclude, there will likely never be a 'magic bullet' for AMD, yet a tailored

therapeutic 'toolbox' of treatments is more likely (Volz & Pauly, 2015). For a complete review of the current potential treatments for AMD, see Cabral de Guimaraes et al. (2021).

Table 1.2 Ongoing clinical trials, based on table from Cabral De Guimaraes et al. (2021).

Drug category/ name	Clinical trial ID (NCT #)	Study phase	Route of delivery	Status	Sponsor	Location	No. of patients	Visual function outcome measures
Antioxidative								
AREDS	NCT00000145	Phase III	Oral	Completed	National Eye Institute (NEI)	USA	3640	Visual Acuity (VA)
AREDS2	NCT00345176	Phase III	Oral	Completed	National Eye Institute (NEI)	USA	4203	VA
OT-551	NCT00306488	Phase II	Topical	Completed	National Institutes of Health Clinical Center (CC)	USA	11	VA and Contrast Sensitivity (CS)
Reduction of toxic by-products								
GSK933776	NCT01342926	Phase II	IV	Completed	GlaxoSmithKli ne	USA	191	VA
RN6G	NCT01577381	Phase II	IV	Terminated	Pfizer	USA	10	VA, Low Luminance VA (LL- VA), CS, Reading Speed (RS), Reading Acuity (RA), Reading Critical Print Size
Visual cycle modulators								
ACU-4429	NCT01802866	Phase IIb/III	Oral	Completed	Kutoba Vision Inc	USA	508	VA
Fenretinide	NCT00429936	Phase II	Oral	Completed	Sirion Therapeutics, Inc	USA	246	N/A
C20-D3- vitamin A (ALK-001)	NCT03845582	Phase III	Oral	Ongoing— recruiting	Alkeus Pharmaceutic als, Inc	USA	300	VA, RS
Anti-inflammatory and complement inhibition								
Eculizumab	NCT00935883	Phase II	IV	Completed	Philip J. Rosenfeld, MD	USA	30	VA
Lampalizumab	NCT02247531	Phase III	Intravitreal	Terminated	Hoffman-La Roche	Multicenter	906	Mesopic Microperimetry (MM), VA, LL-VA, RS
Lampalizumab	NCT02247479	Phase III	Intravitreal	Terminated	Hoffman-La Roche	Multicenter	975	MM, VA, LL-VA, RS
Sirolimus (rapamycin)	NCT00766649	Phase I/II	Subconjuncti val	Completed	National Eye Institute (NEI)	USA	11	VA
Avacincaptad pegol (Zimura)	NCT02686658	Phase II/III	Intravitreal	Completed	IVERIC bio, Inc.	Multicenter	286	VA
Pegcetacoplan (APL-2)	NCT02503332	Phase II	Intravitreal	Completed	Apellis Pharmaceutic als Inc.	Multicenter	246	VA, LL-VA
Pegcetacoplan (APL-2)	NCT03525600	Phase III	Intravitreal	Ongoing— not recruiting	Apellis Pharmaceutic als Inc.	Multicenter	600	N/A
Pegcetacoplan (APL-2)	NCT03525613	Phase III	Intravitreal	Ongoing— not recruiting	Apellis Pharmaceutic als Inc.	Multicenter	600	N/A

Tedisolumab (LFG316)	NCT01527500	Phase II	Intravitreal	Completed	Novartis Pharmaceuticals	USA	150	VA
Risuteganib	NCT03626636	Phase II	Intravitreal	Completed	Allegro Ophthalmics	USA	42	VA
Neuroprotection								
Ciliary nerve trophic factor	NCT00063765	Phase I	Intravitreal	Completed	National Eye Institute (NEI)	USA	10	VA, Visual Fields (VF), ERG
Ciliary nerve trophic factor	NCT00447954	Phase II	Intravitreal	Completed	Neurotech Pharmaceuticals	USA	51	VA, ERG
Brimonidine tartrate	NCT00658619	Phase II	Intravitreal	Completed	Allergan	Multicenter	113	VA, CS, RS
Brimonidine tartrate	NCT02087085	Phase IIb	Intravitreal	Terminated	Allergan	Multicenter	303	VA, VF, LL-VA
Gene therapy								
AAVCAGsCD59	NCT03144999	Phase I	Intravitreal	Completed	Hemera Biosciences	USA	17	VA
GT005	NCT03846193	Phase I/II	Subretinal	Ongoing - Recruiting	Gyroscope Therapeutics	UK	35	VA, VF, RS
Cell-based therapies								
Palucorcel (CNTO-2476)	NCT01226628	Phase I/II	Subretinal	Completed	Janssen Research & Development, LLC	USA	35	VA, LL-VA, Low Luminance Deficit, RS, CS, VF
MA09-hRPE	NCT01344993	Phase I/II	Subretinal	Completed	Astelas Institute for Regenerative Medicine	USA	9	VA, RS
CPCB-RPE1	NCT02590692	Phase I/IIa	Subretinal	Ongoing— not recruiting	Regenerative Patch Technologies	USA	16	VA, VF, ERG
Mitochondrial enhancers								
Elamipretide	NCT02848313	Phase I	Subcutaneous	Completed	Stealth Biotechnologies Inc	USA	40	VA, LL-VA, Dark Adaptometry, RA, MM
Elamipretide	NCT03891875	Phase II	Subcutaneous	Ongoing— recruiting	Stealth Biotechnologies Inc	USA	180	VA, Low Luminance Reading Acuity
Nanosecond laser therapy								
2RT nanosecond laser	NCT01790802	Not applicable	Retinal active laser therapy	Completed	Center for Eye Research Australia	Australia	292	VA

1.6 IMAGING THE RETINA WITH AGE-RELATED MACULAR DEGENERATION

As AMD presence and risk of progression is a structurally defined by the presence of drusen/RPE change; quantification of retinal damage is central to AMD diagnosis and management. Direct ophthalmoscopy offers the most basic examination of the retina but is limited by its small field of view and magnification effects of high refractive errors (Ng et al., 2014). Dilated binocular indirect ophthalmoscopy offers a wider field of view, stereoscopic viewing of raised lesions, and is

independent of refractive errors. This remains the gold standard for fundus examination but is augmented in primary and tertiary care by imaging techniques. Digital CFP has become a standard imaging technique in high street optometric practice and forms the basis of most AMD classification and grading systems. In the hospital eye service, fundus fluorescein angiography has long been used as the gold standard for diagnosis and classification of neovascular AMD. However, due to the advancements in computer, optic and camera technology, new retinal imaging techniques have been introduced and are utilised worldwide, such as OCT, fundus autofluorescence (FAF), and multispectral imaging. For a comprehensive overview of recent developments in retinal imaging, see Soomro et al. (2020) and for an insight into emerging retinal imaging technologies, see Li and Choudhry (2020).

1.6.1 Digital Colour Fundus Photography and Age-Related Macular Degeneration

Digital CFP is used regularly to diagnose and grade AMD disease severity and has been utilised in prominent epidemiological studies (Bird et al., 1995; Klein et al., 1991; Saßmannshausen et al., 2018; Thee et al., 2020). CFP image intensities illustrate the amount of reflected blue, green and red wavelengths (Abramoff, Garvin and Sonka, 2010). There are different types of fundus cameras, often described by the angle of view they offer. The most common angle is 30° which gives an overall view of the retina while smaller angles (20° or less) are used to image lesions such as drusen in AMD with higher magnification (Ng et al., 2014). Drusen appear as yellow/white blobs on CFP images, while areas of GA appear as regions of hypopigmentation with a minimum diameter of 175µm, with increased visibility of underlying large choroidal vessels (See Figure 1.10) (Baumann et al., 2010). Soft drusen are large with an irregular shape and distinct or indistinct borders while hard drusen have well-defined edges and are smaller. SDDs can have a variable appearance on CFP images (Wu et al., 2021). For example, Suzuki et al. (2014) classified three phenotypes: (i) “ribbon” for an interlacing pattern of deposits, (ii) “dot” for distinct dot-like deposits, and (iii) “midperipheral”, as yellow/white coloured globs found outside the vascular arcades (Suzuki, Sato and Spaide, 2014). Filters can be used to highlight certain features. For example, a green filter can be used to highlight retinal lesions, while the blue channel allows better contrast for SDDs. Blue light is preferentially absorbed by melanin thus the RPE appears as a darker background. Zweifel et al (2010) evidenced that as SDDs spatially coincide with abnormal materials above the RPE, they are selectively more visible when the blue filter is used. While some studies utilise CFP to identify SDDS (Finger et al., 2016), the sensitivity of CFP has been found to be lower when compared to other imaging modalities such as SD-OCT (76% and 95%, respectively) (Ueda-Arakawa et al., 2013) and infrared reflectance imaging (88% and 95%, respectively) (Smith et al., 2009) at detecting SDDs despite perfect specificity (100%) (Ueda-Arakawa et al., 2013). Ueda-Arakawa et al. (2013) speculated this may be due to CFP being more hampered by media opacities and recommend multimodal imaging techniques to overcome this. The fundus camera used in this programme of work is the Canon CX-1 Digital Fundus Camera (Canon U.S.A., Inc.).



Figure 1.10 A colour fundus image showing medium and large soft drusen on the left and GA on the right. Sourced from Kanagasingam et al. (2014).

Drusen maximum size and the area of drusen coverage is estimated from the images and then compared to grading classifications (Kanagasingam et al., 2014). Drusen size is often characterised as small (≤ 63 microns [hard drusen or drupelets]), medium ($>63 \leq 125$ microns) or large (>125 microns) (Ferris et al., 2013). In the context of CFP, 63 microns is at the resolution limit of the image, while 125 microns is approximately the width of the central retinal vein as it leaves the optic disc. As aforementioned, severity classifications of AMD like the Beckman classification (Ferris et al., 2013) International classification system (Bird et al., 1995), Wisconsin classification system (Klein et al., 1991), Rotterdam staging system (Van Leeuwen et al., 2003) and the AREDS classification (AREDS Research Group, 2001) all use CFP as they originate from epidemiological studies (Bird et al., 1995; Klein et al., 1991; Saßmannshausen et al., 2018; Thee et al., 2020). However, CFP analysis is marred by relying on clinician's subjectivity and poor image quality can result from background reflectivity (Smith et al., 2005), media opacities and effects from pupil size which impact the grading of drusen (Kanagasingam et al., 2014; Midena et al., 2020). Yet, in studies aiming to compare imaging modalities, CFP has been found to be better than OCT at detecting small, hard drusen with well-defined edges (Jain et al., 2010).

1.6.2 Optical Coherence Tomography and Age-Related Macular Degeneration

Optical coherence tomography uses laser infrared interferometry to provide a non-invasive high-quality, in-vivo cross-sectional image of the retina. OCT was first described in the 1990s by Huang, et al. (1991) and has become the mainstay in clinical imaging. It is increasingly recognised as the imaging modality of choice for the detection of both early and late AMD features. However, an OCT-based severity classification of AMD is yet to be developed as currently used classification systems are based

largely on historical epidemiological studies and appropriate OCT technology did not exist at that time. The programme of work explored in this thesis will explore a potential OCT-based classification of AMD severity (see Chapter 4).

Optical coherence tomography works via the interference pattern developed between light reflected from the target tissue and a local reference signal propagating in the reference arm of a Michelson interferometer (Kalkman, 2017). Simply put, light is used to create a cross-sectional map of the layers within the retina by taking a-scans of the depth of the retina and then aligning them side-by-side to create a b-scan cross-sectional image. The resulting images depend upon the optical properties of the tissues. For example, retinal tissues that disperse (reflect) more light are shown as a lighter colour (or in colour imaging, white and red) while tissues that disperse less light are shown as blue and black. Tissues that moderately reflect light are shown as green and yellow (Garcia-Layana et al., 2009).

Advancements in technology have yielded three main types of OCT imaging: time domain OCT, followed by spectral domain OCT (SD-OCT) and swept-source OCT (SS-OCT). Time domain OCT creates a-scans by moving a reference mirror corresponding to each point along the depth of the a-scan and then scanning the reference arm of a Michelson interferometer for movement. Data regarding intensity in the form of a reflectivity profile in depth, can be extracted from the interference pattern (See Figure 1.11). This is called time domain OCT as time-encoded signals are obtained directly (Gabriele et al., 2011).

Time domain OCT technology was superseded by Fourier-domain OCT systems which measure the interference pattern via a Fourier transformation to acquire all points along the depth of the a-scan rapidly without using reference arm movement. This is completed by assessing the space on a spectrometer using a broadband light source (SD-OCT) (See Figure 1.11) or via time during the wavelength sweep of a narrow bandwidth source (SS-OCT) (Murthy et al., 2016; Nassif et al., 2004). As a result, Fourier-domain OCT systems yield high quality images of retinal tissue with resolution up to one-to-two millimetres deep (Kalkman, 2017) at a faster rate of acquisition and improved axial resolution from $\sim 10\mu\text{m}$ to up to $2\mu\text{m}$ (but $\sim 5\text{-}6\mu\text{m}$ is standard) (See Figure 1.12) (Gabriele et al., 2011).

Advancements in OCT technology means volumetric 3D imaging is feasible, giving a greater understanding into structural abnormalities of retinal disease. However, despite the introduction of these more advanced OCT systems with better imaging processing capabilities, severe segmentation errors can still occur resulting in unreliable retinal thickness measurement, particularly in patients with complicated structural abnormalities like PED (Sadda et al., 2009).

As SD-OCT is the only method used in this thesis, explanations will be limited to this type. For a review of the development and impact of OCT, see Fujimoto and Swanson (2016). The SD-OCT devices used in the studies described in this thesis are Heidelberg Spectralis SD-OCT (Heidelberg Engineering, Heidelberg, Germany).

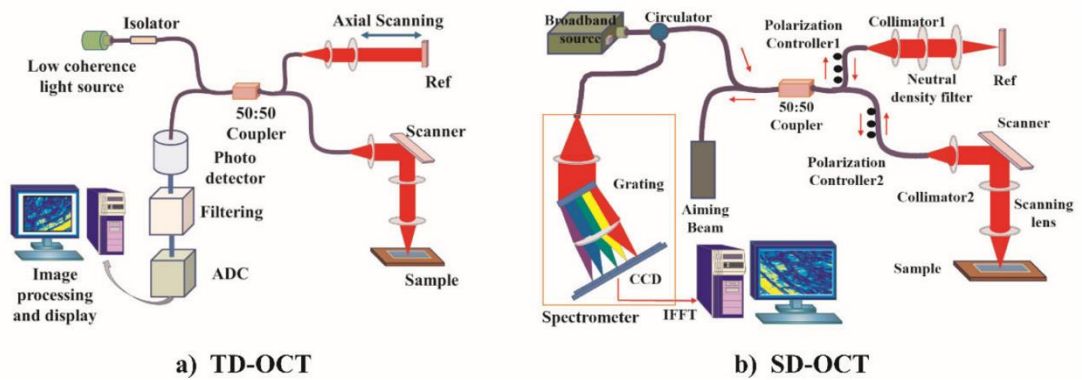


Figure 1.11 Panel A features a diagram for time-domain OCT while panel B features a diagram of spectral-domain OCT. Sourced from Wang et al. (2022).

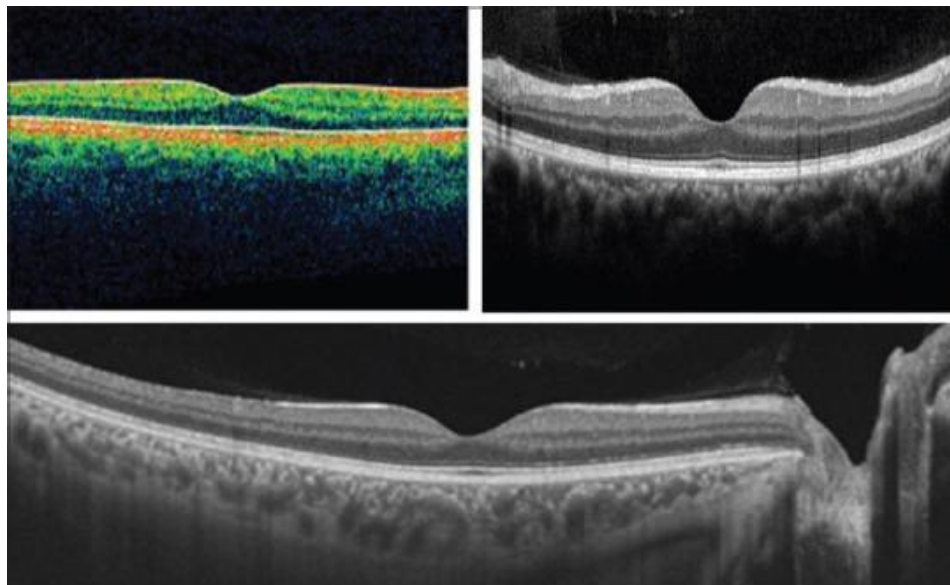


Figure 1.12 Images from a time-domain OCT (top-left), SD-OCT (top-right) and SS-OCT (bottom). Note the differences in resolution achieved the Fourier-domain OCT systems. Sourced from Bhende et al. (2018).

As OCT offers a tomographic view of the retina, the presence of drusen are shown via dome-shaped distortions of the retinal strata (see Figure 1.13). Drusen can appear with varying levels of reflectivity, depending upon the material beneath them (Keane et al., 2012). Hyperreflective regions can also be sometimes seen in conjunction with drusen, believed to be due to resultant changes in the surrounding retinal layers above (Schuman et al., 2009). Aside from classic drusen, OCT is the method of choice to identify and categorise SDDs (see section 1.1.4.1). Through the use of OCT, it was determined that SDDs occur in subretinal space between the RPE and photoreceptor layers and the granular hyperreflective material corresponds with SDDs seen with different imaging modalities

(Zweifel et al., 2010). Furthermore, SD-OCT has confirmed photoreceptor layer thinning over drusen in vivo in eyes with non-neovascular AMD (Schuman et al., 2009), correlating with previous histopathological investigations (Curcio, Medeiros and Millican, 1996).

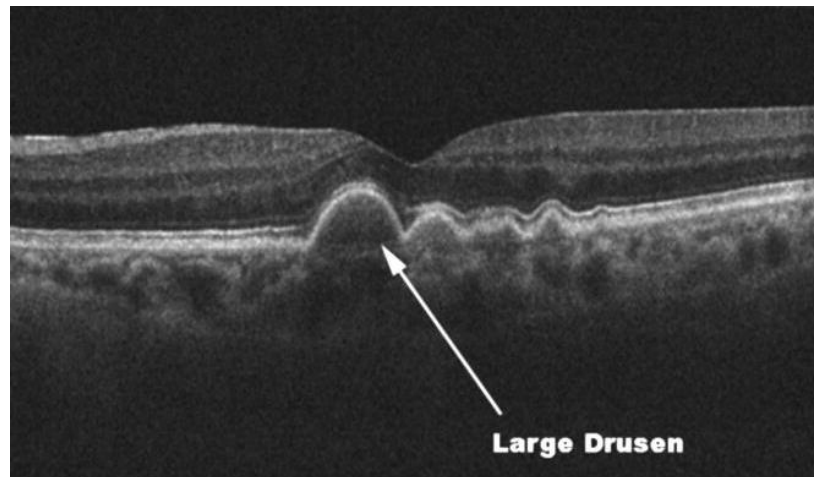


Figure 1.13 An OCT image (Cirrus HD-OCT; Carl Zeiss Meditec), showing a large druse, visible as a large dome RPE-elevation. Sourced from Keane et al. (2012).

1.6.3 Optical Coherence Tomography versus Colour Fundus Photography

A number of studies have compared imaging modalities and concluded good agreement between SD-OCT and CFP with respect to drusen evaluation (Jain et al., 2010; Rosenfeld et al., 2011). However, Jain et al. (2010) found that SD-OCT had increased sensitivity in detecting SDD presence in people with later stage AMD compared to CFP. SD-OCT allows for the quantitative and reproducible assessment of AMD and allows for automated measurement of drusen area and volume (problematic with CFP) (Kanagasingam et al., 2014). Yet, Jain et al. (2010) found CFP to be better at detecting smaller drusen, while producing precise delineation of drusen borders still proves difficult for both. Furthermore, as OCT is still relatively new, image interpretation can be difficult (due to lack of formal training and multifaceted phenotypes seen on OCT images) (Joeres et al., 2007; Keane et al., 2012). Therefore, CFP is still useful in screening for early AMD (Kanagasingam et al., 2014). A multimodal approach to imaging AMD appears to be the most sensible solution given both device's strengths and limitations (Kanagasingam et al., 2014). For a considered review of retinal imaging analysis in AMD and comparisons between modalities, see Kanagasingam et al. (2014).

1.6.4 Other imaging modalities

Other imaging modalities are found in AMD research, despite being beyond the scope of this thesis, they will be described in brief. Such examples include fluorescein angiography and FAF. Fluorescein angiography was first introduced in the early 1960s and remains a key tool in the diagnosis of retinal disorders. Fluorescein angiography is performed by injecting fluorescein sodium dye into a vein. Fluorescein sodium fluoresces when exposed to blue light (465-490nm) and results in fluorescence at yellow-green wavelengths (520-530nm). A fundus camera or scanning laser ophthalmoscope is then used to capture an image of the eye (See Figure 1.14). Fluorescein angiography offers insights into the presence, activity, and severity of retinal disease not immediately apparent via clinical examination alone (Patel & Kiss, 2014), particularly exudative lesions in neovascular AMD (Tomi & Marin, 2014).

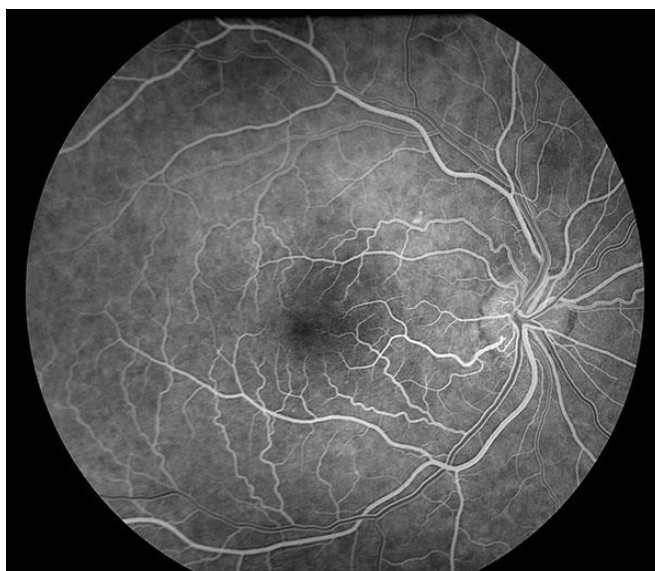


Figure 1.14 A fluorescein angiogram image of a normal fundus in early venous phase, showing the fluoresceine dye beginning to fill the veins. Accessed from The University of Iowa.

Unlike fluorescein angiography, FAF does not need contrast dye but instead uses the natural fluorescent properties of lipofuscin within the RPE. Lipofuscin is a by-product of the phagocytosis of distal segments of photoreceptors by RPE cells. Lipofuscin absorbs blue light (peak of 470nm) and as a result fluoresces yellow-green light with a peak of 600nm. As RPE dysfunction is characteristic of AMD impairment and progression, changes in levels of lipofuscin can be detected and monitored with FAF thus can be used as a marker for the disease (See Figure 1.15) (Bhagat, 2021).

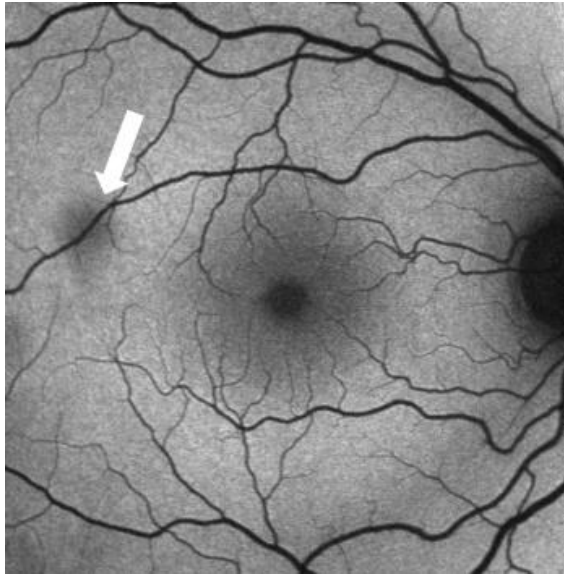


Figure 1.15 A blue light short-wavelength FAF image of normal fundus. The arrow indicates an artefact from a vitreous opacity. Sourced from Bhagat (2021).

1.7 ASSESSING VISUAL FUNCTION IN AGE-RELATED MACULAR DEGENERATION

1.7.1 Visual Acuity

Visual acuity forms an integral component of vision assessment and screening for all ocular pathology. Simply put, VA is the ability to resolve detail at a high level of contrast. Since 1862, the high contrast letter Snellen chart has adorned optometrist's walls, yet there are established limitations of the chart such as uneven crowding effects and steps in acuity between lines, and different numbers of letters on each line (McGraw, Winn and Whitaker, 1995). This led to the development of charts that follow geometric progression (the optotypes size changes in logarithmic steps) (Holladay, 2004) such as the Early Treatment Diabetic Retinopathy Study (ETDRS) (Ferris et al., 1982) and Bailey–Lovie charts (Bailey & Lovie, 1976) (see Figure 1.16). These charts utilise recognition acuity as they rely on the examinee to recognise the optotypes presented (Heinrich & Bach, 2013). Their main advantages over the traditional Snellen charts are that their design standardises crowding effects between lines by having the same numbers of optotypes per line, equal spacing between letters and lines (proportional to letter size), and equal steps between lines. The log minimum angle of resolution (logMAR) and letter by letter scoring methods used within these charts can be readily statistically analysed, compared to the complex Snellen fractions. These charts are now standard in research but have not been universally adopted into clinics, perhaps due to the unfamiliar scoring system (Lim et al., 2009).

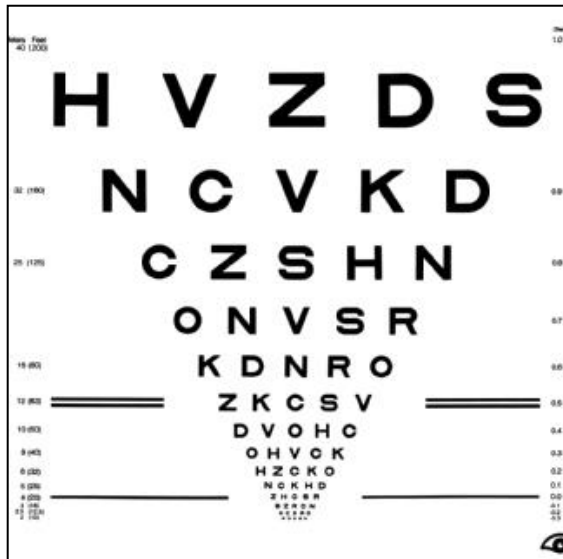


Figure 1.16 An ETDRS chart Image from National Eye Institute, National Institutes of Health.

Visual acuity is a frequently used measure of visual function in AMD research including in clinical trials. This is despite the fact that VA has been shown to be poor at distinguishing between healthy controls and the different severity levels of AMD prior to the onset of late-stage manifestations (Owsley, Clark, et al., 2016). In early AMD, incremental decreases in VA may be disguised by its wide test-retest variability while, in late AMD, VA yields limited information about GA status (Hogg & Chakravarthy, 2006). Furthermore, longitudinal studies have found VA to be a poor predictor of progression into wet AMD (Mayer et al., 1994). Yet, VA will likely continue to be used in research and in low vision clinic due to its ease and widespread availability. Furthermore, NICE guidelines for anti-VEGF therapy eligibility are based on VA metrics (6/12-6/96), hence VA forms an important aspect of clinical decision making (NICE Recommendations for Age-Related Macular Degeneration NG82, 2018).

1.7.2 Contrast Sensitivity

Contrast refers to the light-dark transition of an edge of an image. CS describes the ability to resolve a target at varying levels of contrast (Owsley, 2003). Measurement of a CS function evaluates the contrast threshold at different spatial frequencies (See Figure 1.17). VA is analogous to the high spatial frequency cut off of the CS function i.e. the minimum spatial frequency resolvable at maximum contrast. The CS function is considered a more well-rounded assessment of visual function as it assesses visual ability across the whole range of spatial frequency channels rather than at a single point. However, it is time consuming to evaluate and in a clinical setting, like VA, CS is measured via chart-based assessments, either with wave-gratings or letters. This does not provide full information

about the CS function but, alongside VA, does at least provide an extra point of reference with respect to spatial vision. Examples of charts that use gratings are Arden's Gratings (Arden & Jacobson, 1978) and the Cambridge Low Contrast Gratings (Langdon et al., 1988). The most popular chart favoured by both researchers and clinicians is the Pelli-Robson chart (Pelli, Robson and Wilkins, 1988) which uses letters (see Figure 1.18). For a thorough review of CS, see Owsley (2003).

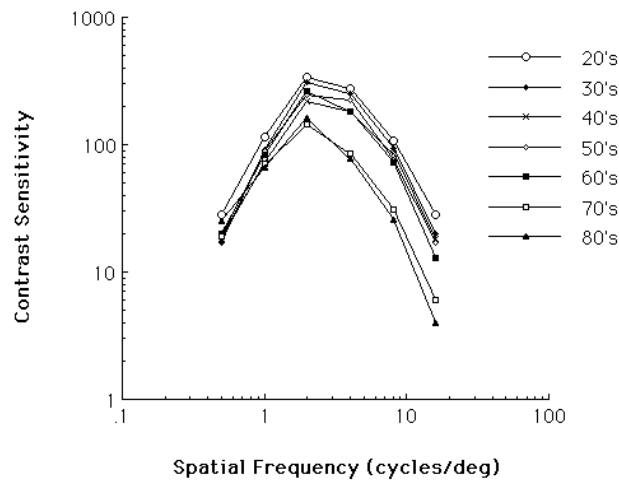


Figure 1.17 CS functions of seven different age groups. Sourced from Schieber (1992).

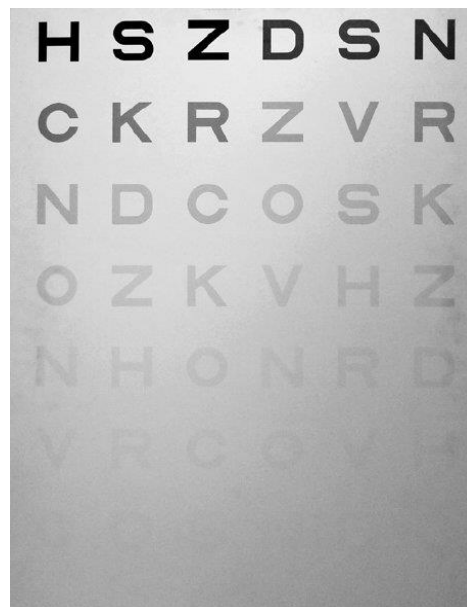


Figure 1.18 Pelli-Robson CS chart. Sourced from Parede et al. (2013).

Compared to VA, CS assessed to moderate spatial frequencies correlates better with ability to perform everyday visual activities like driving (Owsley & McGwin, 2010) walking (Geruschat, Turano and Stahl,

1998), and the ability to recognize faces (West et al., 2002). Lateral inhibition due to the centre-surround antagonism within receptive fields in the visual pathway forms the neurophysiological basis for CS. For a review of the literature on CS assessment in people with AMD, see Hogg and Chakravarthy (2006). Hogg and Chakravarthy (2006) hypothesise that the reason why CS may be reduced in AMD is may be due to a reduction in photopigment which would result in a reduction in quantum catch ability of photoreceptors. In an early study by Sjöstrand and Frisén (1977) it was established that 11 people with various causes of macular impairment (e.g. AMD, macular oedema and diabetic retinopathy) aged 19-78 years had impaired CS across all spatial frequencies investigated using sinusoidal gratings compared to 10 healthy controls aged 19-61 years. The varying degree of severity and different causes of macular impairment featured in this study makes it hard to apply these results across AMD population as a whole. Moreover, the participants appear to have advanced macular impairment hence it is unsurprising that visual loss might be extensive. GA has been noted to be associated with significantly reduced CS in a longitudinal study of two years by Sunness et al. (1997) in 74 eyes with late non-neovascular AMD. There are inconsistent findings supporting a link between reduced early and intermediate stage AMD and CS, with some groups finding a difference between these stages of AMD and healthy controls in photopic (Feigl et al., 2004; Lott et al., 2021) and mesopic conditions (Maynard, Zele and Feigl, 2016), while others have not (Owsley, Huisingh, et al., 2016). Up until recently there were no reports of assessing the full CS function under both photopic and mesopic conditions in people with early and intermediate stage AMD. However, a recent study by Ridder et al. (2022) assessed the difference of CS performance in 24 people with early and intermediate stage AMD (mean age [SD] 76 [7] years) and 25 healthy controls (mean age [SD] 73 [7] years) under different lighting conditions. No difference was found in the mesopic or photopic CS condition between people with early AMD and 25 controls, although the authors did report people with iAMD had significantly reduced CS compared to controls using the mesopic conditions. Unfortunately, demographic details were given for the whole AMD group rather than indicating characteristics per severity group.

Contrast sensitivity can be limited by a range of conditions, including cataracts and media opacities which are very common in older adults. Thus, it is difficult to separate the AMD effects from other conditions (similar to colour vision). Yet, like VA, as CS tests are easy to conduct and low-cost, their use will likely continue. Both have been used as outcome measures in interventional studies which allows comparison of the two functional measures. For example, in a two-year longitudinal study, Bellmann et al. (2003) found changes in VA and CS do not consistently show the same progression in vision loss, indicating both as independent and important to continue, including in trials.

1.7.3 Microperimetry

The healthy visual field extends 70° superiorly, 80° inferiorly, 60° nasally and 100° temporally. The sensitivity to stimuli presented in the visual field increases from the periphery to the centre, peaking at the fovea. As mentioned previously, AMD is associated with loss of rods in the parafoveal region (Curcio, Medeiros and Millican, 1996). Perimetry is a comprehensive functional assessment of various points of the visual field and can be used in mesopic and scotopic conditions. In spite of this, in most cases clinicians continue to monitor AMD impairment using visual assessments that are dominated by cone function i.e. in photopic or mesopic conditions (Midena & Pilotto, 2017). For an overview of microperimetry in AMD research, see Midena and Pilotto (2017).

When a static perimetric test is carried out, the participant fixates on a central target while stimuli are presented in different locations at variable intensity to assess the detection threshold at specific points in the visual field. Thresholds are reported in decibels (dB), and are presented graphically in numerous ways, including grey scale plots indicating areas of reduced sensitivity in darker tones, total deviation plots indicating the deviation of the threshold at each point from that of age-matched controls, pattern deviation plots, and pseudo-colour maps indicating regions of elevated threshold (above normal range for age) (see Fig 1.19). Reliability checks for perimetry data are conducted as part of good clinical practice. These include checking for fixation losses, whereby a fixation loss of $\geq 30\%$ are considered likely inaccurate and the test may need to be repeated. Another example is if 95% Bivariate Contour Ellipse Area (BCEA) value is greater than 50 deg², the test may be inaccurate.

There are different types of static perimetry (e.g., standard automated perimetry), but the type focused on and utilised in this thesis will be microperimetry. Microperimetry (also known as fundus automated perimetry) has the advantage over standard automated perimetry by utilising tracking technology to compensate for eye movements to enable stimuli to be presented to precise retinal locations. This occurs by establishing the Preferred Retinal Locus (PRL) for fixation and although most of the times it is near the fovea, in people with impaired visual fields, this location can be altered (Greenstein et al., 2008). Hence, microperimetry can account for undesirable eye movements in people with AMD that may be attributable to fixation instability, a potential result of macular damage. There are various commercially available microperimeters, such as the S-MAIA microperimeter (Macular Integrity Assessment; CenterVue, Padova, Italy), used in the studies featured in this programme of work described in Chapter 5. In addition, the introduction of mesopic and more recently scotopic microperimetry (Crossland et al., 2011) allows enhanced testing of rod photoreceptors.

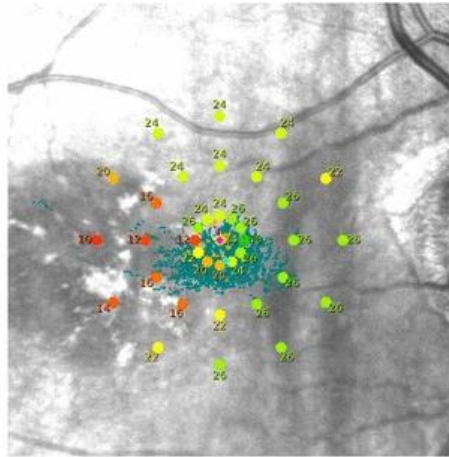


Figure 1.19 Image from MAIA microperimeter report. Green colour indicate normal values while red indicate abnormal. The dark green dots indicate participant fixation which was relatively unstable. Adapted from Estudillo et al. (2017).

The microperimeter output provides a map of threshold overlaid on the central fundus image. Precise correlation between AMD macular pathology and analogous functional impairment (Ratra et al., 2012) makes microperimetry an excellent tool to assess the structural-functional relationship in AMD. Impairment of retinal sensitivity has been evidenced to develop earlier than measurable VA changes (Midea et al., 2007). As a result, microperimetry has been shown to detect longitudinal changes in sensitivity in early AMD when VA remained stable (Wu et al., 2015). These changes were found mainly localised in the parafoveal region known to be susceptible to photoreceptor loss (Curcio, Medeiros and Millican, 1996). Presence of SDDs has been shown to correlate with a reduction of mean retinal sensitivity, confined to the macular area (Ooto et al., 2013). Scotomas associated with later stage AMD can similarly be identified via microperimetry. The assessment of fixation stability and PRL enabled by microperimetry also has clinical value when assisting patients to adapt to visual loss. For example, Sunness et al. (1996) investigated fixation patterns in 41 people with AMD who had central scotomas using microperimetry and found a preference for the PRL to be to the left of the scotoma (believed to be reading-driven), followed by below the scotoma (cortex-driven). The process of eccentric viewing training may be guided by an understanding of the PRL adopted by participants in studies such as these (Gaffney et al., 2014).

1.7.4 Dark Adaptation

Dark adaptation is the recovery of photoreceptor sensitivity to stimuli after a large proportion of visual pigment has been bleached by a high intensity light source (Owsley et al., 2007) and is the key assessment of visual function in this thesis. DA can be measured in both photoreceptor types, but this thesis will focus on RMDA. DA relies upon the biological mechanisms featured in visual cycle (see

section 1.1.2.1), which in turn are dependent on the function of photoreceptors, BM, choroid and, above all, RPE. DA influences the capacity of the visual system to adjust to light level changes, which can have a significant impact on an individual's ability to perform daily activities e.g. turning on a bedside lamp in the middle of the night and struggling to see to get to the bathroom (Yazdanie et al., 2017).

Measuring DA can likely be traced back to the 19th century, when Aubert (1865) first assessed DA using the glow of a just visible platinum wire as a stimulus. Developments have since been made; from the early DA curves plotted by Hecht, Haig and Chase (1937) to the landmark mathematical model of DA by Lamb and Pugh (2004). For a review of the history of DA literature from 1961-2011, see Reuter (2011). Specifically designed dark adaptometers are now used to investigate DA and have been instrumental in assessing the phenomenon in people with AMD. For example, the adapted Humphrey Visual Field Perimeter (HVFP; Carl Zeiss Meditec, Inc, Dublin, California, USA), the Medmont Dark Adapted Chromatic perimeter (MDAC; Medmont Pty Ltd, Melbourne, Australia) and the AdaptDx.

The AdaptDx is commercially available and since the protocol was first introduced by (Jackson & Edwards, 2008), its use to assess RMDA is prevalent in the literature studies (Jackson and Edwards, 2008; Clark et al., 2011; Jackson, Clark, et al., 2014; Jackson, Scott, et al., 2014; Flamendorf et al., 2015; Owsley, Clark, et al., 2016; Owsley, Huisingh, et al., 2016; Owsley, McGwin, et al., 2016; Sevilla et al., 2016; Neely et al., 2017; Laíns et al., 2017; Owsley, Clark and McGwin, 2017; Yazdanie et al., 2017; Binns et al., 2018; Cocce et al., 2018; Laíns, Miller et al., 2018; Laíns, Park, et al., 2018; Thompson et al., 2018; Beirne and McConnell, 2019; Chen et al., 2019; Mullins et al., 2019). The AdaptDx measures the RIT. The RIT is defined as the time taken for retinal sensitivity to recover to reach a threshold located within the second component of rod recovery (i.e. 5×10^{-3} scotopic cd/m² [3 log units of stimulus attenuation]). The AdaptDx is used in the studies described in this programme of work (See Figure 1.20). See section 1.5 for a dedicated systematic review of current literature regarding DA and AMD.



Figure 1.20 Image of AdaptDx. Accessed from Maculogix (www.maculogix.com)

1.7.4.1 Measuring Dark Adaptation using the AdaptDx

There is some debate as to whether pre-adapting participants is a necessary step in the AdaptDx DA procedure. There is no explicit guidance to pre-adapt participants as the general assumption is that after the bleaching flash all participants will receive the same level of photopigment bleach. However, Binns et al. (2018) found that for lower intensity bleaching the previous adaptation state of the patient was significant, and so a pre-adaptation period of 30 minutes was introduced.

As DA is a scotopic assessment, the assessment must take place in a totally dark room (See Figure 1.21). In an effort to prevent any stray light from hampering the dark adapting session, a red filter is used on the AdaptDx touch screen. Briefly, the non-study eye is patched and the participant is asked by the examiner to focus on the red fixation light and is told that a bleaching light flash will occur. They are asked to press the response button whenever this blue-green stimuli becomes visible. Then there is brief practice session whereby a low intensity bleach is presented and the patient can carry out the test until the examiner is confident that they have grasped the instructions. To standardise retinal illumination during the testing procedure, the AdaptDx automatically calculates pupil size and accounts for this in retinal illuminance calculations. The participant is advised to ensure throughout the assessment they remain fixated on the red fixation light.

The study eye is bleached using a flash 0.25ms in duration at a retinal location subtending 4° and centred at either 5° or 12° inferiorly in the vertical meridian. The location of the flash is also the location of the test target. The strength of this flash is dependent upon the desired percentage of bleaching the photoreceptors receive. For example, a bleaching flash intensity of 1.8×10^4 scotopic cd/m²s results in an equivalent rhodopsin bleach of approximately 76%, while a flash of 5.8×10^4 scotopic cd/m²s intensity produces an equivalent bleach of 82-83% (Pugh, 1975a, 1975b). Binns et al. (2018) recently compared different bleaching protocols in people with and without AMD (65%, 70% and 76% equivalent rhodopsin bleach at either 5° or 12° inferior field). It was concluded that 76% bleach at 12° eccentricity allowed for separation between groups in the sample and reduced recovery time to under 20 minutes, compared to a more extended recovery times in the 5° location.

The stimulus for the threshold measurement (the blue/green spot) is a 2° diameter, 500nm circular target which begins 15 seconds after the bleaching. The initial stimulus presentation starts at 1 log units of stimulus attenuation. Log thresholds are expressed as sensitivity in log units of attenuation as a function of time from bleaching offset and are estimated using a modified, 3-down-1-up staircase procedure. The test continues until either the RIT is obtained, or the test protocol ends, whichever first occurs. When the RIT is not obtained within the test duration, a capped value of the total duration of the test can be assigned for analysis (e.g. 20 minutes). Alternatively, some studies utilise the estimated recovery time based on the observed trend up to the maximum recording time. However, when the parameter cannot be extrapolated, it usually is again set to the experimental cut-off time (Jackson, Scott et al, 2014) Conversely, Owsley et al. (2017) has reported setting the unknown RIT

value to 'indeterminate' rather than allocate an estimated RIT. Consequently, RIT data represents a challenge for statistical analysis. Many authors use standard statistical approaches to analyse groups of RIT values such as a student's t-test (Owsley et al., 2014; Owsley, Huisingh, et al., 2016; Owsley, McGwin, et al., 2016; Laíns et al., 2017; Cocce et al., 2018; Laíns, Park, et al., 2018) or non-parametric equivalents (Jackson, Clark, et al., 2014; Jackson, Scott, et al., 2014; Flamendorf et al., 2015; Owsley, Clark and McGwin, 2017). However, the t-test may not be appropriate when capping distorts the distribution of data. Furthermore, the value of non-parametric tests is limited by their relative lack of power and inability to generate CI (see Chapter 3 for an alternative method of assessing RIT data).

The originally published AdaptDx test duration was 20 minutes or when the RIT is reached (Jackson & Edwards, 2008), and a subsequent modified protocol suggests an even shorter cut off at 6.5 minutes (Jackson, Scott, et al., 2014). However, both protocols were developed as diagnostic tests, whereby patients who fail to reach a RIT within a pre-specified test duration are considered to have abnormal rod mediated DA. Many people with delayed DA due to AMD fail to reach the rod intercept within the test time therefore, whilst this has value as a diagnostic test, it is limiting in terms of a test monitoring patients over time and an extended test duration is required to obtain an actual value for the RIT. For example, Owsley et al. (2017) found some people with iAMD required ~100 minutes to reach the RIT.

The AdaptDx device records the percentage of threshold points which indicate a fixation error (determined as points where the change in threshold from one threshold to the next is physiologically implausible). If fixation errors exceed 30%, previous studies have tended to deem the test unreliable and to exclude from analysis (Jackson, Scott, et al., 2014).

The AdaptDx has been described in the literature as having high levels of diagnostic sensitivity and specificity (Jackson, Scott, et al., 2014) when comparing healthy controls and people with AMD. Jackson, Scott, et al. (2014) reported results for 127 people with AMD and 21 visually healthy people. Using an RIT of ≤ 6.5 minutes as the threshold for being test negative; the AdaptDx yielded a sensitivity of 91% and a specificity of 91%. However, 14 people could reportedly not do the examination. This bias is noteworthy as authors did not include this in their estimates of diagnostic precision. Furthermore, the small sample of controls meant that the lower bound of the 95% CI for specificity was ~70%. For a detailed assessment of diagnostic precision of the AdaptDx featured in recent literature (see Chapter 2).

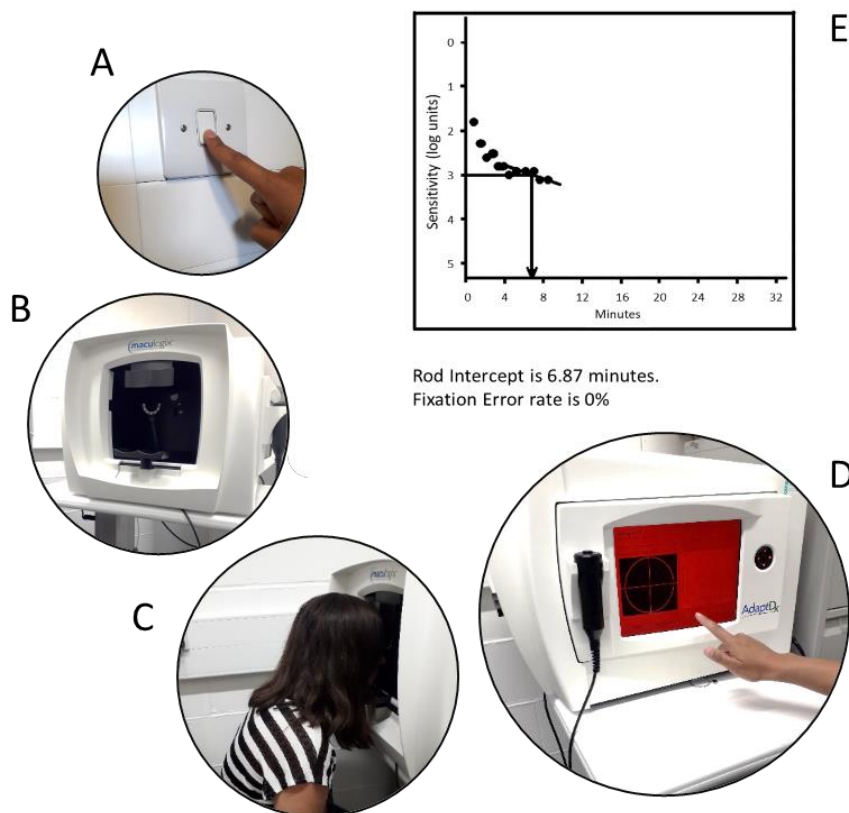


Figure 1.21 Diagram of setting up for the AdaptDx testing procedure. Anticlockwise: A. Assessment must take place in scotopic conditions (with or without a period of pre adaptation, as discussed above). B. AdaptDx machine has a chinrest that participant is instructed to place their chin on and given the response button to press when they see the stimuli. C. Participant is instructed to fixate on the fixation cross. D. Examiner uses the red filter on the AdaptDx to reduce stray light and ensures the bleach will be given to the correct location on the retina. E. The AdaptDx produces a DA curve, indicating the RIT and fixation errors. Note: Images were taken under photopic conditions for ease of photography, the assessment is conducted in scotopic conditions. Source: Author's own.

1.7.5 Other Measures of Visual Function

There are other examples of psychophysical assessments that have been investigated in people with AMD which are not the topic of this thesis. Such measurements have been reviewed by Hogg and Chakravarthy (2006). Examples include assessing chromatic sensitivity in people with AMD, which have found to illustrate a loss in yellow/blue discrimination (O'Neill-Biba et al., 2010). A further example includes sensitivity to flickering stimuli, for example Phipps et al. (2004) concluded flicker sensitivity to be reduced in the early stages of AMD. Lastly, electrophysiological measurements of visual function will not be explored in this thesis but provide an interesting avenue of AMD research. An example includes electroretinograms (ERG) which offer an objective method to assess the retina (Seiple et al., 1986). Impairments in full-field ERG have been reported in people with AMD (Walter et

al., 1999), however other studies have found the full-field ERG to be relatively insensitive to the localised dysfunction associated with AMD (Holopigian et al., 1997; Sunness et al., 1985). Multifocal ERGs and focal ERGs which selectively assess macular function are likely to be a more promising avenue for visual function assessment in AMD (Binns & Margrain, 2007; Gerth, 2009; Moschos & Nitoda, 2018).

1.8 DARK ADAPTATION AND AGE-RELATED MACULAR DEGENERATION

1.8.1 An Overview

The rate of DA is dependent on the rate of rhodopsin regeneration in photoreceptors, which in turn is dependent upon the choroidal circulation, BM, and, crucially, the RPE's functional integrity (Lamb & Pugh, 2004). Early AMD is characterised by a thickening and reduced permeability of BM (Curcio & Johnson, 2012), as well a reduced density of choroidal vessels and decreased choroidal blood flow (Grunwald et al., 2005), which together are likely to impact on the supply of metabolites to the outer retina necessary to support the visual cycle. Furthermore, the RPE, which is the site of the critical enzymatic conversion of bleached all-trans retinal to the 11-cis configuration (Lamb & Pugh, 2004), is also believed to be at the centre of the AMD disease mechanism (Ambati & Fowler, 2012). Therefore, it is unsurprising that DA has been proposed as a functional biomarker for AMD (Owsley, McGwin, et al., 2016). DA has been found to be delayed in people with AMD compared to their visually healthy counterparts (Jackson and Edwards, 2008; Clark et al., 2011; Jackson, Clark, et al., 2014; Jackson, Scott, et al., 2014; Flamendorf et al., 2015; Owsley, Clark, et al., 2016; Owsley, Huisingh, et al., 2016; Owsley, McGwin, et al., 2016; Láins et al., 2017; Yazdanie et al., 2017; Binns et al., 2018; Cocce et al., 2018; Láins, Miller, et al., 2018; Beirne and McConnell, 2019; Chen et al., 2019; Mullins et al., 2019). This is also reflected in the common complaint of poor night vision in people with AMD (Ying et al., 2008). Despite VA being the gold standard in psychophysical testing, under photopic conditions it is unaffected in earlier stages of AMD. Yet, DA has been reported as delayed in people with AMD before other metrics of visual dysfunction can be measured (Dimitrov et al., 2011; Owsley et al., 2001; Ying et al., 2008).

The localised lack of availability of 11-cis retinal associated with AMD has been hypothesised to impact rod adaptation more than cones as they preferentially rely on vitamin A to be supplied from the RPE and choroid while cones also source from an intraretinal supply via Muller cells (Owsley, McGwin, et al., 2016). However, cone adaptation has also been shown to be delayed in AMD despite the different mechanism of visual pigment regeneration (Phipps, Guymer and Vingrys, 2003; Dimitrov et al., 2008; Gaffney, Binns and Margrain, 2013); and has been proposed as a more clinically viable means of assessment of adaptational deficits in AMD as cone adaptation proceeds relatively more rapidly than

that of rods and so may be assessed in a shorter timeframe. The photostress test is one means of rapidly assessing cone adaptation, whereby the time taken for cone function (usually assessed using VA) to return to a pre bleach level is assessed after exposure to a bright adapting light (Margrain & Thomson, 2002).

Owsley et al. (2001) examined rod-mediated kinetics of DA in 20 people with early AMD compared to 16 older controls using a modified Humphrey Field Analyzer (Zeiss Humphrey Systems, Dublin, CA). They assessed sensitivity at 12° on the vertical meridian in the inferior visual field following a 98% bleaching flash. This test location was chosen as it has been demonstrated to suffer from photoreceptor loss in the earliest stages of AMD (Curcio, Medeiros and Millican, 1996). They reported that people with early AMD showed statistically significant delays in almost all parameters of rod mediated DA (Owsley et al., 2001). Importantly, it was also found that individuals were more likely to fall outside the normal reference range for kinetic measures of adaptation rates, than for steady state measures of sensitivity. For example, 85% of people with early AMD had at least one abnormal DA kinetic parameter, whereas this figure was only 25% with respect to steady-state scotopic sensitivity. Ergo, this data supported the hypothesis that people with AMD exhibit slowed visual cycle as abnormal modifications in the BM-RPE complex may lead to a reduction of 11-cis-retinal to the photoreceptors (Curcio, Owsley and Jackson, 2000). Several years later, Owsley et al. compared the impairment of cone and RMDA using the same methodology in 83 older adults with AMD (ranging from early to advanced) and 43 controls (Owsley et al., 2007). This study evidenced that RMDA was reduced more than cone-mediated DA in people with AMD compared to visually healthy controls. Moreover, the data revealed parameters of RMDA worsened as AMD severity increased. This study was the first to simultaneously assess both cone and rod-mediated parameters of DA at the same retinal location. Dimitrov et al. (2008) developed a novel cathode-ray-tube monitor-based technique to assess both rod and cone-mediated DA in 27 people with AMD and 22 age-matched controls at a 4° central location. Authors reported both slowed cone and rod recovery and a delayed rod-cone-break (RCB) in eyes with AMD. This study highlighted that cone recovery can also be used as an indicator of AMD with a high level of diagnostic accuracy according to receiver operator characteristic assessment (ROC) (area under the curve [AUC]; 0.98 ± 0.01), compared to rod recovery (AUC, 0.92 ± 0.04). The authors also indicate that their modest bleaching level (30%) and the length of the test (30 minutes) makes it suitable for clinical application (Dimitrov et al., 2008).

More recently, technology has advanced such that DA testing can be conducted rapidly in people with AMD (≤ 6.5 minutes), whereas the procedure was previously plagued by long testing times (Jackson, Scott et al., 2014). This shortening of test time makes the assessment easier to include in a battery of tests in clinical trials alongside other scotopic assessments (Finger et al., 2019), and indeed allows it to become clinically practical. Furthermore, advancements in genotyping technology have allowed correlations to be assessed between functional tests such as DA and known genes associated with AMD. For example, Mullins et al. (2019) reported a novel association wherein older adults with no

evidence of AMD but who had high-risk ARMS2 genotype were more likely to demonstrate delayed RIT, where those who had the high risk CFH genotype did not show delays. However, the presence of the high risk CFH genotype was associated with delayed RIT in people with AMD. For a full review of functional and structural correlations with DA in people with AMD (see Chapter 2).

1.8.2 Metrics of Dark Adaptation in Age-Related Macular Degeneration

Classic results from Hecht et al. (1937) (Figure 1.22) illustrate the visual thresholds of a healthy eye measured following five different intensities of bleaching. A biphasic curve of recovery of visual sensitivity can be seen when a large proportion of the visual pigment has been bleached. DA curves are characterised by a rapid cone recovery phase followed by a plateau, in turn followed by two slower rod recovery phases (S2 and S3), followed by a final plateau reflecting the absolute threshold of the eye when fully dark adapted (Lamb & Pugh, 2004). The time at which the cone recovery ends and the rod recovery begins is called the RCB. Classically, mathematical modelling of the cone and rod components of the DA function has employed two exponential functions to describe the two components (Hollins & Alpern, 1973). More recent models have described rod recovery using three linear components (S1-S3) (Leibrock, Reuter and Lamb, 1998; McGwin, Jackson and Owsley, 1999), where S1 is obscured by the cone branch of the DA function. Metrics of cone DA reported in the literature include cone absolute threshold (Owsley, McGwin, Jackson, et al., 2006; Owsley, McGwin, Scilley et al., 2006; Owsley et al., 2007; Dimitrov et al., 2008, 2011; Gaffney, Binns and Margrain, 2011, 2013; Tahir et al., 2018), and exponential cone time constant (Owsley, McGwin, Jackson, et al., 2006; Owsley, McGwin, Scilley, et al., 2006; Owsley et al., 2007; Gaffney, Binns and Margrain, 2011, 2013; Grant Robinson et al., 2019; Rodrigo-Diaz et al., 2019), whilst more recent analysis has suggested that cone DA is better described by the ‘maximum rate’ parameter of a model based on Michaelis Menton kinetics (Mahroo & Lamb, 2004; Paupoo et al., 2000). For a full review of mathematical models applied to DA curves, see Lamb and Pugh (2004).

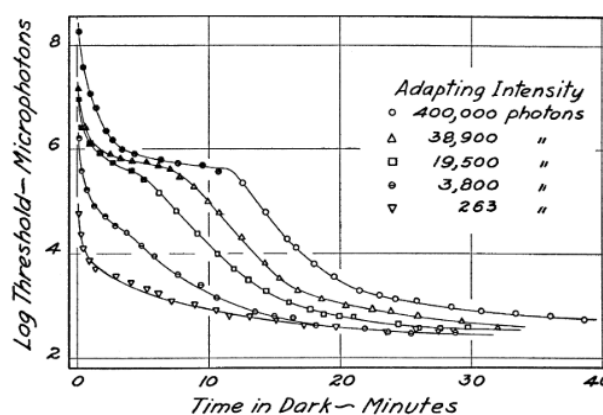


Figure 1.22 DA curves for healthy eye. Sourced from Hecht, Haig and Chase (1937).

A rightward shift can be seen in the DA curves of elderly eyes as DA takes longer with increasing age (Owsley et al., 2001). This is believed to be due to changes in the BM–RPE complex which leads to a reduction of 11-cis-retinal to the photoreceptors and hence a slowed visual cycle. However, this rightward shift is exacerbated in AMD eyes which exhibit thickening of BM/reduced choroidal blood flow and RPE dysfunction (Owsley et al., 2001). See Figure 1.23. This is reflected in longer recovery time or shallower gradients of rod components S2 and S3, fitted using Lamb’s linear model (Owsley et al., 2001, 2007; Dimitrov et al., 2008). Elevated cone and rod final thresholds are also noted in people with AMD, which may be attributable to photoreceptor loss or dysfunction (Owsley et al., 2001). For example, in a study by Clark et al. (2011) 57 people with non-neovascular AMD and 17 people without AMD using the Clinical Age- Related Maculopathy Staging (CARMS) system were assessed for differences in both DA and retinal thickness. DA data were fitted with a biological model of RMDA and the authors measured the slopes of the second and third components of recovery, final threshold recorded during the 20 minute test period, and ‘mean threshold’ (the average of all thresholds after 300 seconds post bleach). The authors concluded that retinal thinning was associated with reductions in mean threshold and final threshold even after adjustment for covariates such as age and VA. The time to the RCB can also be assessed. A delayed RCB has been reported in AMD, which is indicative of DA impairment (Jackson, Felix, & Owsley, 2006; Owsley, McGwin, Jackson, et al., 2006; Owsley, McGwin, Scilley et al., 2006; Owsley et al., 2007; Dimitrov et al., 2008, 2011; Gaffney, Binns and Margrain, 2011, 2013; Tahir et al., 2018; Rodrigo-Diaz et al., 2019).

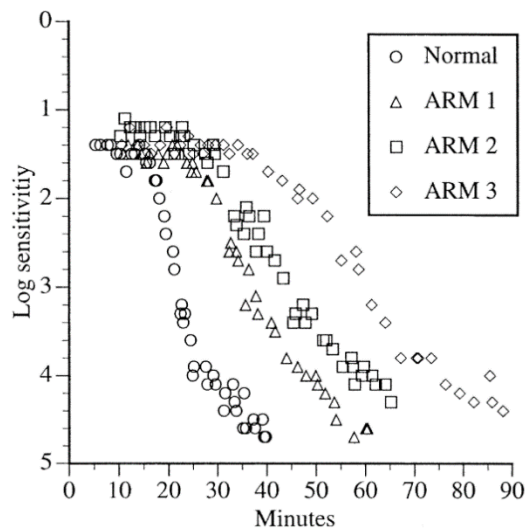


Figure 1.23 A plot showing the DA functions for three people with AMD at different severity levels and one older healthy control. All participants have 20/25 VA or better. ARM 1 is >5 small drusen ($\leq 63\mu\text{m}$). ARM 2 is defined as ≥ 1 large drusen ($>63\mu\text{m}$), focal hyperpigmentation, or both. ARM 3 is drusen and CNV. Sourced from Owsley et al. (2001).

Once DA curves are produced, the most frequent way in current devices to measure RMDA in people with AMD is by assessing the time taken to reach a set criterion of recovery within the S2, like the RIT (Jackson and Edwards, 2008; Jackson, Clark, et al., 2014; Jackson, Scott, et al., 2014; Flamendorf et al., 2015; Owsley, Clark, et al., 2016; Owsley, Huisingh, et al., 2016; Owsley, McGwin, et al., 2016; Sevilla et al., 2016; Neely et al., 2017; Laíns et al., 2017; Owsley, Clark and McGwin, 2017; Yazdanie et al., 2017; Binns et al., 2018; Cocce et al., 2018; Laíns, Miller, et al. 2018; Laíns, Park, et al., 2018; Thompson et al., 2018; Beirne and McConnell, 2019; Chen et al., 2019; Mullins et al., 2019). RIT is estimated by linear interpolation for the sensitivity responses (Flamendorf et al., 2015). In people with AMD, the RIT takes longer to achieve (Flamendorf et al., 2015; Jackson, Scott et al., 2014; Jackson & Edwards, 2008). In some case of more severe AMD, it cannot be reached in the experimental time (Jackson, Scott et al., 2014). For example, Jackson and Edwards (2008) introduced the AdaptDx protocol and suggested that RITs longer than 12.5 minutes should be classified as evidence of impaired DA when testing a location at 5° in the inferior field after an 83% bleach. This metric was proposed as it was the upper limit of the normative reference range (Jackson & Edwards, 2008). Owsley, McGwin, et al. (2016) used a similar reference of 12.3 minutes in a later study. Note: For a full review of currently used methodology to assess DA in people with AMD, see Chapter 2.

1.8.3 Dark Adaptation and Subretinal Drusenoid Deposits

Subretinal drusenoid deposit presence is a topic of interest in DA research in people with AMD (Flamendorf et al., 2015; Laíns et al., 2017; Chen et al., 2019; Grewal et al., 2022). DA impairment has been shown to be worse in people SDDs (Flamendorf et al., 2015; Sevilla et al., 2016; Neely et al., 2017; Flynn, Cukras and Jeffrey, 2018; Laíns, Park, et al., 2018; Nguyen et al., 2018; Chen et al., 2019; Grewal et al., 2022) compared to those without SDDs, therefore a potential structure-function relationship may be evident. In short, SDDs are accretions of material within the RPE that extend through the ellipsoid zone (Spaide, Ooto and Curcio, 2018) best seen on OCT rather than CFP (Zweifel et al., 2010) (see section 1.1.4.1). Flamendorf et al. (2015) looked at the relationship between SDD presence and DA in people with AMD and reported significantly longer RITs in 15 people who had SDDs (with 80% reaching the test ceiling of 40 min) (Flamendorf et al., 2015). However, the study was limited by a small cohort with SDDs that were significantly older than the controls; this is noteworthy. Neely et al. (2017) found SDD presence in controls did not significantly impact DA and postulated scarce SDD manifestation coupled with minimal RPE abnormalities in people with a healthy macula was insufficient to negatively impact DA (Neely et al., 2017). It has been suggested that SDD presence should be seen as a prognostic biomarker for AMD progression in people with early-stage disease (Chen et al., 2019; Clark et al., 2011; Huisingh et al., 2016). Recently, Grewal et al. (2022) evaluated functional clinical endpoints including RMDA and structural correlations in 11 controls and 39 people

with AMD (17 people with iAMD and no SDDs, 11 people with iAMD with SDDs and 11 people with non-foveal atrophic AMD, respectively). The authors found people with iAMD and SDDs had significantly delayed RIT compared to people with iAMD and no SDDs. As a result, the authors concluded that SDD presence is a biomarker of photoreceptor abnormalities, comparable to that of non-central atrophy (Grewal et al., 2022). However, it should be noted that the group with SDDs were significantly older than the group without SDDs, and age is known to play a role in delayed DA. See Chapter 2 for an overview of literature evaluating DA in people with AMD with and without SDD and see Chapter 4 for our investigation into the association between SDD presence and DA at different AMD severity grades, using an OCT-based classification. This analysis also forms part of a manuscript which is currently under review for publication.

1.8.4 Is Dark Adaptation a Potential Clinical Biomarker for Age-Related Macular Degeneration?

A clinical biomarker, a portmanteau of 'biological marker', refers to a measurable characteristic that indicates a medical state of a patient e.g. a sign of pathogenic processes or a response to therapy (Strimbu & Tavel, 2010). Biomarkers can be split into prognostic or predictive biomarkers. Prognostic biomarkers are associated with outcomes and classify people who are likely to experience a future clinical event, be that disease progression or recurrence. They are used to decide who will receive treatment (or indeed who will not) with expected clinical outcomes. Predictive biomarkers classify people who will react (or not) to a treatment in a certain way and aid in helping spare patients from ineffective treatment options (Verdaguer, Saurí and Macarulla, 2016). To ascertain if a biomarker is clinically relevant, it must demonstrate it can be used to divide people into groups with different recommended clinical management (Freidlin, McShane and Korn, 2010).

Optimal photoreceptor function relies upon the RPE cells' involvement in the visual cycle. Hence, not only does DA assessment examine the number and integrity of the photoreceptors, but also the status of the outer retinal complex that supports the photoreceptors such as the RPE, Müller Cells, BM and the choriocapillaris. The outer retinal complex suffers impairment as a result of AMD which gets worse as the disease progresses (see section 1.2.2). Perhaps unsurprisingly, some studies have shown the time taken for DA to occur has also been shown to progressively increase with increasing severity of AMD, suggesting it has potential not only as a diagnostic tool, but also as a biomarker for disease progression (i.e. a prognostic biomarker) (Dimitrov et al., 2012; Jackson, Scott, et al., 2014; Owsley, Clark and McGwin, 2017).

Owsley, McGwin, et al. (2016) recently evidenced that RMDA is a functional prognostic biomarker of incident early AMD. Elderly, visually healthy controls at baseline who were classed as having 'abnormal' DA (≥ 12.3 minutes) were on average two-times more likely to have early AMD three years

later compared with controls with 'normal' RITs (Owsley, McGwin, et al., 2016). However, the evidence for measurement of DA being able to discriminate early AMD cases from elderly controls and differentiate between groups of varying AMD severity is weak (Higgins, Taylor, et al., 2021). See Chapter 2 for a full review of recent literature in DA assessment in people with AMD, including a focus on the evidence of precision in detecting the onset and progression of AMD.

1.9 RATIONALE AND AIMS OF PHD THESIS

It is necessary to find functional prognostic biomarkers in early and intermediate stage non-neovascular AMD. Prognostic biomarkers are needed to aid the advancement of clinical trials of potential therapies and to help identify patients at risk for progressing to later stage AMD. The expense associated with running clinical trials with end-stage disease as the endpoint is extortionate, largely due to the need for a large number of participants to ensure a sufficient number end up progressing to advanced AMD. Biomarkers allow us to develop surrogate endpoints which can be evaluated in a shorter period, making it more cost-effective to run clinical trials. Prognostic biomarkers are particularly useful in highlighting people at risk of progression to later stage AMD who need to be monitored more closely. Functional tests which are sensitive to disease progression also help us in clinic to determine how effective a treatment has been for a particular patient. Furthermore, it would be preferable if these functional biomarkers correlated with structural biomarkers, such as drusen, which form the basis of our current understanding of AMD pathophysiology and our current severity grading systems. RMDA as a potential functional biomarker is gaining more traction in AMD research, with dark adaptometers such as the AdaptDx becoming commercially available and making the assessment of DA feasible within a clinically acceptable timeframe.

The studies described in this PhD thesis seek to better understand how DA is assessed in people with AMD, and its limitations and strengths as a potential functional biomarker for AMD. The overarching aim of this work, therefore, was to identify, evaluate and improve upon methodology used to assess RMDA in people with early and intermediate non-neovascular AMD and to compare it to other measures of visual function.

Specifically, the following aims were investigated:

- I. To systematically review the current methodology used to assess DA in people with AMD, the evidence of precision in detecting the onset and progression of AMD, and the relationship between DA and other functional and structural measures (see Chapter 2).
- II. To test the efficacy of utilising time-to-event (survival) analysis on RIT data using the AdaptDx (see Chapter 3).

- III. To assess the differences in DA between different grades of AMD severity using a novel OCT-based classification system compared to the Beckman CFP-based classification. Also to assess the association between SDD presence and DA at different AMD severity grades, using the OCT-based classification. (see Chapter 4).

- IV. To assess the between-test variability and discrimination performance of rod mediated DA (AdaptDx) compared to parameters of scotopic and mesopic microperimetry (S-MAIA) in eyes with iAMD as part of the observational multicentre MACUSTAR study (see Chapter 5).

Chapter 6 provides a brief summary of the key findings from this research and discusses these in the context of potential future work.

2 CHAPTER 2; ARE CURRENT METHODS OF MEASURING DARK ADAPTATION EFFECTIVE IN DETECTING THE ONSET AND PROGRESSION OF AGE-RELATED MACULAR DEGENERATION? A SYSTEMATIC LITERATURE REVIEW

2.1 INTRODUCTION

As outlined in Chapter 1, AMD is the primary cause of sight-loss in ageing populations of the developed world (Bourne et al., 2014). It is therefore important to identify AMD in its earliest stages so disease progression can be potentially delayed. In order to reduce the duration and costs associated with trials for new treatments of AMD, sensitive biomarkers for disease progression are also required (Finger et al., 2019). The RPE is believed to be the fulcrum of the AMD disease process (Ambati & Fowler, 2012), whilst the provision of 11-cis retinal from the RPE to the photoreceptors is the limiting factor in the rate of visual pigment regeneration in photoreceptors. Therefore, DA has been proposed as a functional biomarker for AMD onset and progression (Owsley et al., 2001). Dark adaptometers have been designed for clinical use with commercially available instruments designed to assess DA in conditions like AMD.

The most recent systematic review considering DA assessment in people with AMD was published as part of a wider review on visual function tests by (Hogg & Chakravarthy, 2006). Since then, new studies on DA measurement have been published. Moreover, some instruments for measuring DA have become commercially and widely available, such as the AdaptDx adaptometer (Jackson, Scott, et al., 2014; Jackson & Edwards, 2008). DA is also one of the candidate biomarkers being examined by a large multi-centre longitudinal study aiming to find better ways of detecting progression in AMD (Finger et al., 2019).

This systematic review was conducted in order to evaluate current methodology used to assess DA in people with AMD. The review specifically examined the evidence of diagnostic precision of these methods in detecting the onset of AMD, as well as the sensitivity to disease progression. The review focussed on the AdaptDx instrument as the device most widely used in the recent literature. Furthermore, associations between DA and functional vision measures, structural measures, patient reported outcome measures (PROMs) and outcomes from performance-based studies (involving assessment of visually guided tasks such as face-recognition or mobility assessments) were explored. This systematic review followed PRISMA guidelines and a detailed protocol has been published on PROSPERO (registration number: CRD42019129486).

The work presented in this chapter is published as a paper in *Ophthalmology and Therapy* (Higgins, Taylor, et al., 2021) (see list of supporting publications). The co-authors of this work are Bethany E. Higgins (BEH), Deanna J. Taylor (DJT), Alison M. Binns (AMB) and David P. Crabb (DPC). BEH and DPC conceived the idea of doing the systematic review. BEH and DJT read and screened abstracts and full-text articles for inclusion and BEH appraised study quality. Any disagreements or uncertainties during the screening and quality appraisal process were referred to AMB. BEH extracted data from articles selected for inclusion and wrote the manuscript, which was reviewed, edited, and approved by DJT, AMB and DPC.

2.2 METHODS

To be eligible for inclusion, studies had to be: (1) published in the English language; (2) dated from January 2006 to January 2020 to include studies following the review by (Hogg & Chakravarthy, 2006); (3) include participants with AMD (of any stage) and (4) include a dynamic measurement of rod and/or cone DA. Studies were excluded if they were review articles, letters to the Editor, published protocols or conference abstracts.

The following databases were searched: CINAHL, MEDLINE, PsycINFO and PsycARTICLES (via EBSCO) and EMBASE and AMED (via OVID) for publications published between 01/01/2006 and 27/01/2020. An indicative list of search terms and the search query used is provided in Supplemental Table S2.1 (see section 8.1). Key terms regarding AMD, DA and dynamic photostress testing were used. The reference lists of the included literature were examined as a further source of relevant studies. Covidence software (Veritas Health Innovation, 2019) was used for extraction, organisation and screening of the literature.

Duplicates were automatically removed by Covidence software (Veritas Health Innovation, 2019). Two authors (BEH and DJT) independently assessed for eligibility for inclusion through screening titles and abstracts. The same two authors then independently read the full texts of potential eligible studies with any disagreements about inclusion resolved through discussion and then arbitration by a third author (AMB).

Two authors (BEH and DJT) evaluated the quality of included studies independently. The Critical Appraisal Skill programme tool (CASP, 2013) was used to assess cohort, case-control and randomised controlled trial study designs. The Joanna Briggs Institute critical appraisal tool (JBI, 2017) was used to assess cross-sectional and case-series design types. These tools are recommended by the UK NICE guidelines. The summarised quality appraisal results are shown in Supplemental Table S2.2 (see section 8.1).

Study characteristics were extracted into a data synthesis table (Supplemental Table S2.3; see section 8.1). A meta-analysis was not appropriate given the range of stimulus and bleach parameters employed by different studies. Data were analysed based upon reported DA and/or photostress procedure (Supplemental Table S2.4; see section 8.1), diagnostic accuracy and repeatability measures reported (Supplemental Table S2.5; section 8.1) and reported vision and structural outcome measures compared to parameters of DA (Supplemental Table S2.6; section 8.1). Data on reported outcome measures compared to parameters of DA, unrelated to vision were also recorded but not analysed (Supplemental Table S2.7; section 8.1).

2.3 RESULTS

The search of bibliographic databases performed on 27th January 2020 identified 512 publications. During this screening procedure, most studies (n=397) were excluded, principally due to not reporting measures of dynamic DA or not including a study population with people who have AMD. Sixty-seven full texts screened were removed primarily because their format was ineligible for this systematic review (e.g. conference abstract, protocol or review) resulting in 48 papers deemed appropriate for the final review process (Figure 2.1).

The included 48 publications were subjected to quality appraisal. The CASP tool was used for cohort (n=4), case-control (n=20) and randomised controlled trial (n=4) study designs. The JBI tool was used for cross-sectional (n=17) and case studies (n=3). The grading of all papers can be found in Table S2.2 (see section 8.1). The main source of bias was selection bias, whereby most observational studies did not explicitly report their recruitment strategies. Moreover, some studies were conducted on small sample sizes that could lead to systematic over or under-estimation of effects. In addition, a large percentage of the studies did not report SD or CI for the DA parameter, which made it difficult to judge the precision of the results. These factors were considered when analysing the results.

What follows is a short narrative summary of the main findings of the 48 studies included in this systematic review with a focus on the 21 studies that used the AdaptDx and AdaptRx devices (Apeliotus Technologies, Atlanta, GA). The other 27 studies used a myriad of lab-based dark adaptometers, dynamic photostress tests devices and the occasional commercially available instrument like the Roland Consult Dark Adaptometer (RCDA; Roland Consult GmbH, Germany) (Rodriguez et al., 2018). Full detail about each study is in the Tables S2.3-S2.7 (see section 8.1).

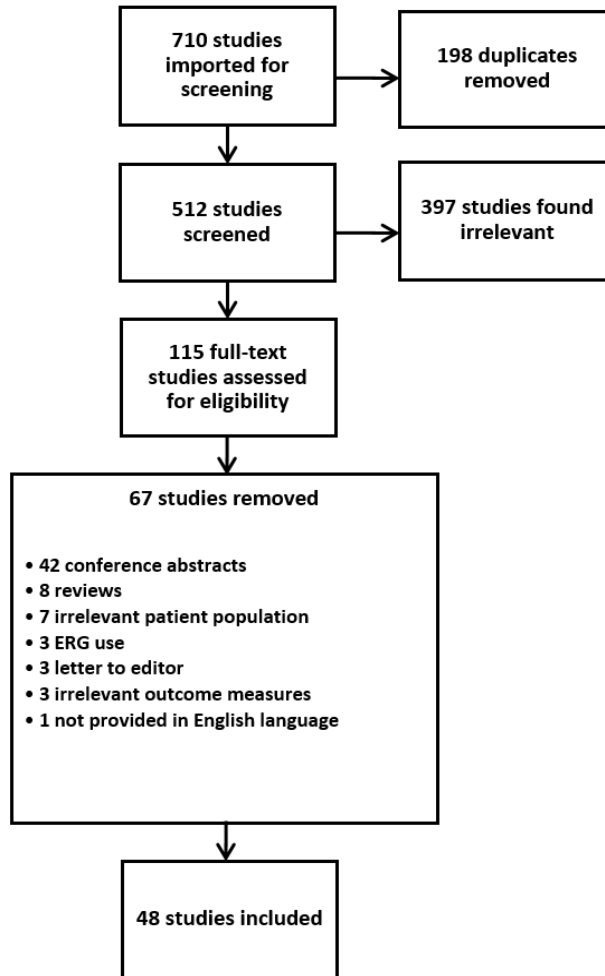


Figure 2.1 Flowchart of study selection process

2.3.1 AdaptDx: Testing Procedures

For full details of the testing procedures used by studies with the AdaptDx, see Table 2.1. AdaptDx and AdaptRx were used to measure RMDA in 21 studies. The AdaptRx methodology appeared identical to the AdaptDx and was reported once in the reviewed literature by Flamendorf et al., (2015). The most frequently reported DA parameter was RIT (20 out of 21 studies), an estimate of the time duration for the rods to recover to an established criterion sensitivity (i.e. $5 \times 10^{-3} \text{ cd/m}^2$) after focal bleaching (Jackson & Edwards, 2008). Clark et al. (2011) was the only study which fitted AdaptDx threshold data with a biological model of RMDA and analysed the slopes of the second and third components of recovery, final threshold recorded during the 20 minute test period, and ‘mean threshold’ (the average of all thresholds after 300 seconds post bleach).

There were different approaches to bleaching magnitude and target position reported in the literature that varied dependent upon the aim of the study. For example, the most recurrently reported

bleaching procedure in these studies was an 82-83% photoreceptor bleach using a flash of 5.8×10^4 scotopic cd.s/m² intensity or equivalent for 0.25-milliseconds (12 out of 21 studies). This bleaching light has been reported by (Jackson & Edwards, 2008) to be sufficient in magnitude to demonstrate impaired DA in people with early AMD when using the 20 minute duration AdaptDx protocol. Another reported bleaching procedure in the literature was a 76% photoreceptor bleach using a flash of 1.8×10^4 scotopic cd.s/m² intensity for 0.8 milliseconds (10 out of 21 studies) which has been also reported as sufficient in highlighting the AMD-related DA impairment (Jackson, Scott et al, 2014). Chen et al., (2019) reportedly used both an 82% and a modified 76% bleaching. Only a handful of explicitly studies reported the wavelength of the bleach as 505nm (7 out of 21 studies) (Beirne & McConnell, 2019; Cocce et al., 2018; Jackson, Scott et al, 2014; Láins et al., 2017; Láins, Miller, et al., 2018; Láins, Park, et al., 2018; Thompson et al., 2018).

The most often reported testing location of the bleaching procedures and subsequent location of threshold measurements was centred at 5° on the inferior vertical meridian (19 out of 21 studies) which is consistent with evidence of preferential damage to the parafoveal retina in the earliest stages of AMD (Curcio, Medeiros and Millican, 1996; Owsley et al., 2000). Three studies reported a test location of 11/12° eccentricity. In two of these cases, both 5° and 12° locations were evaluated (Binns et al., 2018; Chen et al., 2019). Binns et al., (2018) recently compared different bleaching protocols (65%, 70% and 76% photoreceptor bleach at either 5° or 12° inferior field). It was concluded that 76% bleach at 12° eccentricity allowed for separation between the groups in the sample and reduced recovery time to under 20 minutes, compared to a more extended recovery times in the 5° location (Binns et al., 2018).

The AdaptDx has a threshold stimulus size of 1.7-2.0° with a wavelength of 500-505nm, centred on a bleached area subtending 4°. Eight studies reported that the stimulus was first presented 15-seconds after bleaching onset while two reported that it started immediately after bleaching (Beirne & McConnell, 2019; Láins et al., 2017). The most often reported maximum test time (or cut-off time) was 20 minutes (13 out of 21 studies) followed by 40 minutes (5 out of 21 studies), 45 minutes (Beirne & McConnell, 2019; Jackson, Clark, et al., 2014) (2 out of 21 studies) and 30 minutes (Binns et al., 2018) (1 out of 21 studies). For the rapid procedure, the DA functions were truncated to 6.5 minutes (Binns et al., 2018; Jackson, Scott et al, 2014) (2 out of 21 studies).

Twelve studies allocated the participant an RIT value (in most cases, the cut-off time) if they failed to recover within the duration of the test. It was not clearly reported by six studies what this value was set to if the participant surpassed the cut-off time. Two studies appeared to use an estimated recovery time based on the observed trend up to the maximum recording time but when the parameter was unable to be extrapolated, it was again set to the experimental cut-off time (Jackson, Scott et al., 2014; Thompson et al., 2018). Conversely, Owsley et al. (2017) set the value to 'indeterminate' rather than allocate an estimated RIT.

Table 2. 1 Dark adaptation methodology adopted with the AdaptDx/AdaptRx

Procedure used	Frequency	Studies
Dark adaptometer used		
AdaptDx/AdaptRx	21	Jackson and Edwards (2008); Jackson, Clark, et al. (2014); Jackson, Scott, et al. (2014); Flamendorf et al. (2015); Owsley, Clark, et al. (2016); Owsley, Huisingh, et al. (2016); Clark et al. (2011) ; Owsley, McGwin, et al. (2016); Sevilla et al. (2016); Neely et al. (2017); Laíns et al. (2017); Owsley, Clark and McGwin, (2017); Yazdanie et al. (2017); Binns et al. (2018); Cocce et al. (2018); Laíns, Park, et al. (2018); Laíns, Miller, et al. (2018); Thompson et al., (2018); Beirne and McConnell (2019); Chen et al. (2019); Mullins et al. (2019)
DA parameters		
Rod-intercept time (an estimate of the time duration for the rods to recover to an established criterion sensitivity (i.e. 5×10^{-3} cd/m ²) after focal bleaching)	20	Jackson and Edwards (2008); Jackson, Clark, et al. (2014); Jackson, Scott, et al. (2014); Flamendorf et al. (2015); Owsley, Clark, et al. (2016); Owsley, Huisingh, et al. (2016); Owsley, McGwin, et al. (2016); Sevilla et al. (2016); Neely et al. (2017); Laíns et al. (2017); Owsley, Clark and McGwin, (2017); Yazdanie et al. (2017); Binns et al. (2018); Cocce et al. (2018); Laíns, Park, et al. (2018); Laíns, Miller, et al. (2018); Thompson et al., (2018); Beirne and McConnell (2019); Chen et al. (2019); Mullins et al. (2019)
Slopes of the 2 nd and 3 rd components of rod recovery, final threshold recorded and mean threshold recorded	1	Clark et al. (2011)
Bleaching magnitude		
82-83% photoreceptor bleach using a flash of 5.8×10^4 scotopic cd.s/m ² intensity or equivalent for 0.25-milliseconds	12	Jackson and Edwards (2008); Clark et al. (2011); Jackson, Clark, et al. (2014); Flamendorf et al. (2015); Owsley, Clark, et al. (2016); Owsley, Huisingh, et al. (2016); Owsley, McGwin, et al. (2016); Sevilla et al. (2016); Neely et al. (2017); Yazdanie et al. (2017); Chen et al. (2019); Mullins et al. (2019)

76% photoreceptor bleach using a flash of 1.8x10 ⁴ scotopic cd.s/m ² intensity for 0.8 milliseconds	10	Jackson, Scott, et al. (2014); Láins et al. (2017); Owsley, Clark and McGwin (2017); Binns et al. (2018); Cocce et al. (2018); Láins, Miller, et al. (2018); Láins, Park, et al. (2018); Thompson et al. (2018); Beirne and McConnell (2019); Chen et al. (2019)
---	----	--

Testing location

5° on the inferior vertical meridian	20	Jackson and Edwards (2008); Clark et al. (2011); Jackson, Clark, et al. (2014); Jackson, Scott, et al. (2014); Flamendorf et al. (2015); Owsley, Clark, et al. (2016); Owsley, Huisingsh, et al. (2016); Owsley, McGwin, et al. (2016); Sevilla et al. (2016); Neely et al. (2017); Láins et al. (2017); Yazdanie et al. (2017); Cocce et al. (2018); Láins, Park, et al. (2018); Láins, Miller, et al. (2018); Thompson et al., (2018); Beirne and McConnell (2019); Binns et al. (2018); Chen et al. (2019); Mullins et al. (2019)
--------------------------------------	----	--

11/12° eccentricity	3	Owsley, Clark and McGwin (2017); Binns et al. (2018); Chen et al. (2019)
---------------------	---	--

Time stimulus presented

15-seconds after bleaching	8	Clark et al. (2011); Owsley, Clark, et al. (2016); Neely et al. (2017); Owsley, Huisingsh, et al. (2016); Owsley, McGwin, et al. (2016); Owsley, Clark and McGwin (2017); Binns et al. (2018); Mullins et al. (2019)
----------------------------	---	--

Immediately after bleaching	2	Beirne and McConnell (2019); Láins et al. (2017)
-----------------------------	---	--

Maximum test-time

20 minutes	13	Jackson and Edwards (2008); Clark et al. (2011); Jackson, Scott, et al. (2014); Owsley, Clark, et al. (2016); Owsley, Huisingsh, et al. (2016); Owsley, McGwin, et al. (2016); Sevilla et al. (2016); Neely et al. (2017); Láins et al. (2017); Cocce et al. (2018); Láins, Miller, et al. (2018); Láins, Park, et al. (2018); Thompson et al. (2018)
------------	----	---

40 minutes	5	Flamendorf et al. (2015); Owsley, Clark and McGwin (2017); Yazdanie et al. (2017); Chen et al. (2019); Mullins et al. (2019)
------------	---	--

45 minutes	2	Beirne & McConnell (2019); Jackson, Clark, et al. (2014)
30 minutes	1	Binns et al. (2018)
6.5 minutes	2	Binns et al. (2018); Jackson, Scott et al (2014)

When a participant failed to recover

Allocated an RIT (in most cases the maximum test time)	12	Beirne & McConnell (2019); Binns et al. (2018); Chen et al. (2019); Flamendorf et al. (2015); Láins et al. (2017); Jackson, Clark, et al. (2014); Jackson & Edwards (2008); Láins, Miller, et al. (2018); Láins, Park, et al. (2018); Mullins et al. (2019); Yazdanie et al. (2017), Cocce et al. (2018)
Unclear from methodology	6	Clark et al. (2011); Owsley, Clark, et al. (2016); Owsley, Huisingh, et al. (2016); Owsley, McGwin, et al. (2016); Sevilla et al. (2016); Neely et al. (2017)
estimated recovery time based on the observed trend up to the maximum recording time	2	Jackson, Scott et al. (2014; Thompson et al. (2018)
Set value to 'indeterminate'	1	Owsley, Clark and McGwin (2017)

2.3.2 AdaptDx: Diagnostic Precision, Repeatability and Longitudinal Studies

Three studies specifically reported estimates of diagnostic performance (sensitivity and specificity) of AdaptDx to separate people with AMD from visually healthy controls (Binns et al., 2018; Jackson, Scott, et al., 2014; Jackson & Edwards, 2008). Only one of these studies had this as its primary aim (Jackson, Scott, et al., 2014). A third reported the prognostic performance of the test at identifying healthy individuals who would develop AMD within three years of baseline testing (Owsley, McGwin, et al., 2016).

Jackson and Edwards (2008) introduced the AdaptDx 20 minute protocol in a study of controls (17, eight young participants [mean age 32.6 years] and nine old participants [mean age 73.1 years]) and 17 participants with AMD. The threshold for being test negative was ≤ 12.5 minutes; this yielded a sensitivity of 88% and specificity of 100%. Notably, nine participants with AMD (incidentally, the whole of the iAMD and late AMD cohort) were unable to complete the test so were assigned an RIT of 20 minutes. The small sample size yielded wide CIs and is considered insufficient to allow analysis of the true diagnostic precision of the 20 minute procedure.

Jackson, Scott, et al. (2014) reported results from a prospectively planned cross-sectional study (at three centres) of 127 people with AMD and 21 visually healthy people. The reference standard was clinical examination and grading of CFP. The AdaptDx rapid protocol was the index test with RIT of ≤ 6.5 minutes as the threshold for being test negative; this yielded a sensitivity of 91% and a specificity of 91%. Fourteen people could reportedly not do the examination; this is a noteworthy bias because authors failed to include this in their estimates of diagnostic precision. Moreover, the small sample of controls meant that the lower bound of the 95% CI for specificity was $\sim 70\%$, but this was not reported in the abstract. Further examination revealed that sensitivity was reduced (81%) in people investigators classified as having early AMD. The groups were not age-related (controls were mean eight years younger) and this is another limitation of the results.

Binns et al. (2018) primarily aimed to determine optimal test conditions for evaluating DA in iAMD using the AdaptDx. Authors used estimates of diagnostic precision (ROC assessment; AUC) to conclude that a 76% bleach at 5° eccentricity provided 'optimal' separation between AMD and controls, however this was at the expense of a long recording duration. An alternative test location was suggested at 12° to provide adequate diagnostic accuracy whilst reducing recording time by more than 50%. Authors reported estimates of diagnostic precision at different cut-offs (sensitivity and specificity of 89% and 63% respectively for the optimal condition, for example) but the small sample size (16 people with AMD and 10 controls) was insufficient to allow evaluation of the true diagnostic precision of the procedure.

In a well-designed cohort study, albeit at a single centre, Owsley, McGwin, et al. (2016) primarily aimed to examine whether slowed RIT (measured with an extended AdaptDx protocol) in 325 adults

with normal macular health at baseline was associated with the incidence of AMD 3-years later. After adjustment for age and smoking, those with abnormal DA (defined as RIT ≥ 12.3 minutes) at baseline were approximately two times more likely to have AMD in that eye by the time of the FU visit, compared with those who had normal DA at baseline. The purpose of this study was not to evaluate the diagnostic precision, but authors reported a sensitivity and specificity of 33% and 83% respectively for incident AMD in those in normal macular health at baseline.

Only one paper explicitly gives data about the repeatability of DA measurement with the AdaptDx. Flamendorf et al. (2015), using the AdaptRx, conducted a cross-sectional, single centre study of 116 participants (>50 years) with and without AMD. Patients were stratified by fundus features, with 36% having 'no large drusen'. Authors primarily demonstrated that RIT was associated with age, AMD severity and subfoveal choroidal thickness. A subsample of 87 participants did repeat examination ~1 week later and authors report a mean (\pm SD) RIT difference of 0.02 ± 2.26 minutes; this translates into 95% limits of agreement (LoA) of -4.41 to 4.46 minutes, which is quite wide given the average RIT. Authors claimed that repeatability did not differ significantly between AMD groups but it is not explicitly clear how they analysed this. Authors did provide a Bland-Altman (BA) graph showing the differences in test-retest variability which did not seem to increase with worse RIT. Yet on inspection, it appeared those participants recording a RIT below 10-minutes had better RIT repeatability.

There is clear evidence for an association between delayed DA and presence of AMD. However, we only identified five longitudinal studies assessing DA measurements from AdaptDx over time (Jackson, Clark, et al., 2014; Owsley, Clark, et al., 2016; Owsley, McGwin, et al., 2016; Owsley, Clark and McGwin, 2017; Chen et al., 2019).

Jackson, Clark et al. (2014) prospectively collected DA, VA, and CFP at baseline and at 6-months and 12-months in 26 people with AMD. Investigators observed worsening of DA in five participants in 12-months of observation, despite seemingly stable VA and fundus appearance. The study was limited by the small sample size and had only had six participants in the control group who were not age-related. Four AMD participants exhibited large changes in DA at 6-months, which was inconsistent with their DA at 12 months.

The previously mentioned cohort study reported by Owsley, McGwin, et al. (2016) focused on elderly people without AMD and showed delayed DA at baseline was associated with development of AMD at 3-years. Owsley, Clark, et al. (2016) reiterated this finding in another paper comparing the association of impaired visual function to AMD incidence 3-years later (using the previously reported DA results for 363 eyes). Impaired mesopic acuity was found to have a weaker association to AMD incidence compared to DA. The same research group was responsible for another two year longitudinal study reporting on 23 eyes with iAMD and measurable RITs (Owsley, Clark and McGwin, 2017). This paper reported RMDA slows in iAMD over 2-years in most eyes and gave useful data on expected average RIT change over time but concluded there was wide variability both in RIT at baseline, and in the extent to which it increased over 24-months.

Chen et al. (2019) conducted a notable longitudinal study of changes in RIT in 77 people with a range of AMD severities over four years; they indicated that decline in DA accelerated in eyes with greater AMD severity and especially in eyes that had SDD both at baseline and at 4 years (see below).

2.3.3 AdaptDx: Relationship with Other Measures

The secondary aim of this systematic review was to assess the relationship of DA measures with other factors. The latter includes measures of visual function, structural measures from photographs or images, PROMs and potentially performance-based metrics within the literature. For this review, all factors directly (and statistically) compared to DA parameters were recorded for each study in their entirety (see section 8.1). These were then categorised into relevant themes and are summarised briefly below.

The most frequent factor directly compared to RIT in the literature was AMD presence and severity of AMD (19 out of 21 studies) See Table 2.2 for details. It was generally reported by authors that a presence of AMD was associated with slowed or 'abnormal' RIT when compared to visually healthy controls, although one cross-sectional study found no significant difference in average RIT between people with AMD and controls once data was age-adjusted (Sevilla et al., 2016). Most of these studies reported difference in RIT between controls and the AMD group as a whole (Clark et al., 2011; Jackson, Clark, et al., 2014; Jackson, Scott et al, 2014) or between controls and people with iAMD/advanced AMD (Flamendorf et al., 2015; Laíns et al., 2017; Owsley, Clark and McGwin, 2017; Yazdanie et al., 2017; Binns et al., 2018; Cocce et al., 2018; Laíns, Miller, et al., 2018; Beirne and McConnell, 2019; Chen et al., 2019). Cocce et al. (2018) found a significant difference in RIT between early and iAMD. Few studies found significant differences between those with early AMD and controls (Jackson and Edwards, 2008; Owsley, Clark, et al., 2016; Owsley, Huisingh, et al., 2016; Owsley, McGwin, et al., 2016). For example, Owsley, McGwin, et al. (2016) reported controls with abnormal DA were almost two times more likely to have AMD in the tested eye three years. Furthermore, Jackson and Edwards (2008) reported the mean RIT for six people with early AMD was nearly twice as slow as the nine people in the control group, but no p-values were offered.

Table 2. 2. Table of studies that compared DA parameters to presence and severity of AMD

Measure compared to DA	Frequency	Studies
Presence of and/or severity of AMD	19	Jackson and Edwards (2008); Jackson, Clark, et al. (2014); Jackson, Scott, et al. (2014); Flamendorf et al. (2015); Owsley, Clark, et al. (2016); Owsley, Huisingh, et al. (2016); Clark et al. (2011); Owsley, McGwin, et al. (2016); Sevilla et al. (2016); Laíns et al. (2017); Owsley, Clark and McGwin, (2017); Yazdanie et al. (2017); Binns et al. (2018); Cocce et al. (2018); Laíns, Miller, et al. (2018); Thompson et al., (2018); Beirne and McConnell (2019); Chen et al. (2019) Mullins et al. (2019)

The effect of presence of SDDs on RIT was considered in a number of studies (Chen et al., 2019; Flamendorf et al., 2015; Laíns et al., 2017; Neely et al., 2017; Sevilla et al., 2016; Yazdanie et al., 2017). Overall, the results indicated that SDD presence in people with AMD correlated with slowed RIT (Chen et al., 2019; Flamendorf et al., 2015; Laíns et al., 2017; Neely et al., 2017; Sevilla et al., 2016; Yazdanie et al., 2017), whether the SDDs were in the testing location or not (Laíns et al., 2017). Neely et al. (2017) reported that SDD presence in controls did not significantly impact RIT, while eyes with both early AMD and SDD presence did have markedly slower RIT. However, this association was lost when data was adjusted for age. Flamendorf et al. (2015) reported significantly slowed RIT in 15 participants with SDD presence with 80% reaching the test ceiling (40 minutes); although it is noteworthy that the SDD group was significantly older than the controls. Chen et al. (2019) described a key association between presence of SDD and accelerated worsening of DA in their longitudinal study. Conversely, peripheral classic drusen (both presence and number) have not been found to be associated with slowed RIT (Laíns, Park, et al., 2018).

The literature indicates that other structural abnormalities also impact on DA. For example, delayed RIT may appear more likely in pseudophakic eyes which may have implications on the routine clinical use of the instrument (Flamendorf et al., 2015; Laíns, Miller, et al., 2018; Owsley, McGwin, et al., 2016). Chen et al. (2019) observed huge changes in RIT across the study visits just preceding and after cataract extraction. Markedly, age and AMD stage are evidenced to negatively impact this association when applied in multivariate analysis (Laíns, Miller, et al., 2018; Owsley, McGwin, et al., 2016) and some studies report no significant differences for lens status (Laíns et al., 2017).

Others have reported an association between impaired DA and changes in choroidal thickness (Flamendorf et al., 2015), reticular pigmentary changes, and presence of a mottled decreased FAF pattern in the midperipheral zone (Laíns, Park, et al., 2018). When the effect of age and VA is controlled for in the analysis of DA parameters, an association has also been identified in changes in retinal thickness and DA (Clark et al., 2011). Laíns et al. (2017) found structural abnormalities (such as classic drusen, ellipsoid zone disruption and serous PED) to affect DA whether they were in the testing

location or not, even after controlling for AMD stage and age. The level of macular pigment has not been found to correlate with RMDA in people with AMD (Beirne & McConnell, 2019). Sevilla et al. (2016) reported presence of hyper-reflective foci, lower RPE-drusen-complex volume and greater RPE-drusen-complex abnormal thinning volume were associated with slowed RIT. While no significant differences were found between groups (early AMD, iAMD, 'no-apparent visual ageing' controls and 'normally ageing' controls) in RPE-drusen-complex, retinal volumes, or inner and outer retinal volumes and, when the data were age-adjusted, group differences in RIT was also lost.

Genotyping of well-defined populations is another route to discover what might happen in early disease stages in AMD. Mullins et al. (2019) reported a cross-sectional analysis of RIT and genetic risk factors in 543 people aged ≥ 60 years with either evidence of normal visual ageing or AMD in one or both eyes. A novel association was found wherein older adults with no evidence of AMD but who had high-risk ARMS2 genotype were more likely to demonstrate delayed RIT, but not for those who had CFH genotype. While presence of the CFH genotype was associated with delayed RIT in people with AMD. Further research into understanding ARMS2 function has been suggested to be a research priority.

Few studies directly compared visual function measurements to RIT (4 out of 21 studies) and with differing results (Beirne & McConnell, 2019; Chen et al., 2019; Flamendorf et al., 2015; Láins, Miller, et al., 2018). Flamendorf et al. (2015) and Láins et al. (2018) found that best corrected VA (BCVA) and worse eye BCVA, respectively, correlated with delayed. In the Chen et al. (2019) longitudinal study, changes in RIT occurred over four years while BCVA remained largely unchanged with a mean of only 1.8 letters lost. Authors suggested that RIT appears to show functional loss that BCVA cannot, although the study could not exclude the effects of lens removal which may affect longitudinal measures of BCVA. Beirne and McConnell (2019) did not find a relationship between RIT and VA in people with iAMD, although it was significantly associated with CS. This was the only study found in the featured AdaptDx literature that compared CS to RIT.

Few PROMs have been directly compared to RIT. One example includes the Low Luminance Questionnaire (LLQ) (Chen et al., 2019; Thompson et al., 2018; Yazdanie et al., 2017). Yazdanie et al. (2017) found a correlation between lower scores on the LLQ and RIT, with the strongest association found for the driving-related subscale. Despite BCVA yielding a statistically significant association with LLQ, the correlations found were marginally weaker than those found for RIT. Yazdanie et al. (2017) specifically reported that problems with night vision and low luminance may not be explained by traditional metrics of visual function measured in clinic. This correlation between the LLQ and RIT has also been found in another study (Thompson et al., 2018) and when compared to RIT progression over time (Chen et al., 2019). However, Thompson et al. (2018) found that the correlation between the LLQ and RIT in people with early and iAMD was not significant once the data were controlled for AMD severity, speculated to be due to the lack of late-stage AMD participants (Thompson et al., 2018).

In addition to the medical history questionnaire used by Laíns et al. (2018), the study also incorporated a food frequency questionnaire and the Rapid Assessment of Physical Activity test. After adjusting data for age and AMD stage, body mass index, taking AREDS supplements, and family history of AMD were significantly associated with delayed RIT and alcohol intake was significantly associated with RIT ≥ 6.5 minutes.

There were no studies comparing measurement of RIT with performance-based measures.

2.3.4 Other Adaptometers and Photostress Tests

For full details of the testing procedures used by studies with the AdaptDx, see Table 2.3. A total of 27 studies presented data collected using devices other than the AdaptDx. This included studies evaluating parameters of either cone, rod adaptation or both. Nineteen of these studies reported DA data collected using some form of dark adaptometer while six studies reported data collected using a photostress test protocol, whereby time is recorded for cone function (e.g. cone threshold or VA) to return to a specified level. Dimitrov et al. (2011 & 2012) assessed using both techniques. Eight studies used an adapted HVFP and eight utilised 'in-house' adaptometer, with methods developed by investigators. Other adaptometers, featuring in more than one study, included the MDAC (5 out of 27 studies) and the Macular Disease Detection MDD-2[®] device (Health Research Science, LLC, Lighthouse Pt, FL, USA) (2 out of 27 studies) (Richer et al., 2013, 2014). The Scotopic Sensitivity Tester-1 (SST-1; LKC Technologies, Gaithersburg, MD, USA) (Jackson, Felix, & Owsley, 2006), RCDA (Rodriguez et al., 2018), KOWA AS14B NightVision Tester (KOWA Optimed, Tokyo, Japan) (Richer et al., 2011), and Eger macular stressometer (EMS; Gulden Ophthalmics, PA, USA) (Wolffsohn et al., 2006) were used in one study each. What follows is a brief narrative of these papers.

The most frequently reported parameters of DA in studies that did not use the AdaptDx were RCB (10 out of 27 studies), cone absolute threshold (8 out of 27 studies), cone time constant (7 out of 27 studies) and RIT (7 out of 27 studies). Other parameters in the reviewed papers included rod absolute threshold (5 out of 27 studies) and 'second slope' or rod slope (5 out of 27 studies) which refers to the second phase of rod recovery when threshold data are fitted with a model based on the physiological process of DA (Lamb & Pugh, 2004).

There was a wide variation in procedures used by these studies. However, some similarities exist, such as the stimulus used. The most frequently reported was a 1.7-2° circular stimulus with a wavelength of ~500nm similar to the threshold stimulus seen in the AdaptDx (8 out of 27 studies). To examine cone-mediated DA, frequently reported stimulus wavelengths of ~620nm or 650nm were seen in the literature. Eight studies used a threshold location of 12° eccentricity, seven studies used a 6° location, six studies used an ~4° location, six studies used a foveal location, five studies used an 8° location and two studies used a 3° location (Rodrigo-Diaz et al., 2019; Tahir et al., 2018).

No cut-off times signifying the end of the DA assessment were reported for the photostress tests as the nature of the examination is for the patient to return to baseline sensitivity which occurs relatively quickly (Wolffsohn et al., 2006; Dhalla et al., 2007; Newsome & Negreiro, 2009). The most often reported cut-off time for the DA procedure was 30 minutes (7 out of 27 studies) followed by 60 minutes (3 out of 27 studies). Four of these studies reported that the recovery parameter was set to the maximum test time as a censored data-point, similar to the procedure followed by studies that used the AdaptDx.

Table 2. 3. Table of procedures adopted by included studies that did not use the AdaptDx

Procedure used	Frequency	Studies
Dark adaptometer or photostress device used		
Adapted Humphrey Automated Perimeter	8	Owsley, McGwin, Jackson, et al. (2006); Owsley, McGwin, Scilley, et al. (2006); Dhalla et al. (2007); Owsley et al. (2007); Gaffney, Binns and Margrain (2011), (2013); Robinson et al. (2018); Grant Robinson et al. (2019)
'in house' adaptometer	8	Dimitrov et al. (2008), (2011), (2012); Newsome & Negrerio (2009); Akuffo, Beatty, et al. (2017); Akuffo, Nolan, et al. (2017); Tahir et al. (2018); Rodrigo-Diaz et al. (2019)
Medmont Dark Adapted Chromatic perimeter	5	Fraser et al. (2016); Flynn, Cukras and Jeffrey (2018); Luu et al. (2018); Nguyen et al. (2018); Tan et al. (2019)
Macular Disease Detection MDD-2	2	Richer et al. (2013), (2014)
Scotopic Sensitivity Tester-1	1	Jackson, Felix, & Owsley (2006)
Roland Consult Dark Adaptometer	1	Rodriguez et al. (2018)
KOWA AS14B NightVision Tester	1	Richer et al. (2011)
Eger macular stressometer	1	Wolffsohn et al. (2006)
DA parameter(s)		

Rod-cone break	10	Jackson, Felix, & Owsley (2006); Owsley, McGwin, Jackson, et al. (2006); Owsley, McGwin, Scilley, et al. (2006); Owsley et al. (2007); Dimitrov et al. (2008), (2011); Gaffney, Binns and Margrain (2011), (2013); Tahir et al. (2018); Rodrigo-Diaz et al. (2019)
Cone absolute threshold	8	Owsley, McGwin, Jackson, et al. (2006); Owsley, McGwin, Scilley, et al. (2006); Owsley et al. (2007); Dimitrov et al. (2008), (2011); Gaffney, Binns and Margrain (2011), (2013); Tahir et al. (2018)
Cone time constant	7	Owsley, McGwin, Jackson, et al. (2006); Owsley, McGwin, Scilley, et al. (2006); Owsley et al. (2007); Gaffney, Binns and Margrain (2011), (2013); Grant Robinson et al. (2019); Rodrigo-Diaz et al. (2019)
Rod-intercept time (an estimate of the time duration for the rods to recover to an established criterion sensitivity (i.e. 5×10^{-3} cd/m ²) after focal bleaching)	7	Dimitrov et al. (2008), (2011); Fraser et al. (2016); Flynn, Cukras and Jeffrey (2018); Luu et al. (2018); Nguyen et al. (2018); Tan et al. (2019)
Rod absolute threshold	5	Owsley, McGwin, Jackson, et al. (2006); Owsley, McGwin, Scilley, et al. (2006); Owsley et al. (2007); Dimitrov et al. (2008), (2011)
Slopes of the 2 nd component of rod recovery	5	Owsley, McGwin, Jackson, et al. (2006); Owsley, McGwin, Scilley, et al. (2006); Owsley et al. (2007); Tahir et al. (2018); Rodrigo-Diaz et al. (2019)
Stimulus wavelength used		
500nm	8	Owsley, McGwin, Jackson, et al (2006); Owsley, McGwin, Scilley, et al. (2006); Owsley et al. (2007); Fraser et al. (2016); Flynn, Cukras and Jeffrey (2018); Luu et al. (2018); Nguyen et al. (2018); Tan et al. (2019)
620nm	2	Fraser et al. (2016); Flynn, Cukras and Jeffrey (2018)
650nm	2	Owsley et al. (2007); Owsley, McGwin, Jackson, et al. (2006)

Testing location

12° eccentricity	8	Owsley, McGwin, Jackson, et al. (2006); Owsley, McGwin, Scilley, et al. (2006); Owsley et al. (2007); Fraser et al. (2016); Flynn, Cukras and Jeffrey (2018); Luu et al. (2018); Nguyen et al. (2018); Tan et al. (2019)
6° eccentricity	7	Fraser et al. (2016); Flynn, Cukras and Jeffrey (2018); Luu et al. (2018); Nguyen et al. (2018); Tahir et al. (2018); Rodrigo-Diaz et al. (2019); Tan et al. (2019)
4° eccentricity	6	Dimitrov et al. (2011); Fraser et al. (2016); Flynn, Cukras and Jeffrey (2018); Luu et al. (2018); Nguyen et al. (2018); Tan et al. (2019)
fovea	6	Dimitrov et al. (2008), (2011); Gaffney, Binns and Margrain (2011), (2013); Robinson et al. (2018); Grant Robinson et al. (2019)
8° eccentricity	5	Fraser et al. (2016); Flynn, Cukras and Jeffrey (2018); Luu et al. (2018); Nguyen et al. (2018); Tan et al. (2019)
3° eccentricity	2	Rodrigo-Diaz et al. (2019); Tahir et al. (2018)

Maximum test-time

30 minutes	7	Dimitrov et al. (2008), (2011), (2012); Gaffney, Binns and Margrain (2013); Flynn, Cukras and Jeffrey (2018); Luu et al. (2018); Tan et al. (2019)
60 minutes	3	Owsley et al. (2007); Owsley, McGwin, Jackson, et al. (2006); Rodrigo-Diaz et al. (2019)

When a participant failed to recover

Allocated a time
(in most cases the maximum test time)

4

Gaffney, Binns and Margrain (2013); Nguyen et al. (2018); Rodrigo-Diaz et al. (2019); Tan et al. (2019)

Most studies that did not use AdaptDx demonstrated DA and photostress measurements to be altered in AMD (Jackson, Felix, & Owsley, 2006; Dhalla et al., 2007; Owsley et al., 2007; Newsome & Negrerio, 2009; Dimitrov et al., 2011, 2012; Gaffney, Binns and Margrain, 2011, 2013; Fraser et al., 2016; Flynn, Cukras and Jeffrey, 2018; Nguyen et al., 2018; Rodriguez et al., 2018; Grant Robinson et al., 2019; Rodrigo-Diaz et al., 2019). However, use of small cohorts and/or comparative control groups (≤ 10 people) (Dhalla et al., 2007; Gaffney, Binns and Margrain, 2011, 2013; Fraser et al., 2016; Flynn, Cukras and Jeffrey, 2018; Luu et al., 2018; Nguyen et al., 2018; Rodriguez et al., 2018; Rodrigo-Diaz et al., 2019) hampered many of these studies. Two studies suggested the techniques were not useful for AMD (Jackson, Felix, & Owsley, 2006; Wolffsohn et al., 2006). The following narrative focuses on notable results of the remaining studies.

Newsome and Negrerio (2009) assessed photorecovery in 144 controls, 118 people with non-neovascular and 36 people with neovascular using an in-house photostress test. Prolonged photorecovery was evident in people with non-neovascular AMD with GA compared to controls, but not if only drusen were present. Worsening non-neovascular AMD was shown to be accompanied by prolonged photostress recovery.

Using the adapted HVFP, Owsley et al. (2007) reported that 83 people with AMD severity ranging from early to late compared to 43 controls exhibited a significantly longer average RMDA, while cone-mediated DA did not differ between groups (Owsley et al., 2007). Conversely, Dimitrov et al. (2012) used the same modality and reported 293 people with hard and/or intermediate drusen and advanced fundus changes demonstrated significantly abnormal cone photostress recovery and RMDA when compared to 64 controls. However, these parameters did not discriminate between people with different severities of AMD (Dimitrov et al., 2012).

Grant Robinson et al. (2019), using an in-house system to assess cone adaptation in 19 controls and 81 people with AMD status varying from early to advanced, reported mean differences in cone time constant between groups. Authors speculated on the measurement being a potential biomarker for AMD (Grant Robinson et al., 2019). Fifty participants with early AMD, iAMD and contralateral neovascular AMD reported significant delay in mean cone tau when reassessed 12 months later in the ALIGHT trial (McKeague et al., 2014).

Various attempts at quantifying diagnostic accuracy of DA techniques other than AdaptDx in identifying early AMD have been undertaken. Two studies by Gaffney, Binns and Margrain (2011, 2013) aimed to identify pre-adapting light intensity and test location that generated the maximum separation in the parameters of cone DA and time to RCB between participants with early AMD and controls in the minimum recording time, using a custom built adaptometer (Gaffney, Binns and Margrain, 2011, 2013). Sample sizes were prohibitively small, but authors reported estimates of sensitivity and specificity at different thresholds and bleach conditions.

Dimitrov et al. (2008) assessed diagnostic capacity using ROC (AUC) assessments of rod and cone-mediated DA parameters using an in-house adaptometer in small samples of people (27 people with AMD of varying severity and 22 healthy peers). Cone-mediated parameters gave smaller AUC curves than rod-mediated parameters (Dimitrov et al., 2008). This result was replicated in a study in large numbers by the same team (Dimitrov et al., 2011). where RMDA was found to have the best diagnostic capacity (AUC, 0.93 ± 0.016), followed by cone photostress recovery (AUC, 0.85 ± 0.021). Tahir et al. (2018) used an in-house experimental adaptometer designed to present stimuli at two inferior field locations, (3° and 5.5°) measuring cone and RMDA. AUC was used to justify the optimal testing procedure (Tahir et al., 2018). A small number of 15 controls were used so estimates have little value in terms of assessing diagnostic suitability of this paradigm.

Few longitudinal studies were found. Rodriguez et al. (2018) primarily demonstrated cone-mediated visual function recovery, measured using a RCDA, could separate a small sample of 12 people with early AMD from 17 visually healthy controls with relatively high sensitivity and specificity (>85%) (Rodriguez et al., 2018). Repeatability and reproducibility of the RCDA was assessed in eight early AMD participants and four visually healthy participants. Both baseline cone threshold and recovery half-life were found to have a high degree of repeatability across all visits (intraclass correlation coefficient (ICC)=0.88; and ICC=0.93, respectively). RCB exhibited poor repeatability (ICC=0.40). A FU after 1 year illustrated high reproducibility of the adaptometer (baseline cone threshold (ICC=0.84) and the recovery half-life (ICC=0.84) (Rodriguez et al., 2018). However, the very small sample sizes leaves these data insufficient in judging true repeatability and reproducibility of the adaptometer.

Tan et al. (2019) evaluated longitudinal rod function at 14 different eccentricities using the MDAC perimeter in 23 controls, 12 people with iAMD and 13 people with SDDs. Over 12 months a significant decrease in rod recovery rate was found in the iAMD group (at the 12° test-point alone), while no significant changes were found in RIT across all groups. Wolffsohn et al. (2006) used a longitudinal study to show that EMS photostress recovery time did not predict those whose vision decreased over the following year compared with those among whom it remained stable. Moreover, this was the only study, not using AdaptDx, that compared visual function measurements (near and distance VA and CS) to rates of adaptation. However, no significant relationships were found.

Measurement of DA, not using AdaptDx, and photostress parameters have been shown to be altered, for example, in SDD presence (Fraser et al., 2016; Flynn, Cukras and Jeffrey, 2018; Luu et al., 2018; Nguyen et al., 2018; Tan et al., 2019), macular oedema (Newsome et al., 2009), serous macular detachment (Newsome & Negrerio, 2009), abnormal new vessels (Newsome & Negrerio, 2009) and inner segment ellipsoid zone disruption (Flynn, Cukras and Jeffrey, 2018). Level of macular pigment has not been found to correlate with photostress recovery (Akuffo, Nolan, et al., 2017). Furthermore, Rodrigo-Diaz et al. (2019) found that parameters of the DA curves such as the rod-mediated second slope and the RCB were associated with FAF changes and CFP grading. However, only a moderate correlation at best was found between cone time constant and measures from FAF and CFP grading.

Three studies, not using the AdaptDx, compared measurement of DA directly to PROM data. Owsley, McGwin, Scilley, et al. (2006) used measures of rod and cone-mediated DA to validate the newly developed LLQ, using the adapted HVFP. DA was assessed in 41 participants who exhibited normal retinal ageing and 84 participants with AMD of varying severity. An association was established between greater difficulties with emotional distress linked with low-luminance activities and worsening RMDA, including RCB. The highest correlation coefficients were seen between RMDA parameters (in particular rod threshold, defined as the average of the last three thresholds of the rod second slope) and the driving subscale. However, no LLQ subscales were associated with cone-mediated DA. A significant association between RMDA and LLQ results was also reported by Owsley, McGwin, Jackson, et al. (2006), who assessed the effect of a 30 day course of retinol on DA in 104 participants. It was found that the change from baseline to day 30 in the mobility subscale was significantly associated with changes in slope of the second component of rod recovery. No such correlations were found in cone parameters. A non-validated questionnaire on self-reported difficulties with glare recovery was reported by Wolffsohn et al. (2006) but no association between reported self-difficulties and EMS photostress recovery time was found.

The National Eye Institute Visual Function Questionnaire (NEI-VFQ) (Akuffo, Beatty, et al., 2017; Akuffo, Nolan, et al., 2017; Owsley et al., 2007; Richer et al., 2011), Veterans Affairs Low Vision Visual Function Questionnaire (VFQ-48) (Robinson et al., 2018), the EuroQoL-5D Instrument (EQ-5D) (Robinson et al., 2018) and Pittsburgh Sleep Quality Index (PSQI) (Robinson et al., 2018) also featured in the literature but were not compared to DA metrics.

There are no studies comparing measurement of DA with performance-based measures.

2.4 DISCUSSION

Our systematic review clearly indicates that a delay in measured rate of DA is associated with the presence of AMD; this is our main finding. Yet the evidence for measurement of DA being able to discriminate early AMD cases from elderly controls and differentiate between groups of varying AMD severity is weaker. Selection bias, problems with experimental design, poor reporting of precision of estimates and small sample sizes seem to characterise many of the studies that specifically considered diagnostic precision of the AdaptDx. Still, some of the studies, from the Owsley group for example, point to adequate levels of diagnostic precision (Owsley, McGwin, et al., 2016) and one well-designed cohort study indicates DA becomes impaired in some eyes with iAMD over time (Owsley, Clark and McGwin, 2017). Even here, there was wide variability in measurement of DA (RIT) at baseline and in the extent to which it increased over 24 months. We conclude that more longitudinal studies are required to test whether a measure of DA is truly a biomarker for changes in AMD severity.

The most common method used to assess DA in people with AMD was measuring RIT using the AdaptDx adaptometer (see Table 2.1). Since the protocol was first introduced by Jackson and Edwards (2008), the AdaptDx has been used frequently in RMDA research. Despite this, there is no consensus on how RIT is recorded for people who surpass the different, experimental cut-off times set and then how it is statistically assessed. To reiterate, this systematic review found the current evidence for the true diagnostic capabilities of this instrument to be quite weak. For example, no study specifically designed to satisfy STARD (Standards for the Reporting of Diagnostic accuracy studies) guidelines turned up in our review (Bossuyt et al., 2003; Fidalgo, Crabb and Lawrenson, 2015). In fact, the original Jackson and Edwards (2008) report, which has more than 60 citations at the time of writing, is often widely cited as evidence for the device being able to, “sensitively and specifically detect early AMD”, yet the sample sizes included were small (n=17 per group), and consequently CIs for diagnostic precision were wide.

Our systematic review indicates there is reasonably good evidence (Eisner et al., 1992) for people with drusen and/or atrophic changes having impaired slowed DA, particularly those with SDDs (Flamendorf et al., 2015; Fraser et al., 2016; Sevilla et al., 2016; Neely et al., 2017; Láíns et al., 2017; Flynn, Cukras and Jeffrey, 2018; Láíns, Miller, et al., 2018; Luu et al., 2018; Nguyen et al., 2018; Chen et al., 2019). Most published literature on DA is characterised by CFP which remains the gold standard for AMD diagnosis and grading, despite the recognised limitations of the device (Danis et al., 2013; Láíns et al., 2017). This review showed that recent studies utilised imaging devices (such as OCT) to further examine the evident structure-function relationship that has emerged in DA research (Chen et al., 2019; Láíns et al., 2017; Sevilla et al., 2016). Subsequently, further relationships with AMD macular anatomy and DA such as choroidal (Flamendorf et al., 2015) and retinal thickness (Chen et al., 2019) have been found, both at and beyond the DA testing location (Láíns et al., 2017).

This systematic review identified a number of studies which evaluated parameters of cone adaptation in addition to or instead of rod adaptation. This was either through direct assessment of parameters of the cone branch of the DA function or by assessment of cone photostress recovery (see Table 2.3). Whilst Owsley et al. (2007) reported a greater deficit in rates of rod than cone adaptation in people with AMD, other studies included in this review did find evidence of significant delays in cone adaptation (Dimitrov et al., 2008, 2011, 2012; Gaffney, Binns and Margrain, 2011, 2013; Robinson et al., 2018; Rodriguez et al., 2018; Tahir et al., 2018; Grant Robinson et al., 2019; Rodrigo-Diaz et al., 2019). This has been suggested to have clinical implications in light of the more rapid rate of cone than rod sensitivity, and the resultant reduction in the clinical testing time (Gaffney, Binns and Margrain, 2013).

Our review revealed some other findings. Only a small number of the studies directly compared DA to a measure of visual function, and findings were mixed (Beirne & McConnell, 2019; Chen et al., 2019; Flamendorf et al., 2015; Láíns, Miller, et al., 2018). Whilst lack of concordance with other measures of visual function can be interpreted as offering new information about the functional deficits of the

condition, this notion needs to be formally tested in a prospective study. This review highlighted the importance to control for age as it is a confounder in case control and other observational studies (Neely et al., 2017; Sevilla et al., 2016). We noticed that some studies did not use an age-matched or age-related control group often resulting in large differences in ages between groups (Jackson, Scott, et al., 2014).

Association between measurement of DA and subjective complaints of visual dysfunction were first reported more than 30 years ago (Brown & Kitchin, 1983). Yet, this review highlights a surprising lack of studies investigating the relationship between PROMs and DA parameters. A series of notable exceptions led to Owsley, McGwin, Scilley, et al. (2006) developing a 32-item LLQ, which was evaluated in some of the studies included in this review (Owsley, McGwin, Jackson, et al., 2006; Owsley, McGwin, Scilley, et al., 2006; Yazdanie et al., 2017; Thompson et al., 2018; Chen et al., 2019). The LLQ builds on reports from people with AMD that visual function is more impaired under low lighting conditions (Feigl et al., 2011; Finger et al., 2011; Owsley, Clark, et al., 2016; Owsley, McGwin, Scilley, et al., 2006). Interestingly, Owsley and team found a lack of correlation between the outcomes from the PROM and cone-mediated DA in two separate studies (Owsley, McGwin, Jackson, et al., 2006; Owsley, McGwin, Scilley, et al., 2006), which may be surprising as cone adaptation is important in early adjustment in vision when moving from high to low level of luminance. Moreover, we did not find a single study looking at how measures of DA could be associated with people with AMD performing real world visually guided tasks, or surrogates of them (sometimes referred to as performance-based tasks). Such tasks could measure face-recognition, search performance, visuomotor control or mobility (Taylor, Smith and Crabb, 2017; Taylor et al., 2018; Taylor et al., 2020). For example, DA would be expected to impact mobility in low lighting, and this could be a promising area of research.

Our review indicates other gaps in the literature too. Many of the studies used the AdaptDx instrument (21 out of 48) but surprisingly, there was little data on the repeatability and reproducibility of measurements from this device. Apart from the Flamendorf et al. (2015) study there was no data on the practise effect or learning effect with the task; this is surprising given the psychophysical nature of the test.

We consider our systematic review to be timely. The most recent prior assessment of the literature on examination of DA in AMD was published, as part of a larger review of the literature on visual function tests in AMD, 14 years ago (Hogg & Chakravarthy, 2006). We found 48 new studies published since then on DA and photostress testing in people with AMD that satisfied the inclusion and exclusion criteria for our review. In addition, new adaptometers have been introduced and are now being used clinically. Our review and the results reported have some limitations. First, this review combined observations on photostress testing and alternative DA procedures to AdaptDx which differ in their experimental design. This was necessary due to the inherent heterogeneity of DA assessment. Second, only studies published in peer-reviewed journals were included and we excluded protocols and non-English language manuscripts. Third, we limited our search to studies including an evaluation of the

kinetics of DA and, as such, we did not consider studies which evaluated thresholds in the absence of a prior photostress. Furthermore, pachychoroid diseases have been brought to attention as a possible explanation for AMD pathogenesis and are thought to be clinically separate from drusen-driven AMD (Yamashiro et al., 2020; Zhang & Sivaprasad, 2021). As a result, DA measurement may be different in AMD associated with pachychoroid, a factor not considered in this systematic review which requires further analysis.

2.5 CONCLUSION

This systematic review was the first in 14 years to assess the growing literature in DA assessment in AMD. This review highlights the variety of experimental methodology currently used in the field. Assessment of DA is a very promising measure of visual function and it may play an important role in early detection and monitoring of AMD in clinical practice and in experimental studies.

We have highlighted the need for further evidence of the discriminatory power of DA measurement to better differentiate early-stage AMD and normative macular ageing. Further data on repeatability, reproducibility, practice effects and the true diagnostic precision of RIT as recorded by AdaptDx is needed too. There is reasonably good evidence on how structural abnormalities such as SDDs negatively impact DA. However, more research on the relationship between DA and VA, CS, measures from microperimetry, PROMs and performance-based measures are required to see how this assessment fits in with the spectrum of measuring visual function in AMD.

2.6 UPDATE TO SYSTEMATIC LITERATURE REVIEW

The above systematic review literature search identified publications published between 01/01/2006 and 27/01/2020. To identify any new and relevant work appearing since then, the search was replicated to identify literature published between 28/01/2020 and 1/10/2022. An additional 16 studies meeting inclusion criteria and what follows is a brief narrative summary of the main findings of the 16 studies, relevant to this review.

Table 2. 4 Dark adaptation methodology adopted by the 16 studies published 2020-2022

Procedure used	Frequency	Studies
Device used		
AdaptDx/AdaptRx	11	Owsley et al. (2022); Hess et al. (2022), Lad et al. (2022); Grewal et al. (2022); Lains et al. (2022); Allingham et al. (2021); Mendez et al. (2021); Lee et al. (2020); Echols et al. (2020); Gunvant Davey et al. (2020); Kar et al. (2020)
Medmont Dark Adapted Chromatic perimeter	4	Jeffrey et al. (2022); Guymer et al. (2021); Uddin et al. (2020); McGuinness et al. (2020)
In-house photostress test	1	Lott et al. (2021)
DA parameter(s)		
Rod-intercept time (an estimate of the time duration for the rods to recover to an established criterion sensitivity (i.e. 5×10^{-3} cd/m ²) after focal bleaching)	15	Owsley et al. (2022); Hess et al. (2022), Lad et al. (2022); Grewal et al. (2022); Lains et al. (2022); Allingham et al. (2021); Mendez et al. (2021); Lee et al. (2020); Echols et al. (2020); Gunvant Davey et al. (2020); Kar et al. (2020); Jeffrey et al. (2022); Guymer et al. (2021); Uddin et al. (2020); McGuinness et al. (2020)
Area under the (recovery) curve	3	Mendez et al. (2021); Lains et al. (2022); Hess et al. (2022)
Cone decay, cone plateau, time to rod-cone break, rod adaptation rate	1	Hess et al. (2022)
Cone sensitivity, final threshold, RITslope (measured from the first plateau prior to the rod-cone break)	1	Uddin et al. (2020)

time required to identify all three letters of the triplet on the MARS card

1

Lott et al. (2021)

Bleaching magnitude

82-83% photoreceptor bleach using a flash of 5.8×10^4 scotopic cd.s/m² intensity or equivalent for 0.25-milliseconds

7

Owsley et al. (2022); Hess et al. (2022), Grewal et al. (2022); Lee et al. (2020); Echols et al. (2020); Guvant Davey et al. (2020); Kar et al. (2020)

76% photoreceptor bleach using a flash of 1.8×10^4 scotopic cd.s/m² intensity for 0.8 milliseconds

3

Mendez et al. (2021); Lains et al. (2022); Lad et al. (2022)

20-30% photoreceptor bleach using customized Ganzfeld stimulator

4

Jeffrey et al. (2022); Guymer et al. (2021); Uddin et al. (2020); McGuinness et al. (2020)

Testing location

5° on the inferior vertical meridian

11

Owsley et al. (2022); Hess et al. (2022), Lad et al. (2022); Grewal et al. (2022); Lains et al. (2022); Allingham et al. (2021); Mendez et al. (2021); Lee et al. (2020); Echols et al. (2020); Guvant Davey et al. (2020); Kar et al. (2020)

4° superior and inferior to the fovea

4

Guymer et al. (2021); McGuinness et al. (2020); Uddin et al. (2020); Jeffrey et al. (2022)

6° superior and inferior to the fovea

3

Guymer et al. (2021); McGuinness et al. (2020); Uddin et al. (2020)

8° superior and inferior to the fovea

4

Guymer et al. (2021); McGuinness et al. (2020); Uddin et al. (2020); Jeffrey et al. (2022)

12° superior and inferior to the fovea

3

Guymer et al. (2021); McGuinness et al. (2020); Uddin et al. (2020);

unclear 1 Lott et al. (2021)

Maximum test-time

20 minutes 6 Lad et al. (2022); Grewal et al. (2022); Lains et al. (2022); Allingham et al. (2021); Mendez et al. (2021); Lee et al. (2020); Guntant Davey et al. (2020)

30-45 minutes 6 Owsley et al. (2022); Jeffrey et al. (2022); Hess et al. (2022), Guymer et al. (2021); Uddin et al. (2020); McGuinness et al. (2020)

unclear 3 Lott et al. (2021); Echols et al. (2020); Kar et al. (2020)

When a participant failed to recover

Allocated an RIT
(in most cases the maximum test time) 3 Lad et al. (2022); Grewal et al. (2022); Mendez et al. (2021)

Participants were offered a different testing protocol using a reduced bleach 2 Hess et al. (2022); Allingham et al. (2021)

unclear 2 Owsley et al. (2022); Jeffrey, et al. (2022); Hess et al. (2022), Lains et al. (2022); Guymer et al. (2021); Lott et al. (2021); Lee et al. (2020); Echols et al. (2020); Guntant Davey et al. (2020); Kar et al. (2020)

2.6.1 Update on Testing Procedures

Eleven out of the 16 studies reviewed utilised the AdaptDx and nearly all of the 16 studies measured the RIT. Therefore, the methodology was near-identical to the 21 procedures reviewed prior in section 2.3.1. This highlights the retained relevance of this systematic literature review as overall, no major changes in the methodology to assess RMDA in people with AMD has yet occurred. See Table 2.4 for the full details of the procedures adopted by the 16 studies.

A metric that has been used several times in the assessment of RMDA in the last two years and suggested as an alternative to RIT, is the AUC. This is justified as a more suitable metric compared to the frequently used RIT as sometimes recovery cannot be recorded within a maximum allowed time for the test (Jackson, Clark, et al., 2014; Owsley, Clark and McGwin, 2017; Binns et al., 2018). Furthermore, the AUC is a familiar and standardised statistic used frequently in ROC analysis. Three out of the 16 studies adopted the AUC as well as the RIT as method to assess RMDA (Mendez et al., 2021; Lains et al., 2022; Hess et al., 2022) and Hess et al. directly compared the two parameters. Hess and colleagues evaluated both cone and rod-mediated metrics from 1329 DA curves of 191 people with AMD and controls and found RIT had the greatest association with age, AMD severity, and SDDs ($R^2=0.38$) (Hess et al., 2022). It appears from the recent literature that the RIT is here to stay for a while longer. Indeed, new imaging biomarkers have recently been discovered using deep learning algorithms in association with RIT, providing further justification for its use as an outcome measure in clinical trials (Lee et al., 2020).

2.6.2 Update on Diagnostic Precision, Repeatability and Longitudinal Studies

Only two studies examined repeatability of DA metrics measured in people with AMD in the last two years. Hess et al. (2022) compared cone and rod-mediated metrics from the AdaptDx including cone decay, cone plateau, RCB, RIT rod adaptation rate (S2), and AUC. The authors assessed intrasession reliability via Bland Altman analysis between tests conducted roughly 2-weeks from each other in a large cohort of 191 people with varying levels of AMD. RIT illustrated the greatest reliability ($ICC=0.88$) out of all the parameters. Hess et al. highlighted that these findings emphasise the RIT as suitable for an outcome measure to be used in clinical trials (Hess et al., 2022).

Uddin et al (2020) was the second study that assessed test–retest variability of both cone-mediated and RMDA, this time using the MDAC adaptometer. The authors evaluated repeatability in a small sample of 12 people (n4 with iAMD without SDDs; n5 had iAMD with SDDs and n3 controls) and established a repeatability coefficient for the RIT as 7.6 minutes, along with 3.9 dB for cone threshold,

5.3 dB for final threshold and 0.54 min/degree for RITslope. Not unlike the other studies featured in this SR, a very small sample size hampered the strength of this analysis.

A well-designed (albeit single centre) longitudinal study of early AMD has recently been published on data from the Duke FEATURE study, the aim of which was to assess functional biomarkers to describe disease progression in early AMD and iAMD over a period of 24-months. These tests included BCVA, LLVA, MP, cone contrast tests and DA. Seventy people with early AMD, iAMD and healthy controls completed the 24-month study (n=22, n=31 and n=17, respectively). See Table 2.4 for procedural details. The study concluded that RMDA in people with iAMD revealed slow functional decline over the studied two year period and that a structure–function relationship was demonstrated, potentially impacted by genetic risk factors. The authors identify that DA is a promising an outcome measure to be potentially utilised in clinical trials. However, there remain few appropriate studies on the diagnostic power of RIT.

2.6.3 Update on Relationship with Other Measures

Overall, there are no new, striking findings in the 16 reviewed studies in terms of DA parameter’s relationship with other measures. This again emphasises that the findings of this systematic literature review remain applicable. As expected, studies from the past 2-years demonstrated DA measurements to be altered in AMD (Owsley et al., 2022; Jeffrey et al., 2022; Hess et al., 2022; Lad et al., 2022; Grewal et al., 2022; Guymer et al., 2021; Lott et al., 2021; Echols et al., 2020; McGuinness et al., 2020). This reaffirms this Chapter’s main finding that a delay in measured rate of DA is associated with the presence of AMD. Furthermore, studies that examined the evident structure-function relationship that has emerged previously in DA research have continued to find SDD presence in people with AMD correlated with slowed RIT (Owsley et al., 2022; Grewal et al., 2022). Furthermore, Echols et al. (2020) also found delayed RMDA was strongly associated with hyperreflective foci and hyperreflective specs. This highlights that the future of DA research will likely continue to utilise imaging devices such as OCT to further elucidate structure-function relationships in people with AMD.

3 CHAPTER 3; OPTIMISING ASSESSMENT OF DARK ADAPTATION DATA USING TIME-TO-EVENT ANALYSIS

3.1 INTRODUCTION

As indicated in Chapter 1, measuring DA is fraught with issues around excessive test duration and minimal standardised testing methods (Jackson, Scott et al, 2014). However, more efficient dark adaptometers have been developed and are now commercially available. For example, the AdaptDx dark adaptometer has been used in a number of clinical and research studies (Jackson and Edwards, 2008; Jackson, Scott, et al., 2014; Owsley, McGwin, et al., 2016; Láins et al., 2017; Owsley, Clark and McGwin, 2017).

Assessment of DA in AdaptDx relies on a precise measurement of RIT. At times, especially for advanced AMD cases but sometimes even for those with early and iAMD, recovery cannot be recorded within a maximum allowed time for the test (usually 20-30 minutes) (Jackson, Clark, et al., 2014; Owsley, Clark and McGwin, 2017; Binns et al., 2018). In Chapter 2, it was highlighted that studies statistically analysing RIT data relied upon standard t-tests (Owsley et al., 2014; Owsley, Huisingh, et al., 2016; Owsley, McGwin, et al., 2016; Láins et al., 2017; Cocce et al., 2018; Láins, Park, et al., 2018) or non-parametric equivalents (Jackson, Clark, et al., 2014; Jackson, Scott, et al., 2014; Flamendorf et al., 2015; Owsley, Clark and McGwin, 2017). However, the t-test may not be appropriate when capping distorts the distribution of data. Furthermore, the value of non-parametric tests is limited by their relative lack of power and inability to generate CI. Resampling methods, such as bootstrap techniques, could provide p-values and CIs without the distributional assumptions of asymptotic parametric tests. Yet these methods do not address the issue of bias in the estimates arising from truncation/censoring in the data. Another approach is to consider the failure to recover within the test time as a categorical variable (Flamendorf et al., 2015), although this limits the applicability of the analysis to longitudinal studies, where it is desirable to monitor a change in the variable over time.

In this chapter, time-to-event analysis, commonly referred to as survival analysis, was suggested to be applied to RIT data. Time-to-event analysis is widely used in medical literature (George, Seals and Aban, 2014) and is a method for assessing the length of time until the occurrence of a defined endpoint of interest. Here, time-to-event analysis was used to describe the cumulative proportion of people within each group reaching the rod intercept as a function of time after cessation of the bleach. It was hypothesised this method would offer better statistical power than standard techniques when applied to these types of data. Potential gains would translate into fewer study participants (reduced sample sizes) for trials and studies using measures of DA. A previously published dataset was used to illustrate the method and test the hypothesis (Binns et al., 2018). In addition, a web-based app was

designed and published to implement this technique; this can be freely used by researchers and clinicians wanting to compare groups of people for which RIT values have been measured (<https://bethanyelarahiggins.shinyapps.io/Time-to-EventAnalysis/>).

The work presented in this chapter is published as a paper in *Scientific Reports* (Higgins, Montesano, et al., 2021), see list of supporting publications. The co-authors of this work are Bethany E. Higgins (BEH), Giovanni Montesano (GM), Alison M. Binns (AMB) and David P. Crabb (DPC). The design of the study was conceived by BEH and DPC. The data retrospectively analysed was sourced from AMB on behalf of the authors (Binns et al., 2018). All data analysis, including the conception and development of the published app, was conducted by BEH with support from GM. The paper was written by BEH, and reviewed, edited, and approved by all authors.

3.2 METHODS

3.2.1 Participant Selection

We retrospectively analysed data collected for a previous study by Binns et al. (2018). Institutional research ethical approval was approved by School of Health Sciences, City, University of London. All procedures adhered to the tenets of the Declaration of Helsinki and were carried out in accordance with relevant guidelines and regulations. All the data were anonymised for this study and informed consent was obtained from all subjects. Details on recruitment and inclusion/exclusion criteria can be found in the original paper (Binns et al., 2018). In brief, age-similar visually healthy controls and people with early AMD, iAMD and non-central GA were recruited. Inclusion criteria consisted of BCVA of logMAR 0.7 or better in study eye, >55 years of age, adequately clear ocular media and acceptable pupillary dilation and fixation to allow for quality fundus photography. Exclusion criteria included significant disease, other retinal pathology in the study eye, or a history of medication known to disturb visual function (Binns et al., 2018). For the scope of our analysis, we did not distinguish between different stages of AMD.

3.2.2 Dark Adaptation Procedure

For the purposes of our work, we used the values obtained with the optimal testing conditions as determined by Binns et al. (2018) (76% bleach at 12° eccentricity). Full details of the DA procedure have been published previously (Binns et al., 2018). Briefly, prior to assessment the participant was dark adapted for 30 minutes in a darkened room. An appropriate spherical lens was used (+3.00 DS plus spherical distance prescription) and a patch placed over the non-tested eye. The participant then

viewed a fixation stimulus from a chin rest. Alignment was monitored using an infra-red camera and adjusted by the examiner. Pupil diameter was measured before the administration of the bleaching, 505nm bleaching flash (4° diameter, centred 12° in the inferior visual field, 0.8ms duration, 1.8×10^4 scot cd/s.m², bleaching an estimated 76% of rod visual pigment (Pugh, 1975a). The test stimulus was subsequently shown at the same location as the bleach. Fifteen seconds after the photoflash, the threshold was measured for a 505-nm, 2° diameter target starting. The participant was asked to keep looking at the fixation light and to press a response button when a flashing target became visible. A modified staircase procedure was utilised to estimate the threshold until the RIT was attained or the cut-off time was reached (30 minutes). A 15 second break was given after each threshold. If the RIT was not reached within the test, it was set at the maximum test duration (30 minutes). As in previous studies utilising the AdaptDx (Jackson, Scott et al, 2014), if fixation errors exceeded 30% of threshold points, the test was deemed unreliable (Binns et al., 2018).

To further demonstrate the applicability of our methodology, the same analysis was conducted on a second, supplementary dataset obtained from Binns et al. (2018) (76% bleach at 5° eccentricity). The DA protocol used was identical except the 505nm bleaching flash was centred at 5° in the inferior visual field.

3.2.3 Time-to-event Analysis

We used a parametric time-to-event model widely used in medical literature to describe the time taken for an event such as tumour recurrence or time to death after a treatment (George, Seals and Aban, 2014). Here we use the approach to describe the cumulative proportion of people within each group reaching the rod intercept as a function of time after cessation of the bleach. RIT was not treated as the event itself, but rather the time taken for the participant to recover sensitivity to a stimulus intensity of 5×10^{-3} scot cd/m² (a decrease in threshold of 3 logarithmic units). In this respect, the event recovery can be used in a time-to-event analysis since the RIT is for all intents and purposes the time passed until such an event is observed. In other words, we model RIT values within each group as the cumulative occurrence of recovery over time; a cumulative distribution function $F(t)$. RIT values can be plotted as survival curves using a Kaplan-Meier estimator (Lin & Zelterman, 2002). These curves report the time from bleaching on the horizontal axis and the percentage of recovered subjects on the vertical axis. This is a step graph and changes occur at each observed RIT (downward step). An example of how the survival curve can be plotted from RIT values is reported in Figure 3.1.

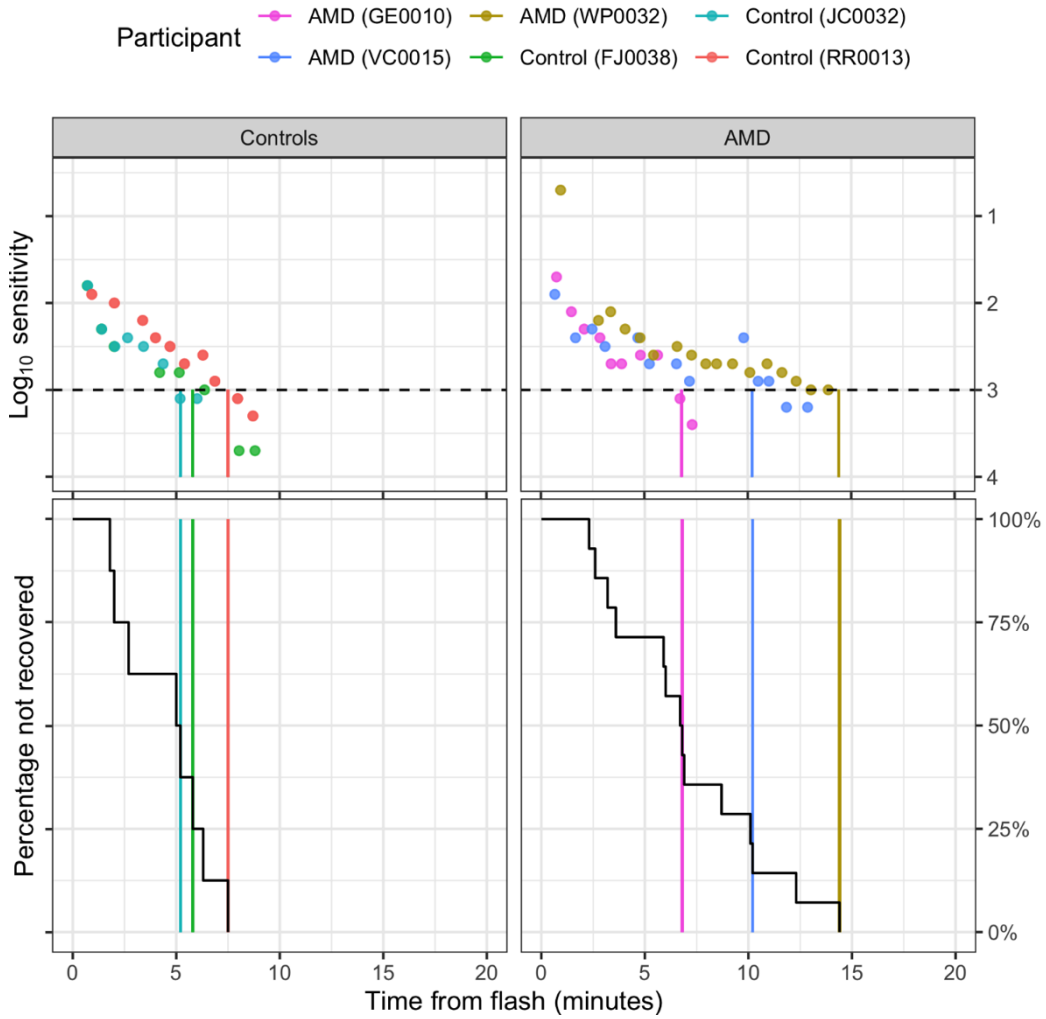


Figure 3.1 The change in Log₁₀ sensitivity for three control subjects and three patients with AMD is plotted in the top panel (filled dots) with the corresponding RIT values (vertical strokes) provided by the device. The horizontal dashed line represents the 3 log-step change in sensitivity used by the device to define the event (recovery from bleaching). The RIT time for each recovery “event” is used to build the survival curves (bottom panels). In this case, the vertical-coloured lines also identify the same RIT values recorded for the curves plotted in the top panels. Notice how each vertical line corresponds to a downward step change in the survival curve (in black). The same process is applied for all RIT values in the dataset to calculate the other step changes that make up the rest of the survival curve.

Its inverse is the time-to-event function $S(t) = 1 - F(t)$. The function $F(t)$ can be modelled as the cumulative distribution function of a variety of distributions. One of the most common is the Weibull distribution, which is then assumed to be the distribution of the observed times-to-event. This is called Accelerated Time Failure model (Equation 1).

Equation 1.
$$\log(T) = \beta_0 + \beta_1 * Group + \sigma W$$

Here T represents the time to recovery, Group denotes the assignment of the subject i (for example AMD or Control), σ denotes a scale factor for the errors and W is the assumed distribution that has $F(t)$ as cumulative distribution function (Weibull in this case).

Additional predictors and interactions can be added to the right-hand side of the function if needed as in a multivariable linear regression (a treatment arm, for example). In our scenario, the expectation is the AMD group will have a proportional increase in “time-to-event time” since more time is needed for the event (recovery from bleaching) to happen, i.e. longer RIT values. One advantage of parametric time-to-event models (as the one proposed) over a semi-parametric Proportional Hazard model (Cox model) is that the baseline time-to-event function is explicitly modelled, thus allowing estimates and inference on time-to-event times. Moreover, delayed/accelerated recovery in one group with respect to the baseline level (for example, AMD with respect to Controls) can be simply calculated as $\exp(\beta_1)$, where $\exp()$ denotes the exponential function. So, for example, a value of $\beta_1 = 0.7$ indicates a two-fold increase in recovery time.

Handling censored data is a key feature of time-to-event analysis (Efron, 1977). In our application, right-censoring happens when the RIT is longer than the maximum time allowed for the test; this can be denoted using a binary variable, commonly assuming a value of 1 when the RIT has been recorded and a value of 0 otherwise. In our dataset the maximum recording time was set at a lengthy 30 minutes (Binns et al., 2018); no subject exceeded this limit. In other studies, especially in a clinical use scenario, this limit is likely lower, e.g. 20 minutes. Therefore, in order to demonstrate how the time-to-event analysis can be used with censored data, we transformed the data with a multiplicative constant ($c=3$) and subsequently capped the data at 20 minutes (see Figure 3.2). This allowed us to explore how the estimates from different modelling approaches change between the capped and the full series. In this specific case the censoring is non-random, as it is set by a predetermined stopping time. The strength of time-to-event analysis is that, using censoring, it is still possible to extract information from unrecorded RIT values as time-to-event analysis can account for the fact that, at termination time (20 minutes), a percentage of subjects have not recovered from bleaching. By contrast, any other method would require to either exclude participants with unrecorded RIT values or to impute the values for the missing data.

3.2.4 Other Parametric Methods

The time-to-event model was compared with two parametric models, the t-test and a generalised linear model (GLM). Both make strong assumptions concerning data structure, such as the independence of each data point and the correct scale of the data. For the t-test, both means of the populations should follow normal distributions and homogeneity of variance is assumed. The GLM

does not require these assumptions. Of course, the former can be interpreted as simple linear model, where the predictor is a binary factor with only two classes (Group). It can be formulated as Equation 2.

Equation 2.
$$RIT_i = \beta_0 + \beta_1 * Group_i + \epsilon_i$$

In this case, the response variable is the RIT for the subject i , the parameter β_0 (Intercept) represents the mean RIT for the baseline Group (Controls in this case), the parameter β_1 represents the estimated difference between the two groups, and ϵ_i is the error, assumed to be Gaussian. This linear model formulation can be extended to GLM, which uses a link function for the mean of the response (Faraway, 2016) (in this specific case, the natural logarithm). This effectively allows the model to have a Gamma distribution (instead of Gaussian) for the error, accounting for the skewed distribution of the data. Note that this is different from a log-transformation of the data: the link function is applied to the mean of the response and is therefore invertible, i.e., the inverse log of the mean response from the GLM produces the corresponding estimate of the RIT in the linear scale. On the contrary, with a log-transformation of the data, the model will estimate the mean of the log-response, which cannot be converted back to the mean of the original response. For both these models, censored data are replaced by the maximum recordable value (20 minutes or 30 minutes).

3.2.5 Power Calculation

Power calculations were used to compare the efficiency of the different statistical approaches. To avoid distributional assumptions on the real data as much as possible, we used a bootstrap procedure to estimate the power of the three methods at different sample sizes. We used random sampling, with replacement, with N subjects from the controls and the same number from the AMD group. Due to replacement, the same subject could be extracted multiple times and arbitrarily large samples could be produced. At each extraction, the three methods were applied and the p-value on the null hypothesis of no difference between RIT in people with AMD and controls from each method was recorded. The sampling was repeated 10000 times at different sample sizes (N from 3 to 50 per Group). The power for each value was calculated as the proportion of extractions where the p-value was below 0.05. As a clarification, the bootstrap was not used to calculate the p-value, which was instead derived from each parametric test, but just to generate the random samples on which the tests were performed. We have used a similar approach in previously published work (Montesano et al., 2019) to perform a post-hoc power calculation.

For our main analysis, when computing the p-values, we adopted the statistical convention for each model: t-test for the parameter derived from the linear model and GLM and the Wald test for the parameters derived from the survival analysis model (Therneau, 2014). However, to prove that the differences in power between the three methodologies were not due a different calculation of the p-values, we performed an additional power analysis using the Wald test for all the models.

3.2.6 Web Application

We designed a purpose written, interactive application to demonstrate the time-to-event analysis technique for RIT data. The application uses Rstudio's Shiny framework and is available in the public domain. It allows a user to upload their own RIT data in .csv format to use the statistical test and produce a time-to-event plot to illustrate the data. The application has the option to use the data illustrated in this paper: (<https://bethanyelurahiggins.shinyapps.io/Time-to-EventAnalysis/>).

All analyses were performed in R 3.5.2 (<http://www.r-project.org/>) under R Studio, version 1.1.463 (RStudio, Boston, MA, USA). For time-to-event analysis the parametric time-to-event regression provided in the Survival package for R was implemented (Lin & Zelterman, 2002). Figures were generated using the ggplot2 package (Wickham, 2016).

3.3 RESULTS

Table 3.1 Clinical characteristics of all participants.

Participant ID	logMAR test eye	AMD status test eye	AMD status fellow eye	RIT (minutes)
RR0013	0.16	1	1	7.5
JE0008	0.00	1	1	6.3
JC0032	0.16	1	1	5.2
GM0035	-0.04	1	1	1.8
BW0037	0.00	1	1	5.0
MI0033	0.16	1	1	2.7
SF0034	0.10	1	1	2.0
FJ0038	0.16	1	1	5.8
KM0003	0.16	2	2	3.6
DH0005	0.44	3	3	2.6
MM0006	0.20	3	3	6.7
GE0010	0.00	3	3	6.8
PS0012	0.20	3	3	6.9
GD0014	-0.04	3	3	6.0
VC0015	0.02	3	4	10.2
PN0009	0.06	3	4	5.9
JB0018	0.00	3	3	10.1
WP0032	0.40	3	3	14.4
JG0027	0.20	4	4	12.3
EC0011	0.44	4	4	8.7
AF0028	0.50	4	4	3.2
PF0031	0.12	4	4	2.3

AMD graded according to the Beckman classification (Ferris et al., 2013). Eyes were grouped as normal ageing (1), early AMD (2), iAMD (3), and late AMD (4) (GA and/or neovascular lesions)

Of those who participated in the previous study, 14 people with variable stages of AMD and eight age-similar controls provided valid data for the 76° bleach, 12° eccentricity test condition and were used to determine optimal test conditions for acquiring RIT with the AdaptDx instrument. The study reported no significant difference in age (mean [SD] controls: 69±8 years; mean [SD] AMD: 71±8 years, independent samples t-test, $p=0.73$) between control participants and those with AMD (Binns et al., 2018). Table 3.1 summarises the clinical characteristics of the included participants.

Fitted curves are shown in Figure 3.2. The central estimates for the three methods are reported in Table 3.2. A statistically significant difference (at $p<0.05$) between groups was only detected with the time-to-event model (Table 3.2) in the original data. The p-values for the original and the scaled uncapped RITs were identical, the second being simply the same data scaled by a constant. With capped data, both the GLM and the linear model yielded very biased estimates, especially in the AMD group (larger number of capped values). In contrast, the results of the time-to-event model were much closer to the values obtained without capping. With capped data, the CIs were larger for the time-to-event model but smaller for both the GLM and the linear model.

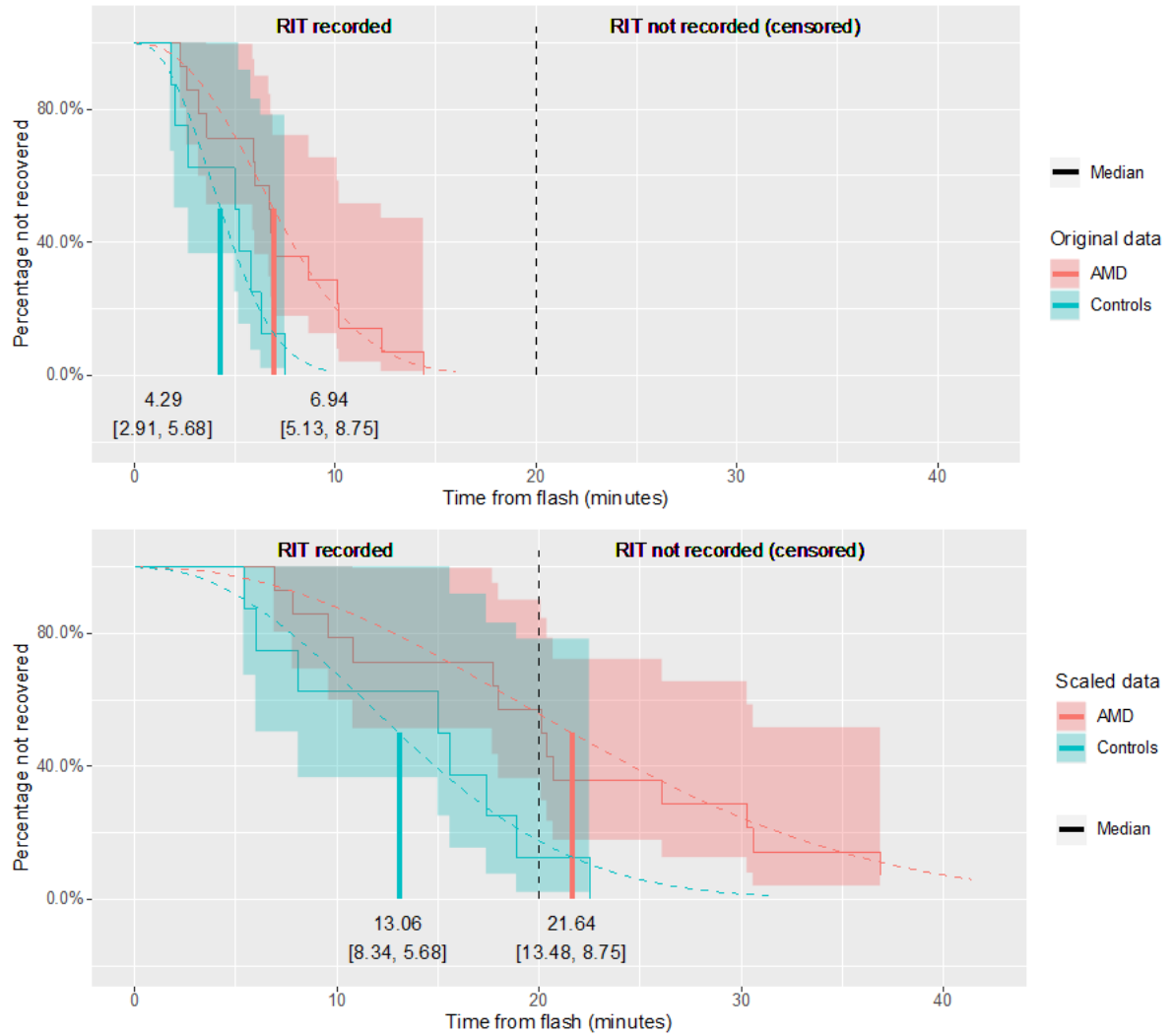


Figure 3.2 Empirical curves for the original (top) and the transformed (bottom) data, scaled to illustrate RITs that surpass a cut off time. The vertical dashed line indicates the capping limit of 20 minutes. For the scaled data, both the fitted survival curves from the mode (dashed curves) and the median values (vertical solid lines) were calculated from capped data. However, the time-to-event model fits the data well even beyond the cut off time. For the scaled AMD data, the time-to-event model correctly predicts a median value beyond the capping limit.

Table 3.2 Central estimates [95% CI] of RIT values (in minutes) with the three methods considered

		Estimate [95% CIs]		
		AMD	Controls	p-value
Original data	Survival model	6.94 (5.13, 8.75)	4.29 (2.91, 5.68)	0.014
	GLM	7.12 (5.26, 8.98)	4.54 (5.26, 8.98)	0.055
	Linear model	7.12 (5.44, 8.81)	4.54 (5.44, 8.81)	0.085
Scaled data, uncapped	Survival model	20.81 (15.38, 26.25)	12.88 (8.72, 17.03)	0.014
	GLM	21.36 (15.78, 26.95)	13.61 (15.78, 26.95)	0.055
	Linear model	21.36 (16.31, 26.42)	13.61 (16.31, 26.42)	0.085
Scaled data, capped	Survival model	21.64 (13.48, 29.79)	13.06 (8.34, 17.79)	0.066
	GLM	16.49 (13.33, 19.64)	13.3 (13.33, 19.64)	0.199
	Linear model	16.49 (13.63, 19.34)	13.3 (13.63, 19.34)	0.202

For the linear model (t-test) and the GLM, the mean is reported. For the survival model the estimate for the median is reported. The third column reports the effect [95% CIs] measured by the three methods, which is the basis for the calculation of the p-value. Significant p-values at an alpha level of 0.05 are shown in bold. The effect is the ratio between the mean RITs of AMD and controls for the survival model and the GLM, and the difference between the two groups for the linear model. Notice how the estimate from the survival model is much less affected by capped values.

When we investigated the power of the three methods via bootstrap, the time-to-event model was superior. This is demonstrated by the power curves as a function of sample size in Figure 3.3. The number of subjects needed per group to detect a significant difference ($\alpha=0.05$) at 80% power are reported in Table 3.3. When censored observations were introduced, the power of all methods was decreased, but the time-to-event model still performed better than the linear model and GLM, and this is noteworthy. The estimated effect was much less affected by capping with the time-to-event model compared to the other two methods; this offers a considerable practical advantage in studies where participants' RIT could exceed the maximum time set in a protocol.

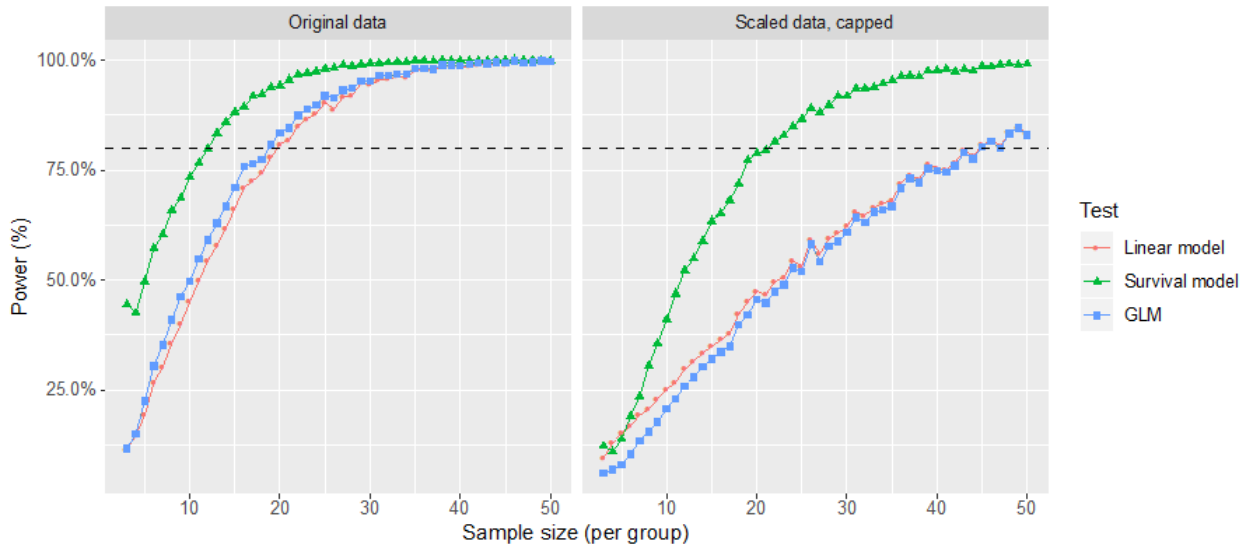


Figure 3.3 Power curves as a function of sample size for the three methods considered with and without capping for the scaled data. The power curves for the original data (not scaled) are identical to the scaled uncapped data and are therefore not reported (10,000 bootstrap simulations for each step in the sample size).

Table 3.3 Sample size (to whole number) of each group required to reach 80% power at $\alpha=0.05$ with the three methods considered

	Uncapped data	Capped data
	Sample size at 80% Power (per group)	Sample size at 80% Power (per group)
Survival model	12	21
GLM	18	44
Linear model	20	45

A supplementary analysis was conducted to further demonstrate the applicability of our proposed methodology in a second, censored dataset (Binns et al., 2018). Sixteen people from the same cohort used for the main analysis with various stages of AMD and eight age-similar controls provided valid data for the 76% bleach, 5° eccentricity test condition. This dataset features censored data because three RITs were not accrued within the test time and were capped at 30 minutes. Demographic characteristics of the included participants in this second analysis can be found in Supplemental Table S3.1 (see section 8.1). In this supplemental dataset, it is clear that the survival analysis offers a smaller p-value when testing the difference between the two groups, compared to both the GLM and linear model. This result is in line with the improved statistical power shown with our bootstrap experiment. Furthermore, the CIs for the central estimates are wider, exemplifying that censored data only provide limited information. However, as for our main calculations, accounting for censored data provides larger differences because it reduces the downward bias induced by capped data (see Supplemental Tables S3.1-S3.2 and Supplemental Figures S3.1-S3.2; section 8.1-8.2). Lastly, to further demonstrate

how the web application can be used on different datasets featuring RMDA data for different levels of AMD, the dataset featured in Chapter 5 has been entered into the app. The results from the censored RIT data can be found in supplemental materials for controls, early AMD, iAMD and late AMD, classified by the Beckman classification. The central estimates (CI) pulled from the app were 3.56 (2.85, 4.44), 5.72 (4.41, 7.43), 6.27 (5.44, 7.22) and 13.85 (8.25, 23.24) minutes, respectively. (See Supplemental Table S3.3 and Supplemental Figure S3.3). Despite the test being capped at 20 minutes, the time-to-event analysis correctly predicts the RIT for the late-stage AMD to stretch beyond this capped value. For details of these participant cohorts and methodology used, see Chapter 5.

3.4 DISCUSSION

We have shown how time-to-event analysis can be applied to the data yielded from psychophysical measurements of DA. Compared to alternative statistical methods, the proposed time-to-event model achieved higher statistical power in discriminating between people with AMD and healthy controls. Our method is statistically correct, by which we mean it can accommodate for both skewed data and censored data points. Time-to-event analysis offers the advantage of significantly reducing sample sizes when planning studies where this functional test is an outcome measure. The latter is important because designing trials and studies more efficiently equates to newer treatments likely being examined more efficiently. Our method may also have application to longitudinal studies and trials such as evaluation of proof-of-concept or phase II clinical trials aimed at early intervention. Moreover, this model offers flexibility and allows for additional covariates to be added to the analysis (e.g. presence of SDDs or age), making a wide range of RIT analysis possible. We have made the technique freely available via a simple App.

Both the GLM and the time-to-event model are able to account for the skewed distribution of the data; the former employs a Gamma distribution for the error, whereas the latter makes use of a Weibull distribution. However, time-to-event analysis can also accommodate censored observations. This feature is expected to prove useful for the assessment of DA impairment in people with AMD because examination time is usually capped at a maximum for practical reasons e.g. 20-30 minutes; a deficient RIT may exceed the maximum time of the test (Owsley, McGwin, et al., 2016). This issue has been addressed in different ways in previous studies, for instance simply using the capped value as if it was an actual measured RIT (Binns et al., 2018; Jackson & Edwards, 2008; Láíns, Park, et al., 2018; Owsley, McGwin, et al., 2016). We adopted the same solution for our simulated capping when using the GLM and the linear model. Of course, the major drawback of artificial capping is that it will create a false peak at the capped value. This is similar to what is observed in sensitivities in visual field examination with standard automated perimetry, where thresholds below 0 dB cannot be tested, resulting in a zero inflated distribution (Zhu et al., 2014). With our results, we showed that such an

approach can severely bias the central estimates. For example, in the scaled capped data for people with AMD (the group with largest amount of capped values), the estimates for the mean are much smaller than the correct values obtained from uncapped data. Moreover, the CIs are narrower with capped data and do not include the correct value for the mean. In contrast, the estimate of the median from the time-to-event model is very close to the value calculated without capping. The CIs are also wider, correctly reflecting the fact that censored data only provide partial information. Finally, the time-to-event model can correctly predict a median value beyond the capping limit (20 minutes). This would not be possible with a raw calculation of the median.

One alternative solution to deal with capped data is to use values estimated from the DA recovery curve. The AdaptDx is able to fit a decay model to the acquired values and extract a RIT value by projecting the estimated curve forward in time. This allows for missing data points and has been employed by some researchers (Owsley, Clark and McGwin, 2017). However, this is subject to the assumptions of the fitted curve and to measurement variability in the acquired data; it is unable to fit the decay model where limited recovery has taken place within the duration of the test, and thus capped data points still remain.

Our technique should have wide application in the context of studies measuring DA. For example, functional deficit in DA has been shown to become apparent before other clinical measures of visual function are affected (Dimitrov et al., 2011; Owsley, McGwin, et al., 2016). Moreover, evidence suggests that delayed DA may manifest before the appearance of structural features of AMD such as drusen and focal pigmentary changes (Owsley et al., 2001, 2007, 2014; Chen et al., 2019; Jackson et al., 2005; Owsley, McGwin, Jackson, et al., 2006; Fraser et al., 2016; Owsley, Huisingh, et al., 2016; Owsley, Clark and McGwin, 2017), indicating that DA is a pertinent clinical measure. Indeed, a series of studies, of varying quality, have shown a measure of DA to be a diagnostic indicator of AMD (Owsley et al., 2001; Dimitrov et al., 2008, 2011; Jackson and Edwards, 2008). The rate of DA has been shown to increase with increasing severity of AMD (Jackson, Clark, et al., 2014; Jackson, Scott, et al., 2014; Flamendorf et al., 2015; Owsley, Clark and McGwin, 2017)

The unusual statistical properties and subsequently skewed distribution of RIT values has been largely overlooked in previous reports (Cocce et al., 2018; Owsley et al., 2014). This can have important negative effects on the power of statistical tests, as illustrated by our power analysis. In many cases, researchers resorted to non-parametric tests, acting on the ranks of the data, because they do not make assumptions on the distribution of the data. However, classical non-parametric tests are less powerful than their parametric alternatives and they do not provide CIs on the estimates.

There are some limitations to what we have proposed. For the purposes of this study, we did not attempt to distinguish between stages of AMD. However, the use of a disease vs. non disease dataset was sufficient to demonstrate the reduction in sample size associated with the statistical techniques

used, and the methods would be equally applicable to studies designed to discriminate between different disease severities. Our method is primarily meant to compare RIT values among groups of people involved in a study or clinical trial. In fact, it is focused on the estimation of group effects as global changes in time scale of recovery and would provide little information on individual subjects. Future work could focus on the application of our methodology to larger datasets and longitudinal data; we hope our App for using this technique will help facilitate this.

Furthermore, while the app is currently unsuitable for clinical application as it cannot be used to analyse individual patients, there is scope for the censoring element of the methodology to be developed further. For example, censored data is not only an issue in measuring DA, but an issue in the assessment of declining retinal sensitivity via visual fields. Values censored at 0 dB are often considered to be actual 0 dB for the scope of analysis, which can introduce positive biases in the measured progression rate. The app methodology could be adapted to conduct a censored regression that can be applied to the uploaded data, where the error term is a censored distribution, making it applicable for wider clinical data analysis. Another perceived limitation of our study is our use of a dataset that does not feature RITs >15 minutes and scaling the dataset to reflect censored data. However, this allowed us to demonstrate the strength of the time-to-event method by showing how the estimates obtained with capped data would compare to those obtained from fully measured RITs. Such a comparison would have been impossible had censoring been present in the original data, because the true underlying distribution of RITs would have been unknown. However, we have also included a supplemental analysis on a second dataset with actually censored RIT values to further highlight the real-life applicability of this methodology.

The RIT measurement itself has limitations as it is not only dependent on DA kinetics but also on parameters such as pupil size and the number of photoreceptors (known to vertically scale sensitivity). Analysis of other metrics of DA measurements such as slope of the S2 component may be more demonstrable of DA kinetics (Dimitrov et al., 2008; Lamb & Pugh, 2004, 2006). Furthermore, the intent of this report was only to assess the RIT as produced by the analysis responses from the machine. We have not reanalysed the responses themselves in order to offer a different strategy for estimating the RIT. Larger datasets would also provide the opportunity to test other distributions for our time-to-event analysis (see Chapter 4). In fact, despite being widely used in parametric time-to-event analyses for its flexibility, the Weibull distribution might not necessarily be the best choice for this type of data. Finally, as explained in the methods section, these models do not describe the data in exactly the same way: both the GLM and the time-to-event model perform the comparisons in the logarithmic scale. This implies that, opposite to the linear model, they model the changes as proportions rather than linear differences. This is a common choice in many fields where strictly positive values are expected (such as with RIT values) since this data usually exhibit a heteroscedastic behaviour whereby the variance increases with the predicted mean. Log-scale models account for this behaviour (Faraway,

2016). Moreover, the logarithmic scale reduces the influence of large values which would otherwise greatly affect the mean calculated in the linear scale.

One final important aspect is that different conventions to calculate p-values are used for survival analyses (Wald test) and linear models/GLMs (t-test). We address this issue in a supplemental analysis, where we show that the improvement in power obtained with the time-to-event analysis is unchanged when the p-values are calculated using the Wald test for all the models.

3.5 CONCLUSION

In summary, the use of a time-to-event analysis is a more powerful statistical measure compared to other statistical approaches, for the assessment of RITs of people with AMD. We propose that time-to-event curves are a useful tool to visualise RIT in groups of people. We make full use of this in our freely available app, providing a user-friendly interface for clinical scientists to visualise and analyse RIT data more efficiently.

4 CHAPTER 4; ASSESSMENT OF A CLASSIFICATION OF AGE-RELATED MACULAR DEGENERATION SEVERITY FROM THE NORTHERN IRELAND SENSORY AGING STUDY USING A MEASURE OF DARK ADAPTATION

4.1 INTRODUCTION

As stated in Chapter 1, retinal imaging is used clinically to assess fundus-based structural abnormalities. The Beckman classification (Ferris et al., 2013) incorporates structural features detected on CFP. It has been well studied with a consensus-based approach and has been extensively adopted in both clinical and research settings (including a notable ongoing clinical study (Finger et al., 2019)) because it is pragmatic and easily applied. SD-OCT provides detailed images of the macular retina and is increasingly recognised as the imaging modality of choice for the detection of both early and late AMD features. However, longstanding AMD classification systems are based on CFP as they originate from prior epidemiological studies (Bird et al., 1995; Klein et al., 1991), while analogous SD-OCT based classifications were not feasible as this technology did not exist at that time.

Visual function testing has potential to enhance granularity of AMD staging when assessed in tandem with structural classification (Flamendorf et al., 2015). As aforementioned, there is accumulating evidence that delayed RMDA has been proposed as a diagnostic indicator of AMD (Jackson & Edwards, 2008; Owsley, McGwin, et al., 2016) that worsens with disease severity (Flamendorf et al., 2015; Owsley, Clark and McGwin, 2017). RMDA impairment has been shown to be worse in people with SDDs (Chen et al., 2019; Flamendorf et al., 2015; Neely et al., 2017) compared to those without SDDs. SDDs are best seen on OCT rather than CFP (Zweifel et al., 2010) and are considered a risk factor for atrophy and CNV (Finger et al., 2014). Histopathological studies of eyes with SDDs have found resulting changes in retinal structure such as shortened photoreceptor outer segments which may explain the association between impaired RMDA and SDD presence (Curcio et al., 2013).

Most studies on RMDA in AMD have used disease presence and severity graded from CFP, despite the limitation of classifications using this approach. The Beckman classification was not designed to incorporate SDDs (Spaide, Ooto and Curcio, 2018), even though CFP can identify SDDs using colour channel separation (Spaide & Curcio, 2010). The absence of an AMD classification system that includes SDD in the severity staging poses a potential issue as researchers want to further refine AMD disease status and staging. To compensate, some studies have placed people with SDDs in their own independent subgroup for analysis (Chen et al., 2019; Flamendorf et al., 2015; Sevilla et al., 2016).

However, this does not illustrate the impact of SDD presence within the different existing severity grades.

OCT has many advantages over CFP, such as better differentiating between structural abnormalities such as SDDs (Zweifel et al., 2010) in three-dimensions (Yehoshua et al., 2013). Chapter 2 highlighted OCT-based studies that have revealed new relationships between AMD macular anatomy (such as SDDs) and RMDA (Chen et al., 2019; Flamendorf et al., 2015; Láíns et al., 2017; Láíns, Park, et al., 2018; Sevilla et al., 2016). However, the sample sizes of the SDD cohorts ($n < 20$) (Chen et al., 2019; Flamendorf et al., 2015; Sevilla et al., 2016) have been small and few included age-adjusted control groups. This weakness of existing studies is particularly pertinent as age is a confounding variable associated with RMDA (Jackson, Owsley and McGwin, 1999).

The idea that OCT is a more accurate tool to assess AMD phenotypes is not a novel viewpoint (Lei et al., 2017). However, incorporating structural abnormalities detected on SD-OCT into a severity grading that CFP cannot readily image may provide a better understanding of associated RMDA impairment. To explore this idea we take advantage of a large volume of data collected from a community-based observational study. Our primary aim is to estimate RMDA deficits between different levels of AMD severity using an OCT-based classification and the Beckman classification with a hypothesis that differences between AMD grading severities will be more discernible with the OCT classification. Our secondary aim is to assess the impact of incorporating SDD presence into the OCT-based classification to measure the association between SDD presence and RMDA metrics.

The work presented in this chapter has been published in *Ophthalmology Science*, see list of supporting publications. The co-authors of the work presented in this chapter are split across City, University of London and Queens University, Belfast: Bethany E. Higgins (BEH), Giovanni Montesano (GM), Timos Naskas (TK), Katie Graham (KG), Usha Chakravarthy (UC), Frank Kee (FK), David Wright (DW), Ruth Hogg (RH) and David P. Crabb (DPC). The design of the study was conceived by BEH and DPC. The data was sourced from the Northern Ireland Cohort of Longitudinal Study of Aging (NICOLA) study, of which TK, KG, UC, FK, DW and RH are part of. Data collection was completed in Belfast by TN and KG. All data analysis was conducted by BEH with support from GM. The manuscript was written by BEH, and reviewed, edited, and approved by GM, UC, DW, RH and DPC. This work has been presented as a paper presentation at the European Society of Retina Specialists 2021 virtual meeting, and at the British Congress of Optometry and Vision Science 2021 virtual meeting where BEH was awarded Best Early Career Researcher Presentation. The work has also been presented in poster format at the Association for Research in Vision and Ophthalmology 2022 Annual Meeting in Denver, Colorado and BEH was awarded a travel grant from the ARVO Foundation.

4.2 METHODS

We used prospectively collected data from the case-control study: the Northern Ireland Sensory Aging (NISA) study, which was part of the long-term, ongoing epidemiological NICOLA study conducted at Queen's University, Belfast. NISA adhered to the tenets of the Declaration of Helsinki with ethical approval from the School of Medicine, Dentistry and Biomedical Sciences Ethics Committee, Queens University Belfast (Ref. 14.25v4). Participants provided written informed consent prior to enrolment. For full details of methodology used in the NISA study including details on how clinical phenotypes like SDDs were identified and categorised, see Supplemental Methods 8.3.1.

Both eyes (if eligible) were imaged and classified into AMD stage. A single grader (TN) evaluated the SD-OCT and the CFP images. A senior retina specialist (UC) with extensive experience of reviewing multi-modal retinal images reviewed all images classified as containing RPE abnormalities given the novelty of this phenotype, as well a random selection of 10% of remaining sample. Graders and the arbitrator were masked to all participant characteristics including age and RMDA data. CFP-based AMD grading systems consider drusen size, location and appearance. For more details of the Beckman clinical grading (Ferris et al., 2013), see Supplemental Table S4.1 (see section 8.1). Note, this study does not include people with late stage (GA and/or exudative) AMD, therefore this Beckman stage has been omitted. This study will refer to Beckman stages: controls, early ageing changes, early AMD and iAMD as Beckman 0-3, respectively. On colour imaging, SDD presence was assigned when a clear pattern of yellowish interlacing ribbons or dot like patterns were detected.

4.2.1 Brief Review of NISA Study Methodology

The NICOLA study is a long-term epidemiological study which commenced in January 2014. The recruitment strategy consisted of extracting an unclustered sample of addresses in which at least one person living at the residence was over the age of 50 from the Business Services Organization Family Practice Register. It was expected out of the 6000 people targeted, approximately 400 people with signs of AMD could be extracted (considering prevalence and drop-out rate of 50%). This cohort was used in the add-on NISA study, which features in this chapter.

The NISA study incorporates a large, enriched population sample size and a large cohort of people with SDDs. It's methodological strengths include the full-range ocular imaging undertaken and that AMD was graded using a multimodal imaging protocol that was independently graded by the NetwORC UK reading centre to ensure impartiality. Furthermore, a single optometrist conducted all the 400 participant's visual assessment during a single visit, which ensures repeatability and avoids inter-observer variation. However, there are also drawbacks to the methodology utilised specific to the data used in this analysis.

For example, for the Heidelberg Spectralis SD-OCT/SLO was utilised with a 30x25 degree grid. This is the maximum grid employed by the Spectralis and should be sufficient to detect most SDDs in the macular as well as covers the area tested by the AdaptDx. However, the scan density was only 61 scans, meaning that some SDDs or drusen may be caught between scans therefore missed. Furthermore, the in-built Heidelberg Eye Explorer (HEYEX) review software segmentation system was used and images were visually inspected by a grader and corrected if necessary. The automated segmentation is limited as it simply does not work well for drusen and SDDs, particularly where there is overlying pigment atrophy. It would be unreasonable to not individually check segmentations to ensure they are correct. While manually checking the segmentation may introduce human error and no repeatability measures were taken for this process, it is important to note that thickness measures were not used in this analysis.

In terms of the identification of SDD presence, these were defined as granular hyper-reflective material lying between the RPE and the boundary between the inside and outside sections of the photoreceptors. This is a standardised classification of SDDs described by Zweifel et al. (2010). SDDs were graded as present, absent or questionable. Unsurety over the presence of SDDs could be due to image quality and ultimately those agreed upon as 'questionable' were ultimately graded as absent. All grading was completed by a single optometrist (TN) and a senior retina specialist (UC) assessed a random sample of 50 participant images on two occasions. This was conducted simply as a concordance exercise and no repeatability analysis was conducted on this data. Therefore, the possibility of intra-observer variation cannot be completely ruled out and evidence of no inter-observer variation cannot be empirically illustrated. This serves as a limitation for the methodology and the subsequent analysis featured in this chapter as SDD presence is a main outcome measure.

Lastly, a single SDD was deemed sufficient for grading of SDD presence, as per previous studies (Gabrielle et al., 2019; Zarubina et al., 2016). Yet, more recent studies published in the field have typically used a strategy of a minimum of five SDDs to be present on a single B scan and present on >1 B-scan in an OCT volume (Grewal et al., 2021). Furthermore, many definitions require OCT presence with an additional requirement of appearance on a 2D modality. For the NISA study, the presence of a single SDD was chosen based upon the "Image Level" definition featured in The Alabama Study on Early Age- Related Macular Degeneration (ALSTAR study) and the same definition has been published as a supplemental material in Zarubina et al. (2016). Furthermore, more recently the Montrachet Study also used a single SDD as definite presence of SDDs (Gabrielle et al., 2019). It is worth mentioning that the NICOLA study protocol was written in 2016 and therefore grading may not reflect more recent definitions in the literature. However, it is the perception of the authors (and the team that developed the NICOLA protocol) that an instance where only a few SDDs present would be a very rare occurrence so the definition used in this study is sufficient. Yet, as a result, the findings of this study may not be comparable across recent literature that use a different definition of SDD presence.

4.2.2 Statistical Analysis

All analyses were performed in R 3.5.2 (<http://www.r-project.org/>) under R Studio, version 1.1.463 (RStudio, Boston, MA, USA). First, we cross-tabulated participants staging from the Beckman and OCT gradings. Descriptive statistics for demographic and standard visual function measures stratified by the two classification methods were generated. A Kruskal-Wallis test, was used to assess differences in descriptive variables such as age. Our primary analysis focused on how average RMDA (the RIT parameter) differed between groupings assigned using the different classification techniques. Here we specifically used a time-to-event analysis as described in Chapter 3 (Higgins, Montesano, et al., 2021). In short, the time-to-event analysis can be conveniently used to model the time taken to recover from bleaching while accounting for predictors of interest, such as differences between groups, and correcting for covariates such as age or other attributes (Higgins, Montesano, et al., 2021). Kaplan-Meier curves were plotted to visually represent the comparisons of the results from the models. The parametric time-to-event regression (using a Weibull distribution) provided in the Survival package for R was implemented. We take $p < 0.05$ as level of statistical significance and we correct for multiple comparison via Bonferroni Holm's method. This is pertinent because the CFP-classification has four groups and six contrasts whilst the OCT-classification has three groups yielding three contrasts. The use of a parametric model is justified by its ability to predict the behaviour of the data beyond the censoring imposed by the cap in RIT recordings. Weibull models are a common choice for this type of problems, owing to their flexibility, and a strong support for any specific model does not exist for our data. Alternative distributions and their associated Akaike Information Criterion (AIC) values are reported as supplemental analysis, including an assessment of similarly performing distributions (Supplemental Tables S4.5-S4.6; section 8.1). From this analysis, it is evident that models using a strictly positive distribution (Weibull, Log-Normal, Log-Logistic and Log-Gaussian) performed the best, and importantly much better than the semi-parametric alternative (Supplemental Table S4.5). Therefore, any of these distributions might be an adequate, or better, description of the data. However, and importantly, the specific choice of model did not change our results (Supplemental Table S4.6). Despite it not being the focus of this study, a Spearman's correlation test was also used to assess the relationship between age and RMDA in the control cohort.

4.3 RESULTS

Complete data were available for 459 participants (249 [54%] females) and numbers are shown as stratified by the Beckman and OCT classification in Figure 4.1. Cross tabulation of these numbers, shown in the same figure, indicate some similarities but also some marked differences between the results of the two classifications. For example, 62 participants (18%; 95% CI 14-23%) were classified

as having no drusen or pigmentary changes on the Beckman scale but were shown to have some features of early AMD on the OCT classification. Conversely, eight participants (11%; 95% CI 5-21%) classified as having large drusen and/or AMD pigmentary changes on the Beckman scale were observed to have no drusen or RPE abnormalities on the OCT classification. These discrepancies show that the classifications based on CFP and OCT do not agree in all cases or, in other words, indicates that the two classifications are providing different information on the eyes.

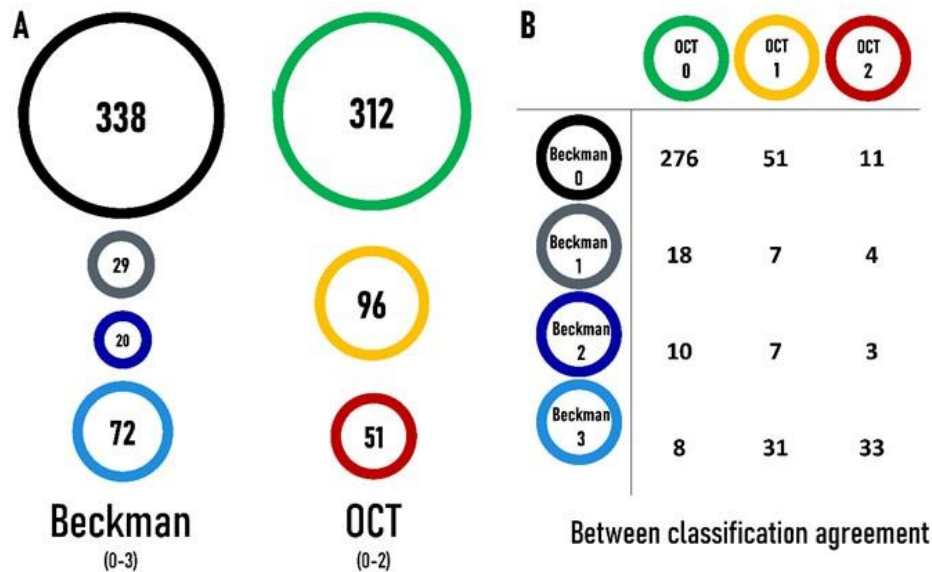


Figure 4.1 The 459 participants were graded by the Beckman classification (0-3) and the OCT classification (0-2). Section A. shows the participant cohorts in each class and Section B shows the agreement between the two classifications. For the participants with the greatest discordance between classifications ($n=8$ in OCT 0 and Beckman 3 and $n=11$ in OCT 2 and Beckman 0) a further check was completed of the grading by RH. Reasons for disagreement were confirmed to be due to the different imaging technologies. Note: As repeatability assessment was not conducted, it cannot be ruled out that these differences are due to lack of consistency in classifications.

Descriptive statistics for the demographic data and visual function variables stratified using the Beckman classification and OCT classification are shown in Table 4.1 and 4.2 respectively. The average age differences between groups using both classifications are noteworthy, see Figure 4.1. There were some small, but unsurprising, average differences between average VA and average CS between some of the various groupings. A correlational analysis was conducted to assess any changes of DA with age in the control group for both classifications. A Spearman's correlation was computed, and a weak negative correlation was found between RMDA and Beckman 0 ($\rho = -0.33$; $p < .001$) and OCT 0 ($\rho = -0.36$; $p < .001$). For both classifications, RMDA was more delayed in older participants.

Table 4.1 Summary statistics for demographic and visual function data stratified using Beckman classification.

Stage Name	Stage Description	Frequency (n)	Gender (% female)	Mean (\pm SD)			Median (IQR)	
				Age (years)	BCVA (letters)	CS (logCS)	RMDA (min)	
Beckman 0	No obvious ageing changes	338	54%	64 (8)	85.7 (5.9)	1.6 (0.2)	6.0 (4.5, 8.7)	
Beckman 1	Normal ageing changes	29	52%	69 (8)	82.6 (12.7)	1.5 (0.2)	6.6 (4.7, 10.5)	
Beckman 2	Early AMD	20	75%	66 (6)	84.2 (4.6)	1.5 (0.2)	5.7 (4.4, 7.4)	
Beckman 3	Intermediate AMD	72	53%	71 (9)	82.0 (7.6)	1.4 (0.2)	13.2 (6.0, 21.1)	

Table 4.2 Summary statistics for demographic and visual function data stratified using OCT classification

Stage Name	Stage Description	Frequency (n)	SDDs present (n)	Gender (% female)	Mean (\pm SD)			Median (IQR)	
					Age (years)	BCVA (letters)	CS (logCS)	RMDA (min)	
OCT 0	Controls	312	55	56%	64 (7)	86.8 (5.7)	1.6 (0.2)	5.8 (4.5, 8.5)	
OCT 1	Drusen only	96	30	53%	68 (8)	83.3 (8.9)	1.5 (0.2)	8.4 (5.2, 13.3)	
OCT 2	Drusen and/or RPE abnormalities	51	24	45%	72 (10)	82.6 (8.3)	1.4 (0.2)	11.1 (5.3, 20.1)	

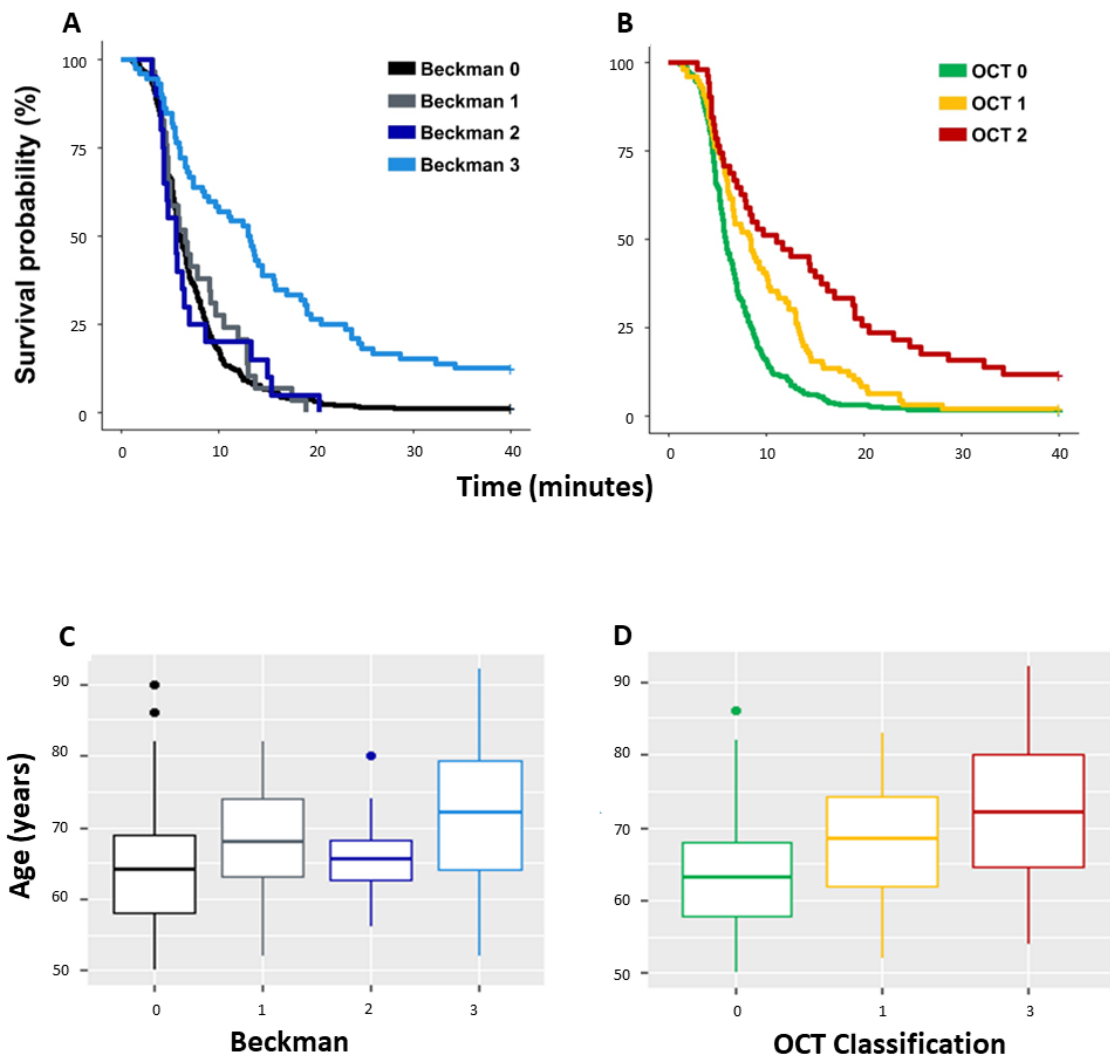


Figure 4.2 Upper row: Kaplan-Meier curves illustrating the time taken for participant sensitivity to recover to a value of 5.0×10^{-3} scotopic cd/m^2 (3.0 log units of stimulus attenuation). This time taken is the RIT. The two plots show survival times for the control and AMD groups stratified by Beckman classification (left) and OCT classification (right). Bottom row: Age distribution for each classification. Visually, it seems like there is significant difference in OCT-classification in RIT, but after correction for age this is lost in earlier stages of AMD disease. Note: these differences might be expected given there are four levels of classification using the OCT-based criterion compared to just three in the Beckman classification, with smaller sample sizes found in the Beckman Classification (Early AMD; Beckman 1 has 20 people only).

Our main visual function measure of interest was median (interquartile range; IQR) RMDA. In the four groups in the Beckman classification this was 6.0 (4.5, 8.7), 6.6 (4.7, 10.5), 5.7 (4.4, 7.4) and 13.2 (6.0, 21.1) minutes respectively. Median (IQR) RMDA appeared different for the three groups in the OCT classification being 5.8 (4.5, 8.5), 8.4 (5.2, 13.3) and 11.06 (5.3, 20.1) minutes respectively. These

summary statistics suggest differences in RMDA are more discernible between different grades of AMD severity when an OCT-based criterion is used as compared to the Beckman classification; this is illustrated by the observed separation in the time-to-event curves shown in Figure 4.2. Yet these differences might be expected given there are four levels of classification using the OCT-based criterion compared to just three in the Beckman classification.

The time-to-event analysis (uncorrected for age) indicated that only eyes with iAMD (Beckman 3) had significantly worse RMDA compared to each of the other groups in the Beckman classification (vs Beckman 0, Beckman 1, Beckman 2; $p < 0.0001$ all). In contrast, no statistically significant differences were found between any of the other Beckman groups. Yet, statistically significant differences were found between all OCT groups. Eyes in OCT 2 had worse RMDA compared to OCT-defined controls (OCT 0) ($p < 0.0001$) and eyes in OCT 1 ($p < 0.001$). Eyes in OCT 1 (drusen presence only) had worse RMDA compared to OCT-defined controls ($p < 0.001$). This was in line with our observations on the 'raw' median RIT data. However, the results were less clear when we subjected the data to time-to-event analysis correcting for age. Eyes in Beckman 3 remained significantly worse than Beckman 0, Beckman 1 and Beckman 2 ($p < 0.005$ all). There also remained no statistically significant differences in mean RMDA between any of the other pairs of groups in the Beckman classification. In contrast, while eyes in OCT 2 had worse RMDA compared to eyes in OCT 0 ($p < 0.001$) and eyes in OCT 1 ($p = 0.009$), the mean difference in RMDA between eyes in the OCT 0 and OCT 1 groups was not statistically significant ($p = 0.195$).

Summary statistics in Supplemental Table S4.2 (see section 8.1) suggest minimal differences in RMDA between people without SDDs, compared to the larger differences found between to people with SDDs graded by the OCT criterion. The effect of adding the presence of SDDs to the time-to-event model and time-to-event curves are shown in Figure 4.3. The differences in the plots indicate that presence of SDDs in each group worsens RMDA, certainly for OCT 1 and OCT 2. We assessed these differences formally by including an interaction term between SDD presence and OCT grading added to the time-to-event model. SDD presence significantly worsened average RMDA within OCT 2 ($p < 0.001$) and OCT 1 ($p < 0.05$) but not within OCT 0 ($p = 0.45$). Once again, when we adjusted our model for age, these results were less clear. SDD presence significantly worsened average RMDA within OCT 2 ($p < 0.01$) but not within OCT 1 ($p = 0.28$). On the contrary, in OCT 0 the presence of SDDs improved RMDA ($p = 0.013$) once age adjusted.

Participants with SDDs had their SDDs graded into Stages 1-3 (see Supplemental Tables S4.3-S4.4; section 8.1). Due to the small number of Stage 3 SDDs, only Stages 1-2 were used in analysis ($n = 99$). For these participants (Stage 1 $n = 55$; Stage 2 $n = 44$), median (IQR) RMDA was 5.3 (4.1, 7.7) and 7.9 (5.1, 13.9), respectively. A time-to-event model was used to assess the interaction of SDD stage with RMDA and found that Stage 2 SDDs were associated with significant slowing of RMDA compared to Stage 1 ($p < 0.01$). This association between delayed RMDA and more severe stage SDDs remained

when age was added as a covariate controlled for ($p < 0.05$), see Supplemental Figure S4.2 (section 8.2).

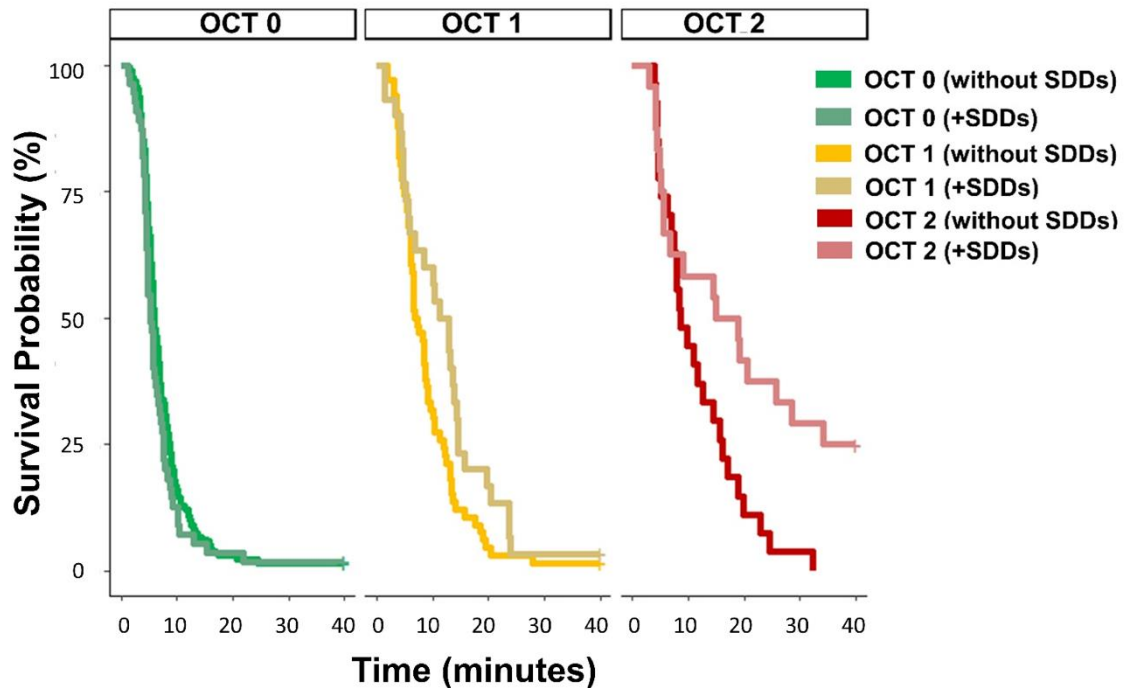


Figure 4.3 Kaplan-Meier curves illustrating the time taken for participant sensitivity to recover to a value of 5.0×10^{-3} scotopic cd/m^2 (3.0 log units of stimulus attenuation). This time taken is the RIT. Survival curves shown for control group and AMD group stratified by OCT classification and SDD presence

4.4 DISCUSSION

We assessed how RMDA, as a reference standard functional measure, varied between groups of eyes with different severity of AMD using structural measures. Differences in RMDA, as described by simple summary measures, appeared more discernible between different grades of AMD severity when an OCT-based criterion is used as compared to the Beckman classification. Yet these differences might be expected given there are four levels of classification using the OCT-based criterion compared to just three in the Beckman classification. After correcting for age, RMDA function was found to be significantly delayed in people with a structural definition of iAMD when compared to less severe AMD and healthy controls, regardless if they are classified using a CFP or OCT based criterion. This is the main finding from our study. For those defined to have less severe AMD or normal ageing by either OCT or CFP classifier after correcting for age, no statistically significant difference in RMDA between the groups was found. SDD presence (assessed via the OCT-based classification) has some effects on RMDA at different severity levels of AMD. Results from this study represent new knowledge about classifying people with and without AMD using structural measures. The two classifications provide

unique information on eyes, potentially due to CFP underestimating drusen size since it is essentially showing depigmentation whereas OCT reveals the dome, seen previously (Kim et al., 2021). Recent insights afforded by high-resolution histologic imaging of RPE indicates pigmentary changes visible in the fundus are caused by RPE shape changes just as much if not more so than changes in the content or size of melanosomes and melanolipofuscin (Chen et al., 2022). OCT offers an alternative to CFP that better illustrates structural changes in three-dimensions and incorporating it into classifiers could improve phenotyping of people with drusen and SDDs.

The idea that OCT could provide better assessment of morphological changes associated with AMD is not a novel one. An OCT-based classification of AMD has been proposed by Lei et al. (2017), inclusive of high central drusen volume, SDD presence, intraretinal hyperreflective foci (IRHF) and hyporefective drusen cores (HDC). However, automated software used to assess drusen volume is machine specific (Cirrus [Carl Zeiss Meditec, Dublin, CA]) and therefore not widely applicable (Lei et al., 2017). We feel that in addition to our novel methodology using RMDA as our reference standard to measure visual function and use of the statistically correct time-to-event analysis to effectively assess RMDA, this study offers a widely applicable, simple, feature-based classifier that can be easily applied. This can be used alongside the accessible online web application to run the time-to-event analysis on other data, detailed in the previous chapter. Moreover, this study has important implications for both AMD classifier and RMDA research in people with AMD.

Regardless of the structural classifier used to identify people with AMD our results are meaningful because they support the previously reported notion that RMDA is substantially delayed in people with iAMD compared to controls (Binns et al., 2018; Chen et al., 2019; Flamendorf et al., 2015; Laíns et al., 2017) and people with early AMD (Cocce et al., 2018). However, our results were less clear when age was considered, which is not unusual in RMDA literature (Sevilla et al., 2016). RMDA is affected by normal ageing changes (Jackson, Owsley and McGwin, 1999), due to retinal structural changes that impact metabolic exchange between the photoreceptors and the choroid (Lamb & Pugh, 2004). This age-effect may have been underestimated in previous studies measuring RMDA in people with AMD as we discuss below.

Our analysis also suggests a possible structure-function relationship between SDD presence visible on OCT and functional loss assessed as slowed RMDA in people with AMD. This association between SDD presence and RMDA is evidenced in the literature (Chen et al., 2019; Flamendorf et al., 2015; Laíns et al., 2017; Neely et al., 2017; Sevilla et al., 2016). For example, Flamendorf et al. (2015) reported significantly worse RMDA in 15 people who had SDDs, with 80% reaching the test ceiling of 40 minutes (Flamendorf et al., 2015). However, the small cohort with SDDs in their study were significantly older than the controls; this limitation in their study is noteworthy. While we too found that people with SDDs in groups OCT 1 and OCT 2 had significantly worse RMDA compared to people without, we also went on to include age as a covariate in the time-to-event analyses. Despite the results becoming less clear, SDD presence within OCT 2 group was still associated with slower average RMDA compared to

those without SDDs. We can infer from our data that SDD presence is associated with greater rod dysfunction in people with structurally defined iAMDAMD, regardless of age-effects. This complements previous histopathological studies that SDDs tend to be located in rod-dominated retinal locations and that SDD presence has been associated with changes in photoreceptor morphology such as shortened photoreceptor outer segments (Curcio et al., 2013). Indeed several papers describe how photoreceptors are shortened or bent over SDDs when using multimodal imaging including adaptive optics SLO (AOSLO) (Zhang et al., 2020) and histological surveys (Echols et al., 2020). However, rod dysfunction occurs where rods are sparse, such as near the rod-free fovea (Owsley et al., 2000) and where rod degeneration occurs due to ageing and AMD. For example, we have recently found that slowing of RMDA has been found to be worse at 5° compared to 12° in people with AMD (Binns et al., 2018). Therefore, SDD presence may not be directly related to slow RMDA but rather serve as a marker for another process. Furthermore, we did not restrict our screening of pathology to within the RMDA testing spot, meaning our data supports prior studies that SDD presence associated with delayed RMDA regardless of whether the SDDs were in the testing location or not (Lains et al., 2017).

We found SDD presence in controls did not significantly impact RMDA prior to age-adjusting the results. Similar findings were seen by Neely et al. (2017), whom postulated sparse SDD manifestation along with lack of RPE abnormalities in people without AMD was insufficient to negatively impact RMDA (Neely et al., 2017), suggesting that SDD presence should be seen as a structural biomarker for AMD disease progression in controls (Chen et al., 2019; Clark et al., 2011; Huisinigh et al., 2016). However, when we corrected estimates for age, we found a surprising indication that the presence of SDDs improved RMDA (on average) in our large cohort of OCT-defined controls. We speculate this may be due to incomplete bleaching due to the irregular structure of the retina caused by SDDs but there is no literature in the field to support or explain this finding. Yet, we acknowledge the discordance of this finding and believe this would be an interesting case for future investigation explored with rigorous age-matching.

Despite not being the focus of this paper, we also found evidence to suggest a structure-function relationship between larger, more distinct SDDs and delayed RMDA function in people with AMD. When deposited hyperreflective materials in the interdigitation zone were sufficient enough to alter the contour of the ellipsoid zone (Stage 2 SDDs) (Zweifel et al., 2010), they were significantly more likely to be associated with worse RMDA compared to those with less 'pronounced' SDDs (Stage 1). This remained the case when our data was age-adjusted. Due to our small sample sizes per AMD group, we cannot determine if this relationship is irrespective of AMD status. We believe this finding to be novel but it must be replicated in future studies to be confirmed.

Findings from this study suggest other avenues for future research. For example, SDD presence and indeed stage of SDD severity appears relevant when assessing functional vision such as RMDA and further research is critical in order to understand the pathophysiology of earlier stages of AMD with

these structural phenomena. In addition, SDD presence in controls would be a pertinent focus of future investigation to determine if SDD presence is an appropriate structural biomarker for AMD disease progression, given the perhaps surprising result found in this study.

We also think our findings are relevant to the debate about designing future clinical trials looking to grade AMD. Furthermore, an OCT-based classification of AMD that takes into account SDD presence would be an important tool for studies investigating automated grading of retinal images using deep learning algorithms (Farsiu et al., 2014; Lee et al., 2017; Srinivasan et al., 2014). The potential of using artificial intelligence in tandem with an OCT-based classification of AMD severity includes disease screening as well as guidance of therapies. In fact, new imaging biomarkers have recently been discovered using deep learning algorithms in association with measures of RMDA, providing further justification for its use as an outcome measure in clinical trials (Lee et al., 2020).

Our study has various strengths. We used a large, enriched population sample size and a large cohort of people with SDDs; this is uncommon when compared to recent RMDA research in people with AMD (Chen et al., 2019; Flamendorf et al., 2015; Sevilla et al., 2016). Furthermore, the use of the standardised Beckman grading for AMD allows for comparisons across relevant literature. We also utilised a time-to-event model (sometimes referred to as a survival model) to assess the magnitude of measurement differences in RMDA. This model is a statistically correct method for this data and offers advantages over alternative methods like t-tests and non-parametric tests, described previously in Chapter 3. While we were not the first to identify age as a possible confounder in RIT analyses, another strength of our methodology was that we compensated for age-effects. For example, previous work from Owsley et al (Owsley et al., 2014; Owsley, Huisingh, et al., 2016) did not correct the estimates of RIT but rather applied a correction for age and other factors to the estimated odds-ratios of having an abnormal RIT based on pre-defined cut-offs. An approach more similar to ours was taken by Laíns et al. (Laíns et al., 2017; Laíns, Park, et al., 2018) where a multivariate model having the RIT as a response variable was applied to correct for age and other factors. However, such a linear model does not account for heteroscedasticity or for censoring. In fact, the authors explicitly state that they assigned a value of 20 minutes to all the observations not recovering within the maximum allocated time. In our previous paper (Higgins, Montesano, et al., 2021), we have shown this to introduce important distortions in the estimates of RIT. Our approach retains all the advantages of allowing for correction of covariates while addressing fundamental properties of the specific nature of the data. The consideration of age-effects in this study subsequently weakened the relationship between AMD severity and RMDA; this in itself is notable and has been demonstrated in the literature before (Sevilla et al., 2016).

There are limitations to our study. Firstly, there are drawbacks associated with the methodology used in the NISA study, of which this chapter yields its cross-sectional data from. Ultimately, data collection was not originally designed for the purpose of testing our hypotheses. Of note, there was no ethnicity data made available for this dataset, meaning inferences from the findings cannot be applied to

specific ethnic groups. A brief review of the NISA methodology can be found in section 4.2.1 but the two most prominent limitations to this study was as follows.

Firstly, no inter-rater nor intra-rater repeatability data was captured during the classification of AMD for both CFP and OCT criteria or for the classification of SDD presence. Measuring consistency of agreement in classification-based decisions is vital when proposing novel criteria for disease severity and the lack of this data is noteworthy. While the aim of this study was not to definitively propose a novel grading system, we recognise that further validation would be required. However, it is also worth noting that there is a well-analysed lack of concordance and interrater variability in image analysis in people with AMD (Reeves et al., 2016).

Secondly, while the NISA study chose to classify SDD presence when a single SDD was found (based upon the "Image Level" definition featured in ALSTAR study), more recently developed classification systems consist of a minimum of five SDDs to be present on a single B scan and present on >1 B-scan in an OCT volume (Grewal et al., 2021). Furthermore, many definitions require OCT presence with an additional requirement of appearance on a 2D modality. Nevertheless, the team that developed the NICOLA protocol (which the NISA study incorporated) felt that an occasion where only one-to-five SDDs was present would be an incredibly rare occurrence. The team felt the definition used in this study was therefore sufficient. However, this data may over-estimate the number of people with SDDs in the cohort. For example, the SDD classification used found 55 visually healthy controls with SDDs, which seems unlikely and perhaps the number of people would not be as high if the minimum number of SDDs was >5. This limitation should be taken into consideration when interpreting the SDD-related findings from this study.

In terms of limitations of the data analysis featured in this chapter, a caveat associated with our findings surrounds the number of groups in each of the classifications we compared. The OCT classification has three levels while the Beckman has four. Therefore, the number of eyes in each group for the Beckman classification are smaller for the statistical analysis (for example, only 20 people in the Early AMD group) which may not be sufficiently powered to detect a difference between the groups. While Early stage AMD is a notoriously difficult group to recruit for (as most people present to clinic when they experience symptoms which is typically later in the disease timeline), to effectively compare the classifications, further study with a larger sample size would be needed. In addition, there were statistically significant age differences between the AMD groups in both classifications (see Figure 4.2). Yet, we ameliorated this limitation by using age-corrected analyses. Also, while we know size, homogeneity and location are important when grading drusen (Spaide & Curcio, 2010), incorporating these attributes along with other OCT-based features into a grading scale has not yet been widely adopted in the literature, despite efforts to create one (Lei et al., 2017). There also remains disagreement over the best way to stratify features of AMD across standardised CFP-based classifications. Hence, our study featured a simple feature-based scheme using the presence or absence of classical drusen, pigmentary irregularities and SDDs. However, by grouping different

phenotypes together in the levels of this classification such as different types of drusen (e.g. soft drusen and hard drusen) all in one level (e.g. OCT1), their independent effects on RMDA cannot be teased apart. It is therefore possible that a more detailed OCT-based classification that considers these phenotypes separately and additional factors may give a more distinct separation of RMDA between groups. For example, the OCT criterion created by Lei et al. (2017) incorporated IRHF, found to be associated with progression to late-stage AMD. IRHF was absent from our classification, a further shortcoming of this OCT criterion (Lei et al., 2017).

4.5 CONCLUSION

To summarise, we provide evidence to suggest that RMDA function is delayed in eyes with a structural definition of iAMD regardless if classified using CFP or OCT based criterion. In this study, RMDA does not differ between groups of eyes defined to have early AMD or normal ageing, regardless of using OCT or CFP classifications after data is age corrected. Our findings certainly add to the debate about how we stratify disease severity in AMD. For example, SDD presence was evidenced to have some effect on RMDA at different levels of AMD severity using the OCT classification.

5 CHAPTER 5; PROPERTIES OF MEASUREMENTS FROM MICROPERIMETRY AND DARK ADAPTATION ASSESSMENT IN PEOPLE WITH INTERMEDIATE AGE-RELATED MACULAR DEGENERATION

5.1 INTRODUCTION

The prospective multicentre clinical study MACUSTAR aims to develop endpoints for clinical trials in people with AMD. The design of MACUSTAR is described in detail elsewhere (Finger et al., 2019); it has a cross-sectional and longitudinal component with the former designed to assess measurement properties of structural and functional candidate endpoints and ability to distinguish between normal ageing changes and Beckman (Ferris et al., 2013) classified AMD severity stages. The longitudinal component, to be completed in 2024, is designed to mainly evaluate how different structural and functional measures might track progression in people with iAMD and how these measures might relate to changes in self-reported vision related QoL. Testing of visual function may elicit a greater sensitivity, or at least additional information, about disease status in AMD when compared to grading scales based on structural appearance alone (Saßmannshausen et al., 2018). Therefore, one aim of MACUSTAR is to assess a set of functional vision tests that might characterise changes in iAMD before late-stage AMD (Finger et al., 2019).

Aside from interest in visual function measures for trials, there is growing investment by clinics in instruments for measuring visual function beyond those using conventional charts. Examples include microperimetry (fundus controlled perimetry) and dark adaptometry technology. In the literature there is evidence to support the role of both mesopic and scotopic microperimetry (Cassels et al., 2018; Wong et al., 2017) in assessing people with AMD especially in research and as study endpoints (Yang & Dunbar, 2021). Moreover, measures of RMDA may provide a sensitive measure of AMD progression (Chen et al., 2019; Owsley et al., 2014; Owsley, McGwin, et al., 2016). In this context, a specific aim of MACUSTAR is to evaluate measurements from mesopic and scotopic microperimetry (S-MAIA) and dark adaptometry (AdaptDx) as potential functional biomarkers for iAMD. These instruments are the subject of this study, with the MACUSTAR assessment of other chart-based methods of assessing visual function described in a previous report (Dunbar et al., 2022).

Repeated measurements on the same subject vary around a true value because of measurement error. Confusingly, different terms are used to describe measurement error including, for example, precision, repeatability, inter-test variability and test-retest variability. For simplicity we will adopt the last. An understanding of the test-retest variability of a measurement, possibly estimated by the

difference in two repeated measures recorded over a short period of time, is critical for the clinical use of the measurement, or adoption in trials. This must be linked to the minimal clinically significant difference insofar as a 'real' change can only be registered, in FU for example, if it exceeds the test-retest variability. Assessment of test-retest variability for a device is sometimes inadequately done in studies of small numbers of visually healthy people. For instance, in Chapter 2, only one study was found to have adequately attempted to assess test-retest variability of the AdaptDx and this did not specify the disease status of the cohort recruited (Flamendorf et al., 2015). Better reports on the topic for measurements from S-MAIA exist (Pfau, Lindner, Fleckenstein, et al., 2017; Welker et al., 2018; Yang & Dunbar, 2021). Still, MACUSTAR offers a unique opportunity to estimate test-retest variability of these visual function measures in a large number of people with iAMD; this is the main focus of our study.

We primarily aim to estimate test-retest variability for measurements from mesopic and scotopic assessments using S-MAIA microperimetry and AdaptDx DA in eyes with iAMD from the MACUSTAR cross-sectional study. We also conduct a series of secondary analyses including an assessment of how well summary measurements from the devices distinguish people with iAMD from people with early AMD and visually healthy controls. We also estimate other measurement properties of the devices, including reliability, participant compliance to complete the examinations and practice/learning effects. Such data will be particularly useful for those planning to use these measures of visual function in clinical trials in iAMD.

The co-authors of work presented in this chapter are: Bethany E. Higgins (BEH), Giovanni Montesano (GM), Hannah M.P. Dunbar (HMPD), Alison M. Binns (AMB), Deanna R. Taylor (DRT), Charlotte Behning (CB), Amina Abdirahman (AA), Matthias C. Schmid (MCS) Jan H. Terheyden (JHT), Nadia Zakaria (NZ), Stephen Poor (SP), Robert P. Finger (RPF), Sergio Leal (SL), Frank G. Holz (FGH), Gary S. Rubin (GSR), Ulrich F.O. Luhmann (UFOL) and David P. Crabb (DPC). The design of the study was conceived by BEH, AMB and DPC. The data was sourced from the MACUSTAR CONSORTIUM, of which GM, HMPD, AMB, DRT, CB, AA, MCS, JHT, NZ, SP, RPF, SL, FGH, GSR, UFOL AND DPC are members of. Data collection was completed in 18 European ophthalmology centres across Europe, overseen by the MACUSTAR CONSORTIUM. All data analysis was conducted by BEH with support from GM. The manuscript was written by BEH, and reviewed, edited, and approved by GM, HMPD, AMB and DPC. The manuscript is currently under review with the MACUSTAR CONSORTIUM publications committee. Part of this work has been accepted as a presentation by the Imaging and Perimetry Society (IPS) for the IPS Symposium in August 2022 in Berkley (California, USA) and BEH has been awarded a travel grant.

5.2 METHODS

The design of the MACUSTAR study (Registration NCT03349801; www.clinicaltrials.gov) has been described previously (Finger et al., 2019) with participants recruited from 18 clinical sites from seven European countries. For the present study, we only extracted data collected from participants in the cross-sectional component of MACUSTAR; this comprised of a baseline and a short-term FU visit (14±7 days) with at least 150 people with iAMD planned to be recruited. In addition, people with early AMD, late-stage AMD and normal ocular ageing changes only (controls) were also recruited. The Beckman scale (Ferris et al., 2013) was used for all classifications as determined by a central reading centre on the basis of multi-modal imaging from a dedicated screening visit; the detail of this and a full description of inclusion and exclusion criteria are given elsewhere (Terheyden et al., 2021). All participants gave written informed consent and the study conformed to the Declaration of Helsinki. At both cross-sectional study visits participants performed tests of visual function, as well as imaging and completing questionnaires. A study eye for each participant was defined as one with the better BCVA determined at the screening visit using the ETDRS chart. Our focus is solely on the device-based tests of visual function, namely mesopic and scotopic microperimetry (S-MAIA) and DA (AdaptDx). These device-based tests were done after the conventional chart-based tests. We assessed data from these devices in participants who successfully had BCVA recorded at the two visits. This inclusion criterion makes our results representative of a study population that can adequately perform chart based visual function assessment; this is noteworthy because one of the properties of a device should simply be how many people, from a defined population, can do the test and provide reliable data.

The device-based visual field testing (S-MAIA followed by AdaptDx) was carried out by certified technicians in accordance with standard operating procedures (SOP) put together by MACUSTAR. What follows is a brief description of these examinations.

S-MAIA is a modified version of the macular integrity assessment microperimeter that can assess both mesopic testing with achromatic stimuli and dark adapted two-colour scotopic testing with cyan (505nm) and red (627nm) stimuli (Steinberg et al., 2017). Scotopic testing is thought to be more relevant when probing visual dysfunction function in AMD but it is more inconvenient because of the need for DA (Nebbioso, Barbato and Pescosolido, 2014; Steinberg et al., 2017). The study eye was dilated (1% tropicamide) and the participant was dark adapted for five minutes prior to beginning the mesopic microperimetry. The participant was positioned on the chin rest (non-study eye occluded) and then instructed to respond (press button) to stimuli whilst fixating on a red fixation circle. The technician used the device to determine the optic disc centre and the participant's PRL was estimated automatically by the S-MAIA in order to correctly centre the grid. This study used a customised stimulus grid of 33 points located at 0°, 1°, 3°, 5°, and 7° from fixation (Welker et al., 2018). First, mesopic microperimetry was performed using achromatic stimuli (Goldmann III) presented for 200ms using a 4-2 staircase strategy with a background luminance of 1.27 cd/m² and an initial target

brightness of 2.6 ± 0.5 abs. Next, after a further 30 minutes of DA, scotopic microperimetry was performed using a red (627nm) stimulus (Goldmann III) presented for 200ms using a 4-2 staircase strategy with no background illumination and an initial target brightness of 0.01 abs. A red filter was in place on the S-MAIA screen during scotopic testing to ensure the participant remained dark adapted throughout testing. The tests were expected to take approximately five minutes each (Welker et al., 2018). Both tests used the 33-point test pattern. In addition, the SOP instructed technicians to use the FU mode for both tests for the FU visit; this ensures the same retinal locations are examined on retesting, which makes sense in endpoint-exploring studies. (The FU mode on the S-MAIA also shortens test times.) The SOP also instructed technicians to note if tests failed either of two reliability criteria (fixation losses $\geq 30\%$ or if the 95% BCEA $> 50 \text{ deg}^2$) but not to repeat tests. It is important to note that at the baseline visit participants first performed a microperimetry practice session, based on a 9-point grid, done with the aim of mitigating any practice/learning effects.

Dark adaptation assessment, using the AdaptDX, was conducted after the scotopic microperimetry and the participant remained dark adapted. The participant was positioned on the adjustable chin rest (non-study eye occluded) and asked to focus on the red fixation light with the technician aligning the eye to the eye tracker. The participant was advised there would be a bleaching flash followed by a blue-green spot and they were then instructed to press the button when this was seen. Pupil size was automatically assessed by the device to standardise retinal illumination during the testing procedure. The study eye was bleached using a 0.25ms flash at 8×10^4 scotopic $\text{cd/m}^2\text{s}$, equivalent to a 76% bleach, at a retinal location subtending 4° and centred at 12° inferiorly in the vertical meridian (location of the test target). The stimulus for the threshold measurement was a 2° diameter, 500nm circular target which began 15 seconds after the bleaching offset. The initial stimulus presentation was at 1 log units of stimulus attenuation. Log thresholds were estimated using a modified, 3 down-1 up staircase procedure. The procedure continued with a 15 second break between each threshold measurement. This continued until either the RIT was obtained, or the test protocol ended (30 minutes), whichever first occurred. RIT is defined as time taken for retinal sensitivity to recover to reach a threshold located within the second component of rod recovery (5×10^{-3} scotopic cd/m^2 [3 log units of stimulus attenuation]). When the RIT was not obtained within the test duration, a capped value of 30 minutes was assigned for analysis.

AdaptDx records the percentage of threshold points which indicate a fixation error. If fixation errors exceeded 30%, the test was deemed unreliable and excluded. Where fixation error rate was between 30-40%, or recovery occurred faster than two minutes, test data were evaluated manually by author AMB (while masked to AMD status) to determine eligibility for inclusion according to specific criteria. Other reasons for exclusion of data were if the rod intercept could not be calculated by the device due to ineffective bleach delivery (e.g. due to fixation loss at the time of bleaching), or if the test was terminated early by the technician due to participant fatigue. When practical, participants repeated the test after a 30 minute washout period if their test data were deemed unreliable.

A scheme for data quality control and data export was followed as set out in the SOPs. As reasoned before we only considered data from participants who had successfully recorded BCVA at both visits. First, we identified missing data, following the SOP for what we describe as examination procedural errors (screening phase 1) excluding participants because of problems, for example, with the examination set-up (technician responsibility), even though they had BCVA recorded. Next, we identified missing data for participant issues (screening phase 2) resulting from, for example, an abandoned examination, even though they had BCVA recorded. Finally, we identified data, following MACUSTAR protocols, deemed unreliable (screening phase 3) because of, for example, too many fixation errors, insufficient DA, and incomplete bleaching. Results from this exercise alone will be useful for those planning future studies/trials wanting to estimate attrition rates of data when using measurements from S-MAIA and AdaptDx.

We used the main instrument determined summary measures of visual function as the measurements of interest, namely Mesopic S-MAIA Average Threshold (MMAT[dB]); Scotopic S-MAIA Average Threshold (SMAT[dB]) and RIT(min). Descriptive statistics were calculated for these measures along with age and BCVA, at baseline for the different participant groups. For our primary analysis, test-retest variability estimates for MMAT, SMAT and RIT were estimated by the difference in the respective indices at baseline and the FU visit (denoted MMATd, SMATd and RITd). A BA analysis was used to generate 95% LoA calculated as ± 1.96 times the SD of the test-retest differences (Bland & Altman, 1986), with the mean of these differences, denoted bias, being an estimate of the average magnitude of practice or learning effect between sessions. The upper LoA from the BA analysis can be loosely interpreted as a value for the smallest detectable change (SDC) that needs to be observed to be confident that the observed change is real and not, potentially, a product of measurement error in the instrument. Sensitivity (dB) values at individual points for S-MAIA (scotopic and mesopic) grouped by eccentricity (1°, 3°, 5°, 7° from fixation) were analysed and results from these data can be found in supplemental materials.

For fairness of comparison between the two instrument types, RIT data were also transformed by $10 \times \log^{10}$ to mimic the logged (dB) output of the S-MAIA. A ratio of variability metric was calculated to also compare the test-retest variability performance of the measures, defined as the SD of the test-retest differences (noise) divided by SD of the average (signal), with the latter being the average of the measurement recorded over the two visits. A relatively large value for this metric would indicate large test-retest differences (high level of noise) and/or a small dynamic range (short span over the values for the averages). For completeness we also calculated the ICC for each measure using the standard approach (Koo & Li, 2016). ICCs are thought to capture measurement reliability with ICCs with values above 0.75 loosely interpreted to be good/adequate. We restricted our primary analysis to the participants defined as having iAMD.

To compare discrimination performance between the three measures to separate iAMD from early AMD, late AMD and controls, ROC and AUC values with 95% CI were computed for baseline data. AUC values support comparison of the discriminatory power between test whereby, loosely speaking, values greater than 0.9 indicate excellent discrimination, 0.8 – 0.9 good, 0.7 – 0.8 fair, 0.6 – 0.7 poor and 0.6 or less represent a failure to discriminate (Pines et al., 2012). Note that age was not adjusted for in these analyses because we are only making relative comparisons between the measures. However, despite it not being the focus of this study, a Spearman’s correlation test was used to assess the relationship between age and RMDA in the control cohort. All data analyses were performed in R 4.0.5 (<http://www.r-project.org/>) under R Studio, version 1.1.463 (RStudio, Boston, MA, USA) including use of ggplot2, BlandAltmanLeh and pROC packages.

5.3 RESULTS

Three-hundred and one people participated in the MACUSTAR cross sectional study. Of these, 290 participants attended both visits and had complete BCVA data (controls [n=54], early AMD [n=28], iAMD [n = 167], late AMD [n = 41]). Median time between sessions was 14 days (IQR; 12-18 days). Mean (\pm SD) age was 68 (6), 72 (6), 71 (8), 75 (6) years for controls, early AMD, iAMD and late AMD groups respectively. Mean (\pm SD) BCVA was -0.04 (0.08), 0.01 (0.08), 0.02 (0.10), 0.78 (0.24) logMAR, respectively.

Results from the data screening exercise for the participants with iAMD are shown in the flow-chart in Figure 5.1. Results are presented in the same way for the other participant groups in Supplemental Figures S5.1-5.3 (see section 8.2). In short, a significant quantity of data had to be excluded for mesopic (n=39; 23%) and scotopic (n=36; 22%) microperimetry. This data attrition rate was even higher for AdaptDx data (n=64; 38%).

A significant proportion of these data for all tests were excluded because of procedural errors (screening phase 1) which includes events attributed to examiner errors. For example, on 26 occasions when a participant with iAMD had their mesopic microperimetry assessed for the second time, follow-up mode was not chosen by the examiner during test set-up (which ensures the same retinal locations were tested again). This meant that the second dataset couldn’t not be directly compared to the first, rendering both useless for this study. However, reporting on site errors was dependent on the group and not always reported specifically (i.e., sometimes just reported as ‘site error’). The procedural errors indicate a need for further training of examiners at each centre and may be due to that training was given virtually due to the Covid-19 pandemic. Perhaps in-person training would have reduced the number of procedural errors as examiners would have benefitted from hands-on training practice with technicians skilled in this methodology. The large proportion of data excluded in screening phase 3 (unreliable data because of fixation errors and incomplete bleaching) for AdaptDx (n=46; 27%) is

noteworthy as it illustrates errors made by the participant and indicates difficulty of the task itself. In short, we had complete data for 128, 131 and 103 participants for the mesopic and scotopic microperimetry data and AdaptDx data respectively and this was used in our primary analysis. We also grouped data for 81 (49%) of the 167 participants with iAMD who were able to complete all three tests. We report an analysis for this subset in supplemental materials (see section 8.1-8.2).

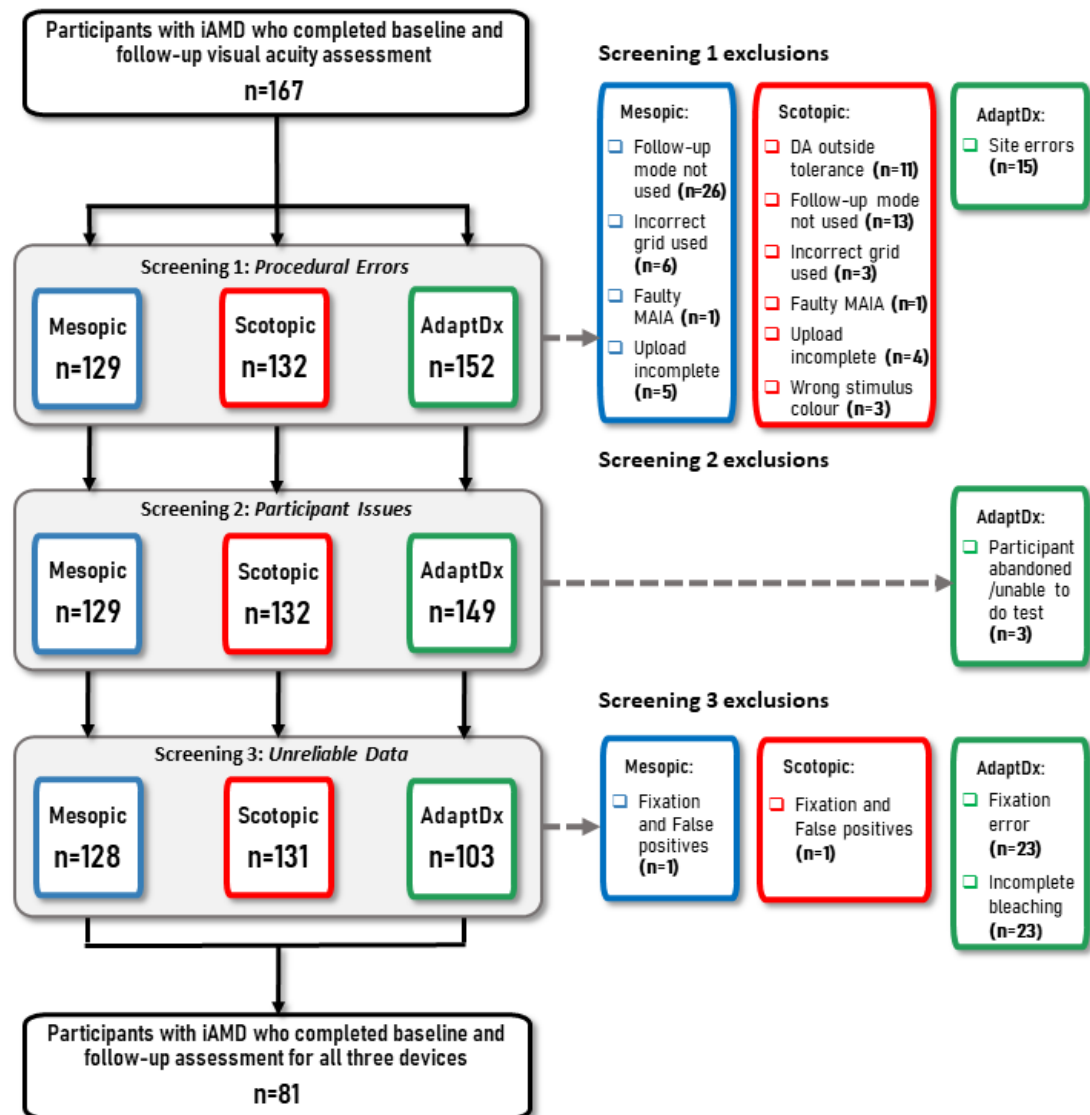


Figure 5.1 Flowchart of participant screening with iAMD. (In some cases, multiple reasons for removal were recorded for a participant. In this case, whatever reason that occurred first in the screening processes was reported here. For example, if a participant was recorded as having ‘DA outside tolerance’ (screening 1 exclusion) and recorded an unsuitable false-positive rate (screening 3 exclusion), the participant was removed based on the screening 1 exclusion.)

Test-retest variability estimates for MMAT, SMAT and RIT for the iAMD participants are described in Table 5.1 and Figure 5.2. In short, MMAT and SMAT had very similar test-rest variability. The upper LoA (SDC) was about 5dB for both devices. It is difficult to compare BA plots when the measures under

scrutiny are recorded on different scales. Still, BA plots for RIT (and the transformed RIT) seem similar to those for MMAT and SMAT. None of the BA plots indicate heteroscedastic behaviour, meaning for example, that test-retest variability worsens as the measurement worsens, and this is a positive feature of the measurements. Moreover, and remarkably, there was no evidence of any statistically significant bias in MMAT, SMAT or RIT. For example, indicating no evidence of better sensitivity or shorter RIT as a result of improved performance between visits (practice/learning effect). Taken together, the test-retest variability estimates for RIT (variability ratio and ICCs) were worse than those returned for MMAT and SMAT. The upper LoA (SDC) for RIT was about 8 minutes in the untransformed data.

We present secondary results of the same measures stratified by individual study centres ($n \geq 10$ participants and iAMD only) to identify any cross-centre effects in test-retest variability. Data showing test-retest measures and participant screening/attrition stratified by individual study centres are given in Table S5.1 (see section 8.1). We also present results from a similar analysis as applied to visually healthy controls, early AMD and late AMD. Test-retest variability estimates for MMAT, SMAT and RIT for controls, early AMD and late AMD groups are given in Supplemental Tables S5.2-S5.4 and Figures S5.4-S5.6 (see section 8.1-8.2). Note the smaller sample sizes for these groups. Data grouped by eccentricity (1°, 3°, 5°, 7° from fixation) were analysed and results from these data can be found in Supplemental Tables S5.6-S5.7; see section 8.1).

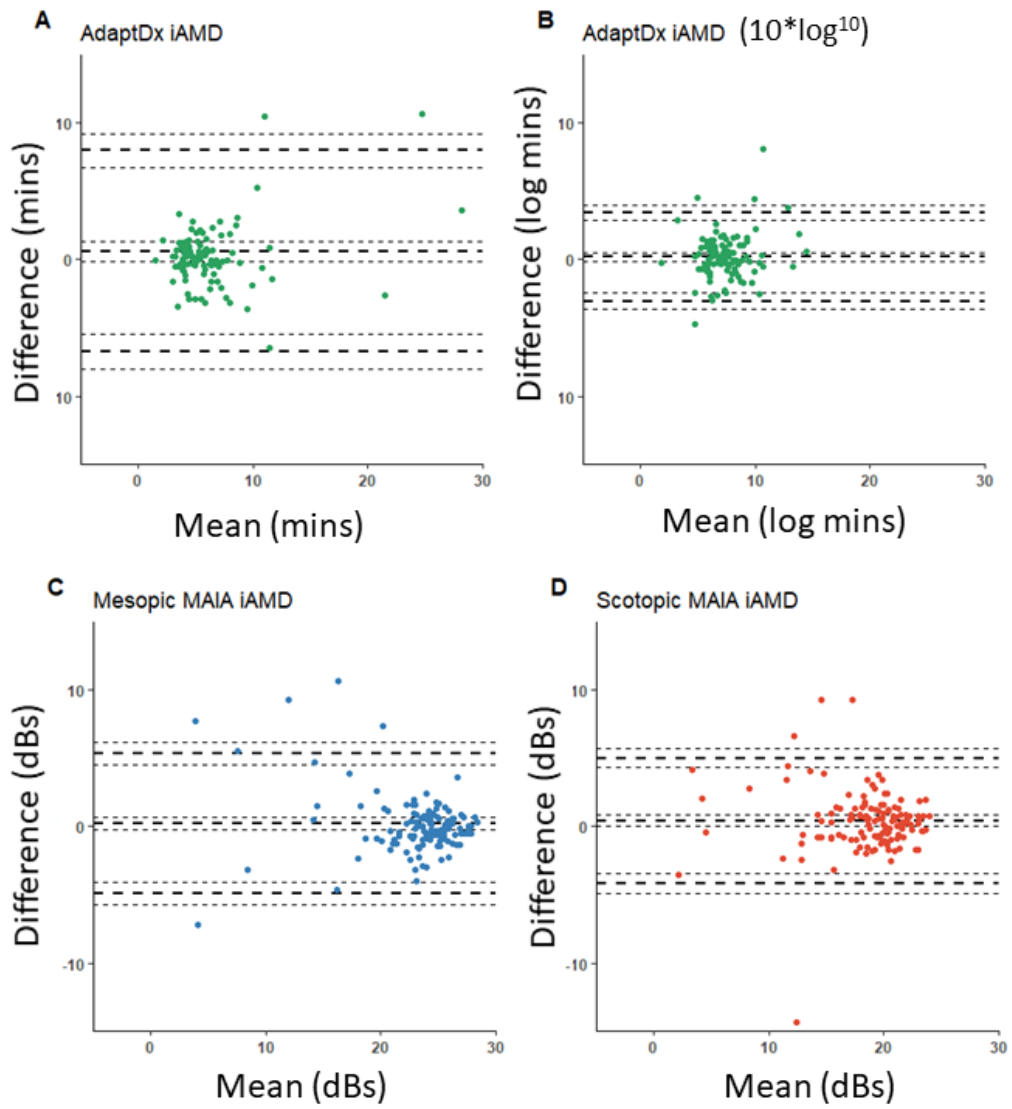


Figure 5.2 BA plots to show the test-retest agreement for the three metrics for participants with iAMD. (Note RIT data [B] has been transformed by $10 \cdot \log^{10}$ for better comparison).

Table 5.1 Test-retest variability assessment results for AdaptDx (RIT[mins]) and S-MAIA (MMAT (dB) and SMAT (dB)) in people with iAMD

Test	N	Mean (±SD)	BaselineMean FU (±SD)	Bias (95% CI)	SD of differences	Lower LoA (95% CI)	Upper LoA (95% CI)	Interclass Correlation Coefficient (95% CI)	Variability Ratio
RIT (mins)	103	6.82 (5.41)	6.20 (3.76)	0.62 (-0.12, 1.34)	3.75	-6.73 (-7.99, -5.47)	7.96 (6.70, 9.22)	0.67 (0.55,0.77)	0.88
RIT (10*log ¹⁰)	103	7.60 (2.30)	7.40 (2.04)	0.20 (-0.12, 0.52)	1.65	-3.03 (-3.58, -2.48)	3.43 (2.88, 3.98)	0.63 (0.49, 0.73)	0.82
MMAT (dB)	128	23.12 (4.25)	22.89 (5.14)	0.23 (-0.23, 0.69)	2.62	-4.90 (-5.69, -4.12)	5.36 (4.58, 6.15)	0.85 (0.79, 0.89)	0.58
SMAT (dB)	131	18.68 (4.15)	18.27 (4.27)	0.42 (0.01, 0.82)	2.35	-4.18 (-4.88, -3.49)	5.02 (4.32, 5.71)	0.84 (0.78, 0.89)	0.58

The results of our discrimination analysis are summarised in Figure 5.3 and Figure 5.4. MMAT, SMAT and RIT had fair and equivalent discriminatory power when distinguishing between people with iAMD and controls. Yet all three methods completely fail to distinguish between people with iAMD and early AMD.

We give AUC values for all contrasts between controls, early AMD, iAMD and late AMD for the three different measures in Supplemental Tables S5.7-S5.9. In short, while both MMAT and SMAT give excellent separation, RIT only gives good-fair separation between late AMD and the other groups (Pines et al., 2012). A different comparison was done by only using data where a participant had successfully recorded all three measurements. The results were generally the same with, MMAT, SMAT and RIT having equivalent discriminatory power when distinguishing between people with iAMD and controls (see Supplemental Table S5.10; section 8.1).

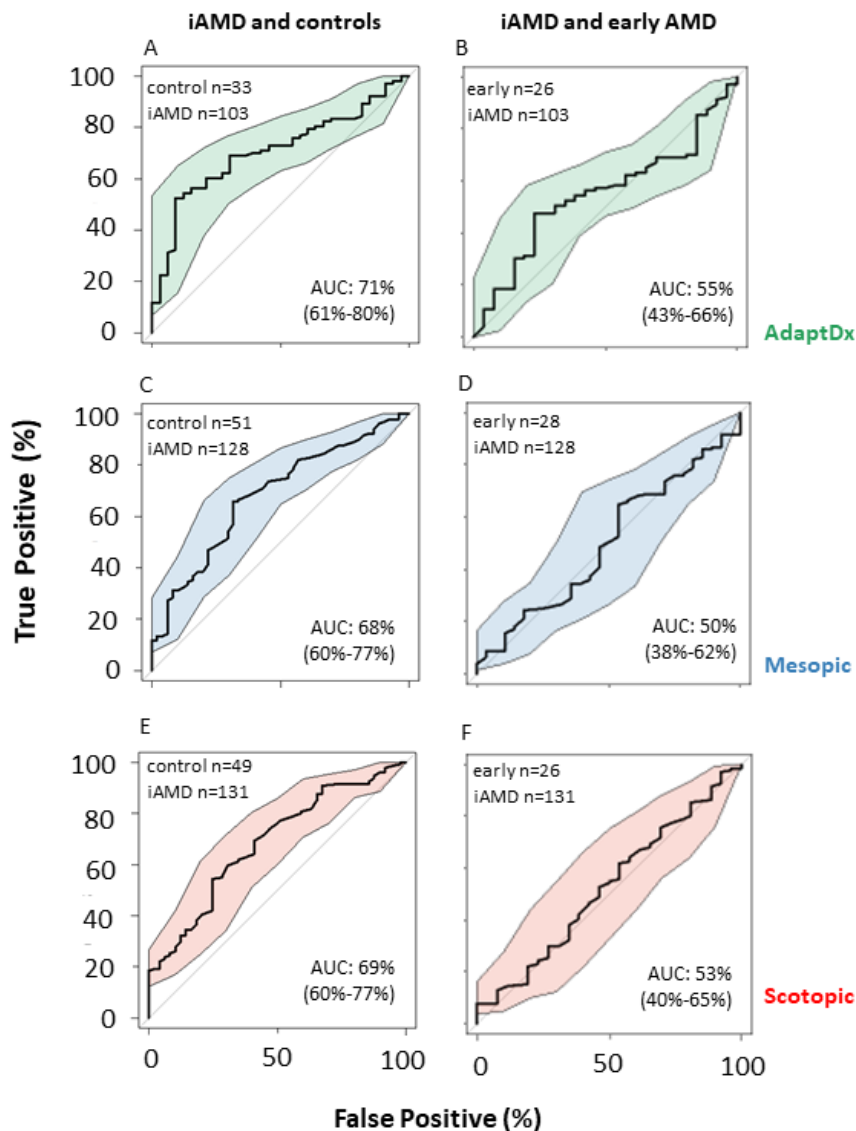


Figure 5.3 ROCs to show discrimination performance between the three measures' individual ability to separate people with iAMD from controls and people with early AMD using baseline visit data.

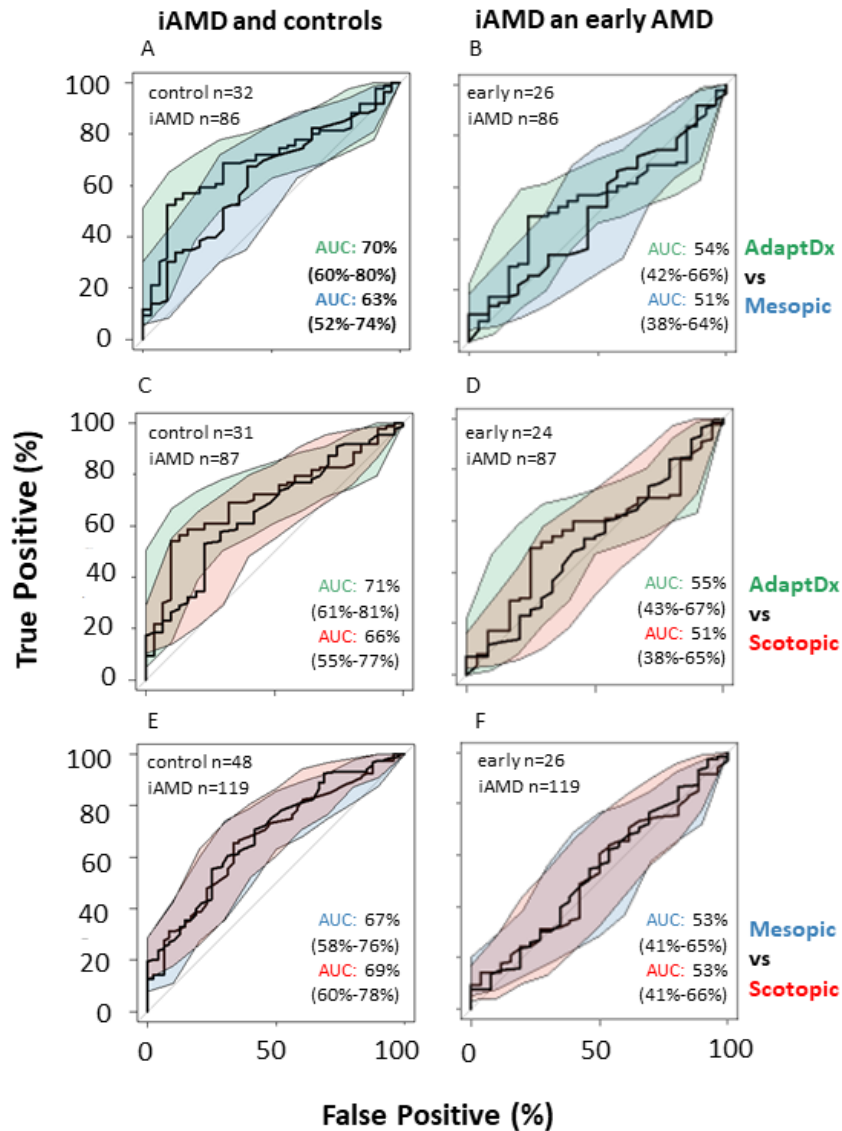


Figure 5.4 ROCs to compare discrimination performance between the measures' ability to separate people with iAMD from healthy controls and people with early AMD using baseline visit data. (Note the smaller sample sizes representing participants from each group that performed both tests plotted e.g. 24 participants with early AMD successfully performed both AdaptDx and scotopic S-MAIA testing.)

A correlational analysis was conducted to assess any changes of DA with age in the control group for baseline visit. A Spearman's correlation was computed, and no statistically significant correlation was found between the two variables ($\rho = -0.283$; $p = 0.11$). This may be due to the small sample size of 33 visually healthy controls in this cohort.

5.4 DISCUSSION

We primarily assessed mesopic (MMAT) and scotopic (SMAT) microperimetry and AdaptDx (RIT) in a large number of people with iAMD from the multi-centre MACUSTAR cross-sectional study. A proportion of test results from these devices could not be used despite assessment following trial like SOPs; this overall proportion was worst in measurements from AdaptDx. MMAT and SMAT had similar levels of test-retest variability which in turn were better than those of RIT from AdaptDx. RIT manifesting marginally worse test-retest variability when compared to results from microperimetry is supported by the different metrics of test-retest variability we calculated, including ICCs. However, in a secondary analysis we found MMAT, SMAT and RIT to be equivalent in having fair discriminatory power when separating people with iAMD and controls. Yet, all three assessments were unable to discriminate between people with iAMD and people with early AMD. We found no average differences between baseline and FU measurements in these device-based tests indicating no evidence of learning or practice effects; this is surprising given what is often experienced in study participants in perimetry and other psychophysical measures of visual function (Jones et al., 2016; Wu et al., 2013). Short practice tests as directed by the SOPs likely helped here. Indeed, our SOPs will be useful for those designing studies using the device-based tests we have reported on here.

Results from our study are mainly useful to those planning clinical trials using S-MAIA and AdaptDx in people with iAMD. Having accurate values for test-retest variability of the metrics from these instruments and estimates of usable/reliable data are invaluable for trial design and sample size calculations. We could only use microperimetry data from about one in four participants who had successfully completed chart-based assessments. This data attrition was worse (about one in three) for the measures from the AdaptDx. We think these findings are important to highlight despite the data being acquired following SOPs. However, device-based testing of visual function was done at the end of a long battery of testing performed on the day (Dunbar et al., 2022) and this might explain the attrition of good data; participant fatigue can never be underestimated in such studies. Furthermore, attrition was worst in the smaller sites that collected data from <10 people. Still, ICC values for MMAT and SMAT are no worse than those reported in our companion study of simple to administer chart-based tests (Dunbar et al., 2022). Furthermore, data we report here cannot predict the potential of measures from these more complicated test modalities being most effective in tracking disease progression to be revealed by the longitudinal component of MACUSTAR.

Some more discussion of our secondary analyses, in what we describe as discrimination performance of the S-MAIA and AdaptDx is pertinent. First, the MACUSTAR cross-sectional study was not designed to truly assess the diagnostic accuracy of these device-based tests. None of these analyses were powered appropriately because the sample sizes for the non iAMD groups were small and what we report would not satisfy guidelines for diagnostic accuracy studies (Fidalgo, Crabb and Lawrenson, 2015). Note also our AUCs are constructed on fewer participants for RIT meaning those estimates are

biased with the likelihood that discrimination is worse than estimated here. After all, missing data is often not random but results from a test not being completed because of, for example, unreliability or lack of participant compliance. (Unfortunately, this uncertainty in the estimates is not reflected by greatly wider CIs for the AUC (Cho, Matthews and Harel, 2019).) Still, it is reasonable to conclude that MMAT, SMAT and RIT have equivalent discriminatory power when distinguishing between people with iAMD and controls, for example. AUC values we report were equivalent to the measurements from most of the chart-based tests reported in our companion paper but not as good as CS measured by Pelli-Robson, which afforded best discrimination between iAMD and controls (AUC: 0.77); this is noteworthy given it would be more conveniently measured.

We have shown that measurements from scotopic and mesopic microperimetry have a very similar profile and this is interesting. MMAT and SMAT offer almost identical test-retest variability (see Supplemental Figure S5.7 and Supplemental Tables S5.5-5.6 to show similarities in different revisions of the visual field). MMAT and SMAT have very similar discriminatory power too. The latter suggest that mesopic microperimetry ought to be a first choice because it is a more convenient examination to do. Yet, we do not know how measurements from these two modalities will perform in the longitudinal data from MACUSTAR. It might be that scotopic microperimetry may pick up subtle changes in people with iAMD that might be predictive of them progressing to advanced disease (Pfauf et al., 2018). Presently the more inconvenient test, and perhaps challenging test for the patient, does not yield a great level of measurement noise and this is useful new knowledge supporting findings from smaller studies (Pfauf, Lindner, Müller, et al., 2017).

There are few reports in the literature similar to ours. Flamendorf et al (2015) assessed test-retest variability between the two visits (± 7 days) of RIT in 87 people with AMD (RIT mean (\pm SD) difference was 0.02 (\pm 2.26) minutes (Flamendorf et al., 2015). AMD severity of these participants was not reported, but they were likely visually healthy or earlier stage AMD as they did not reach the AdaptDx test ceiling (Chen et al., 2019; Flamendorf et al., 2015) and this is notable. Elsewhere in the literature there is overwhelming evidence of an association between impaired DA and AMD but the studies of the discrimination performance of RIT in separating people with different levels of AMD are of poor quality (Higgins, Taylor, et al., 2021). Good levels of test-retest variability of the S-MAIA (both mesopic and scotopic conditions) have been previously reported using coefficient of repeatability (CoR) metrics. For example, Welker et al (2018) reported CoR of 4.4 dB (mesopic) and 4.52 dB (scotopic) for pointwise sensitivity in a small number ($n=23$) of volunteers with iAMD (Welker et al., 2018). Barkana et al (2021) assessed test-retest variability of 'abnormal' microperimetry points only (defined if threshold sensitivity was at least 5% lower than expected values in healthy eyes). The authors reported better test-retest variability for this subset of points, with lower 95% LoA compared to all grid points (Barkana et al., 2021). Pfauf et al. (2017) assessed 47 visually healthy eyes and reported slightly worse CoRs than Welker et al (2018) (4.75dB and 4.06dB, respectively) (Pfauf, Lindner, Fleckenstein, et al., 2017). von der Emde et al (2019) assessed test-retest variability in 28 people with

neovascular AMD in both cyan and red scotopic testing conditions using the S-MAIA and reported CoR of 6.14 dB and 6.06 dB, respectively (von der Emde et al., 2018). While CoR tend to be used to assess test-retest variability, we used a variability ratio metric. With this the measurements from the devices are penalised both for having large test-retest variability (large noise) and for having small dynamic range (short span over the values for the averages).

There are few studies in the literature that have assessed discriminatory performance of the S-MAIA in people with AMD. Pondorfer et al. (2020) reported that the S-MAIA could successfully discriminate between 83 people with iAMD and 24 controls. AUC values were better than what we reported (88% mesopic and 82% scotopic). Still, CIs around these estimates were wider reflecting the smaller sample sizes and their study was only done at one centre (Pondorfer et al., 2020). Interestingly, their study also assessed performance of chart-based tests including Pelli Robson CS and reported it to have a marginally higher-level discriminatory power.

Our study has strengths and limitations. For example, the data is unique because of its size and being yielded from so many different centres, following SOPs we have made freely available. We did not randomise the order of the visual function assessments in the MACUSTAR cross-sectional study and this is a limitation. Indeed, the device-based testing reported here was done at the end of series of chart-based tests and other assessments. As stated before, this might explain some of the data attrition especially with the DA assessment that was scheduled at the very end of an extensive examination session. Despite following SOPs there were a large amount of data lost due to procedural error, indicating a need for further training of examiners. These errors may be due to training being reduced to video calls as a result of the Covid-19 pandemic. Perhaps in-person training would have reduced the number of procedural errors as examiners would have benefitted from hands-on training practice with technicians skilled in this methodology. While this study has shown it is possible to train technicians virtually to yield a reasonably high level of useable and repeatable data, this illustrates where improvements on the study design can be made in the future. There are minor limitations associated with what we describe as our discriminatory analyses, such as not correcting estimates of AUC for age, sex or phakic status but we have already outlined that these analyses were comparative and never designed as a formal assessment of diagnostic accuracy of the device-based tests.

5.5 CONCLUSIONS

To sum up we have reported on the properties of measurements from device-based testing of visual function, namely mesopic and scotopic microperimetry and DA. The SOPs, estimates of test-retest variability and test completion rates will potentially contribute to the design of future trials for treatments for AMD when using this technology. Ultimately the results from the longitudinal

component of MACUSTAR will tell us more about the prognostic power of measurements from these devices when tracking progression in iAMD.

6 CHAPTER 6; OVERVIEW OF FINDINGS AND FUTURE WORK

6.1 OVERVIEW OF FINDINGS

6.1.1 Research Summary

The overarching aim of this work was to identify and then improve upon methodology used to assess RMDA in people with early and iAMD and to compare it to similar measures of visual function with respect to diagnostic accuracy and repeatability metrics. This thesis has reviewed recent literature assessing DA in people with AMD and revealed that the AdaptDx device is the most widely used technique in a research setting to measure RMDA (using the RIT) in people with AMD. However, despite the popularity of this metric as a reference standard of visual function, this thesis has also highlighted the lack of recent research into both repeatability and discriminatory power of DA to separate people with earlier stages of AMD and visually healthy controls.

This thesis supports the growing body of research measuring RMDA in people with AMD by offering a better way to statistically assess RIT data, and through reporting important information regarding the performance of RMDA, which is relevant to the design of clinical trials and studies planning on utilising the AdaptDx. Overall, RMDA is a potentially useful visual function biomarker of iAMD and worsening disease severity, but its ability to distinguish early AMD stages and early ageing changes from visually healthy controls is decidedly weaker. Furthermore, there are important considerations to take into account when designing trials using the AdaptDx such as the number of participants who are unable to provide usable, reliable data in a multicentre setting. In addition, this thesis has found that delayed RMDA appears to relate to SDD presence, but less obviously in earlier stages of AMD disease severity. Therefore, this thesis highlights the importance to identify SDDs within cohorts of participants of AMD by use of OCT when using RMDA as an outcome measure.

6.1.2 Systematic Literature Review Summary

Chapter 2 aimed to systematically review the current literature describing methodology used to assess DA in people with AMD, the evidence of precision in detecting the onset and progression of AMD, and the relationship between DA and other functional and structural measures. Forty-eight studies that included the assessment of DA in people with AMD published between January 2006 and January 2021 were assessed. The literature identified in the review clearly indicated that a delay in measured rate of DA is associated with the presence of AMD (Higgins, Taylor, et al., 2021); this was the main finding.

Yet, there was less evidence of an association between early AMD and delayed DA when compared to visually healthy controls. The AdaptDx was the most popular dark adaptometry device in the literature, but there was a lack of methodological continuity (e.g., statistical analysis, test cut-off times used and AMD severity classifications). There was an absence of studies reporting test-retest variability assessment of RIT data and evidence for diagnostic capabilities of the AdaptDx was weak. Chapter 2 highlighted the requirement for further studies to plug these clear gaps in the literature and, perhaps most importantly, identified avenues this body of work could go on to explore.

6.1.3 Time-to-event Analysis and Rod-Intercept Time Data

Chapter 2 revealed that the majority of studies statistically analysing RIT data relied upon standard t-tests (Owsley et al., 2014; Owsley, Huisinigh, et al., 2016; Owsley, McGwin, et al., 2016; Láíns et al., 2017; Cocce et al., 2018; Láíns, Park, et al., 2018) or non-parametric equivalents (Jackson, Clark, et al., 2014; Jackson, Scott, et al., 2014; Flamendorf et al., 2015; Owsley, Clark and McGwin, 2017). Yet, these standard statistical tests are suboptimal in handling the characteristics of RIT data (skewed and censored data).

In the study described in Chapter 3, the efficacy of utilising time-to-event (survival) analysis was explored. This analysis was conducted on retrospectively collected RIT data sourced from Binns et al. (2018). The time-to-event analysis was compared to standard, alternative statistical methods: the student's t-test and GLM. As a result, time-to-event analysis was found to achieve higher statistical power in discriminating between people with AMD and healthy controls compared to both alternative methods. For example, at 80% power (at $\alpha = 0.05$), potential trial sample sizes could be reduced by between 40-53% by using the time-to-event analysis compared to a standard t-test of means. Thus, time-to-event analysis offers the potential advantage of reducing sample sizes if the method is chosen for analysing RIT data in future trials, for example. This is noteworthy for those designing trials as more efficient methodology equates to newer treatments likely being examined more efficiently. In addition, to help improve the accessibility of this methodology for RIT data, a free, web-based app was designed and published to implement this statistical technique (<https://bethanyelurahiggins.shinyapps.io/Time-to-EventAnalysis/>).

6.1.4 Optical Coherence Tomography-based Classification of Age-Related Macular Degeneration Disease Severity

In Chapter 2, it was reported there is reasonably good evidence for people with drusen and/or atrophic changes having slowed DA, particularly those with SDDs (Flamendorf et al., 2015; Fraser et al., 2016; Sevilla et al., 2016; Neely et al., 2017; Láins et al., 2017; Flynn, Cukras and Jeffrey, 2018; Láins, Miller, et al., 2018; Luu et al., 2018; Nguyen et al., 2018; Chen et al., 2019). Yet, the majority of published literature investigating DA in people with AMD features severity grading systems characterised by CFP, despite its subpar ability to image SDDs when compared to OCT (Jain et al., 2010).

The work described in Chapter 4 compared a novel OCT-based classification of AMD disease severity to the Beckman CFP-based classification, using RMDA as a reference standard for visual function. The secondary aim was to assess the association between SDD presence and DA at different AMD severity grades, using the OCT-based classification. To assess RMDA, time-to-event analysis was used, as described in Chapter 3. After correcting for age, it was found that RMDA was delayed in people graded as having iAMD, regardless of if they were classified using a CFP or an OCT-based system. This was the main finding from this study. In addition, RMDA did not differ between eyes classified as having less severe AMD, and those with normal ageing changes, irrespective of the classification system used, after correcting for age. Also, SDD presence (assessed via OCT) was found to be associated with impaired RMDA at more severe levels of AMD, but this was less clear after correcting for age. Results from this chapter represent new knowledge about classifying people with and without AMD using structural measures, as well as novel methodology using RMDA as our reference standard to measure visual function.

6.1.5 Test-retest variability and discrimination performance of the AdaptDx versus S-MAIA

Lastly, the work featured in Chapter 2 highlighted the dearth of research into both test-retest variability and discriminatory power of DA to separate people with earlier stages of AMD and visually healthy controls. This is noteworthy as the AdaptDx is widely cited as able to “sensitively and specifically detect early AMD” (Jackson & Edwards, 2008). To address this, Chapter 5 aimed to compare the performance of repeated measures of the AdaptDx device (RIT) to measures of the S-MAIA (MMAT and SMAT) in eyes with iAMD as part of the multicentre MACUSTAR study. As a result, MMAT and SMAT were found to have adequate test-retest variability levels, which were slightly better than those of RIT. All measures were moderately good (AUC; ~70%) at separating people defined as having iAMD from controls. Yet, early AMD was indistinguishable from iAMD on all measures (AUC:

<55%). We did not find evidence of practice/learning effects, which was surprising, but may be due to the SOPs featured (see section 8.3). Furthermore, the analysis presented in this chapter indicated that incomplete results and unreliable data using both devices need to be considered when designing trials using these technologies. Awareness of test-retest variability of the metrics from these devices and estimates of usable/reliable data are invaluable for study design and represent a significant contribution to the knowledge base provided by the work in this chapter.

6.2 IDEAS FOR FUTURE WORK

The studies reported in this thesis go some way towards understanding how DA is currently assessed in people with AMD the studies also suggest improvements upon methodology currently used and to compare it to similar measures of visual function. Yet the completed studies also raise a number of issues which have the potential to be addressed in future research. Specific ideas relating to each individual project were discussed in the preceding chapters. What follows is a brief ‘think-aloud’ description of some additional ideas that arise from the body of work as a whole and might be considered subjects of future work.

The results from the systematic literature review in Chapter 2 and the work described in Chapter 4 highlighted that SDD presence is associated with greater rod dysfunction in people with more severe AMD. While this finding supports histopathological studies that SDDs tend to be located in rod-dominated retinal locations and are associated with changes in photoreceptor morphology (Curcio et al., 2013), rod dysfunction tends to occur where there are fewer rods due to location (e.g. the fovea) or degeneration (ageing or AMD) (Owsley et al., 2000). Therefore, we concluded SDD presence may serve as a structural biomarker for another process and further work needs to be completed in increasing our understanding of SDD pathophysiology. For example, SDD presence can be seen in other pathologies involving the RPE-BM such as Sorsby’s macular dystrophy, it would be conducive to compare RMDA and structural features on OCT in these conditions.

The app developed as part of Chapter 3 featuring time-to-event analysis is currently unsuitable for clinical application as it cannot be used to analyse individual patients. Yet, there is scope for the censoring element of the time-to-event analysis methodology to be developed further and potentially be broadened to other visual function measures. For example, censored data is not only an issue in measuring DA, but an issue in the assessment of declining retinal sensitivity via visual fields. Values censored at 0dB are often considered to be actual 0dB for the scope of analysis, which can introduce positive biases in the measured progression rate. The freely available app’s methodology could be adapted further to conduct a censored regression that can be applied to the uploaded data, where the error term is a censored distribution, making it applicable for wider clinical data analysis. This app

could then be used in clinical trials or longitudinal studies looking and changes in visual field data over time.

Despite not being the focus of work in Chapter 4, we also found evidence to suggest a structure-function relationship between larger, more distinct SDDs and delayed RMDA function in people with AMD. This was still the case when the time-to-event analysis was age adjusted. Yet, the experimental design of the study yielding the data did not allow for meaningful comparisons across different levels of AMD severity. This would be an interesting focus of a future study to ascertain if this potential structure-function relationship occurs only in more severe cases of AMD. In turn, this could be done with other disease-related morphology or also in visually healthy controls and earlier cases of AMD disease.

In keeping with the theme of exploring RMDA in other pathologies, it would be an interesting topic of future research to examine RMDA using the AdaptDx in young people with inherited retinal eye disease. For example, genetic diseases characterised by retinal degeneration in which nyctalopia is a common symptom such as Usher syndrome(El-Amraoui & Petit, 2014) may be a potential group to benefit from RMDA assessment. In fact, the time-to-event methodology developed as part of this thesis in Chapter 3 will soon be applied to RMDA data collected by a research team at the Institute of Ophthalmology at UCL alongside Moorfields Eye Hospital in young people and adults with choroideremia. Choroideremia is caused by a mutation in the CHM gene is its phenotypes include progressive degeneration of the RPE, photoreceptors and the choriocapillaris and like Usher syndrome, night blindness is a common symptom.

Furthermore, recruitment is underway for a new research study with patients seen at Moorfields Eye Hospital with CRB1 mutations. When mutations exist in the CRB1 gene, individuals can develop different patterns of sight loss. Some individuals are severely affected, experiencing sight loss from birth and blindness within the first few years of life. This is called Leber congenital amaurosis (LCA). CRB1 accounts for between 7-17% of LCA cases. Other individuals can develop progressive sight loss from later in childhood or early adulthood, with night vision then peripheral vision affected first, followed by central vision. This is called retinitis pigmentosa (RP) and mutations in the CRB1 gene account for up to 9% of such cases. Finally, a smaller proportion of patients may develop loss of central vision first followed by loss of the peripheral field of view, this is known as cone-rod dystrophy and is a rarer form of CRB1-disease. Thirty to forty patients, divided into groups of ~10 with LCA, RP and cone-rod dystrophy will be examined using a battery of visual function tests over a 2-year period to determine vision-related measures that can be used in future clinical trials. One of these tests which will be assessment of RMDA using the AdaptDx. Now that a better statistical assessment of RIT data has been published (Chapter 3) and informative SOPs for the AdaptDx use in a multicentre setting are soon to be available (Chapter 5), this opens the possibility to design and test out appropriate protocols to assess this cohort.

In each of the datasets described in Chapters 3-5, none of the participants were screened for cognitive defects. Thus, it is possible that subtle differences in cognitive ability between participants could have affected the results as it may have impacted the understanding and the orchestration of the DA testing procedure. Furthermore, there have been suggestions in the literature that AMD and impaired cognitive function may be linked (Baker et al., 2009). Future work might use cognitive tests in order to separate out this potential confounder.

Lastly, as defined throughout this thesis, AMD is classified structurally on drusen size and presence/absence of pigmentary abnormalities. While we have highlighted the importance of incorporating SDDs into a classification of AMD severity (Chapter 4), there are other structural biomarkers associated with AMD. For example, drusen volume, hyperreflective foci (HF), retinal layer thicknesses, incomplete RPE, iRORA and cRORA are also not included in the Beckman classification system. Hence, structural phenotypic heterogeneity is to be expected within CFP-based classifications of AMD severity. Furthermore, as iRORA and cRORA have only recently been defined, less is known about the relationship between visual function and presence of these structural biomarkers. Future work could focus on exploring the extent to which there is concordance between these structural biomarkers and those with impaired visual function, using RMDA is a reference standard.

6.3 PEER-REVIEWED MANUSCRIPTS

Higgins BE, Montesano G, Binns AM, Crabb DP (2021). Optimising Analysis of Dark Adaptation Data Using Time-to-Event Analysis. *Scientific Reports*. 11(1), 8323. doi.org/10.1038/s41598-021-86193-3

Higgins BE, Taylor DJ, Bi W, Binns AM, Crabb DP (2021). Are Current Methods of Measuring Dark Adaptation Effective in Detecting the Onset and Progression of Age-Related Macular Degeneration? A Systematic Literature Review. *Ophthalmology Therapy*. 10(1), 21-38. doi:10.1007/s40123-020-00323-0

Higgins BE, Montesano G, Crabb DP, Naskas TT, Graham KW, Chakravarthy U, Kee F, Wright DM, Hogg RE (2022). Assessment of a classification of age-related macular degeneration severity from the Northern Ireland Sensory Aging study using a measure of dark adaptation. *Ophthalmology Science*. 2(4), 100204. doi:org/10.1016/j.xops.2022.100204

6.4 CONFERENCE ABSTRACTS

British Congress of Optometry and Vision Science – BCOVS 2021- Virtual – paper presentation

Assessing an OCT-based Severity Classification of Age-related Macular Degeneration using Dark Adaptation Data from a Large Cohort Study (Northern Ireland Sensory Aging studies – NISA)

Bethany E. Higgins, Giovanni Montesano, Timos Naskas, Katie W. Graham, Usha Chakravarthy, Frank Kee, David M. Wright, Ruth E. Hogg, David P. Crabb

European Society of Retina Specialists - EURetina 2021- Virtual – paper presentation

Assessment of a novel OCT classification of age-related macular degeneration severity using dark adaptation data from a large cohort study (Northern Ireland Sensory Aging studies – NISA)

Bethany E. Higgins, Giovanni Montesano, Timos Naskas, Katie W. Graham, Usha Chakravarthy, Frank Kee, David M. Wright, Ruth E. Hogg, David P. Crabb

The Association for Research in Vision and Ophthalmology- ARVO 2022 Annual Meeting – Denver, Colorado, USA – poster presentation

Evaluating an OCT-based grading of age-related macular degeneration severity from The Northern Ireland Sensory Aging studies using measurement of dark adaptation.

Bethany E. Higgins, Giovanni Montesano, Timos Naskas, Katie W. Graham, Usha Chakravarthy, Frank Kee, David M. Wright, Ruth E. Hogg, David P. Crabb

Imaging and Perimetry Society – IPS Symposium 2022 – Berkley, California, USA - paper presentation

Properties of measurements from the S-MAIA microperimeter in people with intermediate age-related macular degeneration in the MACUSTAR study

Bethany E. Higgins, Giovanni Montesano, Hannah Dunbar, Alison M. Binns, Deanna R. Taylor, Charlotte Behning, Amina Abdirahman, Jan H. Terheyden, Nadia Zakaria, Stephen Poor, Robert P. Finger, Sergio Leal, Frank G. Holz, Michael C. Schmid, Ulrich F.O. Luhman, Gary S. Rubin, David P. Crabb

British Congress of Optometry and Vision Science – BCOVS 2022— poster presentation

Assessing performance of microperimetry and dark adaptometry in people with intermediate AMD. A MACUSTAR report.

Bethany E. Higgins, Giovanni Montesano, Hannah Dunbar, Alison M. Binns, Deanna R. Taylor, Charlotte Behning, Amina Abdirahman, Jan H. Terheyden, Nadia Zakaria, Stephen Poor, Robert P. Finger, Sergio Leal, Frank G. Holz, Michael C. Schmid, Ulrich F.O. Luhman, Gary S. Rubin, David P. Crabb

7 REFERENCES

- Abramoff, M. D., Garvin, M. K., & Sonka, M. (2010). Retinal Imaging and Image Analysis. *IEEE Reviews in Biomedical Engineering*, 3, 169–208. <https://doi.org/10.1109/RBME.2010.2084567>
- Akuffo, K. O., Beatty, S., Peto, T., Stack, J., Stringham, J., Kelly, D., Leung, I., Corcoran, L., & Nolan, J. M. (2017). The impact of supplemental antioxidants on visual function in nonadvanced age-related macular degeneration: A head-to-head randomized clinical trial. *Investigative Ophthalmology and Visual Science*, 58(12), 5347–5360. <https://doi.org/10.1167/iovs.16-21192>
- Akuffo, K. O., Nolan, J. M., Peto, T., Stack, J., Leung, I., Corcoran, L., & Beatty, S. (2017). Relationship between macular pigment and visual function in subjects with early age-related macular degeneration. *British Journal of Ophthalmology*, 101(2), 190–197. <https://doi.org/10.1136/bjophthalmol-2016-308418>
- Allingham, M. J., Mettu, P. S., & Cousins, S. W. (2022). Phase 1 Clinical Trial of Elamipretide in Intermediate Age-Related Macular Degeneration and High-Risk Drusen: ReCLAIM High-Risk Drusen Study. *Ophthalmology Science*, 2(1), 100095. <https://doi.org/10.1016/J.XOPS.2021.100095>
- Ambati, J., Ambati, B. K., Yoo, S. H., Ianchulev, S., & Adamis, A. P. (2003). Age-related macular degeneration: etiology, pathogenesis, and therapeutic strategies. *Survey of Ophthalmology*, 48(3), 257–293. [https://doi.org/10.1016/s0039-6257\(03\)00030-4](https://doi.org/10.1016/s0039-6257(03)00030-4)
- Ambati, J., Atkinson, J. P., & Gelfand, B. D. (2013). Immunology of Age-Related Macular Degeneration. *Nature Reviews Immunology*, 13(6), 438–451. <https://doi.org/10.1038/nri3459>
- Ambati, J., & Fowler, B. J. (2012). Mechanisms of Age-related Macular Degeneration. *Neuron*, 75(1), 26–39. <https://doi.org/10.1016/j.neuron.2012.06.018>
- Anderson, B., & Saltzman, H. A. (1964). Retinal Oxygen Utilization Measured by Hyperbaric Blackout. *Archives of Ophthalmology*, 72(6), 792–795. <https://doi.org/10.1001/archophth.1964.00970020794009>
- Arden, G. B., & Jacobson, J. J. (1978). A Simple Grating Test for Contrast Sensitivity: Preliminary Results Indicate Value in Screening for Glaucoma. *Investigative Ophthalmology and Visual Science*, 17(1), 23–32. <https://iovs.arvojournals.org/article.aspx?articleid=2175483>
- Ardourel, J. E. (2000). Risk Factors Associated with Age-Related Macular Degeneration. A Case-Control Study in The Age-Related Eye Disease Study: Age-Related Eye Disease Study Report Number 3. *Ophthalmology*, 107(12), 2224–2232. [https://doi.org/10.1016/S0161-6420\(00\)00409-7](https://doi.org/10.1016/S0161-6420(00)00409-7)
- AREDS Research Group. (2001). The Age-Related Eye Disease Study System for Classifying Age-Related Macular Degeneration From Stereoscopic Color Fundus Photographs: The Age-Related Eye Disease Study Report Number 6. *American Journal of Ophthalmology*, 132(5), 668–681. [https://doi.org/10.1016/S0002-9394\(01\)01218-1](https://doi.org/10.1016/S0002-9394(01)01218-1)
- AREDS Research Group, Kasseoff, A., Kasseoff, J., Buehler, J., Eglow, M., Kaufman, F., Mehu, M., Kieval, S., Mairs, M., Graig, B., Quattrocchi, A., Jones, D., Locatelli, J., Ruby, A., Capon A., J., Garretson, B., Hassan, T., Trese, M. T., Williams, G. A., ... Crouse, V. D. (2001). A Randomized, Placebo-Controlled, Clinical Trial Of High-Dose Supplementation With Vitamins C And E, Beta Carotene, And Zinc For Age-Related Macular Degeneration And Vision Loss: AREDS report no. 8. *Archives of Ophthalmology*, 119(10), 1417–1436. <https://doi.org/10.1001/archophth.119.10.1417>
- Arjamaa, O., Aaltonen, V., Piippo, N., Csont, T., Petrovski, G., Kaarniranta, K., & Kauppinen, A. (2017). Hypoxia and Inflammation in The Release of VEGF And Interleukins From Human Retinal Pigment Epithelial Cells. *Graefe's Archive for Clinical and Experimental Ophthalmology* 255(9), 1757–1762. <https://doi.org/10.1007/s00417-017-3711-0>

- Arunkumar, R., Calvo, C. M., Conrady, C. D., & Bernstein, P. S. (2018). What do we know about the macular pigment in AMD: the past, the present, and the future. *Eye*, 32(5), 992–1004. <https://doi.org/10.1038/s41433-018-0044-0>
- Aubert H. (1865). *Physiologie der Netzhaut*. E. Morgenstern.
- Augood, C. A., Vingerling, J. R., de Jong, P. T. V. M., Chakravarthy, U., Seland, J., Soubrane, G., Tomazzoli, L., Topouzis, F., Bentham, G., Rahu, M., Vioque, J., Young, I. S., & Fletcher, A. E. (2006). Prevalence of age-related maculopathy in older Europeans: the European Eye Study (EUREYE). *Archives of Ophthalmology*, 124(4), 529–535. <https://doi.org/10.1001/archophth.124.4.529>
- Bailey, I. L., & Lovie, J. E. (1976). New design principles for visual acuity letter charts. *Optometry and Vision Science*, 53(11), 740–745. <https://doi.org/10.1097/00006324-197611000-00006>
- Baker, M. L., Wang, J. J., Rogers, S., Klein, R., Kuller, L. H., Larsen, E. K., & Wong, T. Y. (2009). Early age-related macular degeneration, cognitive function, and dementia: the Cardiovascular Health Study. *Archives of Ophthalmology*, 127(5), 667–673. <https://doi.org/10.1001/archophthalmol.2009.30>
- Barkana, Y., Pondorfer, S. G., Schmitz-Valckenberg, S., Russ, H., & Finger, R. P. (2021). Improved sensitivity of microperimetric outcomes for clinical studies in age-related macular degeneration. *Scientific Reports*, 11(1), 4764. <https://doi.org/10.1038/s41598-021-83716-w>
- Barratt, J., & Weitz, I. (2021). Complement Factor D as a Strategic Target for Regulating the Alternative Complement Pathway. *Frontiers in Immunology*, 12, 3595. <https://doi.org/10.3389/FIMMU.2021.712572/BIBTEX>
- Baumann, B., Götzinger, E., Pircher, M., Sattmann, H., Schütze, C., Schlanitz, F., Ahlers, C., Schmidt-Erfurth, U., & Hitzenberger, C. K. (2010). Segmentation and quantification of retinal lesions in age-related macular degeneration using polarization-sensitive optical coherence tomography. *Journal of Biomedical Optics*, 15(6), 061704. <https://doi.org/10.1117/1.3499420>
- Bavik, C., Henry, S. H., Zhang, Y., Mitts, K., McGinn, T., Budzynski, E., Pashko, A., Lieu, K. L., Zhong, S., Blumberg, B., Kuksa, V., Orme, M., Scott, I., Fawzi, A., & Kubota, R. (2015). Visual cycle modulation as an approach toward preservation of retinal integrity. *PLoS ONE*, 10(5), e0124940. <https://doi.org/10.1371/journal.pone.0124940>
- Beatty, S., Koh, H. H., Phil, M., Henson, D., & Boulton, M. (2000). The role of oxidative stress in the pathogenesis of age-related macular degeneration. *Survey of Ophthalmology*, 45(2), 115–134. [https://doi.org/10.1016/S0039-6257\(00\)00140-5](https://doi.org/10.1016/S0039-6257(00)00140-5)
- Beirne, R. O., & McConnell, E. (2019). Investigation of the relationship between macular pigment levels and rod-mediated dark adaptation in intermediate age-related macular degeneration. *Clinical and Experimental Optometry*, 102(6), 611–616. <https://doi.org/10.1111/cxo.12882>
- Bellmann, C., Unnebrink, K., Rubin, G. S., Miller, D., & Holz, F. G. (2003). Visual acuity and contrast sensitivity in patients with neovascular age-related macular degeneration. *Graefes Archive for Clinical and Experimental Ophthalmology*, 241(12), 968–974. <https://doi.org/10.1007/S00417-003-0689-6>
- Bhagat, N. (2022, July 21). *Fundus Autofluorescence* - EyeWiki. https://eyewiki.aao.org/Fundus_Autofluorescence
- Bhende, M., Shetty, S., Parthasarathy, M. K., & Ramya, S. (2018). Optical coherence tomography: A guide to interpretation of common macular diseases. *Indian Journal of Ophthalmology*, 66(1), 20–35. https://doi.org/10.4103/ijo.IJO_902_17
- Binns, A. M., & Margrain, T. H. (2007). Evaluating Retinal Function in Age-Related Maculopathy with the ERG Photostress Test. *Investigative Ophthalmology & Visual Science*, 48(6), 2806–2813. <https://doi.org/10.1167/iovs.06-0392>

- Binns, A. M., Taylor, D. J., Edwards, L. A., Crabb, D. P. (2018). Determining optimal test parameters for assessing dark adaptation in people with intermediate age-related macular degeneration. *Investigative Ophthalmology & Visual Science*, 59(4), AMD114–AMD121. <http://dx.doi.org.wam.city.ac.uk/10.1167/iovs.18-24211>
- Bird, A. C., Bressler, N. M., Bressler, S. B., Chisholm, I. H., Coscas, G., Davis, M. D., de Jong, P. T. V. M., Klaver, C. C. W., Klein, B. E. K., Klein, R., Mitchell, P., Sarks, J. P., Sarks, S. H., Soubrane, G., Taylor, H. R., & Vingerling, J. R. (1995). An international classification and grading system for age-related maculopathy and age-related macular degeneration. *Survey of Ophthalmology*, 39(5), 367–374. [https://doi.org/10.1016/S0039-6257\(05\)80092-X](https://doi.org/10.1016/S0039-6257(05)80092-X)
- Bland, J. M., & Altman, D. G. (1986). Statistical methods for assessing agreement between two methods of clinical measurement. *Lancet*, 1(8476), 307–310. [https://doi.org/10.1016/S0140-6736\(86\)90837-8](https://doi.org/10.1016/S0140-6736(86)90837-8)
- Bossuyt, P. M., Reitsma, J. B., Bruns, D. E., Gatsonis, C. A., Glasziou, P. P., Irwig, L. M., Lijmer, J. G., Moher, D., Rennie, D., & De Vet, H. C. W. (2003). Toward complete and accurate reporting of studies of diagnostic accuracy: The STARD initiative. *Clinical Chemistry*, 49(1), 1–6. <https://doi.org/10.1373/49.1.1>
- Bott, D., Huntjens, B., & Binns, A. (2018). Nutritional and smoking advice recalled by patients attending a UK age-related macular degeneration clinic. *Journal of Public Health*, 40(3), 614–622. <https://doi.org/10.1093/pubmed/idx115>
- Bourne, R. R. A., Jonas, J. B., Flaxman, S. R., Keeffe, J., Leasher, J., Naidoo, K., Parodi, M. B., Pesudovs, K., Price, H., White, R. A., Wong, T. Y., Resnikoff, S., & Taylor, H. R. (2014). Prevalence and causes of vision loss in high-income countries and in Eastern and Central Europe: 1990-2010. *The British Journal of Ophthalmology*, 98(5), 629–638. <https://doi.org/10.1136/BJOPHTHALMOL-2013-304033>
- Brandl, C., Zimmermann, M. E., Günther, F., Barth, T., Olden, M., Schelter, S. C., Kronenberg, F., Loss, J., Küchenhoff, H., Helbig, H., Weber, B. H. F., Stark, K. J., & Heid, I. M. (2018). On the impact of different approaches to classify age-related macular degeneration: Results from the German AugUR study. *Scientific Reports* 8(1), 1–10. <https://doi.org/10.1038/s41598-018-26629-5>
- Brinkmann, C. K., Adrion, C., Mansmann, U., Schmitz-Valckenberg, S., & Holz, F. G. (2010). Klinische Merkmale, Progression und Risikofaktoren bei geographischer Atrophie. *Der Ophthalmologe*, 107(11), 999–1006. <https://doi.org/10.1007/s00347-010-2158-z>
- Brown, B., & Kitchin, J. L. (1983). Dark adaptation and the acuity/luminance response in senile macular degeneration (SMD). *Optometry and Vision Science*, 60(8), 645–650. <https://doi.org/10.1097/00006324-198308000-00001>
- Brown, D. M., Michels, M., Kaiser, P. K., Heier, J. S., Sy, J. P., & Ianchulev, T. (2009). Ranibizumab versus verteporfin photodynamic therapy for neovascular age-related macular degeneration: Two-year results of the ANCHOR study. *Ophthalmology*, 116(1), 57-65.e5. <https://doi.org/10.1016/j.ophtha.2008.10.018>
- Bunce, C., Zekite, A., Walton, S., Rees, A., & Patel, P. J. (2015). Certifications for sight impairment due to age related macular degeneration in England. *Public Health*, 129(2), 138–142. <https://doi.org/10.1016/j.puhe.2014.12.018>
- Burns, M. E., & Baylor, D. A. (2001). Activation, deactivation, and adaptation in vertebrate photoreceptor cells. In *Annual Review of Neuroscience*, 24, 779–805. <https://doi.org/10.1146/annurev.neuro.24.1.779>
- Cabral De Guimaraes, T. A., Daich Varela, M., Georgiou, M., & Michaelides, M. (2021). Treatments for dry age-related macular degeneration: Therapeutic avenues, clinical trials and future directions. *British Journal of Ophthalmology*, 106, 297-304. <https://doi.org/10.1136/bjophthalmol-2020-318452>

- Campochiaro, P. A. (2004). Ocular neovascularisation and excessive vascular permeability. *Expert Opinion on Biological Therapy*, 4(9), 1395–1402. <https://doi.org/10.1517/14712598.4.9.1395>
- Critical Appraisal Skills Programme (2013). CASP. <https://casp-uk.net/casp-tools-checklists/>.
- Cassels, N. K., Wild, J. M., Margrain, T. H., Chong, V., & Acton, J. H. (2018). The use of microperimetry in assessing visual function in age-related macular degeneration. *Survey of Ophthalmology*, 63(1), 40–55. <https://doi.org/10.1016/j.survophthal.2017.05.007>
- Chakravarthy, U., Williams, M., & AMD Guidelines Group. (2013). The Royal College of Ophthalmologists Guidelines on AMD: Executive Summary. *Eye*, 27(12), 1429–1431. <https://doi.org/10.1038/eye.2013.233>
- Chakravarthy, U., Wong, T. Y., Fletcher, A., Piau, E., Evans, C., Zlateva, G., Buggage, R., Pleil, A., & Mitchell, P. (2010). Clinical risk factors for age-related macular degeneration: A systematic review and meta-analysis. *BMC Ophthalmology*, 10(1), 31. <https://doi.org/10.1186/1471-2415-10-31>
- Chandra, S., McKibbin, M., Mahmood, S., Downey, L., Barnes, B., Sivaprasad, S., Sivaprasad, S., Barnes, B., Barrett, T., Boparai, P., Broom, M., Chandra, S., Crosby-Nwaobi, R., Downey, L., Li, K., Mahmood, S., Mankowska, A., McKibbin, M., Richmond, Z., ... Yelf, C. (2022). The Royal College of Ophthalmologists Commissioning guidelines on age macular degeneration: executive summary. *Eye*, 1–6. <https://doi.org/10.1038/s41433-022-02095-2>
- Chandra, S., Rasheed, R., Sen, P., Menon, D., & Sivaprasad, S. (2022). Inter-rater reliability for diagnosis of geographic atrophy using spectral domain OCT in age-related macular degeneration. *Eye*, 36(2), 392–397. <https://doi.org/10.1038/s41433-021-01490-5>
- Chen, C., Wu, L., Wu, D., Huang, S., Wen, F., Luo, G., & Long, S. (2004). The local cone and rod system function in early age-related macular degeneration. *Documenta Ophthalmologica*, 109(1), 1–8. <https://doi.org/10.1007/s10633-004-1041-0>
- Chen, K. G., Alvarez, J. A., Yazdanie, M., Papudesu, C., Wong, W. T., Wiley, H. E., Keenan, T. D., Chew, E. Y., Ferris, F. L., Cukras, C. A., Ferris 3rd, F. L., Cukras, C. A., Keenan, T. D., Chew, E. Y., Ferris 3rd, F. L., & Cukras, C. A. (2019). Longitudinal Study of Dark Adaptation as a Functional Outcome Measure for Age-Related Macular Degeneration. *Ophthalmology*, 126(6), 856–865. <https://doi.org/10.1016/j.ophtha.2018.09.039>
- Chen, L., Cao, D., Messinger, J. D., Ach, T., Ferrara, D., Freund, K. B., & Curcio, C. A. (2022). Histology and clinical imaging lifecycle of black pigment in fibrosis secondary to neovascular age-related macular degeneration. *Experimental Eye Research*, 214, 108882. <https://doi.org/https://doi.org/10.1016/j.exer.2021.108882>
- Chen, Y., Bedell, M., & Zhang, K. (2010). Age-related macular degeneration: Genetic and environmental factors of disease. In *Molecular Interventions*, 10(5), 271–281. <https://doi.org/10.1124/mi.10.5.4>
- Chen, Y., Zeng, J., Zhao, C., Wang, K., Trood, E., Buehler, J., Weed, M., Kasuga, D., Bernstein, P. S., Hughes, G., Fu, V., Chin, J., Lee, C., Crocker, M., Bedell, M., Salazar, F., Yang, Z., Goldbaum, M., Ferreyra, H., ... Zhang, K. (2011). Assessing susceptibility to age-related macular degeneration with genetic markers and environmental factors. *Archives of Ophthalmology* 129(3), 344–351. <https://doi.org/10.1001/archophthol.2011.10>
- Chew, E. Y., Clemons, T. E., SanGiovanni, J. P., Danis, R., Ferris, F. L., Elman, M., Antoszyk, A., Ruby, A., Orth, D., Bressler, S., Fish, G., Hubbard, B., Klein, M., Chandra, S., Blodi, B., Domalpally, A., Friberg, T., Wong, W., Rosenfeld, P., ... Sperduto, R. (2013). Lutein + Zeaxanthin and Omega-3 Fatty Acids for Age-Related Macular Degeneration: The Age-Related Eye Disease Study 2 (AREDS2) Randomized Clinical Trial. *JAMA*, 309(19), 2005–2015. <https://doi.org/10.1001/JAMA.2013.4997>

- Chew, E. Y., Clemons, T., SanGiovanni, J. P., Danis, R., Domalpally, A., McBee, W., Sperduto, R., & Ferris, F. L. (2012). The Age-Related Eye Disease Study 2 (AREDS2): study design and baseline characteristics (AREDS2 report number 1). *Ophthalmology*, *119*(11), 2282–2289. <https://doi.org/10.1016/j.ophtha.2012.05.027>
- Cho, H., Matthews, G. J., & Harel, O. (2019). Confidence Intervals for the Area Under the Receiver Operating Characteristic Curve in the Presence of Ignorable Missing Data. *International Statistical Review*, *87*(1), 152–177. <https://doi.org/10.1111/insr.12277>
- Christen, W. G., Glynn, R. J., Manson, J. E., Ajani, U. A., & Buring, J. E. (1996). A Prospective Study of Cigarette Smoking and Risk of Age-Related Macular Degeneration in Men. *JAMA*, *276*(14), 1147–1151. <https://doi.org/10.1001/JAMA.1996.03540140035023>
- Clark, M. E., McGwin, G., Neely, D., Feist, R., Mason, J. O., Thomley, M., White, M. F., Ozaydin, B., Girkin, C. A., & Owsley, C. (2011). Association between retinal thickness measured by spectral-domain optical coherence tomography (OCT) and rod-mediated dark adaptation in non-exudative age-related maculopathy. *British Journal of Ophthalmology*, *95*(10), 1427–1432. <https://doi.org/10.1136/bjo.2010.190355>
- Clearkin, L., Ramasamy, B., Wason, J., & Tiew, S. (2019). Anti-VEGF intervention in neovascular AMD: benefits and risks restated as natural frequencies. *BMJ Open Ophthalmology*, *4*, 257. <https://doi.org/10.1136/bmjophth-2018-000257>
- Cocce, K. J., Stinnett, S. S., Luhmann, U. F. O., Vajzovic, L., Horne, A., Schuman, S. G., Toth, C. A., Cousins, S. W., & Lad, E. M. (2018). Visual Function Metrics in Early and Intermediate Dry Age-related Macular Degeneration for Use as Clinical Trial Endpoints. *American Journal of Ophthalmology*, *189*, 127–138. <https://doi.org/10.1016/j.ajo.2018.02.012>
- Colijn, J. M., Buitendijk, G. H. S., Prokofyeva, E., Alves, D., Cachulo, M. L., Khawaja, A. P., Cougnard-Gregoire, A., Merle, B. M. J., Korb, C., Erke, M. G., Bron, A., Anastasopoulos, E., Meester-Smoor, M. A., Segato, T., Piermarocchi, S., de Jong, P. T. V. M., Vingerling, J. R., Topouzis, F., Creuzot-Garcher, C., ... Zwiener, I. (2017). Prevalence of Age-Related Macular Degeneration in Europe: The Past and the Future. *Ophthalmology*, *124*(12), 1753–1763. <https://doi.org/10.1016/j.ophtha.2017.05.035>
- Corvi, F., Chandra, S., Invernizzi, A., Pace, L., Viola, F., Sivaprasad, S., Staurengi, G., Cheung, C. & Teo, K., (2022). Multimodal Imaging Comparison of Polypoidal Choroidal Vasculopathy Between Asian and Caucasian Populations. *American Journal of Ophthalmology*, *234*, 108–116. <https://doi.org/10.1016/j.ajo.2021.08.006>
- Crossland, M. D., Luong, V. A., Rubin, G. S., & Fitzke, F. W. (2011). Retinal specific measurement of dark-adapted visual function: validation of a modified microperimeter. *BMC Ophthalmology*, *11*(5). <https://doi.org/10.1186/1471-2415-11-5>
- Crossland, M., & Rubin, G. (2007). The Amsler chart: absence of evidence is not evidence of absence. *The British Journal of Ophthalmology*, *91*(3), 391–393. <https://doi.org/10.1136/bjo.2006.095315>
- Curcio, C. A., & Johnson, M. (2012). Structure, Function, and Pathology of Bruch's Membrane. In S. J. Ryan, A. P. Schachat, C. P. Wilkinson, D. R. Hinton, S. Sadda, P. Wiedemann (Ed.), *Retina Fifth Edition*, 1, 465-481. <https://doi.org/10.1016/B978-1-4557-0737-9.00020-5>
- Curcio, C. A., Johnson, M., Rudolf, M., & Huang, J. D. (2011). The oil spill in ageing Bruch membrane. *British Journal of Ophthalmology*, *95*(12), 1638–1645. <https://doi.org/10.1136/bjophthalmol-2011-300344>
- Curcio, C. A., Medeiros, N. E., & Millican, C. L. (1996). Photoreceptor loss in age-related macular degeneration. *Investigative Ophthalmology and Visual Science*, *37*(7), 1236–1249. <https://iovs.arvojournals.org/article.aspx?articleid=2180378>

- Curcio, C. A., Messinger, J. D., Sloan, K. R., McGwin, G., Medeiros, N. E., & Spaide, R. F. (2013). Subretinal drusenoid deposits in non-neovascular age-related macular degeneration: morphology, prevalence, topography, and biogenesis model. *Retina* 33(2), 265–276. <https://doi.org/10.1097/IAE.0b013e31827e25e0>
- Curcio, C. A., Owsley, C., & Jackson, G. R. (2000). Spare the rods, save the cones in aging and age-related maculopathy. *Investigative Ophthalmology & Visual Science*, 41(8), 2015–2018. <https://iovs.arvojournals.org/article.aspx?articleid=2123754>
- Curcio, C. A., Sloan, K. R., Kalina, R. E., & Hendrickson, A. E. (1990). Human photoreceptor topography. *Journal of Comparative Neurology*, 292(4), 497–523. <https://doi.org/10.1002/cne.902920402>
- Danis, R. P., Domalpally, A., Chew, E. Y., Clemons, T. E., Armstrong, J., SanGiovanni, J. P., & Ferris, F. L. (2013). Methods and reproducibility of grading optimized digital color fundus photographs in the Age-Related Eye Disease Study 2 (AREDS2 Report Number 2). *Investigative Ophthalmology and Visual Science*, 54(7), 4548–4554. <https://doi.org/10.1167/iovs.13-11804>
- De La Paz, M., & Anderson, R. E. (1992). Region and age-dependent variation in susceptibility of the human retina to lipid peroxidation. *Investigative Ophthalmology & Visual Science*, 33(13), 3497–3499. <https://iovs.arvojournals.org/article.aspx?articleid=2178631&resultClick=1>
- Delori, F. C., Goger, D. G., & Dorey, C. K. (2001). Age-Related Accumulation and Spatial Distribution of Lipofuscin in RPE of Normal Subjects. *Investigative Ophthalmology & Visual Science*, 42(8), 1855–1866. <https://iovs.arvojournals.org/article.aspx?articleid=2200004>
- Dhalla, M. S., Fantin, A., Blinder, K. J., & Bakal, J. A. (2007). The Macular Automated Photostress Test. *American Journal of Ophthalmology*, 143(4), 596–600. <https://doi.org/10.1016/j.ajo.2006.12.033>
- Dimitrov, P. N., Guymer, R. H., Zele, A. J., Anderson & A. J., Vingrys, (2008). Measuring rod and cone dynamics in age-related maculopathy. *Investigative Ophthalmology and Visual Science*, 49(1), 55–65. <https://doi.org/10.1167/iovs.06-1048>
- Dimitrov, P. N., Robman, L. D., Varsamidis, M., Aung, K. Z., Makeyeva, G. A., Guymer, R. H., & Vingrys, A. J. (2011). Visual function tests as potential biomarkers in age-related macular degeneration. *Investigative Ophthalmology and Visual Science*, 52(13), 9457–9469. <https://doi.org/10.1167/iovs.10-7043>
- Dimitrov, P. N., Robman, L. D., Varsamidis, M., Aung, K. Z., Makeyeva, G., Busija, L., Vingrys, A. J., Guymer, (2012). Relationship between clinical macular changes and retinal function in age-related macular degeneration. *Investigative Ophthalmology and Visual Science*, 53(9), 5213–5220. <https://doi.org/10.1167/iovs.11-8958>
- Dunbar, H., Behning, C., Abdirahman, A., Higgins, B. E., Binns, A. M., Terheyden, J. H., Zakaria, N., Poor, S., Finger, R. P., Leal, S., Holz, F. G., Schmid, M., Crabb, D. P., Rubin, G. S., Luhmann, U., & MACUSTAR Consortium (2022). Repeatability and Discriminatory Power of Chart-Based Visual Function Tests in Individuals with Age-Related Macular Degeneration: A MACUSTAR Study Report. *JAMA Ophthalmology* <https://doi:10.1001/jamaophthalmol.2022.2113>
- Dugel, P. U., Koh, A., Ogura, Y., Jaffe, G. J., Schmidt-Erfurth, U., Brown, D. M., Gomes, A. V., Warburton, J., Weichselberger, A., & Holz, F. G. (2020). HAWK and HARRIER: Phase 3, Multicenter, Randomized, Double-Masked Trials of Brolucizumab for Neovascular Age-Related Macular Degeneration. *Ophthalmology*, 127(1), 72–84. <https://doi.org/10.1016/j.ophtha.2019.04.017>
- Echols, B. S., Clark, M. E., Swain, T. A., Chen, L., Kar, D., Zhang, Y., Sloan, K. R., McGwin Jr, G., Singireddy, R., Mays, C., Kilpatrick, D., Crosson, J. N., Owsley, C., & Curcio, C. A. (2020). Hyperreflective Foci and Specks Are Associated with Delayed Rod-Mediated Dark Adaptation in Nonneovascular Age-Related Macular Degeneration. *Ophthalmology. Retina*, 4(11), 1059–1068. <https://doi.org/10.1016/j.oret.2020.05.001>

- Edwards, A. O., Ritter, R. 3rd, Abel, K. J., Manning, A., Panhuysen, C., & Farrer, L. A. (2005). Complement factor H polymorphism and age-related macular degeneration. *Science*, *308*(5720), 421–424. <https://doi.org/10.1126/science.1110189>
- Efron, B. (1977). The efficiency of cox's likelihood function for censored data. *Journal of the American Statistical Association*, *72*(359), 557–565. <https://doi.org/10.1080/01621459.1977.10480613>
- Eisner, A., Klein, M. L., Zilis, J. D., & Watkins, M. D. (1992). Visual function and the subsequent development of exudative age-related macular degeneration. *Investigative Ophthalmology & Visual Science*, *33*(11), 3091–3102. <https://iovs.arvojournals.org/article.aspx?articleid=2178756>
- El-Amraoui, A., & Petit, C. (2014). The retinal phenotype of Usher syndrome: Pathophysiological insights from animal models. *Comptes Rendus Biologies*, *337*(3), 167–177. <https://doi.org/10.1016/J.CRVI.2013.12.004>
- Emeterio Nateras, O. S., Harrison, J. M., Muir, E. R., Zhang, Y., Peng, Q., Chalfin, S., Gutierrez, J. E., Johnson, D. A., Kiel, J. W., & Duong, T. Q. (2014). Choroidal blood flow decreases with age: an MRI study. *Current Eye Research*, *39*(10), 1059–1067. <https://doi.org/10.3109/02713683.2014.892997>
- Estudillo, J. A. R., Higuera, M. I. L., Juárez, S. R., Vera, M. de L. O., Santana, Y. P., & Suazo, B. C. (2017). Visual rehabilitation via microperimetry in patients with geographic atrophy: a pilot study. *International Journal of Retina and Vitreous*, *3*(1), 21. <https://doi.org/10.1186/S40942-017-0071-1>
- Faraway, J. J. (2016). Extending the Linear Model with R. In *Extending the Linear Model with R* (second). CRC Press. <https://doi.org/10.1201/b21296>
- Farsiu, S., Chiu, S. J., O'Connell, R. V., Folgar, F. A., Yuan, E., Izatt, J. A., & Toth, C. A. (2014). Quantitative classification of eyes with and without intermediate age-related macular degeneration using optical coherence tomography. *Ophthalmology*, *121*(1), 162–172. <https://doi.org/10.1016/j.ophtha.2013.07.013>
- Feigl, B. (2009). Age-related maculopathy - linking aetiology and pathophysiological changes to the ischaemia hypothesis. *Progress in Retinal and Eye Research*, *28*(1), 63–86. <https://doi.org/10.1016/j.preteyeres.2008.11.004>
- Feigl, B., Brown, B., Lovie-Kitchin, J., & Swann, P. (2004). Cone-mediated multifocal electroretinogram in early age-related maculopathy and its relationships with subjective macular function tests. *Current Eye Research*, *29*(4–5), 327–336. <https://doi.org/10.1080/02713680490516198>
- Feigl, B., Cao, D., Morris, C. P., & Zele, A. J. (2011). Persons with age-related maculopathy risk genotypes and clinically normal eyes have reduced mesopic vision. *Investigative Ophthalmology and Visual Science*, *52*(2), 1145–1150. <https://doi.org/10.1167/iovs.10-5967>
- Ferrara, N., Damico, L., Shams, N., Lowman, H., & Kim, R. (2006). Development of ranibizumab, an anti-vascular endothelial growth factor antigen binding fragment, as therapy for neovascular age-related macular degeneration. *Retina*, *26*(8), 859–870. <https://doi.org/10.1097/O1.iae.0000242842.14624.e7>
- Ferris, F. L., Fine, S. L., & Hyman, L. (1984). Age-related macular degeneration and blindness due to neovascular maculopathy. *Archives of Ophthalmology*, *102*(11), 1640–1642. <https://doi.org/10.1001/archopht.1984.01040031330019>
- Ferris, F. L., Davis, M. D., Clemons, T. E., Lee, L. Y., Chew, E. Y., Lindblad, A. S., Milton, R. C., Bressler, S. B., & Klein, R. (2005). A simplified severity scale for age-related macular degeneration: AREDS report no. 18. *Archives of Ophthalmology*, *123*(11), 1570–1574. <https://doi.org/10.1001/archopht.123.11.1570>

- Ferris, F. L., Kassoff, A., Bresnick, G. H., & Bailey, I. (1982). New Visual Acuity Charts for Clinical Research. *American Journal of Ophthalmology*, *94*(1), 91–96. [https://doi.org/10.1016/0002-9394\(82\)90197-0](https://doi.org/10.1016/0002-9394(82)90197-0)
- Ferris, F. L., Wilkinson, C. P., Bird, A., Chakravarthy, U., Chew, E., Csaky, K., & Sadda, S. R. (2013). Clinical classification of age-related macular degeneration. *Ophthalmology*, *120*(4), 844–851. <https://doi.org/10.1016/j.ophtha.2012.10.036>
- Fidalgo, B. M. R. R., Crabb, D. P., & Lawrenson, J. G. (2015). Methodology and reporting of diagnostic accuracy studies of automated perimetry in glaucoma: Evaluation using a standardised approach. *Ophthalmic and Physiological Optics*, *35*, 315–323. <https://doi.org/10.1111/opo.12208>
- Finger, R. P., Chong, E., McGuinness, M. B., Robman, L. D., Aung, K. Z., Giles, G., Baird, P. N., & Guymer, R. H. (2016). Reticular pseudodrusen and their association with age-related macular degeneration the melbourne collaborative cohort study. *Ophthalmology*, *123*(3), 599–608. <https://doi.org/10.1016/j.ophtha.2015.10.029>
- Finger, R. P., Fenwick, E., Owsley, C., Holz, F. G., & Lamoureux, E. L. (2011). Visual functioning and quality of life under low luminance: Evaluation of the German low luminance questionnaire. *Investigative Ophthalmology and Visual Science*, *52*(11), 8241–8249. <https://doi.org/10.1167/iovs.11-7858>
- Finger, R. P., Schmitz-Valckenberg, S., Schmid, M., Rubin, G. S., Dunbar, H., Tufail, A., Crabb, D. P., Binns, A., Sánchez, C. I., Margaron, P., Normand, G., Durbin, M. K., Luhmann, U. F. O., Zamiri, P., Cunha-Vaz, J., Asmus, F., & Holz, F. G. (2019). MACUSTAR: Development and clinical validation of functional, structural, and patient-reported endpoints in intermediate age-related macular degeneration. *Ophthalmologica*, *241*(2), 61–72. <https://doi.org/10.1159/000491402>
- Finger, R. P., Wu, Z., Luu, C. D., Kearney, F., Ayton, L. N., Lucci, L. M., Hubbard, W. C., Hageman, J. L., Hageman, G. S., & Guymer, R. H. (2014). Reticular pseudodrusen: A risk factor for geographic atrophy in fellow eyes of individuals with unilateral choroidal neovascularization. *Ophthalmology*, *121*(6), 1252–1256. <https://doi.org/10.1016/j.ophtha.2013.12.034>
- Fisher, C. R., & Ferrington, D. A. (2018). Perspective on AMD Pathobiology: A Bioenergetic Crisis in the RPE. *Investigative Ophthalmology & Visual Science*, *59*(4), AMD41–AMD47. <https://doi.org/10.1167/iovs.18-24289>
- Fisher, D. E., Klein, B. E. K., Wong, T. Y., Rotter, J. I., Li, X., Shrager, S., Burke, G. L., Klein, R., & Cotch, M. F. (2016). Incidence of Age-Related Macular Degeneration in a Multi-Ethnic United States Population: The Multi-Ethnic Study of Atherosclerosis. *Ophthalmology*, *123*(6), 1297–1308. <https://doi.org/10.1016/j.ophtha.2015.12.026>
- Flamendorf, J., Agrón, E., Wong, W. T., Thompson, D., Wiley, H. E., Doss, E. L., Al-Holou, S., Ferris, F. L., 3rd, Chew, E. Y., & Cukras, C. (2015). Impairments in dark adaptation are associated with age-related macular degeneration severity and reticular pseudodrusen. *Ophthalmology*, *122*(10), 2053–2062. <https://doi.org/10.1016/j.ophtha.2015.06.023>
- Flynn, O. J., Cukras, C. A., & Jeffrey, B. G. (2018). Characterization of rod function phenotypes across a range of age-related macular degeneration severities and subretinal drusenoid deposits. *Investigative Ophthalmology and Visual Science*, *59*(6), 2411–2421. <https://doi.org/10.1167/iovs.17-22874>
- Folgar, F. A., Chow, J. H., Farsiu, S., Wong, W. T., Schuman, S. G., O’Connell, R. V., Winter, K. P., Chew, E. Y., Hwang, T. S., Srivastava, S. K., Harrington, M. W., Clemons, T. E., & Toth, C. A. (2012). Spatial correlation between hyperpigmentary changes on color fundus photography and hyperreflective foci on SDOCT in intermediate AMD. *Investigative Ophthalmology & Visual Science*, *53*(8), 4626–4633. <https://doi.org/10.1167/iovs.12-9813>
- Fraser, R. G., Tan, R., Ayton, L. N., Caruso, E., Guymer, R. H., & Luu, C. D. (2016). Assessment of retinotopic rod photoreceptor function using a dark-adapted chromatic perimeter in

- intermediate age-related macular degeneration. *Investigative Ophthalmology and Visual Science*, 57(13), 5436–5442. <https://doi.org/10.1167/iovs.16-19295>
- Freidlin, B., McShane, L. M., & Korn, E. L. (2010). Randomized clinical trials with biomarkers: design issues. *Journal of the National Cancer Institute*, 102(3), 152–160. <https://doi.org/10.1093/jnci/djp477>
- Fritsche, L. G., Igl, W., Bailey, J. N. C., Grassmann, F., Sengupta, S., Bragg-Gresham, J. L., Burdon, K. P., Hebbaring, S. J., Wen, C., Gorski, M., Kim, I. K., Cho, D., Zack, D., Souied, E., Scholl, H. P. N., Bala, E., ELee, K., Hunter, D. J., Sardell, R. J., ... Heid, I. M. (2016). A large genome-wide association study of age-related macular degeneration highlights contributions of rare and common variants. *Nature Genetics*, 48(2), 134–143. <https://doi.org/10.1038/ng.3448>
- Fuchs, S., Nakazawa, M., Maw, M., Tamai, M., Oguchi, Y., & Gal, A. (1995). A homozygous 1-base pair deletion in the arrestin gene is a frequent cause of Oguchi disease in Japanese. *Nature Genetics*, 10(3), 360–362. <https://doi.org/10.1038/ng0795-360>
- Fujimoto, J., & Swanson, E. (2016). The Development, Commercialization, and Impact of Optical Coherence Tomography. *Investigative Ophthalmology & Visual Science*, 57(9), OCT1–OCT13. <https://doi.org/10.1167/iovs.16-19963>
- Gabriele, M. L., Wollstein, G., Ishikawa, H., Kagemann, L., Xu, J., Folio, L. S., & Schuman, J. S. (2011). Optical coherence tomography: history, current status, and laboratory work. *Investigative Ophthalmology & Visual Science*, 52(5), 2425–2436. <https://doi.org/10.1167/iovs.10-6312>
- Gabrielle, P.-H. H., Seydou, A., Arnould, L., Acar, N., Devilliers, H., Baudin, F., Ghezala, I. Ben, Binquet, C., Bron, A. M., Creuzot-Garcher, C., Ben Ghezala, I., Binquet, C., Bron, A. M., & Creuzot-Garcher, C. (2019). Subretinal Drusenoid Deposits in the Elderly in a Population-Based Study (the Montrachet Study). *Investigative Ophthalmology & Visual Science*, 60(14), 4838–4848. <https://doi.org/10.1167/iovs.19-27283>
- Gaffney, A. J., Binns, A. M., & Margrain, T. H. (2013). The effect of pre-adapting light intensity on dark adaptation in early age-related macular degeneration. *Documenta Ophthalmologica*, 127(3), 191–199. <https://doi.org/10.1007/s10633-013-9400-3>
- Gaffney, A. J., Binns, A. M., Margrain T. H. (2011). Topography of cone dark adaptation deficits in age-related maculopathy. *Optometry and Vision Science*, 88(9), 1080–1087. <https://doi.org/10.1097/OPX.0b013e3182223697>
- Gaffney, A. J., Margrain, T. H., Bunce, C. V., & Binns, A. M. (2014). How effective is eccentric viewing training? A systematic literature review. *Ophthalmic & Physiological Optics*, 34(4), 427–437. <https://doi.org/10.1111/opo.12132>
- Garcia-Layana, A., Ciuffo, G., Zarranz-Ventura, J., & Alvarez-Vidal, A. (2017 July). *Optical Coherence Tomography in Age-related Macular Degeneration*. AMDbook.org, <https://amdbook.org/content/optical-coherence-tomography-age-related-macular-degeneration>
- George, B., Seals, S., & Aban, I. (2014). Survival analysis and regression models. *Journal of Nuclear Cardiology*, 21(4), 686–694. <https://doi.org/10.1007/s12350-014-9908-2>
- Gerth, C. (2009). The role of the ERG in the diagnosis and treatment of Age-Related Macular Degeneration. *Documenta Ophthalmologica*. 118(1), 63–68. <https://doi.org/10.1007/s10633-008-9133-x>
- Geruschat, D. R., Turano, K. A., & Stahl, J. W. (1998). Traditional measures of mobility performance and retinitis pigmentosa. *Optometry and Vision Science*, 75(7), 525–537. <https://doi.org/10.1097/00006324-199807000-00022>

- Glaser, T., Doss, E. L., Agrón, E., Nigam, D., Chew, E., & Wong, W. (2013). Significance of Drusen Regression in Intermediate Age-Related Macular Degeneration (AMD) in Progression to Advanced Disease. *Investigative Ophthalmology & Visual Science*, *54*(15), 4151–4151.
- Goralczyk, R. (2009). Beta-carotene and lung cancer in smokers: review of hypotheses and status of research. *Nutrition and Cancer*, *61*(6), 767–774. <https://doi.org/10.1080/01635580903285155>
- Gunvant Davey, P., Henderson, T., Lem, D. W., Weis, R., Amonoo-Monney, S., & Evans, D. W. (2020). Visual Function and Macular Carotenoid Changes in Eyes with Retinal Drusen-An Open Label Randomized Controlled Trial to Compare a Micronized Lipid-Based Carotenoid Liquid Supplementation and AREDS-2 Formula. *Nutrients*, *12*(11), 1–16. <https://doi.org/10.3390/NU12113271>
- Guymier, R. H., Tan, R. S., & Luu, C. D. (2021). Comparison of Visual Function Tests in Intermediate Age-Related Macular Degeneration. *Translational Vision Science & Technology*, *10*(12), 14–14. <https://doi.org/10.1167/TVST.10.12.14>
- Grant Robinson, D., Margrain, T. H., Bailey, C., & Binns, A. M. (2019). An evaluation of a battery of functional and structural tests as predictors of likely risk of progression of age-related macular degeneration. *Investigative Ophthalmology and Visual Science*, *60*(2), 580–589. <https://doi.org/10.1167/iovs.18-25092>
- Greenstein, V. C., Santos, R. A. V., Tsang, S. H., Smith, R. T., Barile, G. R., & Seiple, W. (2008). Preferred retinal locus in macular disease: Characteristics and Clinical Implications. *Retina*, *28*(9), 1234. <https://doi.org/10.1097/IAE.0B013E31817C1B47>
- Grewal, M. K., Chandra, S., Gurudas, S., Rasheed, R., Sen, P., Menon, D., Bird, A., Jeffery, G., & Sivaprasad, S. (2022). Functional clinical endpoints and their correlations in eyes with AMD with and without subretinal drusenoid deposits—a pilot study. *Eye*, *36*(2), 398–406. <https://doi.org/10.1038/s41433-021-01488-z>
- Grimm, C., Wenzel, A., Williams, T. P., Rol, P. O., Hafezi, F., & Remé, C. E. (2001). Rhodopsin-mediated blue-light damage to the rat retina: effect of photoreversal of bleaching. *Investigative Ophthalmology & Visual Science*, *42*(2), 497–505.
- Grunwald, J. E., Metelitsina, T. I., Dupont, J. C., Ying, G.-S., & Maguire, M. G. (2005). Reduced foveolar choroidal blood flow in eyes with increasing AMD severity. *Investigative Ophthalmology & Visual Science*, *46*(3), 1033–1038. <https://doi.org/10.1167/iovs.04-1050>
- Haddad, S., Chen, C. A., Santangelo, S. L., & Seddon, J. M. (2006). The Genetics of Age-Related Macular Degeneration: A Review of Progress to Date. *Survey of Ophthalmology*, *51*(4), 316–363. <https://doi.org/10.1016/j.survophthal.2006.05.001>
- Hafezi, F., Marti, A., Munz, K., & Remé, C. E. (1997). Light-induced apoptosis: Differential timing in the retina and pigment epithelium. *Experimental Eye Research*, *64*(6), 963–970. <https://doi.org/10.1006/exer.1997.0288>
- Hageman, G. S., Luthert, P. J., Victor Chong, N. H., Johnson, L. V., Anderson, D. H., & Mullins, R. F. (2001). An integrated hypothesis that considers drusen as biomarkers of immune-mediated processes at the RPE-Bruch's membrane interface in aging and age-related macular degeneration. *Progress in Retinal and Eye Research*, *20*(6), 705–732. [https://doi.org/10.1016/s1350-9462\(01\)00010-6](https://doi.org/10.1016/s1350-9462(01)00010-6)
- Haines, J. L., Hauser, M. A., Schmidt, S., Scott, W. K., Olson, L. M., Gallins, P., Spencer, K. L., Kwan, S. Y., Noureddine, M., Gilbert, J. R., Schetz-Boutaud, N., Agarwal, A., Postel, E. A., & Pericak-Vance, M. A. (2005). Complement factor H variant increases the risk of age-related macular degeneration. *Science*, *308*(5720), 419–421. <https://doi.org/10.1126/science.1110359>
- Hamilton, W. D. (1966). The moulding of senescence by natural selection. *Journal of Theoretical Biology*, *12*(1), 12–45. [https://doi.org/https://doi.org/10.1016/0022-5193\(66\)90184-6](https://doi.org/https://doi.org/10.1016/0022-5193(66)90184-6)

- Harmening, W. M., & Sincich, L. C. (2019). Adaptive Optics for Photoreceptor-Targeted Psychophysics. In: Bille, J. (eds) High Resolution Imaging in Microscopy and Ophthalmology. Springer, 359–375. https://doi.org/10.1007/978-3-030-16638-0_17
- Hartong, D. T., Berson, E. L., & Dryja, T. P. (2006). Retinitis pigmentosa. *Lancet*, 368(9549), 1795–1809. [https://doi.org/10.1016/S0140-6736\(06\)69740-7](https://doi.org/10.1016/S0140-6736(06)69740-7)
- Hecht, S., Haig, C., & Chase, A. M. (1937). The influence of light adaptation on subsequent dark adaptation of the eye. *Journal of General Physiology*, 20(6), 831–850. <https://doi.org/10.1085/jgp.20.6.831>
- Heier, J. S., Brown, D. M., Chong, V., Korobelnik, J.-F., Kaiser, P. K., Nguyen, Q. D., Kirchhof, B., Ho, A., Ogura, Y., Yancopoulos, G. D., Stahl, N., Vitti, R., Berliner, A. J., Soo, Y., Anderesi, M., Groetzbach, G., Sommerauer, B., Sandbrink, R., Simader, C., & Schmidt-Erfurth, U. (2012). Intravitreal aflibercept (VEGF trap-eye) in wet age-related macular degeneration. *Ophthalmology*, 119(12), 2537–2548. <https://doi.org/10.1016/j.ophtha.2012.09.006>
- Heinrich, S. P., & Bach, M. (2013). Resolution acuity versus recognition acuity with Landolt-style optotypes. *Graefes Archive for Clinical and Experimental Ophthalmology*, 251(9), 2235–2241. <https://doi.org/10.1007/S00417-013-2404-6>
- Hess, K., de Silva, T., Grisso, P., Wiley, H., Thavikulwat, A. T., Keenan, T. D. L., Chew, E. Y., & Cukras, C. A. (2022). Evaluation of Cone- and Rod-Mediated Parameters in Dark Adaptation Testing as Outcome Measures in Age-Related Macular Degeneration. *Ophthalmology. Retina*, 6(12). <https://doi.org/10.1016/J.ORET.2022.05.018>
- Higgins, B. E., Montesano, G., Binns, A. M., & Crabb, D. P. (2021). Optimising assessment of dark adaptation data using time to event analysis. *Scientific Reports*, 11(1), 8323. <https://doi.org/10.1038/s41598-021-86193-3>
- Higgins, B. E., Taylor, D. J., Binns, A. M., & Crabb, D. P. (2021). Are Current Methods of Measuring Dark Adaptation Effective in Detecting the Onset and Progression of Age-Related Macular Degeneration? A Systematic Literature Review. *Ophthalmology and Therapy*, 10(1), 21–38. <https://doi.org/10.1007/s40123-020-00323-0>
- Hogg, R. E. (2014). Reticular pseudodrusen in age-related macular degeneration. *Optometry and Vision Science*, 91(8), 854–859. <https://doi.org/10.1097/OPX.0000000000000287>
- Hogg, R. E., & Chakravarthy, U. (2006). Visual function and dysfunction in early and late age-related maculopathy. *Progress in Retinal and Eye Research*, 25(3), 249–276. <https://doi.org/10.1016/j.preteyeres.2005.11.002>
- Holladay, J. T. (2004). Visual acuity measurements. *Journal of Cataract and Refractive Surgery*, 30(2), 287–290. <https://doi.org/10.1016/J.JCRS.2004.01.014>
- Hollins, M., & Alpern, M. (1973). Dark adaptation and visual pigment regeneration in human cones. *The Journal of General Physiology*, 62(4), 430–447. <https://doi.org/10.1085/jgp.62.4.430>
- Holopigian, K., Seiple, W., Greenstein, V., Kim, D., & Carr, R. E. (1997). Relative effects of aging and age-related macular degeneration on peripheral visual function. *Optometry and Vision Science*, 74(3), 152–159. <https://doi.org/10.1097/00006324-199703000-00026>
- Holz, F. G., Sadda, S. R., Busbee, B., Chew, E. Y., Mitchell, P., Tufail, A., Brittain, C., Ferrara, D., Gray, S., Honigberg, L., Martin, J., Tong, B., Ehrlich, J. S., Bressler, N. M., Sola, F. F., Schlottmann, P., Zambrano, A., Zeolite, C., Arnold, J., ... Wykoff, C. C. (2018). Efficacy and Safety of Lampalizumab for Geographic Atrophy Due to Age-Related Macular Degeneration: Chroma and Spectri Phase 3 Randomized Clinical Trials. *JAMA Ophthalmology*, 136(6), 666–677. <https://doi.org/10.1001/JAMAOPHTHALMOL.2018.1544>

- Holz, F. G., Schmitz-Valckenberg, S., & Fleckenstein, M. (2014). Recent developments in the treatment of age-related macular degeneration. *Journal of Clinical Investigation*, *124*(4), 1430–1438. <https://doi.org/10.1172/JCI71029>
- Holz, F. G., Strauss, E. C., Schmitz-Valckenberg, S., & Van Lookeren Campagne, M. (2014). Geographic atrophy: Clinical features and potential therapeutic approaches. *Ophthalmology*, *121*(5), 1079–1091. <https://doi.org/10.1016/j.ophtha.2013.11.023>
- Hoon, M., Okawa, H., Santina, L. Della, & Wong, R. O. L. (2014). Functional Architecture of the Retina: Development and Disease. *Progress in Retinal and Eye Research*, *42*, 44. <https://doi.org/10.1016/J.PRETEYERES.2014.06.003>
- Huang, D., Swanson, E. A., Lin, C. P., Schuman, J. S., Stinson, W. G., Chang, W., Hee, M. R., Flotte, T., Gregory, K., & Puliafito, C. A. (1991). Optical coherence tomography. *Science*, *254*(5035), 1178–1181. <https://doi.org/10.1126/science.1957169>
- Huang, O. S., Zheng, Y., Tay, W. T., Chiang, P. P. C., Lamoureux, E. L., & Wong, T. Y. (2013). Lack of Awareness of Common Eye Conditions in the Community, *Ophthalmic Epidemiology*, *20*(1), 52–60. <https://doi.org/10.3109/09286586.2012.751429>
- Huisinigh, C., McGwin, G., Neely, D., Zarubina, A., Clark, M., Zhang, Y., Curcio, C. A., & Owsley, C. (2016). The association between subretinal drusenoid deposits in older adults in normal macular health and incident age-related macular degeneration. *Investigative Ophthalmology and Visual Science*, *57*(2), 739–745. <https://doi.org/10.1167/iovs.15-18316>
- Jackson, G. R., Clark, M. E., Scott, I. U., Walter, L. E., Quillen, D. A., & Brigell, M. G. (2014). Twelve-month natural history of dark adaptation in patients with AMD. *Optometry and Vision Science*, *91*(8), 925–931. <https://doi.org/10.1097/OPX.0000000000000247>
- Jackson, G. R., Curcio, C. A., Sloan, K. R., & Owsley, C. (2005). Photoreceptor degeneration in aging and age-related maculopathy. *Macular Degeneration*, *1*(3), 45–62. https://doi.org/10.1007/3-540-26977-0_3
- Jackson, G. R., & Edwards, J. G. (2008). A short-duration dark adaptation protocol for assessment of age-related maculopathy. *Journal of Ocular Biology, Diseases, and Informatics*, *1*(1), 7–11. <https://doi.org/10.1007/s12177-008-9002-6>
- Jackson, G. R., Felix, T., & Owsley, C. (2006). The Scotopic Sensitivity Tester-1 and the detection of early age-related macular degeneration. *Ophthalmic and Physiological Optics*, *26*(4), 431–437. <https://doi.org/10.1111/j.1475-1313.2006.00390.x>
- Jackson, G. R., Owsley, C., & Curcio, C. A. (2002). Photoreceptor degeneration and dysfunction in aging and age-related maculopathy. *Ageing Research Reviews*, *1*(3) 381–396. [https://doi.org/10.1016/S1568-1637\(02\)00007-7](https://doi.org/10.1016/S1568-1637(02)00007-7)
- Jackson, G. R., Owsley, C., & McGwin, G. (1999). Aging and dark adaptation. *Vision Research*, *39*(23), 3975–3982. [https://doi.org/10.1016/S0042-6989\(99\)00092-9](https://doi.org/10.1016/S0042-6989(99)00092-9)
- Jackson, G. R., Scott, I. U., Kim, I. K., Quillen, D. A., Iannaccone, A., & Edwards, J. G. (2014). Diagnostic sensitivity and specificity of dark adaptometry for detection of age-related macular degeneration. *Investigative Ophthalmology and Visual Science*, *55*(3), 1427–1431. <https://doi.org/10.1167/iovs.13-13745>
- Jaffe, G. J., Westby, K., Csaky, K. G., Monés, J., Pearlman, J. A., Patel, S. S., Joondeph, B. C., Randolph, J., Masonson, H., & Rezaei, K. A. (2021). C5 Inhibitor Avacincaptad Pegol for Geographic Atrophy Due to Age-Related Macular Degeneration: A Randomized Pivotal Phase 2/3 Trial. *Ophthalmology*, *128*(4), 576–586. <https://doi.org/10.1016/j.ophtha.2020.08.027>
- Jager, R. D., Mieler, W. F., & Miller, J. W. (2009). Age-Related Macular Degeneration. *The New England journal of medicine*, *358*(24), 2606–2617. <https://doi.org/10.1056/NEJMRA0801537>

- Jain, N., Farsiu, S., Khanifar, A. A., Bearely, S., Smith, R. T., Izatt, J. A., & Toth, C. A. (2010). Quantitative Comparison of Drusen Segmented on SD-OCT versus Drusen Delineated on Color Fundus Photographs. *Investigative Ophthalmology & Visual Science*, 51(10), 4875–4883. <https://doi.org/10.1167/iovs.09-4962>
- Jakobsdottir, J., Conley, Y. P., Weeks, D. E., Mah, T. S., Ferrell, R. E., & Gorin, M. B. (2005). Susceptibility genes for age-related maculopathy on chromosome 10q26. *American Journal of Human Genetics*, 77(3), 389–407. <https://doi.org/10.1086/444437>
- Jeffrey, B. G., Flynn, O. J., Huryn, L. A., Pfau, M., & Cukras, C. A. (2022). Scotopic Contour Deformation Detection Reveals Early Rod Dysfunction in Age-Related Macular Degeneration With and Without Reticular Pseudodrusen. *Investigative Ophthalmology & Visual Science*, 63(6), 23–23. <https://doi.org/10.1167/IOVS.63.6.23>
- Joanna Briggs Institute (2017). *Critical Appraisal Tools - JBI*. <https://jbi.global/critical-appraisal-tools>
- Jiang, H., Shi, X., Fan, Y., Wang, D., Li, B., Zhou, J., Pei, C., & Ma, L. (2021). Dietary omega-3 polyunsaturated fatty acids and fish intake and risk of age-related macular degeneration. *Clinical Nutrition*, 40(12), 5662–5673. <https://doi.org/https://doi.org/10.1016/j.clnu.2021.10.005>
- Jin, K. (2010). Modern Biological Theories of Aging. *Aging and Disease*, 1(2), 72–74. <https://www.ncbi.nlm.nih.gov/pmc/articles/PMC2995895/>
- Joeres, S., Tsong, J. W., Updike, P. G., Collins, A. T., Dustin, L., Walsh, A. C., Romano, P. W., & Sadda, S. V. R. (2007). Reproducibility of Quantitative Optical Coherence Tomography Subanalysis in Neovascular Age-Related Macular Degeneration. *Investigative Ophthalmology & Visual Science*, 48(9), 4300–4307. <https://doi.org/10.1167/IOVS.07-0179>
- Jones, P. R., Yasoubi, N., Nardini, M., & Rubin, G. S. (2016). Feasibility of macular integrity assessment (Maia) microperimetry in children: Sensitivity, reliability, and fixation stability in healthy observers. *Investigative Ophthalmology and Visual Science*, 57(14), 6349–6359. <https://doi.org/10.1167/iovs.16-20037>
- Joselevitch, C. (2008). Human retinal circuitry and physiology. *Psychology & Neuroscience*, 1(2), 141–165. <https://doi.org/10.3922/j.psns.2008.2.008>
- Kalkman, J. (2017). Fourier-Domain Optical Coherence Tomography Signal Analysis and Numerical Modeling. *International Journal of Optics*, 2017. <https://doi.org/10.1155/2017/9586067>
- Kamermans, M., Fahrenfort, I., Schultz, K., Janssen-Bienhold, U., Sjoerdsma, T., & Weiler, R. (2001). Hemichannel-mediated inhibition in the outer retina. *Science*, 292(5519), 1178–1180. <https://doi.org/10.1126/science.1060101>
- Kanagasingam, Y., Bhuiyan, A., Abramoff, M. D., Smith, R. T., Goldschmidt, L., & Wong, T. Y. (2014). Progress on retinal image analysis for age related macular degeneration. *Progress in Retinal and Eye Research*, 38, 20–42. <https://doi.org/10.1016/j.preteyeres.2013.10.002>
- Kaneko, A., & Tachibana, M. (1987). GABA mediates the negative feedback from amacrine to bipolar cells. *Neuroscience Research Supplements*, 6, S239–S251. [https://doi.org/10.1016/0921-8696\(87\)90020-X](https://doi.org/10.1016/0921-8696(87)90020-X)
- Kar, D., Clark, M. E., Swain, T. A., McGwin, G., Crosson, J. N., Owsley, C., Sloan, K. R., & Curcio, C. A. (2020). Local Abundance of Macular Xanthophyll Pigment Is Associated with Rod- and Cone-Mediated Vision in Aging and Age-Related Macular Degeneration. *Investigative Ophthalmology & Visual Science*, 61(8), 46–46. <https://doi.org/10.1167/IOVS.61.8.46>
- Kashani, A. H., Lebkowski, J. S., Rahhal, F. M., Avery, R. L., Salehi-Had, H., Dang, W., Lin, C.-M., Mitra, D., Zhu, D., Thomas, B. B., Hikita, S. T., Pennington, B. O., Johnson, L. V., Clegg, D. O., Hinton, D. R., & Humayun, M. S. (2018). A bioengineered retinal pigment epithelial monolayer for advanced, dry age-related macular degeneration. *Science Translational Medicine*, 10(435). <https://doi.org/10.1126/scitranslmed.aao4097>

- Kaufman, Y., Ma, L., & Washington, I. (2011). Deuterium enrichment of vitamin A at the C20 position slows the formation of detrimental vitamin A dimers in wild-type rodents. *The Journal of Biological Chemistry*, 286(10), 7958–7965. <https://doi.org/10.1074/jbc.M110.178640>
- Kauper, K., McGovern, C., Sherman, S., Heatherton, P., Rapoza, R., Stabila, P., Dean, B., Lee, A., Borges, S., Bouchard, B., & Tao, W. (2012). Two-year intraocular delivery of ciliary neurotrophic factor by encapsulated cell technology implants in patients with chronic retinal degenerative diseases. *Investigative Ophthalmology & Visual Science*, 53(12), 7484–7491. <https://doi.org/10.1167/jiovs.12-9970>
- Kaur, C. (2008). Hypoxia-ischemia and retinal ganglion cell damage. *Clinical Ophthalmology*, 2(4), 879. <https://doi.org/10.2147/opth.s3361>
- Kawamura, S., & Tachibanaki, S. (2021). Molecular bases of rod and cone differences. *Progress in Retinal and Eye Research*, 101040. <https://doi.org/10.1016/j.preteyeres.2021.101040>
- Keane, P. A., Patel, P. J., Liakopoulos, S., Heussen, F. M., Sadda, S. R., & Tufail, A. (2012). Evaluation of Age-related Macular Degeneration with Optical Coherence Tomography. *Survey of Ophthalmology*, 57(5), 389–414. <https://doi.org/10.1016/J.SURVOPHTHAL.2012.01.006>
- Kennedy, C. J., Rakoczy, P. E., & Constable, I. J. (1995). Lipofuscin of the retinal pigment epithelium: A review. *Eye*, 9(6), 763–771. <https://doi.org/10.1038/eye.1995.192>
- Khanifar, A. A., Koreishi, A. F., Izatt, J. A., & Toth, C. A. (2008). Drusen Ultrastructure Imaging with Spectral Domain Optical Coherence Tomography in Age-related Macular Degeneration. *Ophthalmology*, 115(11). <https://doi.org/10.1016/j.ophtha.2008.04.041>
- Khanna, S., Komati, R., Eichenbaum, D. A., Hariprasad, I., Ciulla, T. A., & Hariprasad, S. M. (2019). Current and upcoming anti-VEGF therapies and dosing strategies for the treatment of neovascular AMD: a comparative review. *BMJ Open Ophthalmology*, 4(1), e000398. <https://doi.org/10.1136/bmjophth-2019-000398>
- Kim, D. Y., Loo, J., Farsiu, S., & Jaffe, G. J. (2021). Comparison of Single Drusen Size on Color Fundus Photography and Spectral-Domain Optical Coherence Tomography. *Retina*, 41(8), 1715–1722. <https://doi.org/10.1097/IAE.0000000000003099>
- Klaver, C. C. W., Wolfs, R. C. W., Assink, J. J. M., Van Duijn, C. M., Hofman, A., & De Jong, P. T. V. M. (1998). Genetic risk of age-related maculopathy. Population-based familial aggregation study. *Archives of Ophthalmology*, 116(12), 1646–1651. <https://doi.org/10.1001/ARCHOPHT.116.12.1646>
- Klein, B. E. K., Klein, R., Lee, K. E., Moore, E. L., & Danforth, L. (2001). Risk of incident age-related eye diseases in people with an affected sibling: The Beaver Dam eye study. *American Journal of Epidemiology*, 154(3), 207–211. <https://doi.org/10.1093/aje/154.3.207>
- Klein, R., Davis, M. D., Magli, Y. L., Segal, P., Klein, B. E. K., & Hubbard, L. (1991). The Wisconsin Age-related Maculopathy Grading System. *Ophthalmology*, 98(7), 1128–1134. [https://doi.org/10.1016/S0161-6420\(91\)32186-9](https://doi.org/10.1016/S0161-6420(91)32186-9)
- Klein, R., Klein, B. E. K., & Linton, K. L. P. (1992). Prevalence of Age-related Maculopathy: The Beaver Dam Eye Study. *Ophthalmology*, 99(6), 933–943. [https://doi.org/https://doi.org/10.1016/S0161-6420\(92\)31871-8](https://doi.org/https://doi.org/10.1016/S0161-6420(92)31871-8)
- Klein, R., Klein, B. E. K., Linton, K. L. P., & Demets, D. L. (1993). The Beaver Dam eye study: The relation of age-related maculopathy to smoking. *American Journal of Epidemiology*, 137(2), 190–200. <https://doi.org/10.1093/oxfordjournals.aje.a116659>
- Klein, R., Klein, B. E. K., Tomany, S. C., Meuer, S. M., & Huang, G.-H. (2002). Ten-year incidence and progression of age-related maculopathy: The Beaver Dam eye study. *Ophthalmology*, 109(10), 1767–1779. [https://doi.org/10.1016/s0161-6420\(02\)01146-6](https://doi.org/10.1016/s0161-6420(02)01146-6)

- Klein, R., Meuer, S. M., Knudtson, M. D., & Klein, B. E. K. (2008). The Epidemiology of Progression of Pure Geographic Atrophy: The Beaver Dam Eye Study. *American Journal of Ophthalmology*, 146(5), 692-699.e1. <https://doi.org/https://doi.org/10.1016/j.ajo.2008.05.050>
- Klein, R., Peto, T., Bird, A., & Vannewkirk, M. R. (2004). The epidemiology of age-related macular degeneration. *American Journal of Ophthalmology*, 137(3), 486-495. <https://doi.org/10.1016/j.ajo.2003.11.069>
- Kolb, H. (2005). Facts and Figures Concerning the Human Retina. In H. Kolb (Eds.) et. al., *Webvision: The Organization of the Retina and Visual System*. University of Utah Health Sciences Center. <https://www.ncbi.nlm.nih.gov/books/NBK11530/>
- Kolb, H. (1995). Simple Anatomy of the Retina. In H. Kolb (Eds.) et. al., *Webvision: The Organization of the Retina and Visual System*. University of Utah Health Sciences Center <https://www.ncbi.nlm.nih.gov/books/NBK11530/>
- Koo, T. K., & Li, M. Y. (2016). A Guideline of Selecting and Reporting Intraclass Correlation Coefficients for Reliability Research. *Journal of Chiropractic Medicine*, 15(2), 155-163. <https://doi.org/10.1016/j.jcm.2016.02.012>
- Kumar-Singh, R. (2019). The role of complement membrane attack complex in dry and wet AMD - From hypothesis to clinical trials. *Experimental Eye Research*, 184, 266-277. <https://doi.org/10.1016/j.exer.2019.05.006>
- Kwak, N., Okamoto, N., Wood, J. M., & Campochiaro, P. A. (2000). VEGF is major stimulator in model of choroidal neovascularization. *Investigative Ophthalmology & Visual Science*, 41(10), 3158-3164. <https://iovs.arvojournals.org/article.aspx?articleid=2123593>
- Lad, E. M., Fang, V., Tessier, M., Rautanen, A., Gayan, J., Stinnett, S. S., & Luhmann, U. F. O. (2022). Longitudinal Evaluation of Visual Function Impairments in Early and Intermediate Age-Related Macular Degeneration Patients. *Ophthalmology Science*, 2(3), 100173. <https://doi.org/10.1016/J.XOPS.2022.100173>
- Lains, I., Mendez, K., Nigalye, A., Katz, R., Douglas, V. P., Kelly, R. S., Kim, I. K., Miller, J. B., Vavvas, D. G., Liang, L., Lasky-Su, J., Miller, J. W., & Husain, D. (2022). Plasma Metabolomic Profiles Associated with Three-Year Progression of Age-Related Macular Degeneration. *Metabolites*, 12(1). <https://doi.org/10.3390/METABO12010032>
- Laíns, I., Miller, J. W. J. B., Mukai, R., Mach, S., Vavvas, D., Kim, I. K., Miller, J. W. J. B., & Husain, D. (2018). Health conditions linked to age-related macular degeneration associated with dark adaptation. *Retina*, 38(6), 1145-1155. <https://doi.org/10.1097/IAE.0000000000001659>
- Laíns, I., Miller, J. W. J. B., Park, D. H., Tsikata, E., Davoudi, S., Rahmani, S., Pierce, J., Silva, R., Chen, T. C., Kim, I. K., Vavvas, D., Miller, J. W. J. B., & Husain, D. (2017). Structural Changes Associated with Delayed Dark Adaptation in Age-Related Macular Degeneration. *Ophthalmology*, 124(9), 1340-1352. <https://doi.org/10.1016/j.ophtha.2017.03.061>
- Laíns, I., Park, D. H., Mukai, R., Silverman, R., Oellers, P., Mach, S., Kim, I. K., Vavvas, D. G., Miller, J. W. J. B. J. W., Miller, J. W. J. B. J. W., & Husain, D. (2018). Peripheral Changes Associated With Delayed Dark Adaptation in Age-related Macular Degeneration. *American Journal of Ophthalmology*, 190(9), 113-124. <https://doi.org/10.1016/j.ajo.2018.03.035>
- Lamb, T. D., & Pugh, E. N. (2004). Dark adaptation and the retinoid cycle of vision. *Progress in Retinal and Eye Research*, 23(3), 307-380. <https://doi.org/10.1016/j.preteyeres.2004.03.001>
- Lamb, T. D., & Pugh, E. N. (2006). Phototransduction, dark adaptation, and rhodopsin regeneration the proctor lecture. *Investigative Ophthalmology & Visual Science*, 47(12), 5137-5152. <https://doi.org/10.1167/iovs.06-0187>

- Langdon, R. J., Yousefi, P. D., Relton, C. L., & Suderman, M. J. (1988). Age-related norms for the Cambridge low contrast gratings, including details concerning their design and use. *Clinical Vision Sciences*, 2(3), 201–212. <https://doi.org/10.2/JQUERY.MIN.JS>
- Lee, A. Y., Lee, C. S., Blazes, M. S., Owen, J. P., Bagdasarova, Y., Wu, Y., Spaide, T., Yanagihara, R. T., Kihara, Y., Clark, M. E., Kwon, M. Y., Owsley, C., & Curcio, C. A. (2020). Exploring a structural basis for delayed rod-mediated dark adaptation in age-related macular degeneration via deep learning. *Translational Vision Science and Technology*, 9(2), 1–11. <https://doi.org/10.1167/TVST.9.2.62>
- Lee, C. S., Tying, A. J., Deruyter, N. P., Wu, Y., Rokem, A., & Lee, A. Y. (2017). Deep-learning based, automated segmentation of macular edema in optical coherence tomography. *Biomedical Optics Express*, 8(7), 3440. <https://doi.org/10.1364/boe.8.003440>
- Lei, J., Balasubramanian, S., Abdelfattah, N. S., Nittala, M. G., & Sadda, S. R. (2017). Proposal of a simple optical coherence tomography-based scoring system for progression of age-related macular degeneration. *Graefes Archive for Clinical and Experimental Ophthalmology*, 255(8), 1551–1558. <https://doi.org/10.1007/s00417-017-3693-y>
- Leibrock, C. S., Reuter, T., & Lamb, T. D. (1998). Molecular basis of dark adaptation in rod photoreceptors. *Eye*, 12, 511–520. <https://doi.org/10.1038/eye.1998.139>
- Li, D. Q., & Choudhry, N. (2020). The future of retinal imaging. *Current Opinion in Ophthalmology*, 31(3), 199–206. <https://doi.org/10.1097/ICU.0000000000000653>
- Li, E., Donati, S., Lindsley, K. B., Krzystolik, M. G., & Virgili, G. (2020). Treatment regimens for administration of anti-vascular endothelial growth factor agents for neovascular age-related macular degeneration. *Cochrane Database of Systematic Reviews*, 2020(5), CD012208–CD012208. <https://doi.org/10.1002/14651858.CD012208.pub2>
- Liao, D. S., Grossi, F. V., El Mehdi, D., Gerber, M. R., Brown, D. M., Heier, J. S., Wykoff, C. C., Singerman, L. J., Abraham, P., Grassmann, F., Nuernberg, P., Weber, B. H. F., Deschatelets, P., Kim, R. Y., Chung, C. Y., Ribeiro, R. M., Hamdani, M., Rosenfeld, P. J., Boyer, D. S., ... Francois, C. G. (2020). Complement C3 Inhibitor Pegcetacoplan for Geographic Atrophy Secondary to Age-Related Macular Degeneration: A Randomized Phase 2 Trial. *Ophthalmology*, 127(2), 186–195. <https://doi.org/10.1016/j.ophtha.2019.07.011>
- Lim, L. A., Frost, N. A., Powell, R. J., & Hewson, P. (2009). Comparison of the ETDRS logMAR, ‘compact reduced logMar’ and Snellen charts in routine clinical practice. *Eye*, 24(4), 673–677. <https://doi.org/10.1038/eye.2009.147>
- Lim, L. S., Mitchell, P., Seddon, J. M., Holz, F. G., & Wong, T. Y. (2012). Age-related macular degeneration. *The Lancet*, 379(9827), 1728–1738. [https://doi.org/10.1016/S0140-6736\(12\)60282-7](https://doi.org/10.1016/S0140-6736(12)60282-7)
- Lin, H., & Zelterman, D. (2002). Modeling Survival Data: Extending the Cox Model. *Technometrics*, 44(1), 85–86. <https://doi.org/10.1198/tech.2002.s656>
- Lott, L. A., Schneck, M. E., Haegerstrom-Portnoy, G., Hewlett, S., Stepien-Bernabe, N., Gauer, B. M., Zaidi, A., Fu, A. D., & Brabyn, J. A. (2021). Simple Vision Function Tests that Distinguish Eyes with Early to Intermediate Age-related Macular Degeneration. *Ophthalmic Epidemiology*, 28(2), 93–104. <https://doi.org/10.1080/09286586.2020.1793371>
- Luu, C. D., Tan, R., Caruso, E., Fletcher, E. L., Lamb, T. D., & Guymer, R. H. (2018). Topographic Rod Recovery Profiles after a Prolonged Dark Adaptation in Subjects with Reticular Pseudodrusen. *Ophthalmology Retina*, 2(12), 1206–1217. <https://doi.org/10.1016/j.oret.2018.06.016>
- Ma, L., Liu, R., Du, J. H., Liu, T., Wu, S. S., & Liu, X. H. (2016). Lutein, Zeaxanthin and Meso-zeaxanthin Supplementation Associated with Macular Pigment Optical Density. *Nutrients*, 8(7). <https://doi.org/10.3390/nu8070426>

- Maguire, M. G., Martin, D. F., Ying, G. S., Jaffe, G. J., Daniel, E., Grunwald, J. E., Toth, C. A., Ferris, F. L., & Fine, S. L. (2016). Five-Year Outcomes with Anti-Vascular Endothelial Growth Factor Treatment of Neovascular Age-Related Macular Degeneration: The Comparison of Age-Related Macular Degeneration Treatments Trials. *Ophthalmology*, *123*(8), 1751–1761. <https://doi.org/10.1016/j.ophtha.2016.03.045>
- Mahabadi, N., & Al Khalili, Y. (2019). *Neuroanatomy, Retina*, StatPearls Publishing, <https://www.ncbi.nlm.nih.gov/books/NBK545310/>
- Mahroo, O. A. R., & Lamb, T. D. (2004). Recovery of the human photopic electroretinogram after bleaching exposures: estimation of pigment regeneration kinetics. *The Journal of Physiology*, *554*(2), 417–437. <https://doi.org/10.1113/jphysiol.2003.051250>
- Maller, J., George, S., Purcell, S., Fagerness, J., Altshuler, D., Daly, M. J., & Seddon, J. M. (2006). Common variation in three genes, including a noncoding variant in CFH, strongly influences risk of age-related macular degeneration. *Nature Genetics*, *38*(9), 1055–1059. <https://doi.org/10.1038/ng1873>
- Mares, J. A., & Moeller, S. M. (2006). Diet and age-related macular degeneration: expanding our view. *The American Journal of Clinical Nutrition*, *83*(4), 733–734. <https://doi.org/10.1093/ajcn/83.4.733>
- Margrain, T. H., & Thomson, D. (2002). Sources of variability in the clinical photostress test. *Ophthalmic & Physiological Optics*, *22*(1), 61–67. <https://doi.org/10.1046/j.1475-1313.2002.00005.x>
- Marshall, J. (1987). The ageing retina: Physiology or pathology. *Eye*, *1*(2), 282–295. <https://doi.org/10.1038/eye.1987.47>
- Mata, N. L., Lichter, J. B., Vogel, R., Han, Y., Bui, T. V., & Singerman, L. J. (2013). Investigation of oral fenretinide for treatment of geographic atrophy in age-related macular degeneration. *Retina*, *33*(3), 498–507. <https://doi.org/10.1097/IAE.0b013e318265801d>
- Mata, N. L., Radu, R. A., Clemmons, R. C., & Travis, G. H. (2002). Isomerization and oxidation of vitamin a in cone-dominant retinas: a novel pathway for visual-pigment regeneration in daylight. *Neuron*, *36*(1), 69–80. [https://doi.org/10.1016/s0896-6273\(02\)00912-1](https://doi.org/10.1016/s0896-6273(02)00912-1)
- Mayer, M. J., Ward, B., Klein, R., Talcott, J. B., Dougherty, R. F., & Glucs, A. (1994). Flicker sensitivity and fundus appearance in pre-exudative age-related maculopathy. *Investigative Ophthalmology and Visual Science*, *35*(3), 1138–1149.
- Maynard, M. L., Zele, A. J., & Feigl, B. (2016). Mesopic Pelli-Robson contrast sensitivity and MP-1 microperimetry in healthy ageing and age-related macular degeneration. *Acta Ophthalmologica*, *94*(8), e772–e778. <https://doi.org/10.1111/aos.13112>
- Mazzoni, F., Safa, H., & Finemann, S. C. (2014). Understanding photoreceptor outer segment phagocytosis: use and utility of RPE cells in culture. *Experimental Eye Research*, *126*, 51–60. <https://doi.org/10.1016/j.exer.2014.01.010>
- McCarty, C. A., Mukesh, B. N., Fu, C. L., Mitchell, P., Wang, J. J., & Taylor, H. R. (2001). Risk factors for age-related maculopathy: the Visual Impairment Project. *Archives of Ophthalmology*, *119*(10), 1455–1462. <https://doi.org/10.1001/archophth.119.10.1455>
- McGuinness, M. B., Fraser, R. G., Tan, R., Luu, C. D., & Guymer, R. H. (2020). Relationship Between Rod-Mediated Sensitivity, Low-Luminance Visual Acuity, and Night Vision Questionnaire in Age-Related Macular Degeneration. *Translational Vision Science & Technology*, *9*(6), 30–30. <https://doi.org/10.1167/TVST.9.6.30>
- McGraw, P., Winn, B., & Whitaker, D. (1995). Reliability of the Snellen chart. *British Medical Journal*, *310*(6993), 1481–1482. <https://doi.org/10.1136/BMJ.310.6993.1481>

- McGwin, G. J., Jackson, G. R., & Owsley, C. (1999). Using nonlinear regression to estimate parameters of dark adaptation. *Behavior Research Methods, Instruments, & Computers*, *31*(4), 712–717. <https://doi.org/10.3758/bf03200752>
- McKeague, C., Margrain, T. H., Bailey, C., & Binns, A. M. (2014). Low-level night-time light therapy for age-related macular degeneration (ALight): Study protocol for a randomized controlled trial. *Trials*, *15*(1). <https://doi.org/10.1186/1745-6215-15-246>
- Mendez, K. M., Kim, J., Laíns, I., Nigalye, A., Katz, R., Pundik, S., Kim, I. K., Liang, L., Vavvas, D. G., Miller, J. B., Miller, J. W., Lasky-Su, J. A., & Husain, D. (2021). Association of Human Plasma Metabolomics with Delayed Dark Adaptation in Age-Related Macular Degeneration. *Metabolites* 2021, Vol. 11, Page 183, *11*(3), 183. <https://doi.org/10.3390/METABO11030183>
- Midena, E., Frizziero, L., Torresin, T., Todaro, P. B., Miglionico, G., & Pilotto, E. (2020). Optical coherence tomography and color fundus photography in the screening of age-related macular degeneration: A comparative, population-based study. *PLOS ONE*, *15*(8), e0237352. <https://doi.org/10.1371/JOURNAL.PONE.0237352>
- Midena, E., & Pilotto, E. (2017). Microperimetry in age: related macular degeneration. *Eye*, *31*(7), 985. <https://doi.org/10.1038/EYE.2017.34>
- Midena, E., Vujosevic, S., Convento, E., Manfre, A., Cavarzeran, F., & Pilotto, E. (2007). Microperimetry and fundus autofluorescence in patients with early age-related macular degeneration. *British Journal of Ophthalmology*, *91*(11), 1499–1503. <https://doi.org/10.1136/bjo.2007.119685>
- Miller, J. W., Bagheri, S., & Vavvas, D. G. (2017). Advances in Age-related Macular Degeneration Understanding and Therapy. *US Ophthalmic Review*, *10*(02), 119. <https://doi.org/10.17925/USOR.2017.10.02.119>
- Mimoun, G., Soubrane, G., & Coscas, G. (1990). Les drusen maculaires [Macular drusen]. *Journal francais d'ophtalmologie*, *13*(10), 511–530. <https://pubmed.ncbi.nlm.nih.gov/2081842/>
- Montesano, G., Bryan, S. R., Crabb, D. P., Fogagnolo, P., Oddone, F., McKendrick, A. M., Turpin, A., Lanzetta, P., Perdicchi, A., Johnson, C. A., Garway-Heath, D. F., Brusini, P., & Rossetti, L. M. (2019). A Comparison between the Compass Fundus Perimeter and the Humphrey Field Analyzer. *Ophthalmology*, *126*(2), 242–251. <https://doi.org/10.1016/j.ophtha.2018.08.010>
- Moschos, M. M., & Nitoda, E. (2018). The Role of mf-ERG in the Diagnosis and Treatment of Age-Related Macular Degeneration: Electrophysiological Features of AMD. *Seminars in Ophthalmology*, *33*(4), 461–469. <https://doi.org/10.1080/08820538.2017.1301496>
- Mullins, R. F., McGwin, G., Searcey, K., Clark, M. E., Kennedy, E. L., Curcio, C. A., Stone, E. M., & Owsley, C. (2019). The ARMS2 A69S Polymorphism Is Associated with Delayed Rod-Mediated Dark Adaptation in Eyes at Risk for Incident Age-Related Macular Degeneration. *Ophthalmology*, *126*(4), 591–600. <https://doi.org/10.1016/j.ophtha.2018.10.037>
- Mullins, R. F., Russell, S. R., Anderson, D. H., & Hageman, G. S. (2000). Drusen associated with aging and age-related macular degeneration contain proteins common to extracellular deposits associated with atherosclerosis, elastosis, amyloidosis, and dense deposit disease. *FASEB Journal*, *14*(7), 835–846. <https://doi.org/10.1096/FASEBJ.14.7.835>
- Murthy, R. K., Haji, S., Sambhav, K., Grover, S., & Chalam, K. V. (2016). Clinical applications of spectral domain optical coherence tomography in retinal diseases. *Biomedical Journal*, *39*(2), 107. <https://doi.org/10.1016/J.BJ.2016.04.003>
- Nassif, N. A., Cense, B., Park, B. H., Pierce, M. C., Yun, S. H., Bouma, B. E., Tearney, G. J., Chen, T. C., de Boer, J. F., Huang, D., Swanson, E. A., Lin, C. P., Schuman, J. S., Stinson, W. G., Chang, W., Hee, M. R., Flotte, T., Gregory, K., & Puliafito, C. A. (2004). In vivo high-resolution video-rate spectral-domain optical coherence tomography of the human retina and optic nerve. *Optics Express*, *12*(3) 367-376. <https://doi.org/10.1364/OPEX.12.000367>

- Nebbioso, M., Barbato, A., & Pescosolido, N. (2014). Scotopic microperimetry in the early diagnosis of age-related macular degeneration: Preliminary study. *BioMed Research International*, 2014, 671529. <https://doi.org/10.1155/2014/671529>
- Neely, D., Zarubina, A. V., Clark, M. E., Huisingh, C. E., Jackson, G. R., Zhang, Y., McGwin, G., Curcio, C. A., & Owsley, C. (2017). Association between visual function and subretinal drusenoid deposits in normal and early age-related macular degeneration eyes. *Retina*, 37(7), 1329–1336. <https://doi.org/10.1097/IAE.0000000000001454>
- Newsome, D. A., & Negreiro, M. (2009). Reproducible measurement of macular light flash recovery time using a novel device can indicate the presence and worsening of macular diseases. *Current Eye Research*, 34(2), 162–170. <https://doi.org/10.1080/02713680802647654>
- Ng, E. Y. K., Rajendra Acharya, U., Rangayyan, R. M., & Suri, J. S. (Eds.) (2014). Ophthalmological imaging and applications. (1st ed.) CRC Press <https://doi.org/10.1201/b17026>
- Nguyen, C. T., Fraser, R. G., Tan, R., Caruso, E., Lek, J. J., Guymer, R. H., Luu, C. D., (2018). Longitudinal changes in retinotopic rod function in intermediate age-related macular degeneration. *Investigative Ophthalmology and Visual Science*, 59(4), AMD19–AMD24. <https://doi.org/10.1167/iovs.17-23084>
- National Institute for Health and Care Excellence (NICE) (2013) *Aflibercept solution for injection for treating wet age-related macular degeneration. Technology appraisal guidance [TA294]*. <https://www.nice.org.uk/guidance/ta294>
- National Institute for Health and Care Excellence (NICE) (2018) *Age-related macular degeneration NICE Guideline G82*. <https://www.nice.org.uk/guidance/ng82>
- National Institute for Health and Care Excellence (NICE) (2021) *Brolucizumab for treating wet age-related macular degeneration. Technology appraisal guidance [TA672]*. <https://www.nice.org.uk/guidance/ta672>
- National Institute for Health and Care Excellence (NICE) (2008) *Ranibizumab and pegaptanib for the treatment of age-related macular degeneration. Technology appraisal guidance [TA155]*. <https://www.nice.org.uk/guidance/ta155>
- O’Neill-Biba, M., Sivaprasad, S., Rodriguez-Carmona, M., Wolf, J. E., & Barbur, J. L. (2010). Loss of chromatic sensitivity in AMD and diabetes: a comparative study. *Ophthalmic & Physiological Optics*, 30(5), 705–716. <https://doi.org/10.1111/j.1475-1313.2010.00775.x>
- Ooto, S., Ellabban, A. A., Ueda-Arakawa, N., Oishi, A., Tamura, H., Yamashiro, K., Tsujikawa, A., & Yoshimura, N. (2013). Reduction of retinal sensitivity in eyes with reticular pseudodrusen. *American Journal of Ophthalmology*, 156(6), 1184-1191.e2. <https://doi.org/10.1016/j.ajo.2013.06.036>
- Osterberg. (1937). Topography of the Layer of Rods and Cones in the Human Retina. *Journal of the American Medical Association*, 108(3) 232. <https://doi.org/10.1001/jama.1937.02780030070033>
- Oveson, B. C., Iwase, T., Hackett, S. F., Lee, S. Y., Usui, S., Sedlak, T. W., Snyder, S. H., Campochiaro, P. A., & Sung, J. U. (2011). Constituents of bile, bilirubin and TUDCA, protect against oxidative stress-induced retinal degeneration. *Journal of Neurochemistry*, 116(1), 144–153. <https://doi.org/10.1111/j.1471-4159.2010.07092.x>
- Owsley, C. (2003). Contrast sensitivity. *Ophthalmology Clinics of North America*, 16(2), 171–177. [https://doi.org/10.1016/S0896-1549\(03\)00003-8](https://doi.org/10.1016/S0896-1549(03)00003-8)
- Owsley, C., Clark, M. E., Huisingh, C. E., Curcio, C. A., & McGwin, G. (2016). Visual function in older eyes in normal macular health: Association with incident early age-related macular degeneration 3 years later. *Investigative Ophthalmology and Visual Science*, 57(4), 1782–1789. <https://doi.org/10.1167/iovs.15-18962>

- Owsley, C., Clark, M. E., & McGwin, G. (2017). Natural History of Rod-Mediated Dark Adaptation over 2 Years in Intermediate Age-Related Macular Degeneration. *Translational Vision Science & Technology*, 6(3), 15. <https://doi.org/10.1167/tvst.6.3.15>
- Owsley, C., Huisin, C., Clark, M. E., Jackson, G. R., McGwin, G. (2016). Comparison of Visual Function in Older Eyes in the Earliest Stages of Age-related Macular Degeneration to Those in Normal Macular Health. *Current Eye Research*, 41(2), 266–272. <https://doi.org/10.3109/02713683.2015.1011282>
- Owsley, C., Huisin, C., Jackson, G. R., Curcio, C. A., Szalai, A. J., Dashti, N., Clark, M., Rookard, K., McCrory, M. A., Wright, T. T., Callahan, M. A., Kline, L. B., Witherspoon, C. D., McGwin, G., McGwin Jr, G., & McGwin, G. (2014). Associations between abnormal rod-mediated dark adaptation and health and functioning in older adults with normal macular health. *Investigative Ophthalmology & Visual Science*, 55(8), 4776–4789. <https://doi.org/10.1167/iovs.14-14502>
- Owsley, C., Jackson, G. R., Cideciyan, A. V., Huang, Y., Fine, S. L., Ho, A. C., Maguire, M. G., Lolley, V., & Jacobson, S. G. (2000). Psychophysical evidence for rod vulnerability in age-related macular degeneration. *Investigative Ophthalmology & Visual Science*, 41(1), 267–273. <https://iovs.arvojournals.org/article.aspx?articleid=2123716>
- Owsley, C., Jackson, G. R., White, M., Feist, R., Edwards, D. (2001). Delays in rod-mediated dark adaptation in early age-related maculopathy. *Ophthalmology*, 108(7), 1196–1202. [https://doi.org/10.1016/S0161-6420\(01\)00580-2](https://doi.org/10.1016/S0161-6420(01)00580-2)
- Owsley, C., McGwin G., Scilley, K., Kallies, K., McGwin, G., Scilley, K., & Kallies, K. (2006). Development of a questionnaire to assess vision problems under low luminance in age-related maculopathy. *Investigative Ophthalmology and Visual Science*, 47(2), 528–535. <https://doi.org/10.1167/iovs.05-1222>
- Owsley, C., & McGwin, G. (2010). Vision and Driving. *Vision Research*, 50(23), 2348. <https://doi.org/10.1016/j.visres.2010.05.021>
- Owsley, C., McGwin, G., Clark, M. E., Jackson, G. R., Callahan, M. A., Kline, L. B., Witherspoon, C. D., Curcio, C. A. (2016). Delayed Rod-Mediated Dark Adaptation Is a Functional Biomarker for Incident Early Age-Related Macular Degeneration. *Ophthalmology*, 123(2), 344–351. <https://doi.org/10.1016/j.ophtha.2015.09.041>
- Owsley, C., McGwin, G., Jackson, G. R., Heimbürger, D. C., Piyathilake, C. J., Klein, R., White, M. F., Kallies, K. (2006). Effect of short-term, high-dose retinol on dark adaptation in aging and early age-related maculopathy. *Investigative Ophthalmology and Visual Science*, 47(4), 1310–1318. <https://doi.org/10.1167/iovs.05-1292>
- Owsley, C., McGwin, G., Jackson, G. R., Kallies, K., & Clark, M. (2007). Cone- and Rod-Mediated Dark Adaptation Impairment in Age-Related Maculopathy. *Ophthalmology*, 114(9), 1728–1735. <https://doi.org/10.1016/j.ophtha.2006.12.023>
- Owsley, C., Swain, T. A., McGwin, G., Clark, M. E., Kar, D., Crosson, J. N., & Curcio, C. A. (2022). How Vision Is Impaired From Aging to Early and Intermediate Age-Related Macular Degeneration: Insights From ALSTAR2 Baseline. *Translational Vision Science & Technology*, 11(7). <https://doi.org/10.1167/TVST.11.7.17>
- Palkar, A. H., & Khetan, V. (2019). Polypoidal choroidal vasculopathy: An update on current management and review of literature. *Taiwan Journal of Ophthalmology*, 9(2), 72–92. https://doi.org/10.4103/tjo.tjo_35_18
- Parede, T. R. R., Torricelli, A. A. M., Mukai, A., Netto, M. V., & Bechara, S. J. (2013). Quality of vision in refractive and cataract surgery, indirect measurers: review article. *Arquivos Brasileiros de Oftalmologia*, 76(6), 386–390. <https://doi.org/10.1590/S0004-27492013000600016>
- Parekh, N., Volland, R. P., Moeller, S. M., Blodi, B. A., Ritenbaugh, C., Chappell, R. J., Wallace, R. B., & Mares, J. A. (2009). Association between dietary fat intake and age-related macular

- degeneration in the Carotenoids in Age-Related Eye Disease Study (CAREDS): an ancillary study of the Women's Health Initiative. *Archives of Ophthalmology*, 127(11), 1483–1493. <https://doi.org/10.1001/archophthalmol.2009.130>
- Patel, M., & Kiss, S. (2014). Ultra-wide-field fluorescein angiography in retinal disease. *Current Opinion in Ophthalmology*, 25(3), 213-220. <https://doi.org/10.1097/ICU.0000000000000042>
- Paupoo, A. A., Mahroo, O. A., Friedburg, C., & Lamb, T. D. (2000). Human cone photoreceptor responses measured by the electroretinogram [correction of electroretinogram] a-wave during and after exposure to intense illumination. *The Journal of Physiology*, 529(2), 469–482. <https://doi.org/10.1111/j.1469-7793.2000.00469.x>
- Pelli, D. G., Robson, J. G., & Wilkins, A. J. (1988). The design of a new letter chart for measuring contrast sensitivity. *Clinical Vision Sciences*, 2(3), 187–199. <https://nyuscholars.nyu.edu/en/publications/the-design-of-a-new-letter-chart-for-measuring-contrast-sensitivi>
- Pfau, M., Lindner, M., Fleckenstein, M., Finger, R. P., Rubin, G. S., Harmening, W. M., Morales, M. U., Holz, F. G., & Schmitz-Valckenberg, S. (2017). Test-Retest Reliability of Scotopic and Mesopic Fundus-Controlled Perimetry Using a Modified MAIA (Macular Integrity Assessment) in Normal Eyes. *Ophthalmologica*, 237(1), 42–54. <https://doi.org/10.1159/000453079>
- Pfau, M., Lindner, M., Gliem, M., Steinberg, J. S., Thiele, S., Finger, R. P., Fleckenstein, M., Holz, F. G., & Schmitz-Valckenberg, S. (2018). Mesopic and dark-adapted two-color fundus-controlled perimetry in patients with cuticular, reticular, and soft drusen. *Eye*, 32(12), 1819–1830. <https://doi.org/10.1038/s41433-018-0183-3>
- Pfau, M., Lindner, M., Müller, P. L., Birtel, J., Finger, R. P., Harmening, W. M., Fleckenstein, M., Holz, F. G., & Schmitz-Valckenberg, S. (2017). Effective Dynamic Range and Retest Reliability of Dark-Adapted Two-Color Fundus-Controlled Perimetry in Patients With Macular Diseases. *Investigative Ophthalmology & Visual Science*, 58(6), BIO158–BIO167. <https://doi.org/10.1167/iovs.17-21454>
- Phipps, J. A., Dang, T. M., Vingrys, A. J., & Guymer, R. H. (2004). Flicker perimetry losses in age-related macular degeneration. *Investigative Ophthalmology & Visual Science*, 45(9), 3355–3360. <https://doi.org/10.1167/iovs.04-0253>
- Phipps, J. A., Guymer, R. H., & Vingrys, A. J. (2003). Loss of Cone Function in Age-Related Maculopathy. *Investigative Ophthalmology & Visual Science*, 44(5), 2277–2283. <https://doi.org/10.1167/iovs.02-0769>
- Pines, J. M., Carpenter, C. R., Raja, A. S., & Schuur, J. D. (2012). *Evidence-Based Emergency Care: Diagnostic Testing and Clinical Decision Rules*. Wiley. <https://doi.org/10.1002/9781118482117>
- Pondorfer, S. G., Heinemann, M., Wintergerst, M. W. M., Pfau, M., Stromer, A. L., Holz, F. G., & Finger, R. P. (2020). Detecting vision loss in intermediate age-related macular degeneration: A comparison of visual function tests. *PLoS ONE*, 15(4). <https://doi.org/10.1371/journal.pone.0231748>
- Pugh, E. N. (1975a). Rushton's paradox: rod dark adaptation after flash photolysis. *The Journal of Physiology*, 248(2), 413–431. <https://doi.org/10.1113/jphysiol.1975.sp010982>
- Pugh, E. N. (1975b). Rhodopsin flash photolysis in man. *The Journal of Physiology*, 248(2), 393–412. <https://doi.org/10.1113/jphysiol.1975.sp010981>
- Pumariega, N. M., Smith, R. T., Sohrab, M. A., Letien, V., & Souied, E. H. (2011). A prospective study of reticular macular disease. *Ophthalmology*, 118(8), 1619–1625. <https://doi.org/10.1016/J.OPHTHA.2011.01.029>

- Quartilho, A., Simkiss, P., Zekite, A., Xing, W., Wormald, R., & Bunce, C. (2016). Leading causes of certifiable visual loss in England and Wales during the year ending 31 March 2013. *Eye*, *30*(4), 602–607. <https://doi.org/10.1038/eye.2015.288>
- Querques, G., Canoui-Poitrine, F., Coscas, F., Massamba, N., Querques, L., Mimoun, G., Bandello, F., & Souied, E. H. (2012). Analysis of progression of reticular pseudodrusen by spectral domain-optical coherence tomography. *Investigative Ophthalmology & Visual Science*, *53*(3), 1264–1270. <https://doi.org/10.1167/IOVS.11-9063>
- Quinn, N., Csincsik, L., Flynn, E., Curcio, C. A., Kiss, S., Sadda, S. V. R., Hogg, R., Peto, T., & Lengyel, I. (2019). The clinical relevance of visualising the peripheral retina. *Progress in Retinal and Eye Research*, *68*, 83–109. <https://doi.org/10.1016/j.preteyeres.2018.10.001>
- Ratra, V., Ratra, D., Gupta, M., & Vaitheeswaran, K. (2012). Comparison between Humphrey Field Analyzer and Micro Perimeter 1 in normal and glaucoma subjects. *Oman Journal of Ophthalmology*, *5*(2), 97–102. <https://doi.org/10.4103/0974-620X.99372>
- Reeves, B. C., Scott, L. J., Taylor, J., Hogg, R., Rogers, C. A., Wordsworth, S., Townsend, D., Muldrew, A., Peto, T., Violato, M., Dakin, H., Cappel-Porter, H., Mills, N., O'Reilly, D., Harding, S. P., & Chakravarthy, U. (2016). The Effectiveness, cost-effectiveness and acceptability of Community versus Hospital Eye Service follow-up for patients with neovascular age-related macular degeneration with quiescent disease (ECHOES): a virtual randomised balanced incomplete block tria. *Health Technology Assessment*, *20*(80), 1–120. <https://doi.org/10.3310/hta20800>
- Remington, L. A. (2012). Retina. In L. A. Remington (Ed.) *Clinical Anatomy and Physiology of the Visual System*, 61–92, Butterworth-Heinemann. <https://doi.org/10.1016/B978-1-4377-1926-0.10004-9>
- Reuter, T. (2011). Fifty years of dark adaptation 1961–2011. *Vision Research*, *51*(21), 2243–2262. <https://doi.org/https://doi.org/10.1016/j.visres.2011.08.021>
- Richer, S. P., Stiles, W., Graham-Hoffman, K., Levin, M., Ruskin, D., Wrobel, J., Park, D. W., & Thomas, C. (2011). Randomized, double-blind, placebo-controlled study of zeaxanthin and visual function in patients with atrophic age-related macular degeneration: The Zeaxanthin and Visual Function Study (ZVF) FDA IND #78, 973. *Optometry*, *82*(11), 667. <https://doi.org/10.1016/j.optm.2011.08.008>
- Richer, S., Patel, S., Sockanathan, S., Ulanski, L. J., Miller, L., & Podella, C. (2014). Resveratrol based oral nutritional supplement produces long-term beneficial effects on structure and visual function in human patients. *Nutrients*, *6*(10), 4404–4420. <https://doi.org/10.3390/nu6104404>
- Richer, S., Stiles, W., Ulanski, L., Carroll, D., & Podella, C. (2013). Observation of human retinal remodeling in octogenarians with a resveratrol based nutritional supplement. *Nutrients*, *5*(6), 1989–2005. <https://doi.org/10.3390/nu5061989>
- Ridder, W. H., Comer, G., Oquindo, C., Yoshinaga, P., Engles, M., & Burke, J. (2022). Contrast Sensitivity in Early to Intermediate Age-Related Macular Degeneration (AMD). *Current Eye Research*, *47*(2), 287–296. <https://doi.org/10.1080/02713683.2021.1966478>
- Rieke, F. (2000). Mechanisms of single-photon detection in rod photoreceptor. In J. Abelson, M. Simon, G. Verdine & A. Pyle (Eds), *Methods in Enzymology*, *316*, 186–202. Academic Press. [https://doi.org/10.1016/s0076-6879\(00\)16724-2](https://doi.org/10.1016/s0076-6879(00)16724-2)
- Robinson, D. G., Margrain, T. H., Dunn, M. J., Bailey, C., & Binns, A. M. (2018). Low-level nighttime light therapy for age-related macular degeneration: A randomized clinical trial. *Investigative Ophthalmology and Visual Science*, *59*(11), 4531–4541. <https://doi.org/10.1167/iov.18-24284>
- Rodrigo-Diaz, E., Tahir, H. J., Kelly, J. M., Parry, N. R. A., Aslam, T., & Murray, I. J. (2019). The Light and the Dark of Early and Intermediate AMD: Cone- and Rod-Mediated Changes Are Linked to Fundus Photograph and FAF Abnormalities. *Investigative Ophthalmology and Visual Science*, *60*(15), 5070–5079. <https://doi.org/10.1167/iov.19-27971>

- Rodriguez, J. D., Lane, K., Hollander, D. A., Shapiro, A., Saigal, S., Hertsberg, A. J., Wallstrom, G., Narayanan, D., Angjeli, E., & Abelson, M. B. (2018). Cone photoreceptor macular function and recovery after photostress in early non-exudative age-related macular degeneration. *Clinical Ophthalmology*, *12*, 1325–1335. <https://doi.org/10.2147/OPHTH.S165658>
- Rosenfeld, P. J., Brown, D. M., Heier, J. S., Boyer, D. S., Kaiser, P. K., Chung, C. Y., & Kim, R. Y. (2006). Ranibizumab for neovascular age-related macular degeneration. *The New England Journal of Medicine*, *355*(14), 1419–1431. <https://doi.org/10.1056/NEJM0A054481>
- Rosenfeld, P. J., Dugel, P. U., Holz, F. G., Heier, J. S., Pearlman, J. A., Novack, R. L., Csaky, K. G., Koester, J. M., Gregory, J. K., & Kubota, R. (2018). Emixustat Hydrochloride for Geographic Atrophy Secondary to Age-Related Macular Degeneration: A Randomized Clinical Trial. *Ophthalmology*, *125*(10), 1556–1567. <https://doi.org/10.1016/j.ophtha.2018.03.059>
- Rosenfeld, P. J., Rich, R. M., & Lalwani, G. A. (2006). Ranibizumab: Phase III clinical trial results. *Ophthalmology Clinics of North America*, *19*(3), 361–372. <https://doi.org/10.1016/j.ohc.2006.05.009>
- Rosenfeld, P. J., Sadda, V. S. R., Yehoshua, Z., Penha, F. M., Nittala, M. G., Konduru, R. K., Gregori, G., & Feurer, W. J. (2011). Comparison of Drusen Area Detected by Spectral Domain OCT and Color Fundus Photography. *Investigative Ophthalmology & Visual Science*, *52*(14), 139–139. <https://iovs.arvojournals.org/article.aspx?articleid=2349651>
- Sadda, S. R., Guymer, R., Holz, F. G., Schmitz-Valckenberg, S., Curcio, C. A., Bird, A. C., Blodi, B. A., Bottoni, F., Chakravarthy, U., Chew, E. Y., Csaky, K., Danis, R. P., Fleckenstein, M., Freund, K. B., Grunwald, J., Hoyng, C. B., Jaffe, G. J., Liakopoulos, S., Monés, J. M., ... Staurenghi, G. (2018). Consensus Definition for Atrophy Associated with Age-Related Macular Degeneration on OCT: Classification of Atrophy Report 3. *Ophthalmology*, *125*(4), 537–548. <https://doi.org/10.1016/j.ophtha.2017.09.028>
- Sadda, S. R., Keane, P., Elliott, D., & Scott, I. U. (2009). Pitfalls to consider when using spectraldomain OCT. *Retina Today*, *MARCH*, 38–41. https://retinatoday.com/articles/2009-mar/0309RT_F09_Pearls_Sadda-php
- Salvi, S. M., Akhtar, S., & Currie, Z. (2006). Ageing changes in the eye. *Postgraduate Medical Journal*, *829*(971), 581–587. <https://doi.org/10.1136/pgmj.2005.040857>
- SanGiovanni, J. P., Chew, E. Y., Clemons, T. E., Davis, M. D., Ferris, F. L. 3rd, Gensler, G. R., Kurinij, N., Lindblad, A. S., Milton, R. C., Seddon, J. M., & Sperduto, R. D. (2007). The relationship of dietary lipid intake and age-related macular degeneration in a case-control study: AREDS Report No. 20. *Archives of Ophthalmology*, *125*(5), 671–679. <https://doi.org/10.1001/archophth.125.5.671>
- Sarks, S. H. (1976). Ageing and degeneration in the macular region: A clinico-pathological study. *British Journal of Ophthalmology*, *60*(5), 324–341. <https://doi.org/10.1136/bjo.60.5.324>
- Saßmannshausen, M., Steinberg, J. S., Fimmers, R., Pfau, M., Thiele, S., Fleckenstein, M., Holz, F. G., & Schmitz-Valckenberg, S. (2018). Structure-Function Analysis in Patients With Intermediate Age-Related Macular Degeneration. *Investigative Ophthalmology & Visual Science*, *59*(3), 1599–1608. <https://doi.org/10.1167/iovs.17-22712>
- Schieber, F. (1992). Aging and the Senses. In *Handbook of Mental Health and Aging*, 251–306. Academic Press. <https://doi.org/10.1016/b978-0-12-101277-9.50014-0>
- Schneck, M. E., Lott, L. A., Haegerstrom-Portnoy, G., Hewlett, S., Gauer, B. M., & Zaidi, A. (2021). Visual Function in Eyes with Intermediate AMD with and without Retinal Pigment Abnormalities. *Optometry and Vision Science Academy of Optometry*, *98*(1), 64–72. <https://doi.org/10.1097/OPX.0000000000001624>
- Schuman, S. G., Koreishi, A. F., Farsiu, S., Jung, S. ho, Izatt, J. A., & Toth, C. A. (2009). Photoreceptor Layer Thinning over Drusen in Eyes with Age-Related Macular Degeneration Imaged In Vivo with

Spectral-Domain Optical Coherence Tomography. *Ophthalmology*, 116(3), 488-496
<https://doi.org/10.1016/j.ophtha.2008.10.006>

- Schwartz, R., & Loewenstein, A. (2015). Early detection of age related macular degeneration: Current status. *International Journal of Retina and Vitreous*, 1(1), 1–8. <https://doi.org/10.1186/S40942-015-0022-7/FIGURES/2>
- Schwartz, S. D., Regillo, C. D., Lam, B. L., Elliott, D., Rosenfeld, P. J., Gregori, N. Z., Hubschman, J.-P., Davis, J. L., Heilwell, G., Spirn, M., Maguire, J., Gay, R., Bateman, J., Ostrick, R. M., Morris, D., Vincent, M., Anglade, E., Del Priore, L. V., & Lanza, R. (2015). Human embryonic stem cell-derived retinal pigment epithelium in patients with age-related macular degeneration and Stargardt's macular dystrophy: follow-up of two open-label phase 1/2 studies. *Lancet*, 385(9967), 509–516. [https://doi.org/10.1016/S0140-6736\(14\)61376-3](https://doi.org/10.1016/S0140-6736(14)61376-3)
- Schwartz, S. G., Hampton, B. M., Kovach, J. L., & Brantley, M. A. (2016). Genetics and age-related macular degeneration: a practical review for the clinician. *Clinical Ophthalmology*, 10, 1229. <https://doi.org/10.2147/OPHTH.S109723>
- Seddon, J. M., Ajani, U. A., Sperduto, R. D., Hiller, R., Blair, N., Burton, T. C., Farber, M. D., Gragoudas, E. S., Haller, J., Miller, D. T., Yannuzzi, L. A., & Willett, W. (1994). Dietary Carotenoids, Vitamins A, C, and E, and Advanced Age-Related Macular Degeneration. *JAMA*, 272(18), 1413–1420. <https://doi.org/10.1001/jama.1994.03520180037032>
- Seddon, J. M., George, S., Rosner, B., & Rifai, N. (2005). Progression of Age-Related Macular Degeneration: Prospective Assessment of C-Reactive Protein, Interleukin 6, and Other Cardiovascular Biomarkers. *Archives of Ophthalmology*, 123(6), 774–782. <https://doi.org/10.1001/archophth.123.6.774>
- Seddon, J. M., Santangelo, S. L., Book, K., Chong, S., & Cote, J. (2003). A genomewide scan for age-related macular degeneration provides evidence for linkage to several chromosomal regions. *American Journal of Human Genetics*, 73(4), 780–790. <https://doi.org/10.1086/378505>
- Seiple, W. H., Siegel, I. M., Carr, R. E., & Mayron, C. (1986). Evaluating macular function using the focal ERG. *Investigative Ophthalmology & Visual Science*, 27(7), 1123–1130. <https://iovs.arvojournals.org/article.aspx?articleid=2177580>
- Senger, D. R., Galli, S. J., Dvorak, A. M., Perruzzi, C. A., Harvey, V. S., & Dvorak, H. F. (1983). Tumor cells secrete a vascular permeability factor that promotes accumulation of ascites fluid. *Science*, 219(4587), 983–985. <https://doi.org/10.1126/science.6823562>
- Sevilla, M. B., McGwin, G., Lad, E. M., Clark, M., Yuan, E. L., Farsiu, S., Curcio, C. A., Owsley, C., & Toth, C. A. (2016). Relating Retinal Morphology and Function in Aging and Early to Intermediate Age-related Macular Degeneration Subjects. *American Journal of Ophthalmology*, 165, 65–77. <https://doi.org/10.1016/j.ajo.2016.02.021>
- Shaw, L. T., Mackin, A., Shah, R., Jain, S., Jain, P., Nayak, R., & Hariprasad, S. M. (2020). Risuteganib—a novel integrin inhibitor for the treatment of non-exudative (dry) age-related macular degeneration and diabetic macular edema. *Expert Opinion on Investigational Drugs*, 29(6), 547–554. <https://doi.org/10.1080/13543784.2020.1763953>
- Sieving, P. A., Caruso, R. C., Tao, W., Coleman, H. R., Thompson, D. J. S., Fullmer, K. R., & Bush, R. A. (2006). Ciliary neurotrophic factor (CNTF) for human retinal degeneration: phase I trial of CNTF delivered by encapsulated cell intraocular implants. *Proceedings of the National Academy of Sciences of the United States of America*, 103(10), 3896–3901. <https://doi.org/10.1073/pnas.0600236103>
- Sivaprasad, S., Banister, K., Azuro-Blanco, A., Goulao, B., Cook, J. A., Hogg, R., Scotland, G., Heimann, H., Lotery, A., Ghanchi, F., Gale, R., Menon, G., Downey, L., Hopkins, N., Scanlon, P., Burton, B., Ramsay, C., & Chakravarthy, U. (2021). Diagnostic Accuracy of Monitoring Tests of Fellow Eyes in Patients with Unilateral Neovascular Age-Related Macular Degeneration: Early Detection of

- Neovascular Age-Related Macular Degeneration Study. *Ophthalmology*, 128(12), 1736–1747. <https://doi.org/https://doi.org/10.1016/j.ophtha.2021.07.025>
- Sivaprasad, S., Bird, A., Nitiapapand, R., Nicholson, L., Hykin, P., & Moorfields UCL AMD Consortium (2016). Perspectives on reticular pseudodrusen in age-related macular degeneration. *Survey of Ophthalmology*, 61(5), 521–537. <https://doi.org/10.1016/j.survophthal.2016.02.005>
- Sjöstrand, J., & Frisén, L. (1977). Contrast sensitivity in macular disease: A Preliminary Report. *Acta Ophthalmologica*, 55(3), 507–514. <https://doi.org/10.1111/j.1755-3768.1977.tb06128.x>
- Smith, R. T., Chan, J. K., Nagasaki, T., Sparrow, J. R., & Barbazetto, I. (2005). A method of drusen measurement based on reconstruction of fundus background reflectance. *British Journal of Ophthalmology*, 89(1), 87–91. <https://doi.org/10.1136/BJO.2004.042937>
- Smith, R. T., Sohrab, M. A., Busuioc, M., & Barile, G. (2009). Reticular macular disease. *American Journal of Ophthalmology*, 148(5), 733–743.e2. <https://doi.org/10.1016/j.ajo.2009.06.028>
- Smith, W., Mitchell, P., & Leeder, S. R. (1996). Smoking and age-related maculopathy. The Blue Mountains Eye Study. *Archives of Ophthalmology*, 114(12), 1518–1523. <https://doi.org/10.1001/ARCHOPHT.1996.01100140716016>
- Sommerburg, O., Keunen, J. E. E., Bird, A. C., & van Kuijk, F. J. G. M. (1998). Fruits and vegetables that are sources for lutein and zeaxanthin: the macular pigment in human eyes. *British Journal of Ophthalmology*, 82(8), 907–910. <https://doi.org/10.1136/bjo.82.8.907>
- Soomro, T., Shah, N., Nistrata-Ortiz, M., Yap, T., Normando, E. M., & Cordeiro, M. F. (2020). Recent advances in imaging technologies for assessment of retinal diseases. *Expert Review of Medical Devices*, 17(10), 1095–1108. <https://doi.org/10.1080/17434440.2020.1816167>
- Spaide, R. F. (2018). Improving the age-related macular degeneration construct: A new classification system. *Retina*, 38(5), 891–899. <https://doi.org/10.1097/IAE.0000000000001732>
- Spaide, R. F., & Curcio, C. A. (2010). Drusen characterization with multimodal imaging. *Retina*, 30(9), 1441–1454. <https://doi.org/10.1097/IAE.0b013e3181ee5ce8>
- Spaide, R. F., Ooto, S., & Curcio, C. A. (2018). Subretinal drusenoid deposits AKA pseudodrusen. *Survey of Ophthalmology*, 63(6), 782–815. <https://doi.org/10.1016/j.survophthal.2018.05.005>
- Sparrow, J. R., & Boulton, M. (2005). RPE lipofuscin and its role in retinal pathobiology. *Experimental Eye Research*, 80(5), 595–606. <https://doi.org/10.1016/j.exer.2005.01.007>
- Srinivasan, P. P., Kim, L. A., Mettu, P. S., Cousins, S. W., Comer, G. M., Izatt, J. A., & Farsiu, S. (2014). Fully automated detection of diabetic macular edema and dry age-related macular degeneration from optical coherence tomography images. *Biomedical Optics Express*, 5(10), 3568. <https://doi.org/10.1364/boe.5.003568>
- Steinberg, J. S., Saßmannshausen, M., Pfau, M., Fleckenstein, M., Finger, R. P., Holz, F. G., & Schmitz-Valckenberg, S. (2017). Evaluation of two systems for fundus-controlled scotopic and mesopic perimetry in eye with age-related macular degeneration. *Translational Vision Science and Technology*, 6(4), 7. <https://doi.org/10.1167/tvst.6.4.7>
- Strimbu, K., & Tavel, J. A. (2010). What are biomarkers? *Current Opinion in HIV and AIDS*, 5(6), 463–466. <https://doi.org/10.1097/COH.0b013e32833ed177>
- Sui, G. Y., Liu, G. C., Liu, G. Y., Gao, Y. Y., Deng, Y., Wang, W. Y., Tong, S. H., & Wang, L. (2013). Is sunlight exposure a risk factor for age-related macular degeneration? A systematic review and meta-analysis. *British Journal of Ophthalmology*, 97(4), 389–394. <https://doi.org/10.1136/bjophthalmol-2012-302281>
- Sujak, A., Gabrielska, J., Grudziński, W., Borc, R., Mazurek, P., & Gruszecki, W. I. (1999). Lutein and Zeaxanthin as Protectors of Lipid Membranes against Oxidative Damage: The Structural Aspects.

- Sunness, J. S., Applegate, C. A., Haselwood, D., & Rubin, G. S. (1996). Fixation patterns and reading rates in eyes with central scotomas from advanced atrophic age-related macular degeneration and Stargardt disease. *Ophthalmology*, 103(9), 1458–1466. [https://doi.org/10.1016/S0161-6420\(96\)30483-1](https://doi.org/10.1016/S0161-6420(96)30483-1)
- Sunness, J. S., Massof, R. W., Johnson, M. A., Finkelstein, D., & Fine, S. L. (1985). Peripheral retinal function in age-related macular degeneration. *Archives Of Ophthalmology*, 103(6), 811–816. <https://doi.org/10.1001/ARCHOPHT.1985.01050060071029>
- Sunness, J. S., Rubin, G. S., Applegate, C. A., Bressler, N. M., Marsh, M. J., Hawkins, B. S., & Haselwood, D. (1997). Visual function abnormalities and prognosis in eyes with age-related geographic atrophy of the macula and good visual acuity. *Ophthalmology*, 104(10), 1677–1691. [https://doi.org/10.1016/s0161-6420\(97\)30079-7](https://doi.org/10.1016/s0161-6420(97)30079-7)
- Suzuki, M., Sato, T., & Spaide, R. F. (2014). Pseudodrusen subtypes as delineated by multimodal imaging of the fundus. *American Journal of Ophthalmology*, 157(5), 1005–1012. <https://doi.org/10.1016/j.ajo.2014.01.025>
- Tahir, H. J., Rodrigo-Diaz, E., Parry, N. R. A., Kelly, J. M. F., Carden, D., Aslam, T. M., & Murray, I. J. (2018). Slowed dark adaptation in early AMD: Dual stimulus reveals scotopic and photopic abnormalities. *Investigative Ophthalmology and Visual Science*, 59(4), AMD202–AMD210. <https://doi.org/10.1167/iovs.18-24227>
- Tan, R. S., Guymer, R. H., Aung, K. Z., Caruso, E., & Luu, C. D. (2019). Longitudinal assessment of rod function in intermediate age-related macular degeneration with and without reticular pseudodrusen. *Investigative Ophthalmology and Visual Science*, 60(5), 1511–1518. <https://doi.org/10.1167/iovs.18-26385>
- Tarallo, V., Hirano, Y., Gelfand, B. D., Dridi, S., Kerur, N., Kim, Y., Cho, W. G., Kaneko, H., Fowler, B. J., Bogdanovich, S., Albuquerque, R. J. C., Hauswirth, W. W., Chiodo, V. A., Kugel, J. F., Goodrich, J. A., Ponicsan, S. L., Chaudhuri, G., Murphy, M. P., Dunaief, J. L., ... Ambati, J. (2012). DICER1 loss and Alu RNA induce age-related macular degeneration via the NLRP3 inflammasome and MyD88. *Cell*, 149(4), 847–859. <https://doi.org/10.1016/j.cell.2012.03.036>
- Taylor, D. J., Edwards, L. A., Binns, A. M., & Crabb, D. P. (2018). Seeing it differently: self-reported description of vision loss in dry age-related macular degeneration. *Ophthalmic & Physiological Optics*, 38(1), 98–105. <https://doi.org/10.1111/opo.12419>
- Taylor, D. J., Jones, L., Binns, A. M., & Crabb, D. P. (2019). ‘You’ve got dry macular degeneration, end of story’: a qualitative study into the experience of living with non-neovascular age-related macular degeneration. *Eye*, 34(3), 461–47. <https://doi.org/10.1038/s41433-019-0445-8>
- Taylor, D. J., Smith, N. D., Jones, P. J., Binns, A. M., & Crabb, D. P. (2020). Measuring dynamic levels of self-perceived anxiety and concern during simulated mobility tasks in people with non-neovascular age-related macular degeneration. *The British journal of ophthalmology*, 104(4), 529–534. <https://doi.org/10.1136/bjophthalmol-2019-313864>
- Taylor, D. J., Smith, N. D., Binns, A. M., & Crabb, D. P. (2018). The effect of non-neovascular age-related macular degeneration on face recognition performance. *Graefe’s Archive for Clinical and Experimental Ophthalmology*, 256(4), 815–821. <https://doi.org/10.1007/s00417-017-3879-3>
- Taylor, D. J., Smith, N. D., & Crabb, D. P. (2017). Searching for objects in everyday scenes: Measuring performance in people with dry age-related macular degeneration. *Investigative Ophthalmology and Visual Science*, 58(3), 1887–1892. <https://doi.org/10.1167/iovs.16-21122>
- Terheyden, J. H., Behning, C., Lüning, A., Wintergerst, L., Basile, P. G., Tavares, D., Melício, B. A., Leal, S., Weissgerber, G., Luhmann, U. F. O., Crabb, D. P., Tufail, A., Hoyng, C., Berger, M., Schmid, M., Silva, R., Martinho, C. V., Cunha-Vaz, J., Holz, F. G., ... Zakaria, N. (2021). Challenges, facilitators

and barriers to screening study participants in early disease stages-experience from the MACUSTAR study. *BMC Medical Research Methodology*, 21(1), 54. <https://doi.org/10.1186/s12874-021-01243-8>

The University of Iowa. (n.d.). *Fluorescein Angiography* <https://medicine.uiowa.edu/eye/patient-care/imaging-services/fluorescein-angiography>

Thee, E. F., Meester-Smoor, M. A., Luttikhuisen, D. T., Colijn, J. M., Enthoven, C. A., Haarman, A. E. G., Rizopoulos, D., & Klaver, C. C. W. (2020). Performance of classification systems for age-related macular degeneration in the Rotterdam study. *Translational Vision Science and Technology*, 9(2), 1–11. <https://doi.org/10.1167/TVST.9.2.26>

Therneau, T. M. (2014). A package for survival analysis in S. R package version 2.37-7. <http://CRAN.R-project.org/package=survival>.

Thompson, A. C., Luhmann, U. F. O., Stinnett, S. S., Vajzovic, L., Horne, A., Toth, C. A., Cousins, S. W., Lad, E. M., (2018). Association of low luminance questionnaire with objective functional measures in early and intermediate age-related macular degeneration. *Investigative Ophthalmology and Visual Science*, 59(1), 289–297. <https://doi.org/10.1167/iovs.17-22528>

Thompson, D. A., Gyürüs, P., Fleischer, L. L., Bingham, E. L., McHenry, C. L., Apfelstedt-Sylla, E., Zrenner, E., Lorenz, B., Richards, J. E., Jacobson, S. G., Sieving, P. A., & Gal, A. (2000). Genetics and Phenotypes of RPE65 Mutations in Inherited Retinal Degeneration. *Investigative Ophthalmology & Visual Science*, 41(13), 4293–4299. <https://iovs.arvojournals.org/article.aspx?articleid=2162347>

Tomi, A., & Marin, I. (2014). Angiofluorographic aspects in age-related macular degeneration. *Journal of Medicine and Life*, 7(4), 4–17. <https://www.ncbi.nlm.nih.gov/pmc/articles/PMC4813616/>

Tsacopoulos, M., Poitry-Yamate, C. L., MacLeish, P. R., & Poitry, S. (1998). Trafficking of molecules and metabolic signals in the retina. *Progress in Retinal and Eye Research*, 17(3), 429–442. [https://doi.org/10.1016/S1350-9462\(98\)00010-X](https://doi.org/10.1016/S1350-9462(98)00010-X)

Uddin, D., Jeffrey, B. G., Flynn, O., Wong, W., Wiley, H., Keenan, T., Chew, E., & Cukras, C. (2020). Repeatability of Scotopic Sensitivity and Dark Adaptation Using a Medmont Dark-Adapted Chromatic Perimeter in Age-related Macular Degeneration. *Translational Vision Science & Technology*, 9(7), 31–31. <https://doi.org/10.1167/TVST.9.7.31>

Ueda-Arakawa, N., Ooto, S., Tsujikawa, A., Yamashiro, K., Oishi, A., & Yoshimura, N. (2013). Sensitivity and specificity of detecting reticular pseudodrusen in multimodal imaging in Japanese patients. *Retina*, 33(3), 490–497. <https://doi.org/10.1097/IAE.0B013E318276E0AE>

Van Leeuwen, R., Klaver, C. C. W., Vingerling, J. R., Hofman, A., & De Jong, P. T. V. M. (2003). The risk and natural course of age-related maculopathy: Follow-up at 6 1/2 years in the Rotterdam study. *Archives of Ophthalmology*, 121(4), 519–526. <https://doi.org/10.1001/archophth.121.4.519>

Varma, R., Fraser-Bell, S., Tan, S., Klein, R., & Azen, S. P. (2004). Prevalence of age-related macular degeneration in Latinos: the Los Angeles Latino eye study. *Ophthalmology*, 111(7), 1288–1297. <https://doi.org/10.1016/j.ophtha.2004.01.023>

Verdager, H., Saurí, T., & Macarulla, T. (2016). Predictive and prognostic biomarkers in personalized gastrointestinal cancer treatment. *Journal of Gastrointestinal Oncology*, 8(3), 405–417. <https://doi.org/10.21037/jgo.2016.11.15>

Veritas Health Innovation. (2019). *Covidence systematic review software*. <https://www.covidence.org/>

Volz, C., & Pauly, D. (2015). Antibody therapies and their challenges in the treatment of age-related macular degeneration. *European Journal of Pharmaceutics and Biopharmaceutics*, 95, 158–172. <https://doi.org/10.1016/j.ejpb.2015.02.020>

- von der Emde, L., Pfau, M., Thiele, S., Möller, P. T., Hassenrik, R., Fleckenstein, M., Holz, F. G., & Schmitz-Valckenberg, S. (2018). Mesopic and Dark-Adapted Two-Color Fundus-Controlled Perimetry in Choroidal Neovascularization Secondary to Age-Related Macular Degeneration. *Translational Vision Science & Technology*, 8(1), 7. <https://doi.org/10.1167/tvst.8.1.7>
- Wakatsuki, Y., Shinojima, A., Kawamura, A., & Yuzawa, M. (2015). Correlation of Aging and Segmental Choroidal Thickness Measurement using Swept Source Optical Coherence Tomography in Healthy Eyes. *PLoS One*, 10(12), e0144156. <https://doi.org/10.1371/journal.pone.0144156>
- Wald, G. (1935). Vitamin a in eye tissues. *Journal of General Physiology*, 18(6), 905–915. <https://doi.org/10.1085/jgp.18.6.905>
- Wald, G. (1968). The molecular basis of visual excitation. *Nature*, 219(5156), 800–807. <https://doi.org/10.1038/219800a0>
- Walter, P., Widder, R. A., Lüke, C., Königfeld, P., & Brunner, R. (1999). Electrophysiological abnormalities in age-related macular degeneration. *Graefes Archive for Clinical and Experimental Ophthalmology*, 37(12), 962–968. <https://doi.org/10.1007/s004170050331>
- Wang, A., Qi, W., Gao, T., & Tang, X. (2022). Molecular Contrast Optical Coherence Tomography and Its Applications in Medicine. *International Journal of Molecular Sciences*, 23(6) 3038. <https://doi.org/10.3390/ijms23063038>
- Weeks, D. E., Conley, Y. P., Mah, T. S., Paul, T. O., Morse, L., Ngo-Chang, J., Dailey, J. P., Ferrell, R. E., & Gorin, M. B. (2000). A full genome scan for age-related maculopathy. *Human Molecular Genetics*, 9(9), 1329–1349. <https://doi.org/10.1093/hmg/9.9.1329>
- Weismann, A. (2011). E. B. Poulton, S. Schönland, & A. E. Shipley. (Eds.), *Essays upon heredity and kindred biological problems*. (2nd ed.). Clarendon Press. <https://doi.org/10.5962/bhl.title.28066>
- Welker, S. G., Pfau, M., Heinemann, M., Schmitz-Valckenberg, S., Holz, F. G., & Finger, R. P. (2018). Retest Reliability of Mesopic and Dark-Adapted Microperimetry in Patients With Intermediate Age-Related Macular Degeneration and Age-Matched Controls. *Investigative Ophthalmology & Visual Science*, 59(4), AMD152–AMD159. <https://doi.org/10.1167/iovs.18-23878>
- Wensel, T. G. (2012). Molecular Biology of Vision. In S.T. Brady, G. J. Siegel, R. W. Albers & D. L. Price (Eds) *Basic Neurochemistry*, (8th ed) 889–903. Academic Press. <https://doi.org/10.1016/B978-0-12-374947-5.00051-1>
- West, S. K., Rubin, G. S., Broman, A. T., Muñoz, B., Bandeen-Roche, K., & Turano, K. (2002). How Does Visual Impairment Affect Performance on Tasks of Everyday Life?: The SEE Project. *Archives of Ophthalmology*, 120(6), 774–780. <https://doi.org/10.1001/ARCHOPHT.120.6.774>
- Wickham, H. (2016). *ggplot2: Elegant Graphics for Data Analysis*. Springer Cham. <https://doi.org/10.1007/978-3-319-24277-4>
- Wilson, L. M., Tharmarajah, S., Jia, Y., Semba, R. D., Schaumberg, D. A., & Robinson, K. A. (2021). The Effect of Lutein/Zeaxanthin Intake on Human Macular Pigment Optical Density: A Systematic Review and Meta-Analysis. *Advances in Nutrition*, 12(6), 2244–2254. <https://doi.org/10.1093/advances/nmab071>
- Wolffsohn, J. S., Anderson, S. J., Mitchell, J., Woodcock, A., Rubinstein, M., Ffytche, T., Browning, A., Willbond, K., Amoaku, W. M., & Bradley, C. (2006). Effect of age related macular degeneration on the Eger macular stressometer photostress recovery time. *British Journal of Ophthalmology*, 90(4), 432–434. <https://doi.org/10.1136/bjo.2005.085787>
- Wong, E. N., Chew, A. L., Morgan, W. H., Patel, P. J., & Chen, F. K. (2017). The use of microperimetry to detect functional progression in non-neovascular age-related macular degeneration: A systematic review. *Asia-Pacific Journal of Ophthalmology*, 6(1), 70–79. <https://doi.org/10.22608/APO.201643>

- Wong, K.-H., Nam, H.-Y., Lew, S.-Y., Naidu, M., David, P., Kamalden, T. A., Hadie, S. N. H., & Lim, L.-W. (2022). Discovering the Potential of Natural Antioxidants in Age-Related Macular Degeneration: A Review. *Pharmaceuticals*, *15*(1), 101. <https://doi.org/10.3390/ph15010101>
- Wong, W. L., Su, X., Li, X., Cheung, C. M. G., Klein, R., Cheng, C. Y., & Wong, T. Y. (2014). Global prevalence of age-related macular degeneration and disease burden projection for 2020 and 2040: A systematic review and meta-analysis. *The Lancet Global Health*, *2*(2). [https://doi.org/10.1016/S2214-109X\(13\)70145-1](https://doi.org/10.1016/S2214-109X(13)70145-1)
- Wu, Z., Ayton, L. N., Guymer, R. H., & Luu, C. D. (2013). Intrasection test-retest variability of microperimetry in age-related macular degeneration. *Investigative Ophthalmology and Visual Science*, *54*(12), 7378–7385. <https://doi.org/10.1167/iovs.13-12617>
- Wu, Z., Ayton, L. N., Luu, C. D., & Guymer, R. H. (2015). Longitudinal Changes in Microperimetry and Low Luminance Visual Acuity in Age-Related Macular Degeneration. *JAMA Ophthalmology*, *133*(4), 442–448. <https://doi.org/10.1001/JAMAOPHTHALMOL.2014.5963>
- Wu, Z., Fletcher, E. L., Kumar, H., Greferath, U., & Guymer, R. H. (2021). Reticular pseudodrusen: A critical phenotype in age-related macular degeneration. *Progress in Retinal and Eye Research*, *88*, 101017. doi:10.1016/j.preteyeres.2021.101017
- Xu, H., Chen, M., & Forrester, J. V. (2009). Para-inflammation in the aging retina. *Progress in Retinal and Eye Research*, *28*(5), 348–368. <https://doi.org/10.1016/j.preteyeres.2009.06.001>
- Xu, H., Chen, M., Manivannan, A., Lois, N., & Forrester, J. V. (2008). Age-dependent accumulation of lipofuscin in perivascular and subretinal microglia in experimental mice. *Aging Cell*, *7*(1), 58–68. <https://doi.org/10.1111/j.1474-9726.2007.00351.x>
- Yamashiro, K., Hosoda, Y., Miyake, M., Ooto, S., & Tsujikawa, A. (2020). Characteristics of Pachychoroid Diseases and Age-Related Macular Degeneration: Multimodal Imaging and Genetic Backgrounds. *Journal of Clinical Medicine*. *9*(7), 2034. <https://doi.org/10.3390/jcm9072034>
- Yang, Y., & Dunbar, H. (2021). Clinical Perspectives and Trends: Microperimetry as a Trial Endpoint in Retinal Disease. *Ophthalmologica*, *244*(5), 418–450. <https://doi.org/10.1159/000515148>
- Yazdanie, M., Alvarez, J., Agrón, E., Wong, W. T., Wiley, H. E., Ferris, F. L., Chew, E. Y., Cukras, C. (2017). Decreased Visual Function Scores on a Low Luminance Questionnaire Is Associated with Impaired Dark Adaptation. *Ophthalmology*, *124*(9), 1332–1339. <https://doi.org/10.1016/j.ophtha.2017.05.005>
- Yehoshua, Z., Gregori, G., Sadda, S. R., Penha, F. M., Goldhardt, R., Nittala, M. G., Konduru, R. K., Feuer, W. J., Gupta, P., Li, Y., & Rosenfeld, P. J. (2013). Comparison of Drusen Area Detected by Spectral Domain Optical Coherence Tomography and Color Fundus Imaging. *Investigative Ophthalmology & Visual Science*, *54*(4), 2429–2434. <https://doi.org/10.1167/IOVS.12-11569>
- Ying, G. S., Maguire, M. G., Liu, C., & Antoszyk, A. N. (2008). Night Vision Symptoms and Progression of Age-related Macular Degeneration in the Complications of Age-related Macular Degeneration Prevention Trial. *Ophthalmology*, *115*(11), 1876–1882.e4. <https://doi.org/10.1016/j.ophtha.2008.05.023>
- Yonekawa, Y., & Kim, I. K. (2014). Clinical characteristics and current treatment of age-related macular degeneration. *Cold Spring Harbor Perspectives in Medicine*, *5*(1), a017178. <https://doi.org/10.1101/cshperspect.a017178>
- Youn, H.-Y., McCanna, D. J., Sivak, J. G., & Jones, L. W. (2011). In vitro ultraviolet-induced damage in human corneal, lens, and retinal pigment epithelial cells. *Molecular Vision*, *17*, 237. <https://www.ncbi.nlm.nih.gov/pmc/articles/PMC3025821/>
- Young, R. W. (1967). The renewal of photoreceptor cell outer segments. *The Journal of Cell Biology*, *33*(1), 61–72. <https://doi.org/10.1083/jcb.33.1.61>

- Yu, Y., Bhangale, T. R., Fagerness, J., Ripke, S., Thorleifsson, G., Tan, P. L., Souied, E. H., Richardson, A. J., Merriam, J. E., Buitendijk, G. H. S., Reynolds, R., Raychaudhuri, S., Chin, K. A., Sobrin, L., Evangelou, E., Lee, P. H., Lee, A. Y., Leveziel, N., Zack, D. J., ... Seddon, J. M. (2011). Common variants near FRK/COL10A1 and VEGFA are associated with advanced age-related macular degeneration. *Human Molecular Genetics*, 20(18), 3699–3709. <https://doi.org/10.1093/hmg/ddr270>
- Zampros, I., Praidou, A., Brazitikos, P., Ekonomidis, P., & Androudi, S. (2012). Antivasular Endothelial Growth Factor Agents for Neovascular Age-Related Macular Degeneration. *Journal of Ophthalmology*, 2012, 319728. <https://doi.org/10.1155/2012/319728>
- Zarbin, M. A. (2004). Current Concepts in the Pathogenesis of Age-Related Macular Degeneration. *Archives of Ophthalmology*, 122(4), 598–614. <https://doi.org/10.1001/archophth.122.4.598>
- Zarubina, A. V., Neely, D. C., Clark, M. E., Huisinigh, C. E., Samuels, B. C., Zhang, Y., McGwin, G. J., Owsley, C., & Curcio, C. A. (2016). Prevalence of Subretinal Drusenoid Deposits in Older Persons with and without Age-Related Macular Degeneration, by Multimodal Imaging. *Ophthalmology*, 123(5), 1090–1100. <https://doi.org/10.1016/j.ophtha.2015.12.034>
- Zhang, K., & Sejnowski, T. J. (1999). Neuronal tuning: To sharpen or broaden? *Neural Computation*, 11(1), 75–84. <https://doi.org/10.1162/089976699300016809>
- Zhang, X., & Sivaprasad, S. (2021). Drusen and pachydrusen: the definition, pathogenesis, and clinical significance. *Eye*, 35(1), 121-133. <https://doi.org/10.1038/S41433-020-01265-4>
- Zhang, Y., Wang, X., Sadda, S. R., Clark, M. E., Witherspoon, C. D., Spaide, R. F., Owsley, C., & Curcio, C. A. (2020). Lifecycles of Individual Subretinal Drusenoid Deposits and Evolution of Outer Retinal Atrophy in Age-Related Macular Degeneration. *Ophthalmology. Retina*, 4(3), 274–283. <https://doi.org/10.1016/j.oret.2019.10.012>
- Zhou, H., Zhang, H., Yu, A., & Xie, J. (2018). Association between sunlight exposure and risk of age-related macular degeneration: a meta-analysis. *BMC Ophthalmology*, 18(1), 331. <https://doi.org/10.1186/s12886-018-1004-y>
- Zhu, H., Russell, R. A., Saunders, L. J., Ceccon, S., Garway-Heath, D. F., & Crabb, D. P. (2014). Detecting changes in retinal function: Analysis with non-stationary Weibull error regression and spatial enhancement (ANSWERS). *PLoS ONE*, 9(1), e85654. <https://doi.org/10.1371/journal.pone.0085654>
- Zweifel, S. A., Spaide, R. F., Curcio, C. A., Malek, G., & Imamura, Y. (2010). Reticular Pseudodrusen Are Subretinal Drusenoid Deposits. *Ophthalmology*, 117(2), 303-312.e1. <https://doi.org/10.1016/j.ophtha.2009.07.014>

8 SUPPLEMENTAL MATERIALS

8.1 SUPPLEMENTAL TABLES

Table S2.1 Search Terms for Systematic Literature Review

Search terms
"age-related macular degeneration" or "AMD" or "macular degeneration" or "macular drusen" or "age-related maculopathy"
"dark adaptation" or "dark adaptometer" or "dark adapt*" or "rod-intercept time" or "photopigment regeneration" or "photostress" or "glare recovery" or "bleach recovery"

Table S2.2 Quality assessment of included studies

A. Summary of Quality Assessment of 19 case-control studies using the CASP checklist

Study	Did the study address a clearly focused issue?	Did the authors use an appropriate method to answer their question?	Were the cases recruited in an acceptable way?	Were the controls selected in an acceptable way?	Was the exposure accurately measured to minimise bias?	Aside from the experimental intervention, were the groups treated equally?	Have the authors taken account of the potential confounding factors in the design and/or in their analysis?	Do you believe the results?*	Can the results be applied to the local population?	Do the results of this study fit with other available evidence?
Chen et al (2019)	yes	yes	can't tell	can't tell	yes	yes	yes	yes	yes	yes
Dhalla et al (2017)	yes	yes	yes	can't tell	yes	yes	yes	yes	yes	yes
Dimitrov et al (2008)	yes	yes	can't tell	yes	yes	yes	yes	yes	yes	yes
Dimitrov et al (2011)	yes	yes	can't tell	yes	yes	yes	yes	yes	yes	yes
Dimitrov et al (2012)	yes	yes	can't tell	can't tell	yes	yes	yes	yes	yes	yes
Flynn, Cukras and Jeffrey, (2018)	yes	yes	can't tell	can't tell	yes	yes	yes	can't tell	yes	yes
Fraser et al (2016)	yes	yes	can't tell	can't tell	yes	yes	yes	yes	yes	yes
Gaffney, Binns and Margrain (2011)	yes	yes	can't tell	can't tell	yes	yes	yes	yes	yes	yes
Gaffney, Binns and Margrain (2013)	yes	yes	can't tell	yes	yes	yes	yes	yes	yes	yes
Jackson, Felix and Owsley et al (2006)	yes	yes	yes	yes	yes	yes	yes	yes	yes	yes
Jackson, Clark, et al (2014)	yes	yes	can't tell	can't tell	yes	yes	yes	yes	yes	yes
Jackson and Edwards (2008)	yes	yes	can't tell	can't tell	yes	yes	yes	can't tell	yes	yes
Jackson, Scott, et al (2014)	yes	yes	can't tell	can't tell	yes	yes	yes	yes	yes	yes

Newsome and Negrerio (2009)	yes	yes	can't tell	can't tell	yes	yes	yes	yes	yes	yes	yes
Nguyen et al (2018)	yes	yes	can't tell	can't tell	yes	yes	yes	can't tell	yes	yes	yes
Rodrigo-Diaz et al (2019)	yes	yes	yes	yes	yes	yes	no	can't tell	yes	yes	yes
Rodriguez et al (2018)	yes	yes	yes	yes	yes	yes	yes	yes	yes	yes	yes
Tahir et al (2018)	yes	yes	can't tell	can't tell	yes	yes	no	yes	yes	yes	yes
Tan et al (2019)	yes	yes	can't tell	yes	yes	yes	yes	yes	yes	yes	yes
Thompson et al (2018)	yes	yes	yes	yes	yes	yes	yes	yes	yes	yes	yes

*To answer this, the questions: 'How large was the treatment effect?' and 'How precise was the estimate of the treatment effect?' were considered.

B. Summary of Quality Assessment of four cohort studies using the CASP checklist

Study	Did the study address a clearly focused issue?	Was the cohort recruited in an acceptable way?	Was the exposure accurately measured to minimise bias?	Was the outcome accurately measured to minimise bias?	Have the authors identified all important confounding factors	Have the authors taken account of confounding factors in the design and/or analysis?	Was the follow up of subjects complete enough?	Was the follow up of subjects long enough?	Do you believe the results?*	Can the results be applied to the local population?	Do the results of this study fit with other available evidence?
Owsley, Clark, et al (2016)	yes	can't tell	yes	yes	yes	yes	yes	yes	yes	yes	yes
Owsley, McGwin, et al (2016)	yes	can't tell	yes	yes	yes	yes	yes	yes	yes	yes	yes
Owsley, Clark and McGwin, (2017)	yes	can't tell	yes	yes	yes	yes	yes	yes	yes	yes	yes

Robinson et al (2019)	yes											
-----------------------	-----	-----	-----	-----	-----	-----	-----	-----	-----	-----	-----	-----

*To answer this, the question: 'How precise were the results?' was considered.

C. Summary of Quality Assessment of five randomised control trials using the CASP checklist

Study	Did the study address a clearly focused issue?	Was the assignment of patients to treatments randomised?	Were all the patients who entered the trial properly accounted for at its conclusion?	Were patients, health workers and personnel 'blind' to treatment?	Were the groups similar at the start of the trial	Aside from the experimental intervention, were the groups treated equally?	Can the results be applied to the local population?	Were clinically important outcomes considered?	all	Are the benefits worth the harms and costs?
Akuffo, Beatty, et al (2017)	yes	yes	yes	yes	yes	yes	yes	yes		yes
Owsley, McGwin, Jackson et al (2006)	yes	yes	yes	yes	yes	yes	yes	yes		yes
Richer et al (2011)	yes	yes	yes	yes	yes	yes	yes	yes		yes
Robinson et al (2018)	yes	yes	yes	no	can't tell	yes	yes	yes		no

*The question: 'How precise were the results?' was considered.

D. Quality Assessment of three case-series studies using the JBI checklist

Study	Were there clear criteria for inclusion in the case series?	Was the condition measured in a standard reliable way for all participants?	Were valid methods used for identification of the condition for all participants included?	Did the case series have consecutive inclusion of participants?	Did the case series have complete inclusion of participants?	Was there clear reporting of demographics of the participants in the study?	Was there clear reporting of clinical information of the participants?	Were the outcomes or follow up results of cases clearly reported?	Was there clear reporting of the presenting sites/clinics demographic information	Was the statistical analysis appropriate?
Luu et al (2018)	yes	yes	yes	yes	yes	yes	yes	yes	unclear	n/a
Richer et al (2013)	no	yes	no	unclear	yes	yes	yes	yes	yes	n/a
Richer et al (2014)	no	yes	yes	unclear	yes	yes	yes	yes	yes	n/a

E. Quality Assessment of 18 cross-sectional studies using the JBI checklist

Study	Were the criteria for inclusion in the sample clearly defined?	Were the study subjects and the setting described in detail?	Was the exposure measured in a valid and reliable way?	Were objective, standard criteria used for measurement of the condition?	Were confounding factors identified?	Were strategies to deal with confounding factors stated?	Were the outcomes measured in a valid and reliable way?	Was the statistical analysis appropriate?
Akuffo, Nolan, et al (2017)	yes	yes	unclear	yes	unclear	unclear	yes	yes
Beirne and McConnell (2019)	unclear	yes	yes	yes	yes	yes	yes	yes
Binns et al (2018)	yes	yes	yes	yes	yes	yes	yes	yes
Clark et al (2011)	yes	yes	yes	yes	yes	yes	yes	yes
Cocce et al (2018)	yes	yes	yes	yes	yes	yes	yes	yes

Flamendorf et al (2015)	yes	yes	yes	yes	yes	yes	yes	yes	yes
Lains et al (2017)	yes	yes	yes	yes	yes	yes	yes	yes	yes
Lains, Miller, et al (2018)	yes	yes	yes	yes	yes	yes	yes	yes	yes
Lains, Park, et al (2018)	yes	yes	yes	yes	yes	yes	yes	yes	yes
Mullins et al (2018)	yes	yes	yes	yes	yes	yes	yes	yes	yes
Neely et al (2017)	yes	yes	yes	yes	yes	yes	yes	yes	yes
Owsley, McGwin, Scilley, et al (2006)	yes	yes	yes	yes	yes	yes	yes	yes	yes
Owsley et al (2007)	yes	yes	yes	yes	yes	yes	yes	yes	yes
Owsley, Huisingh, et al (2016)	yes	yes	yes	yes	yes	yes	yes	yes	yes
Sevilla et al (2016)	yes	yes	yes	yes	yes	yes	yes	yes	yes
Wolffsohn et al (2006)	yes	yes	yes	yes	unclear	unclear	yes	yes	yes
Yazdanie et al (2017)	yes	yes	yes	yes	yes	yes	yes	yes	yes

Table S2.3 Data Synthesis Table featuring Study Characteristics

Study	Study Design	Study Aim	Study Population	AMD Severity Grading Type Used	Dark Adaptation Outcome Measures	Outcome measures directly compared to Dark Adaptation parameters	Key Dark Adaptation results
Akuffo, Nolan, et al (2017)	cross-sectional	To investigate the relationship between macular pigment and visual function in subjects with early AMD	121 participants with early AMD, aged 64.77±9.03 years	AREDS	photostress recovery time	macular pigment	Photostress recovery time was unrelated to macular pigment after controlling for age, sex and cataract grade
Akuffo, Beatty, et al (2017)	randomised clinical trial	To evaluate the impact of supplemental macular carotenoids in combination with coantioxidants on visual function in patients with nonadvanced AMD	122 participants with early AMD, aged 64.77±9.03 years	AREDS	photostress recovery time	presence of supplemental macular carotenoids	Statistically significant improvement in photostress recovery time was observed over time and was statistically comparable between interventions.
Beirne and McConnell (2019)	cross-sectional	To determine if rod-mediated dark adaptation is associated with central macular pigment levels in individuals with intermediate stage AMD.	50 participants, split into age-matched controls (23) with a mean age of 74 years and intermediate AMD (27) with a mean age of 76.7 years	International Classification and Grading System for Age-Related Macular Degeneration	rod intercept time	AMD presence and severity, macular pigment, macular pigment optical density, VA, CS	Rod-mediated dark adaptation was significantly delayed in intermediate stage AMD compared with healthy controls. There was no statistically significant correlation between the rod intercept time and the level of macular pigment in those with intermediate AMD. There was no statistically significant relationship between the rod intercept time and logMAR visual acuity

							in the intermediate AMD group; however, there was a statistically significant relationship between the rod intercept time and contrast sensitivity. The rod intercept time was higher in those individuals who had late-stage AMD in the fellow eye, compared those without late AMD in the fellow eye, but this failed to reach statistical significance.
Binns et al (2018)	cross-sectional	To determine optimal test conditions for evaluating dark adaptation in intermediate AMD in order to minimize test time while maintaining diagnostic sensitivity	26 participants, split into controls (10), early AMD (2), intermediate AMD (12) and geographic atrophy (4). Analysis on controls (aged 69±8 years) and iAMD (aged 71±8 years)	Beckman	rod intercept time	bleaching conditions	Statistically significant difference in average rod intercept time between the control and iAMD groups at 5° and at 12° following a 76% bleach. Five participants in the iAMD group had rod intercept times >20 minutes for 76% bleach at 5°, but none for any other test condition.
Chen et al (2019)	case-control	To investigate the natural history of dark adaptation function as measured by the change in rod intercept time over 4 years and to correlate the change with AMD severity	65 participants aged 71±9.3 years, split into Group 0 (34) no large drusen aged 72±8.3 years, Group 1 (9) large drusen 1 eye only aged 69±11 years, Group 2 (16) large drusen both eyes aged 67±10 years, Group 3 (5) large drusen in one eye, late AMD in other aged 77±5.4 years, Group SDD (1) with subretinal drusenoid deposits, aged 84±0 years.	AREDS, but also used categorisation: GO - no large drusen or late AMD (CNV or central geographic atrophy) in either eye. Group 1 - large drusen in 1 eye only and no late AMD in either eye. Group 2 - large drusen in both eyes without any late AMD. Group 3 - large drusen in 1 eye and late AMD in the other eye (central geographic atrophy or CNV).	rod intercept time, slope rod intercept time	AMD presence and severity, change over 4 years, best corrected VA, LLQ score, SDD presence	Higher rates of rod intercept time prolongation were correlated with AMD severity group assignment at baseline and with severity group assignments at year 4. Study eyes that developed SDD during follow-up demonstrated higher rates of rod intercept time prolongation relative to those that did not. Overall, higher rates of rod intercept time

								prolongation were significantly correlated with greater 4-year decreases in LLQ scores. Slope rod intercept time was not correlated with the change in BCVA in study eyes. Slope rod intercept time, however, increased with greater AMD severity. Slope rod intercept time and baseline AMD severity were also correlated when study eyes were Graded using an alternative 9-step AREDS severity scale. Mean slope rod intercept time for eyes in steps 4-9 was significantly greater than that for eyes in steps 1-3.
Clark et al (2011)	cross-sectional	To examine associations between retinal thickness and rod-mediated dark adaptation in older adults with non-exudative ARM or normal macular health	74 participants, aged 77±8 years, split into Group 1 (17), Group 2 (18), Group 3 (20) and Group 4 (19)	Clinical Age-Related Maculopathy Staging (CARMS) system	second slope, third slope, average threshold, final threshold	ARM presence and severity, location of GA on retina, retinal thickness	The second and third slopes were lower and average and final sensitivity decreased with increasing disease severity. The rate of dark adaptation (second and third slopes) was not different between the CARMS group 4 subgroup whereby the test target was positioned over an area of the macula that did not have GA vs the group that did. However, for those participants with the test target positioned amidst GA, their final and average rod-mediated sensitivity was significantly depressed	

							compared to those where the test target was positioned away from the GA. Furthermore, the values from the group where the target was not in the GA area were not significantly different from the CARMS group 3. Thinner retinal thickness was associated with lower average rod-mediated sensitivity and final rod-mediated sensitivity.
Cocce et al (2018)	cross-sectional	To evaluate and quantify visual function metrics to be used as predictors of AMD progression and visual acuity loss in patients with early and intermediate AMD.	101 participants, split into controls (21) aged 71.7±7.4 years, early AMD (33) aged 71.8±8.3 years, intermediate AMD (47) aged 70.4±6.9 years	AREDS	rod intercept time	AMD presence and severity	The rod intercept time was significantly different between AREDS 3 group and the controls and the AREDS 3 group and the AREDS 2 group.
Dhalla et al (2007)	case-control	To introduce a standardized macular photostress test using an automated perimeter as a method to quantify macular disease severity and as a tool to distinguish optic neuropathy from	65 participants aged 65 to 84 years, split into visually healthy (5), mild AMD (5), moderate AMD (5), severe AMD (5), no ocular disease but pseudophakic (5), moderate open angle glaucoma (5) (50 controls were used for analysis purposes from Dhalla et al (2007)).	AMD were stratified into mild, moderate, and severe groups. Patients with mild AMD had best-corrected visual acuity (BCVA) greater than 20/40 and had a maximum of 5 drusen all less than 64 µm in size. Moderate AMD was defined as BCVA less than 20/40 but greater than 20/200. Examination revealed drusen size greater than 64 µm, macular pigment changes, but no geographic atrophy. Geographic atrophy was defined per the International Age-	foveal threshold recovery time	AMD presence and severity, presence of optic nerve pathology	There was a significant delay in recovery time to baseline sensitivity in the participants with AMD. For mild AMD group, the baseline foveal threshold was statistically different to the control group. For moderate and severe AMD groups, the baseline foveal threshold was statistically different to the control group and recovery to baseline foveal sensitivity was significantly longer than the

		macular pathology.		related Maculopathy Epidemiological Study Group as being at least 175 μ m in diameter. ¹⁰ Severe AMD was defined as BCVA worse than 20/200 and geographic atrophy involving the fovea.			normal group. Optic nerve pathology does not affect the foveal response curve.
Dimitrov et al (2008)	case-control	To introduce a cathode-ray-tube monitor-based technique to isolate clinically significant components of dark adaptation and to identify abnormalities in eyes with ARM	49 participants, split into age-matched controls (22) aged 66.8 \pm 5.9 years and ARM (27) aged 67.5 \pm 5.0 years (4 with choroidal neovascularisation, 1 with geographic atrophy)	International Classification and Grading System for Age-Related Maculopathy Bird et al 1995	cone recovery rate, cone absolute threshold, rod-cone break, rod recovery rate, rod absolute threshold, rod intercept time	presence of ARM, high-risk clinical profile subgroups (drusen presence with/without pigmentary changes, AMD in fellow eye, unilateral AMD)	The parameters necessary for effective isolation of cone and early phase rod dark adaptation were a 2.6 ND filter, a 4° foveated, 200-ms, achromatic spot; ~30% pigment bleaching; and a 30-minute test duration. Cone recovery dynamics were significantly slower in the ARM group when compared with age-matched control subjects. Three of the 27 eyes with ARM did not achieve rod-cone break during the allowed duration (30 minutes). The remaining eyes with ARM exhibited a significant delay in rod recovery and the average time to rod-cone break in the ARM group was significantly longer than in the control subjects. The difference between ARM and control group's average cone absolute thresholds was statistically significant. Study eyes with drusen and no pigment change were no different from those that had

							both drusen and pigment change. Study eyes with an AMD fellow eye showed a non-significant trend for slower recovery compared with cases with bilateral ARM. The cases with unilateral AMD also showed a non-significant trend for slower rod-cone break.
Dimitrov et al (2012)	case-control	To investigate the relationship between clinical macular changes and retinal function in AMD	357 participants, split into controls (64) aged 69.16±11.35 years and AMD participants classified into 12 subgroups (293): Group 2 (59) aged 72.09±11.3 years, Group 3 (12) aged 75.06±9.07 years, Group 4 (24) aged 61.97±10.52 years, Group 5 (26) aged 72.04±9.59 years, Group 6 (12) aged 73.33±10.22 years, Group 7 (20) aged 69.04±14.39 years, Group 8 (27) aged 73.76±9.55 years, Group 9 (12) aged 74±6.09 years, Group 10 (14) aged 76.05±9.94 years, Group 11 (17) aged 73.8±11.51 years, Group 12 (14) aged 73.86±9.68 years and Group 13 (56) aged 76.37±8.98 years.	International Classification and Grading System for Age-Related Maculopathy Bird et al 1995	cone recovery rate, rod recovery rate	AMD presence and severity	Both cone recovery rate and rod recovery rate parameters were significantly abnormal when only hard and/or intermediate drusen were evident compared to controls and yielded considerably worse outcomes in cases with more advanced fundus changes, but provided limited ability to discriminate between these cases. Groups 4 and 5 had the worst outcomes across both tests. Group 5 was significantly different from the Group 2 on both measurements, as did Group 4. Group 3 revealed significant functional abnormality when compared to controls for both cone recovery rate and rod recovery rate. Group 2 was significantly different to the control group for both tests. There were no significant differences between groups

									with pigmentary changes (Group 6 vs. Group 7 vs. Group 8). Group 9 did not significantly differ compared to remaining groups Group 10 values were not different from combined groups 4 and 5 and versus combined groups 7 and 8. Lastly, Group 11, 12 and 13's recovery rates were significantly worse than the control group but could not be differentiated between the remaining AMD groups.
Dimitrov et al (2011)	case-control	To evaluate the potential of psychophysical assessments of retinal function to provide diagnostic biomarkers of early AMD	330 participants, split into controls (109) aged 73.07±10.32 years and early AMD (221) aged 72.86±9.94 years. Early AMD was split into: Both eyes = soft drusen (no pigmentary changes) (58) aged 68.73±10.09 years, study eye = soft drusen and pigmentary changes and fellow eye = soft drusen with/without pigmentary changes (71) aged 72.25±10.32 years, study eye = reticular drusen with or without intermediate drusen and fellow eye = CNV (8) aged 71.95±10.67 years, study eye = soft drusen (no pigmentary changes) and fellow eye = GA and/or CNV (13) aged 72.47±10.87 years, study eye = soft drusen and pigmentary changes and fellow eye - GA and/or CNV (71) aged 76.60±07.81 years	International Classification and Grading System for Age-Related Maculopathy Bird et al 1995	cone recovery rate, cone absolute threshold, rod-cone break, rod recovery rate, rod absolute threshold, rod intercept time	between adaptation parameters	dark	All dark adaptation measurements were significantly worse, on average, in the AMD group than in the control group. There were significant correlations between rod-cone break and the rod recovery rate and with rod recovery rate and the rod criterion time. There was a smaller yet still significant correlation between rod-cone break and cone absolute threshold. Static and dynamic parameters showed weak correlations.	

Flamendorf et al (2015)	cross-sectional	To investigate whether ocular and person-based characteristics are associated with dark adaptation measured using the AdaptRx™ device	116 participants, split into Group 0 (42) with no large drusen in either eye, aged 74.8±8.8 years, Group 1 (13) large drusen in the study eye only, aged 71.8±10.8 years, Group 2 (31) large drusen in both eyes, aged 71.8±9.8 years, Group 3 (15) advanced disease in the non-study eye, aged 76.5±8.3 years, Group RPD (15) 1 RPD participant with no large drusen in either eye, 6 RPD participants with large drusen in both eyes, and 8 participants had advanced AMD in their fellow eye, aged 80.9±7.3 years	The control group, Group 0 consists of participants without any large drusen or advanced AMD (CNV or central GA) in either eye. Group 1 consists of participants with large drusen in one eye only and no late AMD in either eye. Group 2 includes participants with large drusen in both eyes without any late AMD. Group 3 includes participants with large drusen in one eye and late AMD in the other eye (either GA or CNV). In addition, colour fundus images (described below) of both eyes of participants were Graded for the presence of large drusen, pigmentary changes, and late AMD (in the fellow eye) to calculate a simplified severity score for each participant using AREDS	rod intercept time	AMD severity, RPD presence, BCVA, replaced lens, choroidal thickness, age	Increased rod intercept time was significantly associated with increasing age, decreasing BCVA, pseudophakia, decreasing subfoveal choroidal thickness. Study eyes with RPD had a significantly greater mean rod intercept time compared to eyes without RPD in any AMD severity group with 80% reaching the DA test ceiling.
Flynn, Cukras and Jeffrey, (2018)	case-control	To examine spatial changes in rod-mediated function in relationship to local structural changes across the central retina in eyes with a spectrum of AMD disease severity	42 participants, split into Group 0 (8) study eye = no drusen>125um, fellow eye = no drusen >125um, aged 76±8 years, Group 1 (7) study eye = drusen >125um, fellow eye = no drusen aged 67±10 years, Group 2 (12) study eye = drusen>125um, fellow eye = drusen>125um, aged 69±11, Group 3 (9) study eye = drusen >125um, fellow eye = advanced amd, wet/dry, aged 72±9, Group SDD (6) study eye subretinal drusenoid deposits, aged 77±10	The control group, Group 0 consists of participants without any large drusen or advanced AMD (CNV or central GA) in either eye. Group 1 consists of participants with large drusen in one eye only and no late AMD in either eye. Group 2 includes participants with large drusen in both eyes without any late AMD. Group 3 includes participants with large drusen in one eye and late AMD in the other eye (either GA or CNV). In addition, colour fundus images (described below) of both eyes of participants were Graded for the presence of large drusen, pigmentary changes, and late AMD (in the fellow	rod intercept time, slope rod intercept time	AMD severity, SDD presence	Dark adaptation was slowed at all loci with SDD or EZ band disruption, and at 32% of loci with no local structural changes. Across AMD groups, there were more points that did not reach criterion in group 3 and SDD (25%) than in groups 0 to 2 (<1%). The superior SDD had a considerably higher number (1.5- to 3-fold) of loci where rod intercept time could not be derived compared with the inferior retina. There was a significant effect of both AMD and eccentricity on rod

				eye) to calculate a simplified severity score for each participant using AREDS			intercept time. There was a significantly longer mean rod intercept time for the SDD group relative to the control group at 4°, 6°, and 8° eccentricity. For all AMD groups, mean rod intercept time increased as a function of decreasing retinal eccentricity. Rod intercept time slope increased as a function of AMD severity. There was a significantly higher mean rod intercept time slope for the SDD group relative to groups 0, 1, and 2; group 3 rod intercept time slope was also significantly greater than for group 0.
Fraser et al (2016)	case-control	To determine the feasibility of using a dark-adapted chromatic perimeter to obtain dark-adapted static and dynamic rod function at multiple retinal locations, and compare these functional parameters between subjects with intermediate AMD and normal controls	30 participants, split into controls (8) aged 67.6±5.5 and intermediate AMD (22) 71.5±6.8 (6 of the 22 AMD eyes had reticular pseudodrusen)	AREDS	rod intercept time	AMD presence	Compared to the control eyes, AMD eyes had an increased in rod intercept time. The region within the central 6° appeared to be the most defective and AMD eyes with RPD seemed to have worse function than eyes without.

Gaffney, Binns and Margrain (2011)	case-control	To quantify the diagnostic potential of cone dark adaptation as a function of retinal eccentricity and compared this with the diagnostic potential of the time to the rod-cone-break	20 participants, split into controls (10) aged 70.0±4.7 years and ARM (10) aged 68.3±7.3 years. ARM split into early ARM (8) and intermediate ARM (2)	AREDS	cone time constant, rod-cone break, cone absolute threshold	AMD presence	Cone time constant of recovery was significantly longer for the ARM group at 2°, 7°, and 12° from fixation, with the greatest significant difference observed at 12°. At this location, the rod-cone break was also significantly different between groups. There were no significant differences in final cone threshold between control and ARM groups for any of the locations studied.
Gaffney, Binns and Margrain (2013)	case-control	To identify the pre-adapting light intensity that generates the maximum separation in the parameters of dark adaptation between participants with early AMD and healthy control participants in the minimum recording time	20 participants, split into controls (10) aged 74.5 (72.3–75.8) years and early AMD (10) aged 73.5(66.5–76) years	International Classification and Grading System for Age-Related Maculopathy Bird et al 1995	cone time constant, rod-cone break, cone absolute threshold	AMD presence, different pre-adapting bleaching intensities	There were significant differences between those with early AMD and controls in cone time constant of recovery and time to rod-cone break at all pre-adapting 'bleaching' intensities.
Jackson, Clark, et al (2014)	case-control	To evaluate whether significant changes in dark adaptation speed could be detected in participants with early to intermediate AMD	32 participants, split into controls (6) aged 65±2 years and AMD (26) aged 71±6 years. AMD was split into Grade 1 (6), Grade 2 (4), Grade 3 (1), Grade 4 (6), Grade 5 (2), Grade 6 (5), Grade 7 (2), Grade 8 (4) and Grade 9 (2)	AREDS	rod intercept time	AMD presence, changes in 12 months	Among AMD subjects, there was a moderate positive correlation between rod intercept time at baseline and disease severity. Rod intercept time was significantly slower for the AMD group than the normal

								at 12 months following baseline dark adaptation measurement	group at each visit. However, the AMD group as a whole did not exhibit significant slowing of DA over 12 months, significant progression of rod intercept time occurred in 5 of 26 (19%) participants. These participants did not progress on AREDS severity step or have a greater than eight-letter change in VA after 12 months. The normal group exhibited stable, mean rod intercept time during the observation period.
Jackson, Felix and Owsley et al (2006)	case-control	To evaluate whether the Scotopic Sensitivity Tester-1 (SST-1) detects early ARMD as defined by fundus appearance.	48 participants, split into young adult controls (12) mean age 23.3 years, old adult controls (17) mean age 69.2 years and early ARMD (19) mean age 74.4 years	WARMGS	rod-cone break, dark adaptation duration, absolute threshold	ARMD age	presence,		The older control group's absolute thresholds were not significantly different to the younger group and the ARMD group. However, the older control group exhibited significantly slower rod-cone break times and dark adaptation duration compared with the younger control group. Although, there was no significant difference when compared to the ARMD group. There was a significant difference between the younger control group and the ARMD group absolute threshold values, rod-cone break time and dark adaptation duration.

Jackson, Scott, et al (2014)	case-control	To evaluate a rapid dark adaptation test (≤6.5 minutes) for the detection of AMD.	148 participants, split into controls (21) mean age 65 (52, 81) years and AMD (127) mean age 73 (51, 93) years. AMD split into early AMD (41), intermediate AMD (72) and advanced (GA or wet) AMD (14)	AREDS	rod intercept time	AMD presence and severity, age	Abnormal DA was detected in 115 of 127 AMD patients, and normal DA was found in 19 of 21 normal adults. For the bleaching intensity used in this study, most normal subjects exhibited a linear sensitivity recovery, lacking distinct cone-mediated features while subjects with early and intermediate AMD typically exhibited a cone plateau and rod-cone break. Subjects with advanced AMD often exhibit minimal or no rod recovery for 20 minutes. The rapid test and the extended test exhibited a significant correlation between rod intercept time and increasing disease severity. There was no significant effect of aging on the rod intercept time which suggests that aging is not a confounding factor for the rapid protocol.
Jackson and Edwards (2008)	case-control	To develop and evaluate a short-duration dark adaptation protocol	26 participants, split into young controls (8) mean age 32.6 years, old controls (9) mean age 73.1 years and ARM (19) mean age 75.1 years	AREDS	rod intercept time	AMD presence, age	ARM patients exhibited substantially slower DA compared with normal old adults; whereas the DA speed was essentially the same for the young and old normal participants. The upper limit of the normal reference range was 12.5 minutes. Individuals with rod

							intercepts longer than 12.5 minutes were classified as having impaired DA. 15 of the 17 ARM patients were classified as having abnormal DA for a diagnostic sensitivity of 88%. All nine normal adults fell within the normal reference range for a diagnostic specificity of 100%.
Lains et al (2017)	cross-sectional	To examine the relationship between dark adaptation and optical coherence tomography - based macular morphology in AMD	137 participants, split into controls (38) mean age 66.1±7.7 years and AMD (99) mean age 8.8±6.4 years. AMD was split into early AMD (22), intermediate AMD (64) and late AMD (13). The late AMD group can be split into, geographic atrophy (6) and neovascular AMD (7)	AREDS	rod intercept time	AMD presence and severity, age, lens status, different oct protocols (edi using 97 lines and edi using 61 lines), structural abnormality presence (ellipsoid disruption, SDD, classic drusen, atrophy, serous ped, hyperreflective foci, subretinal fluid, intraretinal fluid, choroidal neovascularisation, fibrosis, outer retinal tubulations), reduced mean retinal thickness presence, inability to reach testing time	After adjusting for age and AMD stage, the presence of any abnormalities within the DA testing spot as well as any abnormalities in the macula, were significantly associated with delayed rod intercept times and therefore impaired DA. In eyes with no structural changes within the DA testing spot, the presence of any abnormalities in the remaining macula was still associated with delayed rod intercept times. Presence of SDD and ellipsoid zone disruption were a consistent predictor of rod intercept time, whether located within the DA testing spot or anywhere in the macula. Within the testing spot, the presence of classic drusen or serous pigment epithelium detachment was also significantly associated with impairments in DA.

Lains, Park, et al (2018)	cross-sectional	To study the association between peripheral changes in AMD and dark adaptation	128 participants, split into controls (32) mean age 65.9±7.8 years and AMD (96) mean age 68.9±6.4 years. The AMD group can be split into early AMD (9), intermediate AMD (64) and late AMD (13)	AREDS	rod intercept time	presence of peripheral classic drusen, reticular pigmentary changes, peripheral atrophic changes, fundus autofluorescence patterns	The presence of reticular pigmentary changes in the midperipheral and far-peripheral zones was associated with delayed rod intercept times, even after adjusting for confounding factors. The presence, number, and extent of peripheral classic drusen did not show a similar association. The presence of a mottled decreased FAF pattern in the midperipheral zone was also associated with prolonged rod intercept times.
Lains, Miller, et al (2018)	cross-sectional	To determine the association between dark adaption and different health conditions linked with AMD	78 participants, split into controls (19) mean age 66.1±7.7 years and AMD (96) mean age 68.9±6.5 years. The AMD group can be split into early AMD (14), intermediate AMD (34) and late AMD (11)	AREDS	rod intercept time	AMD presence and severity, age, lens status, worst BCVA, diagnosis of heart failure, family history of AMD, taking AREDS vitamins, other multivitamins, other NSAIDs, statins, anticoagulants, bmi, alcohol consumption, autoimmune diseases, presence of drusen, food frequency questionnaire, Rapid Assessment	AMD stage was highly associated with increased rod intercept time. Although there was no significant difference between early AMD and controls, a significant association was observed between controls, intermediate and late. Age, worst BCVA, pseudophakia, diagnosis of heart failure, taking AREDS or other multivitamins and family history of AMD were also significantly associated with delayed rod intercept time. After accounting for age and AMD stage, Body mass index, taking AREDS vitamins, and family history of AMD were

						of Physical Activity questionnaire	significantly associated with worse rod intercept time. Abnormal DA (rod intercept time ≥ 6.5 minutes) was significantly associated with family history of AMD, taking AREDS supplements and alcohol intake.	
Luu et al (2018)	cross-sectional, case-series	To determine rod functional recovery profiles after prolonged dark adaptation in eyes with AMD and reticular pseudodrusen	6 participants with intermediate AMD and RPD, aged 69-79 years	Beckman		rod intercept time	AMD severity, test loci	All cases had delayed rod intercept time at many retinal locations, with test points within the central 6° most affected. The rod intercept time was variable between retinal loci and between subjects, although RPD were present at all test locations. In 5 cases with stage 3 RPD, rod function recovered at all tested locations, but many locations took hours to do so. The case with stage 4 RPD had locations that failed to recover even after 24 hours of DA.
Mullins et al (2018)	cross-sectional	To examine the association between sequence variants in genetic risk factors for AMD and delayed rod-mediated dark adaptation, the first functional biomarker for incident AMD, in older adults with	543 participants with a mean age of 69.3±6 years, split into controls (408), early AMD (124), intermediate AMD(10) and non-central GA (1)	AREDS		rod intercept time	genotypes CFH and ARMS2 (heterozygous and high-risk), AMD presence and severity	For the combined sample, significantly delayed rod intercept time was observed for both the A69S variant in ARMS2 and the Y402H variant in CFH. For healthy participants, the A69S variant in ARMS2 was significantly associated with delayed rod intercept time, whereas the Y402H variant in CFH was not. For AMD patients, the

		normal macular health and early AMD					A69S variant of ARMS2 and the Y402H variant of CFH were significantly associated with delayed rod intercept time. Those with a larger number of high-risk ARMS2 and CFH alleles showed significantly higher rod intercept time, in both healthy and AMD groups.
Neely et al (2017)	cross-sectional	To examine the association between subretinal drusenoid deposits identified by multimodal retinal imaging and visual function in older eyes with normal macular health or in the earliest phases of AMD	1202 participants with a mean age of 69.4(60-92) years, split into controls (958) further split into controls with SDD (185) and controls without SDD (773) and early AMD (244) further split into AMD with SDD (115) and AMD without SDD (129)	AREDS	rod intercept time	SDD presence	In normal eyes SDDs were not associated with impaired rod intercept time. In eyes with early AMD, rod intercept time was markedly delayed in eyes with SDDs versus no SDDs. However this association was no longer significant after age adjustment.
Newsome and Negrerio (2009)	case-control	To determine the safety, sensitivity, and specificity of a novel flash photorecovery timing instrument with response verification in differentiating normal from abnormal maculae, and in detecting worsening macular disease	391 participants, split into controls (144) aged 15-4 years, small drusen only (57), dry AMD (118), wet AMD with subretinal fluid (19) and without subretinal fluid (17), diabetics with background retinopathy with macular oedema (19) and without macular oedema (17) (age not given for remaining groups)	Age-related macular degeneration (AMD) was said to be present if the best corrected acuity was worse than 20/25 (47 or fewer letters correct) and there were visible, typical drusen present within one disc diameter of the foveal centre. Geographic atrophy was noted when present in the dry AMD subjects. Eyes with macular changes such as blood, fluid, lipid, and scarring from wet AMD were tested if the acuity was 20/400 equivalent (at least 2 letters correct) or better.	photostress recovery time	AMD presence and severity, diabetic retinopathy presence, age	Photorecovery lengthened after age 55, nearly doubling that of young subjects by age 80. Macular oedema, serous macular detachment, or worsened dry AMD were accompanied by significantly prolonged photorecovery. When abnormal new vessels or retinal thickening appeared in three serially followed patients, photorecovery at least doubled. In all three,

								photorecovery prolongation occurred without clinical symptoms. None of the 499 tested subjects reported adverse events due to the flash testing.
Nguyen et al (2018)	case-control	To investigate the longitudinal changes in retinotopic rod function in eyes with intermediate AMD	26 participants, split into controls (6) with a mean age of 65.8(63.3–69.0) years and intermediate AMD (20) with a mean age of 72.3(69.2–76.8) years. The intermediate AMD group can be further split into with RPD (6) and without (14)	Beckman	rod intercept time	AMD presence and severity, RPD presence		Significantly declined rod intercept time was found in eyes with iAMD, but there was no significant change in the mean rod intercept time between baseline and follow-up visits in controls. Approximately 25% of test points in iAMD eyes showed a significant increase in rod intercept time over the 12-month period. There was also a significant increase in the number of eyes failing to reach rod intercept time at 20 minutes compared to baseline. Sub-analysis comparing iAMD eyes with and without RPD showed that eyes without RPD had a greater proportion of test points with an increased rod intercept time at follow-up (30%) compared to eyes with RPD.
Owsley, McGwin, Scilley, et al (2006)	cross-sectional	To develop a questionnaire for assessing self-reported visual problems under low luminance and	126 participants with a mean age of 71.5±8.7 years (included in DA testing), split into controls (41), early ARM (45), intermediate ARM (19), advanced ARM (16) and ARM of undetermined severity (5)	AREDS	cone time constant, cone absolute threshold, rod-cone	LLQ subscales		Rod-mediated parameters of dark adaptation were significantly associated with LLQ subscale scores while cone-mediated parameters were not.

		at night for use in studies on ARM			break, rod slope, rod absolute threshold		
Owsley, McGwin, Jackson et al (2006)	randomized clinical trial	To examine the effect of a short course of high-dose retinol (preformed vitamin A) on dark adaptation in older adults with normal retinal health or early ARM	104 participants with AMD, split into the intervention group (52) with a mean age of 71.8±9.3 years and the placebo group (52) with a mean age of 71.7±8.1 years. The intervention group can split into controls (22), early ARM (25) and intermediate ARM (5). The placebo group can be split into controls (19), early ARM (20) and intermediate ARM (13)	AREDS	cone time constant, cone absolute threshold, rod-cone break, rod slope, rod absolute threshold	with and without vitamin A intervention, and LLQ subscales	The parameters of cone time-constant, cone threshold, rod-cone break, and rod threshold did not differ between the intervention group and placebo group. However, the intervention group had significantly larger rod slopes, indicating faster sensitivity recovery, than did the placebo group. Those who had the most self-reported change on the mobility subscale at day 30 were more likely to have greater change in the speed of dark adaptation, as indicated by the rod slope parameter.
Owsley et al (2007)	cross-sectional	To examine impairment in cone- versus rod-mediated dark adaptation in the parafovea of persons with ARM	126 participants, split into controls (43) with a mean age of 68.7±7.0 years, early AMD (45) with a mean age of 72.5±9.0 years, intermediate AMD (21) with a mean age of 75.9±9.4 years and advanced AMD (17) with a mean age of 68.8±7.1 years. The advanced AMD group can be split into choroidal neovascularisation (12) and geographic atrophy (5).	AREDS	cone time constant, cone absolute threshold, rod-cone break, rod slope, rod absolute threshold	AMD presence and severity	ARM patients had significant impairments in rod-cone break, rod slope, rod sensitivity compared to controls, which were increasingly abnormal as disease severity increased. Cone time constant and cone sensitivity were not impaired across all groups and ARM severity.
Owsley, Huisin, et al (2016)	cross-sectional	To compare the ability of several visual functional	640 participants, split into controls (1007 eyes) with a mean age of 68.8±5.7 years and early AMD (253	AREDS	rod intercept time	AMD presence and severity	Adjusting for age and gender, early AMD eyes had two times the odds of having

		tests in terms of the strength of their associations with the earliest phases of AMD	eyes) with a mean age of 71.1±7.0 years				delayed rod intercept time than eyes in normal macular health.
Owsley, McGwin, et al (2016)	cohort	To examine whether slowed rod-mediated dark adaptation in adults with normal macular health at baseline is associated with the incidence of AMD 3 years later	325 participants, split into normal dark adaptation (263) with a mean age of 67.1±5.2 years and abnormal dark adaptation (62) with a mean age of 71.0±5.1 years	AREDS	rod intercept time	changes in AMD presence	After adjustment for age and smoking, those with abnormal DA in the tested eye at baseline were approximately 2 times more likely to have AMD in that eye by the time of the follow-up visit, compared with those who had normal DA at baseline.
Owsley, Clark, et al (2016)	cohort	To examine associations between impaired visual function tests and incident AMD 3 years later	467 visually healthy participants with a mean age of 68.7±5.8 years	AREDS	rod intercept time	AMD incidence	The mesopic acuity association was slightly weaker than the association between abnormal dark adaptation and incident AMD found in Owsley et al (2016) (3)
Owsley, Clark and McGwin, 2017	cohort	To characterize the natural history of rod-mediated dark adaptation over 2 years in eyes with intermediate AMD	30 participants with intermediate AMD. 1 was aged between 50-59 years, 4 were aged between 60-69 years, 18 were aged between 70-79 years and 7 were aged between 80-89 years. The fellow eye of the participants can be split into intermediate AMD (9) and advanced AMD (21). The participants with advanced AMD in the fellow eye can further be split into choroidal neovascularization (16), geographic atrophy (2) or both (3).	AREDS	rod intercept time	change over 24 months, AMD risk factors	Mean change in rod intercept time over 24 months for 30 eyes was 10.5 minutes; 73.3% of eyes had a rod intercept time increase >1 minute, 56.7% had an increase >3 minutes, and 36.7% had an increase >6 minutes; for 26.7% rod intercept time was unchanged (0- to 1-minute increase) or decreased. Greater increase in rod intercept time over 24 months was associated with smoking.

Richer et al (2011)	randomized clinical trial	To evaluate whether dietary supplementation with the carotenoid zeaxanthin raises macula pigment optical density and has unique visual benefits for patients with early atrophic AMD	60 participants with early and moderate AMD, with a mean age of 74.9±10 years, split into 8mg zeaxanthin Group (25), 8mg zeaxanthin plus 9mg lutein Group (25) and 9mg lutein Group (10)	AREDS	glare recovery time	use of dietary supplementation with zeaxanthin	Glare recovery improvement was significant for lutein and particularly the combined lutein plus carotenoid zeaxanthin group with only a trend for improvement with the carotenoid zeaxanthin subgroup.
Richer et al (2013)	case study	A case study of robust improvement of retinal structure and function using an OTC oral resveratrol based nutritional supplement called Longevinex®	3 participants with advanced AMD, split into an 86 year old male with dry AMD, 88 year old female with bilateral wet AMD and 75 year old with wet AMD in one eye and dry in other.	Did not say	cone recovery time	changes over 12 weeks	improvements seen in photo-stress glare recovery
Richer et al (2014)	case study	A case study of long term (two to three year) clinical efficacy of using an OTC oral resveratrol based nutritional supplement called Longevinex®	3 participants with advanced AMD, split into a 64 year old male with atrophic AMD , 89 year old with atrophic AMD and 67 year old with polypoidal choroidal vasculopathy	Did not say	cone recovery time	changes over 2-3 years	improvements seen in photo-stress glare recovery
Robinson et al (2018)	randomized clinical trial	To investigate the safety, acceptability, and effectiveness of light therapy on the progression of	50 participants with early AMD in one eye and neovascular AMD in the fellow eye, split into the control group (29) with a mean age of 77.00±7.02 years and the intervention group (21) with a	AREDS	cone recovery time	changes over 12 months	A significantly larger delay in cone adaptation was observed in the intervention group than in the control group over the follow-up period.

		AMD over 12 months	mean age of 78.43±7.03 years. The control group can be further split into Grade 2 (9), Grade 3 (8) and Grade 4 (12) and the intervention group can be split into Grade 2 (6), Grade 3 (9) and Grade 4 (6)				
Robinson et al (2019)	cohort	To evaluate the ability of visual function and structural tests to identify the likely risk of progression from early/intermediate to advanced AMD, using the Age-Related Eye Disease Study (AREDS) simplified scale as a surrogate for risk of progression. The secondary aim was to determine the relationship between disease severity Grade and the observed functional and structural deficits.	100 participants, split into controls/Grade 0 (19) aged 69.58±8.73 years, Grade 1 (21) aged 7.33±6.44 years, Grade 2 (18) aged 76.56±8.29 years, Grade 3 (23) aged 78.65±6.52 years and Grade 4 (19) aged 77.74±5.37 years	AREDS Simplified Scale	cone time constant	AMD severity, age,	Significant relationships with age were found in control participants for cone time constant. Cone time constant was found to be an independent predictor of increased risk of AMD progression. Mean cone time constant values were significantly lower in grade 0 than grades 1 and 3.
Rodriguez et al (2018)	case-control	To identify parameters from cone function and recovery after photostress that detect functional deficits in early	29 participants, split into young participants (8) with a mean age of 21.8±1.3 years, older participants (9) with a mean age of 66.1±5.6 years and AMD group (12) with a mean age of 70.2±5.8	AREDS	baseline cone sensitivity and cone recovery half-life	AMD presence, age	The mean baseline cone threshold was significantly worse in subjects with early AMD compared to older normal subjects. The cone intercept parameter was not significantly different

		non-exudative AMD and to determine the repeatability of these parameters					between AMD and older normal subject groups. Cone recovery half-life was significantly different between older normal and AMD subject groups. Cone function parameters were significantly different for any group at the 1-year follow-up.
Rodrigo-Diaz et al (2019)	case-control	To describe the extent to which scotopic and photopic measures of visual function predict colour fundus photograph and fundus autofluorescence changes in early and intermediate nonexudative AMD.	69 participants, split into controls (13) with a mean age of 67.77±9.72 years and AMD patients with a mean age of 73±12.98 years	AREDs simplified severity scale	cone threshold, rod-cone break, cone time constant, slope 2 and rod-rod break	AMD severity, FAF category, CFP grade	There were statistically significant effects in slope 2 in patients having intermediate or large drusen compared with healthy normal subjects. In the autofluorescence images, statistically significant differences are evident in patients with focal or patchy FAF patterns and the other FAF category compared with normal subjects. There were strong associations between the fundus photograph, AMD grade, and all DA parameters apart from cone time constant. Of all DA parameters, slope 2 best predicted fundus grading. Similarly, slope 2 showed the strongest association with the severity of FAF changes. It is clear that other DA parameters, notably the rod-rod break (β -point), also predicted the FAF grading. Regarding the photopic DA

								parameters, the highest association was between cone-rod break and fundus photograph grade. Cone-rod break and FAF categories showed correlation. Correspondingly, there were significant differences in rod-cone break between normal subjects and patients in the large drusen group, and this applies to both FAF and CFP. Cone threshold also exhibited a moderate correlation with CFP and FAF, whereas cone time constant did not appear to have a relationship either with CFP or FAF.
Sevilla et al (2016)	cross-sectional	To evaluate relationships between AMD morphology on spectral domain optical coherence tomography and visual function	91 participants, split into No Apparent retinal ageing (15) with a mean age of 66.1±5.1 years, normal ageing (15) with a mean age of 66.9±6 years, early AMD (15) with a mean age of 68.9±5.7 years and intermediate AMD (46) with a mean age of 71.3±6.8 years	Beckman		rod intercept time	AMD presence and severity, presence of SDD, SDOCT volumes	After adjusting for age, there was no difference in rod intercept time between groups. Delayed rod intercept time correlated with lower RPE-drusen-complex volume and greater RPE-drusen-complex abnormal thinning volume. No other retinal volume variables were related to rod-mediated dark adaptation. In eyes with SDD compared to eyes without SDD, rod intercept time was longer. Larger rod intercept times were associated with hyperreflective foci.
Tahir et al (2018)	case-control	To test different stimulus locations	65 participants, split into controls (15) with a mean age of 67.2±9.13	AREDS		cone absolute	stimulus location, AMD presence	There were strong location effects for the healthy group

		to investigate cone function and its relation to rod abnormalities	years and early AMD (50) with a mean age of 73.8±7.29 years		threshold, rod-cone break, second slope, the transition from the second slope to third slope		and the AMD group. Cone threshold was higher for the outer compared with the inner stimulus, slope 2 was steeper for outer compared with inner, α was shorter for outer, and β was shorter for outer than inner.
Tan et al (2019)	case-control	To evaluate rod function longitudinally in intermediate age-related macular degeneration subjects with reticular pseudodrusen and without RPD.	48 participants, split into controls (23), with a mean age of 66.1±9 years, AMD (12) with a mean age of 71.3±8.7 years and RPD (13) with a mean age of 75±7.2 years.	Beckman	rod intercept time and rod recovery time	changes over 12 months, AMD and RPD presence, stimulus location	The average RIT was significantly different between control and AMD groups, AMD and RPD groups, and control and RPD groups both at baseline or 12 months follow-up. At baseline, the rod recovery rate of each ring eccentricity was significantly different between all study groups. Over 12 months, the rod recovery rate for control and RPD groups remained stable, while the AMD group deteriorated, but only at 12°. The RIT was stable in AMD and RPD groups but improved in the control group.
Thompson et al (2018)	case-control	To determine whether Low Luminance Questionnaire scores are associated with objective measures of visual function in early	101 participants, split into controls (21) with a mean age of 71.1±7.4 years, early AMD (33) with a mean age of 71.8±8.26 years and intermediate AMD (47) with a mean age of 70.4±6.85 years	AREDS	rod intercept time	AMD severity, LLQ subscales	LLQ composite scores were significantly associated with rod intercept times, although this was no longer seen when adjusted for AMD status.

		and intermediate AMD					
Wolffsohn et al (2006)	cross-sectional	To assess the repeatability of Eger macular stressometer measures of photostress recovery and determine their association with other measures of visual function	156 participants with a mean age of 78.96±6.64, split into bilateral exudative AMD (90), bilateral atrophic AMD (19) or both (47)	Did not say	photostress recovery time	AMD severity, distance/near VA, CS, presence of central visual defect, questionnaire on self-reported difficulties with glare recovery	The average EMS recovery time was 11.0 (SD 8.9) seconds, decreasing by 1.6 (5.2) seconds on repeated measurement. EMS photostress recovery was not correlated with visual function measures or subjective difficulties with lights. EMS photostress recovery time did not predict those whose vision decreased over the following year compared with those among whom it remained stable
Yazdanie et al (2017)	cross-sectional	To investigate whether responses on a Low Luminance Questionnaire in patients with a range of AMD severity are associated with their performance on focal dark adaptation testing and with choroidal thickness	113 participants, split into controls (41) with a mean age of 72.5±8.4 years, Group 1 (13) with a mean age of 70.5±10.6 years, Group 2 (30) with a mean age of 70.8±9.7 years, Group 3 (15) with a mean age of 75.3±8.4 years and Group RPD (14) with a mean age of 79.3±7.7 years	The control group, Group 0 consists of participants without any large drusen or advanced AMD (CNV or central GA) in either eye. Group 1 consists of participants with large drusen in one eye only and no late AMD in either eye. Group 2 includes participants with large drusen in both eyes without any late AMD. Group 3 includes participants with large drusen in one eye and late AMD in the other eye (either GA or CNV). In addition, colour fundus images (described below) of both eyes of participants were Graded for the presence of large drusen, pigmentary changes, and late AMD (in the fellow eye) to calculate a simplified severity score for each participant using AREDS	rod intercept time	AMD severity, presence of RPD, LLQ subscales	Lower scores on all LLQ subscales were correlated with longer rod intercept time. The strongest association was the LLQ subscale of driving with rod intercept time. Multivariable analysis for each of the LLQ subscale outcomes, adjusted for age, included rod intercept time, with total LLQ score, "driving," "extreme lighting," and "mobility" also including choroidal thickness. In all multivariable analyses, rod intercept time had a stronger association than choroidal thickness. There were significant differences in the mean rod intercept time

between the AMD groups. Most significant differences in rod intercept time were seen in the RPD group with 80% reaching the test ceiling.²³ The mean RIT of groups 2 and 3 was significantly longer than of group 0.

			Germany) with a low- pass glass dichroic filter											
Beirne and McConnell (2019)	AdaptDx	rod intercept time	505nm photoflash of 1.8 x 10 ⁴ cd/m ² s intensity), equivalent to 76% bleaching level for rods, 4° area of the retina centred at 5° on the inferior visual meridian	0.8 millisecond s	2° diameter, 505nm circular test spot, started immediatel y	≥6mm diameter with 0.5% tropic amide	5° on the inferior visual meridian	3-down/1- up modified staircase threshold estimate procedure	45	5x10 ⁻³ cd/m ² (a decrease of 3 log units)	yes	All individuals had a fixation loss of less than 35 per cent (average fixation loss was 14.7 per cent)	no	
Binns et al (2018)	AdaptDx	rod intercept time	5 protocols: (76%) 1.8 x 10 ⁴ @ 5 degrees inferior, (70%) 5.8 x 10 ³ @ 5 degrees inferior, (65%) 2.4 x 10 ³ @ 5 degrees inferior, (76%) 1.8 x 10 ⁴ @ 12	80 millisecond s	2° diameter, 505nm circular test spot, 15 seconds after the bleaching onset	The adaptomet er measures and adjusts for pupil diameter, hence pupil dilation was not required prior to testing	subtended 4° and was centred at either 5° or 12° inferior	3-down/1- up modified staircase threshold estimate procedure	30	unclear	yes	if error exceeded 30%, the test was deemed unreliable	no	

			degrees inferior, (70%) 5.8 x 10 ³ @ 12 degrees inferior										
Chen et al (2019)	AdaptDx	rod intercept time, slope rod intercept time	82% bleach, subtending 4°, was centred at 5° on the inferior vertical meridian, 6.38 log scot Td second-1 intensity. A 12° modified bleach procedure was also used for a subset of participants.	0.25 milliseconds	1.7° diameter, 500nm circular test spot, initial intensity was 5 cd/m ²	study eye is dilated but not specified how	5° on the inferior visual meridian	3-down/1-up modified staircase threshold estimate procedure	40	5x10 ⁻³ cd/m ² (a decrease of 3 log units)	yes	unclear	Yes. Reduced flash intensity equivalent to 76% focal bleach centred on a more eccentric location of 12 on the inferior visual meridian. The modified protocol used the same methodology of staircase threshold estimates continuing until the same target threshold

															was reached.
Clark et al (2011)	AdaptDx	second slope, third average threshold, final threshold	82% bleach, subtending 4°, was centred at 5° on the inferior vertical meridian, 6.38 log scot Td second-1 intensity	0.25 milliseconds	1.7° diameter, 500nm circular test spot, 15 seconds after the bleaching onset	1% tropicamide and 2.5% phenylephrine hydrochloride so that a pupil diameter of ≥ 6 mm was achieved.	5° on the inferior visual meridian	3--down/1-up modified staircase estimate procedure	20	unclear	unclear	unclear	unclear	unclear	no
Cocce et al (2018)	AdaptDx	rod intercept time	505nm photoflash of 1.8 x 10 ⁴ scot cd/m ² s intensity), equivalent to 76% bleaching level for rods, 4° area of the retina centred at 5° on the inferior visual meridian	0.8 milliseconds	2° diameter, 505nm circular test spot, initial intensity was 5 cd/m ²	a drop of tropicamide 1% and phenylephrine 2.5%	5° on the inferior visual meridian	3--down/1-up modified staircase estimate procedure	20	5x10 ⁻³ cd/m ² (a decrease of 3 log units)	yes	if error exceeded 30%, the test was deemed unreliable	no		
Dhalla et al (2007)	in house adaptometer using Humphrey Visual Field	foveal threshold recovery time	60-watt 120V ANSI standard AC bulb held 50cm	30 seconds	dim light stimulus in the centre of the	undilated	unclear	unclear	until sensitivity returned to baseline	baseline level	unclear	unclear	unclear	no	

	Perimeter Model 750		from the eye. Retinal stimulation diameter of 1.9mm ensuring photostress of the fovea.			fixation targets									
Dimitrov et al (2008)	in house adaptometer	cone recovery rate, cone absolute threshold, rod-cone break, rod recovery rate, rod absolute threshold, rod intercept time	30% rod bleach (6.48 log scot Td second ⁻¹) and a 10% cone bleach (5.66 log scot Td second ⁻¹)	11 milliseconds	unclear	0.2-second, foveal, achromatic (1931CIE x 0.267, y 0.318) spot of various sizes 1° to 6°	0.5% tropicamide and 10% phenylephrine hydrochloride diluted to more than 7mm diameter.	centred on fovea	3--down/1-up modified staircase estimate procedure	30	5x10 ⁻³ cd/m ² (a decrease of 3 log units)	unclear	Post hoc analysis removed responses when fixation errors were ≥3°.	no	
Dimitrov et al (2012)	in house adaptometer	cone recovery rate, rod recovery rate	>95% bleach of photopigment for cone recovery and bleaching 30% of photopigment for rod recovery at 12 x 10 ⁶ cd·m ⁻²	unclear	unclear	2° diameter, 0.2-second achromatic (1931CIE; x 0.267, y 0.318)	>7mm diameter with 0.5% tropicamide and 2.5% phenylephrine hydrochloride	3.5° inferior retina along the vertical meridian	4dB up/2dB down staircase procedure	30	5x10 ⁻³ cd/m ² (a decrease of 3 log units)	unclear	Post hoc analysis removed responses when fixation errors were ≥3°.	no	

Dimitrov et al (2011)	in house adaptometer	cone recovery rate, cone absolute threshold, rod-cone break, rod recovery rate, rod absolute threshold, rod intercept time	>95% bleach of photopigment for cone recovery and bleaching 30% of photopigment for rod recovery at $12 \times 10^6 \text{ cd}\cdot\text{m}^{-2}$	unclear	2° diameter, 0.2-second achromatic (1931CIE; x 0.267, y 0.318)	>7mm (0.5% tropicamide and 2.5% phenylephrine hydrochloride)	fovea and two peripheral retinal locations, 3.5° and 10°, in the inferior retina along the vertical meridian	4dB up/2dB down staircase procedure	30	$5 \times 10^{-3} \text{ cd/m}^2$ (a decrease of 3 log units)	unclear	Post hoc analysis removed responses when fixation errors were $\geq 3^\circ$.	no	
Flamendorf et al (2015)	AdaptDx	rod intercept time	82% focal bleach centred at 5° on the inferior visual meridian	0.25 milliseconds	1.7° diameter, 500nm circular test spot. initial intensity was 5 cd/m^2	unclear	5° on the inferior visual meridian	3-down/1-up modified staircase threshold estimate procedure	40	$5 \times 10^{-3} \text{ cd/m}^2$ (a decrease of 3 log units)	yes	excludes fixation errors, but does not specify further	no	
Flynn, Cukras and Jeffrey, (2018)	Medmont dark-adapted chromatic perimeter	rod intercept time, slope rod intercept time	30% bleach at 347 cd/m^2	rod at sc	5 minute	1.73° diameter, red (625nm) and green (505nm) stimulus, measured 2 minutes after bleach	>7.3mm diameter	4°, 6°, 8° and 12° eccentricity, along the vertical meridian.	unclear	30	$5 \times 10^{-3} \text{ cd/m}^2$ (a decrease of 3 log units)	unclear	unclear	no
Fraser et al (2016)	Medmont dark-adapted chromatic perimeter	rod intercept time	30% bleach (6.48 scot	rod log Td	11 milliseconds	1.73° diameter, 620nm and	$\geq 7\text{mm}$ diameter with one drop each	8 test points located at 4°, 6°, 8°	staircase threshold strategy	20	$5 \times 10^{-3} \text{ cd/m}^2$ (a decrease of 3 log units)	unclear	unclear	no

			second-1) and a 10% cone bleach (5.66 log scot Td second-1)		505nm stimulus	of 0.5% tropicamide and 2.5% phenylephrine	and 12° on inferior and superior retina and 12° nasal and temporal retina (12 degree on nasal retina excluded)							
Gaffney, Binns and Margrain I (2011)	in house adaptometer using Humphrey Visual Field Perimeter Model 750	cone time constant, rod-cone break, cone absolute threshold	Maxwellian view optical system was used to deliver an 80% bleach of cone photopigment to the central 43.6° at 5.1 log phot. Td	120 seconds	foveal spot (radius 0.5°) and three achromatic annuli (2, 7, and 12° in radius), all 0.5° wide, centred on the fovea	one drop of 1.0% tropicamide in each eye	centred on fovea	3-down/1-up modified staircase threshold estimate procedure	25 (For the 0.5° stimulus, recovery was only monitored for 10 min, as no RCB was expected for a small stimulus, presented to the rod-free fovea.)	when threshold fell by at least 1 log unit below the cone plateau	unclear	unclear	no	
Gaffney, Binns and Margrain (2013)	in house adaptometer using Humphrey Visual Field Perimeter Model 750	cone time constant, rod-cone break, cone absolute threshold	photopigment bleaches to the central 43.6° of the test eye- Low Bleach denotes the lowest pre-	120 seconds	12° radius amber annulus ($\lambda = 595\text{nm}$; x, y chromaticity coordinates = 0.480,	mean diameter = 7.5mm, one drop of 1.0% tropicamide in each eye	centred on fovea	3-down/1-up modified staircase threshold estimate procedure	30	when threshold fell by at least 1 log unit below the cone plateau	yes	unclear	no	

			adapting intensity, Mod Bleach the middle, and High Bleach the highest pre-adapting intensity)		0.480), 0.5° wide									
Jackson et al (2014) 1	AdaptDx	rod intercept time	83% equivalent bleach at 58,000 scotopic cd/m ² s xenon flash intensity	unclear	2° diameter, 505nm circular test spot	≥6mm diameter with 1% tropicamide and 2.5% phenylephrine hydrochloride	Vertical meridian 5° inferior to the 650nm fixation light.	3-down/1-up modified staircase threshold estimate procedure	45	5x10 ⁻³ cd/m ² (a decrease of 3 log units)	yes	unclear	no	
Jackson, Felix and Owsley et al (2006)	SST-1	rod-cone break, dark adaptation duration, absolute threshold	1000 cd/m ² Ganzfeld. tungsten-halogen bulb (3500 K) for a full-field bleach	1 minute	Produced by the 572nm LED. The stimulus intensity can be set in 0.1 log unit steps over a 3 log unit range with a maximum brightness of 3.8 x 10 ⁴ cd/m ² .	≥6mm diameter with 1% tropicamide and 2.5% phenylephrine hydrochloride	full-field test stimulus	a method of ascending limits	unclear	when two consecutive thresholds were within 0.2 log unit of the pre-bleach absolute threshold	unclear	unclear	no	

Jackson, Scott, et al (2014)	AdaptDx	rod intercept time	505nm photoflash of 1.8×10^4 scot cd/m^2 s intensity), equivalent to 76% bleaching level for rods, 4° area of the retina centred at 5° on the inferior visual meridian	0.8 millisecond s	2° diameter, 505nm circular test spot	≥ 6 mm by using 1% tropicamide and 2.5% phenylephrine hydrochloride.	subtending 4° , was centred at 5° on the inferior vertical meridian	3-down/1-up modified staircase threshold estimate procedure	20 for extended protocol, 6.5 for rapid protocol	sensitivity was twice consecutively measured to be greater than 5×10^{-3} scot cd/m^2 (a decrease of 3 log units)	The algorithm attempts to extrapolate the intersection of the rod recovery with the criterion sensitivity level. If the rod intercept cannot be extrapolated, it is set at maximum test duration.	Invalid dark adaptation test was indicated by a fixation error rate of $\geq 30\%$.	no
Jackson and Edwards (2008)	AdaptDX	rod intercept time	photoflash of $6.38 \log$ scot Td second -1 intensity), 4° area of the retina centred at 5° on the inferior visual meridian	0.25 millisecond s	1.7° diameter, 500nm circular test spot	≥ 6 mm diameter	4° diameter aperture centred at 5° on the inferior visual meridian	3-down/1-up modified staircase threshold estimate procedure	20	5×10^{-4} cd/m^2 (a decrease of 4 log units)	yes	unclear	no
Lains et al (2017)	AdaptDx	rod intercept time	505nm photoflash of 1.8×10^4 scot cd/m^2 s intensity),	0.8 millisecond s	2° diameter, 505nm circular test spot	≥ 6 mm diameter	5° on the inferior visual meridian	3-down/1-up modified staircase threshold	20	5×10^{-3} cd/m^2 (a decrease of 3 log units)	yes	eyes with fixation errors $\geq 30\%$ were excluded	no

			equivalent to 76% bleaching level for rods, 6° area of the retina centred at 5° on the inferior visual meridian						estimate procedure				
Lains, Park, et al (2018)	AdaptDx	rod intercept time	505nm photoflash of 1.8 x 10 ⁴ s intensity), equivalent to 76% bleaching level for rods, 6° area of the retina centred at 5° on the inferior visual meridian	0.8 millisecond s	2° diameter, 505nm circular test spot	≥6 mm diameter	5° on the inferior visual meridian	3-down/1-up modified staircase threshold estimate procedure	20	5x10 ⁻³ cd/m ² (a decrease of 3 log units)	yes	eyes with no fixation errors ≥30% were excluded	
Lains, Miller, et al (2018)	AdaptDx	rod intercept time	505nm photoflash of 1.8 x 10 ⁴ s intensity), equivalent to 76% bleaching	0.8 millisecond s	2° diameter, 505nm circular test spot	≥6 mm diameter	5° on the inferior visual meridian	3-down/1-up modified staircase threshold estimate procedure	20	5x10 ⁻³ cd/m ² (a decrease of 3 log units)	yes	eyes with no fixation errors ≥30% were excluded	

			level for rods, 4° area of the retina centred at 5° on the inferior visual meridian												
Luu et al (2018)	Medmont dark-adapted chromatic perimeter	rod intercept time	a flash of rod photopigment using a customized Ganzfeld light source	unclear	1.73° diameter, 505nm circular test spot, 15 seconds after the bleaching onset	≥7mm diameter with 1 drop of 0.5% tropicamide.	14 test points located at 4°, 5.7°, 8°, and 12°	staircase threshold strategy	30	5x10 ⁻³ cd/m ² (a decrease of 3 log units)	unclear	unclear	unclear	unclear	participants who did not recover within 20 minutes were invited to continue with an extended period of DA (up to 24 hours)
Mullins et al (2018)	AdaptDx	rod intercept time	flash (58,000 scotopic cd/m ² intensity; equivalent ~ 83% bleach) subtending 4°, was centred at 5° on the inferior vertical meridian	0.25 milliseconds	2° diameter, 505nm circular test spot, 15 seconds after the bleaching onset	≥6 mm diameter with 1% tropicamide and 2.5% phenylephrine hydrochloride	subtending 4°, was centred at 5° on the inferior vertical meridian	3-down/1-up modified staircase estimate procedure	40	5x10 ⁻³ cd/m ² (a decrease of 3 log units)	set to 39 minutes	unclear	unclear	no	

Neely et al (2017)	AdaptDx	rod intercept time	flash (58,000 scotopic cd/m ² intensity; equivalent ~ 83% bleach) subtending 4°, was centred at 5° on the inferior vertical meridian	0.25 milliseconds	2° diameter, 505nm circular test spot, 15 seconds after the bleaching onset	≥6 mm diameter with 1% tropicamide and 2.5% phenylephrine hydrochloride	5° on the inferior visual meridian	3-down/1-up modified staircase estimate procedure	20	5x10 ⁻³ cd/m ² (a decrease of 3 log units)	unclear	unclear	no
Newsome and Negrerio (2009)	in house adaptometer	photostress recovery time	xenon arc emitted the flash diffused by the reflective interior surface of the tubular housing, 12mm aperture in the flash tube	unclear	numbers displayed inside the test	undilated	unclear	unclear	unclear	unclear	unclear	unclear	no
Nguyen et al (2018)	Medmont dark-adapted chromatic perimeter	rod intercept time	Ganzfeld light source, bleach 30% of rod photopigments (6.48	11 milliseconds	1.73° diameter, 505nm circular test spot	≥7mm diameter with 0.5% tropicamide and 2.5% phenylephrine	8 test points located at 4°, 6°, 8° and 12° on inferior and superior retina and	4-2 staircase threshold estimate procedure	20	5x10 ⁻³ cd/m ² (a decrease of 3 log units)	yes	unclear	no

													log scot Td second-1)						12° temporal retina				
Owsley, McGwin, Scilley, et al (2006)	in house adaptometer using Humphrey Visual Field Perimeter Model 750	cone time constant, cone absolute threshold, rod-cone break, rod slope, rod absolute threshold	flash of white light (7.65 log scotopic Trolands- second), 98% bleach in the area of the retina to be tested	0.25 millisecond s	1.7° diameter, ≥6 mm diameter with 1% tropicamid e and 2.5% phenylephr ine hydrochlori de	12° in the inferior visual field along the vertical meridian	3-down/1- up modified staircase estimate procedure	unclear	0.3 log units of the previously measured baseline (prebleach) sensitivity	unclear	unclear	no											
Owsley, McGwin, Jackson et al (2006)	in house adaptometer using Humphrey Visual Field Perimeter Model 750	cone time constant, cone absolute threshold, rod-cone break, rod slope, rod absolute threshold	electronic flash of white light (7.65 log scotopic Trolands- second); this flash produced an equivalent approximat ely 98% bleach in the area of the retina	11 millisecond s	1.7° diameter, for the cone- mediated threshold, a 650nm circular test spot (Ealing 35-3961, full width at half maximum [FWHM] 11.4, peak 50%), for	12° in the inferior visual field along the vertical meridian	3-down/1- up modified staircase estimate procedure	60	when rod threshold was stable for 5 minutes after the rod-cone break	no, third component of adaptation removed for analysis	unclear	no											

			bleach in the area of the retina to be tested		[FWHM] 11.4, peak 50%), for rod-mediated threshold was a 500nm circular test spot (Ealing 35-3508, FWHM 7.4, peak 50%). Cone-mediated threshold measurement began immediately after flash offset and Rod-mediated threshold started after 5 minutes									
Owsley, Huisingsh, et al (2016)	AdaptDx	rod intercept time	flash (58,000 scotopic cd/m ² s intensity; equivalent ~ 83% bleach) subtending 4°, was	0.25 milliseconds	2° diameter, 505nm circular test spot, 15 seconds after the bleaching onset	≥6 mm diameter with 1% tropicamide and 2.5% phenylephrine hydrochloride	subtending 4°, was centred at 5° on the inferior vertical meridian	3-down/1-up modified staircase procedure	20	5x10 ⁻³ cd/m ² (a decrease of 3 log units)	>20 minutes' on plot but not explicitly said in results section	unclear	no	

			centred at 5° on the inferior vertical meridian											
Owsley, McGwin, et al (2016)	AdaptDx	rod intercept time	flash (58,000 cd/m ² s intensity; equivalent ~ 83% bleach) subtending 4°, was centred at 5° on the inferior vertical meridian	0.25 milliseconds	2° diameter, 505nm circular test spot, 15 seconds after the bleaching onset	≥6 mm diameter with 1% tropicamide and 2.5% phenylephrine hydrochloride	subtending 4°, was centred at 5° on the inferior vertical meridian	3-down/1-up modified staircase estimate procedure	20	5x10 ⁻³ cd/m ² (a decrease of 3 log units)	>20 minutes' on plot but not explicitly said in results section	unclear	no	
Owsley, Clark, et al (2016)*	AdaptDx	rod intercept time	flash (58,000 cd/m ² s intensity; equivalent ~ 83% bleach) subtending 4°, was centred at 5° on the inferior vertical meridian	0.25 milliseconds	2° diameter, 505nm circular test spot, 15 seconds after the bleaching onset	≥6 mm diameter with 1% tropicamide and 2.5% phenylephrine hydrochloride	subtending 4°, was centred at 5° on the inferior vertical meridian	3-down/1-up modified staircase estimate procedure	20	5x10 ⁻³ cd/m ² (a decrease of 3 log units)	>20 minutes' on plot but not explicitly said in results section	unclear	no	

Owsley, Clark and McGwin, 2017	AdaptDx	rod intercept time	1.8 x 10 ⁴ scot cd/m ² s intensity, an equivalent 76% bleach; subtending 4°, was centred at 11° on the inferior vertical meridian	0.8 milliseconds	2° diameter, 505nm circular test spot, 15 seconds after the bleaching onset	1% tropicamide and 2.5% phenylephrine hydrochloride	subtending 4°, was centred at 5° on the inferior vertical meridian	3-down/1-up modified staircase estimate procedure	40	5x10 ⁻³ cd/m ² (a decrease of 3 log units)	RIT is "indeterminate"	unclear	no
Richer et al (2011)	KOWA AS14B NightVision Tester	glare recovery time	"continuous retinal bleach"	30 seconds	2-line, suprathreshold, low contrast, randomly presented Landolt C	unclear	unclear	unclear	unclear	unclear	unclear	unclear	no
Richer et al (2013)	Macular Disease Detection MDD-2® device	cone recovery time	bright flash	in seconds'	unclear	unclear	unclear	unclear	unclear	unclear	unclear	unclear	no
Richer et al (2014)	Macular Disease Detection MDD-2® device	cone recovery time	bright flash	in seconds	unclear	unclear	unclear	unclear	unclear	unclear	unclear	unclear	no
Robinson et al (2018)	in house adaptometer using Humphrey Visual Field	cone recovery time	Maxwellian view optical system was used to deliver an	120 seconds	foveal spot (radius 0.5°) and three achromatic annuli (2, 7,	one drop of 1.0% tropicamide in each eye	fovea	3-down/1-up modified staircase estimate procedure	25 (For the 0.5° stimulus, recovery was only monitored	when threshold fell by at least 1 log unit below	unclear	unclear	no

	Perimeter Model 750			80% bleach (5.1 log phot. Td) of cone photopigment to the central 43.6°			and 12° in radius), all 0.5° wide, centred on the fovea				for 10 min, as no RCB plateau was expected for a small stimulus, presented to the rod-free fovea.)				
Robinson et al (2019)	in house cone time constant	using Humphrey Visual Field Perimeter Model 751	A handheld bleaching source consisting of a "white" LED overlaid with a diffusing (LEE Filters 216 "white diffusion") and amber filter (LEE Filters HT015 "deep straw") was used. Bleaching ~85% of cone and 74% of rod pigment with a retinal	120 seconds	2° radius, solid yellow circular stimulus (chromaticity coordinates, 0.429, 0.413)	one drop of 1.0% tropicamide in each eye	centred on fovea	3-down/1-up modified staircase threshold estimate procedure	25	1-1/e of the prebleach value	unclear	unclear	unclear	no	

				illuminance of 5.20 log phot Td.s ⁻¹ to a retinal area subtending 12°.												
Rodriguez et al (2018)	Roland Consult dark adaptometer	baseline cone sensitivity and cone recovery half-life	Ora LUX: diffused full-spectrum fluorescent of approximately 40,000 d/m ² , with a dominant peak at 545 nm, 84% cone photoreceptor bleach	90 seconds	red (625nm) stimulus, 2° visual angle	unclear	unclear	unclear	6 dB-down and 2 dB-up stepped fashion	unclear	unclear	unclear	unclear	unclear	unclear	no
Rodrigo-Diaz et al (2019)	in house adaptometer	cone threshold, rod-cone break, cone time constant, slope 2 and rod-rod break	The integrated intensity of the flashgun (Speedlight SB800; Nikon, Tokyo, Japan) was set at either 5.91 or 6.08 log ₁₀ cd.s.m ² ,	0.9 milliseconds	stimuli were segments of annuli, A ViSaGe stimulus generator (Cambridge Research Systems, Rochester, UK) and the Visual Psychophysics Engine	≥5 mm diameter with 1% tropicamide	3.0° and 5.5° eccentricity	and	modified method of adjustment (start point 0.8 log scotopic cd.m ⁻² , step size 0.05 log units)	60	Thresholds were measured using a modified method of adjustment	In cases where the β-point was not reached, the maximum testing time was set at 60 minutes.	unclear	unclear	no	

			which, depending on the pupil size, bleached the photopigment by 70% to 99%.The retinal region of the bleach was 9°x9°			software were used, left half of the screen was covered with a 1.2 log unit neutral density (ND) filter, and the right half with 3.6 log ND filter.									
Sevilla et al (2016)	AdaptDx	rod intercept time	flash (58,000 cd/m ² s intensity; equivalent ~ 83% bleach) subtending 4°, was centred at 5° on the inferior vertical meridian	0.25 milliseconds	2° diameter, 505nm circular test spot	≥6 mm diameter with 1% tropicamide and 2.5% phenylephrine hydrochloride	subtending 4°, was centred at 5° on the inferior vertical meridian	3-down/1-up modified staircase estimate procedure	20	5x10 ⁻³ cd/m ² (a decrease of 3 log units)	unclear	unclear	no		
Tahir et al (2018)	in house adaptometer	cone absolute threshold, rod-cone break, second slope, the	The integrated intensity of the flashgun (Speedlight SB800;	6 milliseconds	stimuli were segments of annuli , A ViSaGe stimulus generator	Control group mean pupil size was 5.47mm and the AMD group	3.0° and 5.5° eccentricity	modified method of adjustment (start point 0.8 log scotopic cd.m 2,	40, If no b point was reached, the test continued for a	unclear	A defined b point required at least 4 to 5 measurements of the S3 phase.	unclear	no		

		transition from the second slope to third slope	Nikon, Tokyo, Japan) was set at either 5.91 or 6.08 log ₁₀ cd.s.m ² , which, depending on the pupil size, bleached the photopigment by 70% to 99%.The retinal region of the bleach was 9°x9°		(Cambridge Research Systems, Rochester, UK) and the Visual Psychophysics Engine software were used, left half of the screen was covered with a 1.2 log unit neutral density (ND) filter, and the right half with 3.6 log ND filter.	had a mean pupil size of 5.32mm using 1% tropicamide		step size further 20 (0.05 log minutes. units)				This meant we could assign patients to either a standard or slow recovery group. As we did not test to absolute threshold sensitivity, the true value of S3 was not determined and S3 is not used in the analysis. Note that, in nine of the AMD subjects, testing continued until 60 minutes with no b point being achieved.	
Tan et al (2019)	Medmont dark-adapted chromatic perimeter	rod intercept time and rod	a customised Ganzfeld flash	unclear	1.73° diameter, 505nm stimulus	≥6 mm diameter with 0.5%	14 locations within	unclear	30	5x10 ⁻³ cd/m ² (a decrease of 3 log units)	yes	unclear	no

		recovery time	bleached approximately 20% with an intensity of 2.45×10^6 scot cd/m ²			tropicamide	central 12° of macular							
Thompson et al (2018)	AdaptDx	rod intercept time	505nm photoflash of 1.8×10^4 scot cd/m ² intensity), equivalent to 76% bleaching level for rods, 4° area of the retina centred at 5° on the inferior visual meridian	0.8 milliseconds	2° diameter, 505nm circular test spot	≥6 mm diameter with 1% tropicamide and 2.5% phenylephrine hydrochloride	subtending 4°, was centred at 5° on the inferior vertical meridian	3-down/1-up modified staircase estimate procedure	6.5	sensitivity was twice consecutively measured to be greater than 5×10^{-3} scot cd/m ² (a decrease of 3 log units)	The algorithm attempts to extrapolate the intersection of the rod recovery with the sensitivity level. If the rod intercept cannot be extrapolated, it is set at maximum test duration.	Invalid dark adaptation test was indicated by a fixation error rate of ≥30%.	no	
Wolffsohn et al (2006)	Eger macular stressometer (EMS)	photostress recovery time	Thyristor photo flash, visual angle 14.2° horizontally and 6.8° vertically	unclear	logMAR near acuity line of capital letters at 40 cm (illuminated by 900 lux)	unclear	unclear	unclear	unclear	one line (0.1 logMAR) larger than their pre-exposure visual acuity was measured	unclear	unclear	no	

Yazdanie et al (2017)	AdaptDx	rod intercept time	flash (58,000 cd/m ² s; scotopic intensity; equivalent ~ 82% bleach) subtending 4°, was centred at 5° on the inferior vertical meridian	0.25 milliseconds	2° diameter, 505nm circular test spot	≥6 mm diameter with 1% tropicamide and 2.5% phenylephrine hydrochloride	subtending 4°, was centred at 5° on the inferior vertical meridian	3-down/1-up modified staircase estimate procedure	40	5x10 ⁻³ cd/m ² (a decrease of 3 log units)	yes	unclear	no
-----------------------	---------	--------------------	--	-------------------	---------------------------------------	---	--	---	----	--	-----	---------	----

*Owsley, Clark, Huising, et al (2016) reports DA values collected as part of an earlier study by the same team (Owsley et al (2016) (3)). The DA procedure used in this previous study has been recorded.

Table S2.5 Diagnostic Accuracy and Repeatability Measures Reported

Study	Device	Receiver Operating Characteristics	Specificity / Sensitivity	Repeatability / Reproducibility
Binns et al (2018)	AdaptDx	The best separation between groups was exhibited by the 76% bleach at 5° AUC = 0.83, CI: 0.64–1.0), and the 76% bleach at 12° (AUC = 0.79, 0.59–0.99 CI).	For the 76% at 5° test condition, using the published diagnostic cut-off for the RIT of 6.5 minutes, five out of the eight control participants for whom valid data were collected were correctly identified (63% specificity) while all 10 iAMD participants were correctly identified as abnormal (100% sensitivity). For the 12° location, specificity remained at 63% (5/8 controls correctly identified) while sensitivity fell to 89% (8/9 AMD for whom data were available) for a 5.5-minute optimal cut-off.	
Dimitrov et al (2008)	in house adaptometer	The recovery rate for cones yields a significantly better diagnostic capacity than does cone absolute threshold (Cone Recovery Rate AUC = 0.983 ± 0.014 vs. Cone Absolute Threshold AUC 0.761 ± 0.069; z = 3.063, p < 0.001). The recovery rate for rods and cones gave similar diagnostic capacity (Cone Recovery Rate AUC = 0.983 ± 0.014 vs. Rod Recovery Rate AUC = 0.924 ± 0.044; z = 1.416, p = 0.078), and although both were better than the Rod Cone Break, the differences were not statistically significant (Cone Recovery Rate AUC = 0.983 ± 0.014 vs. Rod		

Cone Break AUC = 0.904 ± 0.045 , $z = 1.469$, $p = 0.071$;
 Rod Recovery Rate AUC = 0.924 ± 0.044 vs. Rod Cone
 Break AUC = 0.904 ± 0.045 , $z = 0.261$, $p = 0.397$). The
 lack of significant differences between the latter
 parameters most likely reflects the low experimental
 power (0.23) for the sample sizes in our study.

Dimitrov et al (2011)	in house adaptometer	<p>Rod Recovery Rate at 10° returned the lowest diagnostic value, which was significantly lower than the 3.5° DA (AUC; 10° DA, 0.89 ± 0.021 vs. 3.5° DA, 0.93 ± 0.016; $z = 1.82$; $p = 0.034$) but not significantly different from the foveal DA 0.91 ± 0.018; $z = 0.94$; $p = 0.174$). Cone Recovery Rate also had the lowest AUC at this location which was significantly lower than for foveal DA (10° DA, 0.69 ± 0.026 vs. foveal DA, 0.95 ± 0.013; $z = 8.03$; $p < 0.001$) and for the 3.5° DA (10° DA, 0.69 ± 0.026 vs. 3.5° DA, 0.86 ± 0.023; $z = 4.29$; $p < 0.001$). Given that we were able to quantify rod recovery rate at 3.5° eccentricity in a higher number of participants than in the fovea (93% vs. 69%), with similar diagnostic capacity for both locations (3.5° DA 0.93 ± 0.016 vs. fovea 0.91 ± 0.018; $z = 1.21$; $p = 0.114$), and that the cone recovery at 3.5° was of a high AUC value (AUC, 0.86 ± 0.023),</p>	<p>Looking at the proportion of abnormal cases identified with each of the 3.5° DA parameters and the other tests when using a criterion that fails in 2.5% of normal cases (diagnostic capacity at the fixed specificity, 97.5%). It is evident that all dynamic parameters in DA have greater capacity to detect functional abnormality (RR for cones, 62%; rods, 86%) than do static parameters (AT for cones, 32% and for rods, 41%).</p>
--------------------------	-------------------------	---	---

the 3.5° eccentricity most likely represents the optimal location for adaptation testing.

Flamendorf et al 2015	AdaptDx			Bland-Altman plot demonstrated that testing was reproducible with a mean RIT difference of 0.02 ± 2.26 min (mean \pm SD) and 95% limits of agreement of -4.41 to 4.46 min. The distributions of test-retest differences did not differ significantly between AMD groups, indicating that test reproducibility did not vary with AMD severity ($p > 0.05$ for all comparisons).
Gaffney et al (2011)	in house adaptometer using Humphrey Visual Field Perimeter Model 750	ROC showed that the diagnostic potential of DA is greatest for stimuli presented 12° from fixation; for cone [tau] AUC = 0.99 ± 0.02 and for time to RCB, AUC = 0.96 ± 0.04 .	For stimuli presented 12°, this equates to 100% sensitivity and 90% specificity for a cone of 1.04 min and 90% sensitivity and 90% specificity for a RCB of 11.98 min.	
Gaffney, Binns and Margrain (2013)	in house adaptometer using Humphrey Visual Field Perimeter Model 751	For cone tau, the higher two pre-adapting intensities (Med and High Bleach) were equally capable of discriminating participants with early AMD from healthy controls, both yielding an AUC of 0.92 ± 0.07 . This was marginally superior to the AUC of 0.87 ± 0.08 obtained for cone tau at the lowest pre-adapting intensity (Low Bleach); however, there were no statistically significant differences in the AUC obtained for cone tau at any of the pre-adapting	Sensitivity and specificity values of between 80 and 100 % were obtained for optimal cut-off values of cone tau and time to RCB after all of the photopigment bleaches, further illustrating their diagnostic potential.	

intensities ($z < 1.96$) [41, 42] and that there were no significant differences between the AUCs generated for time to RCB at any of the pre-adapting intensities ($z < 1.96$) [41, 42].

Jackson, AdaptDx
Scott, et al
(2014)

The rapid test was found to have a diagnostic test specificity of 90.5% (19/21, $p=0.0271$). The 95% CI for diagnostic specificity had a lower bound of 72.9% and an upper bound of 100%. The rapid test was found to have a diagnostic sensitivity of 90.6% (115/127, $P < 0.001$). The 95% CI for diagnostic sensitivity had a lower bound of 85.1% and an upper bound of 100%. To evaluate whether these false-negative cases were associated with a specific AMD phenotype, diagnostic sensitivity was calculated for each severity of AMD. The diagnostic sensitivities were 80.5% (33/41) for early AMD, 94.4% (68/72) for iAMD, and 100% (14/14) for advanced AMD.

Jackson and AdaptDx
Edwards
(2008)

15 of the 17 ARM patients were classified as having abnormal dark adaptation for a diagnostic sensitivity of 88%. All nine normal adults fell within the normal reference range for a diagnostic specificity of 100%. The sensitivity of the test is 100% for those ARM patients with an AREDS grade 3 and higher.

<p>Newsome in house and Negrerio adaptometer (2009)</p>	<p>For normal eyes and eyes with drusen only, the 95% confidence coefficient of repeatability (CR) confirmed that there was no significant difference between groups, and between initial and 5-min repeat flashes (CR normal right eyes 4.7; normal left eyes 4.5; drusen only right eyes 4.3; drusen-only left eyes 4.8). In order to assess the reproducibility of responses, 10 normal subjects and 10 macular degeneration subjects with visual acuities from 20/40 to 20/70 (28–40 letters correct) participated in serial testing. Subjects were assessed at baseline and again two weeks later and one month later. There was no statistically significant variation in recovery times for normal subjects or for macular degeneration subject's $p > 0.15$ when right eye and left eye times at the two post-baseline time points were compared to baseline.</p>
<p>Owsley, AdaptDx McGwin, et al (2016)</p>	<p>Although the purpose of this study was not to evaluate the sensitivity and specificity of the rod-intercept as a screening test for incident AMD in those in normal macular health at baseline, we used the data to compute sensitivity and specificity, which were 33.3% and 82.8%, respectively.</p>

Rodriguez et al (2018)	Roland Consult dark adaptometer	The baseline cone threshold showed and an AUC of 0.898	The baseline cone threshold showed with specificity of 88.9% and sensitivity of 91.7%	The baseline cone threshold parameter exhibited good short-term ICC =0.88) and long-term (ICC=0.85) repeatability in all subjects. Among all visits at the initial evaluation, both the baseline cone threshold (c) and the recovery half-life (h) were found to have a high degree of repeatability (ICC=0.88; 95% CI 0.8096, 0.9544) and (ICC=0.93; 95% CI 0.8893, 0.9751), respectively. The intercept (a) was determined to have relatively poor repeatability (ICC=0.40; 95% CI 0.1560, 0.6397).The baseline cone threshold (c, ICC=0.84) and the recovery half-life (h, ICC=0.84) were both found to have a high degree of reproducibility.
Tahir et al (2018)	in house adaptometer	The AUC in the ROC for RCB (α) was 0.76 \pm 0.06, regardless of whether the data were from single stimuli or from a combination of both stimuli. However, for S2 there was a more substantial benefit of combining the stimuli, with the AUC changing from 0.88 \pm 0.04 for individual stimuli to 0.94 \pm 0.03 for the combined stimuli.	The technique yielded sensitivity of 88.0% and specificity of 66.7%.	
Wolffsohn et al (2006)	Eger macular stressometer (EMS)			Recovery time was 1.6 (5.2) seconds shorter on intrasession repeated measure (p<0.05). Recovery times were assessed again after a 1 year period. There was no difference in the initial recovery time

among patients with exudative AMD whose distance visual acuity (10.6 (8.7) v 7.9 (3.4) seconds, p=0.15) or contrast sensitivity (10.8 (9.4) v 11.1 (7.5) seconds, p=0.92) deteriorated compared with those among whom these two measures remained stable

Table S2.6 Outcome measures compared to parameters of dark adaptation, related to vision

Eye Related Outcome Measures Compared To Dark Adaptation Parameters			
Outcome Measures	Frequency	Outcome Measures	Frequency
<u>AMD Related</u>		<u>Drusen</u>	
AMD in fellow eye	1	drusen presence	1
AMD incidence from baseline	1	peripheral classic drusen presence	1
AMD presence	23	RPD/SDD presence	7
AMD risk factors	1	<u>PROMs</u>	
AMD severity	22	LLQ score	1
ARM presence	3	LLQ subscales	4
changes in AMD presence	2	<u>Structure</u>	
family history of AMD	1	choroidal thickness	1
high-risk clinical profile subgroups	1	lens status	3
unilateral AMD	1	location of GA on retina	1
<u>Longitudinal Changes</u>		macular pigment	2
changes over 1 year	1	macular pigment optical density	1
changes over 4 years	1	peripheral atrophic changes	1
changes over 12 months	1	presence of central visual defect	1
changes over 12 weeks	1	reticular pigmentary changes	1
changes over 2-3 years	1	retinal thickness	1
<u>DA Procedure</u>		SDOCT volumes	1
different dark adaptation parameters	1	colour fundus photograph grade	1
bleaching conditions/intensities	2	fundus autofluorescence	2
stimulus location	2	<u>Visual Function</u>	
test loci	1	contrast sensitivity	2
<u>Eye Health/Disease</u>		visual acuity	5
diabetic retinopathy presence	1		
presence of optic nerve pathology	1		

Table S2.7 Outcome measures compared to parameters of dark adaptation, unrelated to vision

Non-Eye Related Outcome Measures Compared To Dark Adaptation Parameters	
Outcome Measures	Frequency
<u>Age Related</u>	
age	8
<u>Diet/Lifestyle</u>	
alcohol consumption	1
BMI	1
other multivitamins	1
physically active	1
presence of supplemental macular carotenoids	1
statins	1
taking AREDS vitamins	1
use of dietary supplementation with zeaxanthin	1
without vitamin A intervention	1
<u>Genetics</u>	
ARMS2	1
CFH	1
<u>Health/Disease</u>	
anticoagulants	1
autoimmune diseases	1
diagnosis of heart failure	1
nonsteroidal anti-inflammatory drugs	1

Table S3.1 Clinical characteristics of participants in supplementary analysis

Participant ID	logMAR test eye	AMD status test eye	AMD status fellow eye	RIT (minutes)
RR0013	0.16	1	1	6.5
ET0007	0.34	1	1	5.1
JE0008	0.00	1	1	4.1
JC0032	0.16	1	1	3
GM0035	-0.04	1	1	12.8
BW0037	0.00	1	1	3.1
MI0033	0.16	1	1	21.5
FJ0038	0.16	1	1	7.5
AG0002	0.20	2	2	12.3
KM0003	0.16	2	2	14.5
DH0005	0.44	3	3	10.8
MM0006	0.20	3	3	7.6
GE0010	0.00	3	3	12
PS0012	0.20	3	3	30*
GD0014	-0.04	3	3	29
VC0015	0.02	3	4	30*
BB0016	0.42	3	4	30*
PN0009	0.06	3	4	7.3
JB0018	0.00	3	3	12.3
WP0032	0.40	3	3	30*
JG0027	0.20	4	4	4.6
EC0011	0.44	4	4	10.6
AF0028	0.50	4	4	14
PF0031	0.12	4	4	3.8

These values were obtained by Binns et al (2018) using a DA procedure consisting of 76% bleach at 5° eccentricity, detailed in manuscript. AMD was graded according to the Beckman classification (Ferris et al., 2013).

Table S3.2 Central estimates of RIT values (in minutes) with the three methods considered for the supplementary analysis.

		Estimate (95% CIs)		
		AMD	Controls	p-value
Original data	Survival model	16.37 (9.62, 23.12)	6.74 (3.17, 10.32)	0.007
	GLM	16.18 (10.8, 21.55)	7.95 (10.8, 21.55)	0.024
	Linear model	16.18 (11.79, 20.56)	7.95 (11.79, 20.56)	0.045

For the linear model (t-test) and the GLM, the mean is reported. For the survival model the estimate for the median is reported. In this supplemental dataset censored at 30 minutes, it is clear that the survival analysis offers a more statistically significant difference (at $p < 0.05$) between groups compared to the GLM and linear model.

Table S3.3 Plain text comparison of RMDA between different levels of AMD severity according to the Beckman classification utilising easy-to-use output from the web app. Dataset sourced from baseline data collected in Chapter 5.

	Controls	Early AMD	iAMD
Early AMD	RITs for Early AMD group are 61% longer than Control group ($p = .01$)	-	-
iAMD	RITs for iAMD group are 76% longer than Control group ($p = .00$)	RITs for Early AMD group are 9% shorter than iAMD group ($p = .53$)	
Late AMD	RITs for control group are 74% shorter than late AMD group ($p = .01$)	RITs for Early AMD group are 59% shorter than Late AMD group ($p = .00$)	RITs for iAMD group are 55% shorter than Late group ($p = .00$)

Table S4.1 The Beckman Classification of AMD severity, adapted from Ferris et al. (2013)

Beckman Stage Number	Beckman Stage Name	Definition (areas of lesions within 2 disc diameters from the foveal centre)
0	No obvious ageing changes	No Drusen – No pigmentary changes*
1	Normal ageing changes	Only Drusen $\leq 63\mu\text{m}$ – No AMD pigmentary abnormalities*
2	Early AMD	Medium drusen $>63\mu\text{m}$ and $\leq 125\mu\text{m}$ – No AMD pigmentary abnormalities*
3	Intermediate AMD	Large Drusen $>125\mu\text{m}$ - any other AMD pigmentary changes*

*AMD pigmentary changes = any definite hyper- or hypopigmentation with medium or large drusen not associated with any known disease entities

Table S4.2 OCT Classification of AMD severity

Stage Number	Stage Description	SDDs	Frequency	Mean Age in years (SD \pm)	Median RMDA (IQR)
0	Controls	No	257	63 (7)	6.0 (4.6, 8.7)
		Yes	55	66 (9)	5.3 (4.4, 7.6)
1	Drusen only	No	66	66 (8)	7.1 (5.1, 11.8)
		Yes	30	73 (7)	12.1 (5.3, 14.6)
2	Drusen and/or RPE abnormalities	No	27	69 (10)	8.6 (5.7, 15.9)
		Yes	24	75 (8)	17.0 (5.4, 35.7)

Table S4.3 SDD classification by Zweifel et al. (2010)

Stage Number	Description
0	Diffuse deposition of granular hyperreflective material in the interdigitation zone
1	Mounds of accumulated material sufficient to alter the contour of the ellipsoid zone
2	Material with conical appearance breaking through the ellipsoid zone

Table S4.4 SDD presence stratified using OCT classification and Zweifel et al. (2010) SDD staging

OCT Group	Participants with SDDs	SDD Stage		
		Stage 1	Stage 2	Stage 3*
0	55	34	20	1
1	30	14	13	3
2	24	7	11	6

*Due to small number of Stage 3 SDDs, these were omitted from further analysis

Table S4.5 AIC values for both age-corrected survival models for both classifications using all available distributions

Classification	Distribution	Type of distribution	AIC
Beckman	Weibull	Parametric	2607
OCT	Weibull	Parametric	2625
Beckman	Cox	Semi-parametric	4549
OCT	Cox	Semi-parametric	4555
Beckman	Exponential	Parametric	2787
OCT	Exponential	Parametric	2792
Beckman	Gaussian	Parametric	2974
OCT	Gaussian	Parametric	2994
Beckman	Logistic	Parametric	2825
OCT	Logistic	Parametric	2839
Beckman	Lognormal	Parametric	2509
OCT	Lognormal	Parametric	2516
Beckman	Loglogistic	Parametric	2473
OCT	Loglogistic	Parametric	2484
Beckman	Rayleigh	Parametric	2640
OCT	Rayleigh	Parametric	2667
Beckman	Loggaussian	Parametric	2509
OCT	Loggaussian	Parametric	2516
Beckman	T	Parametric	2722
OCT	T	Parametric	2733
Beckman	Extreme	Parametric	3313
OCT	Extreme	Parametric	3344

Analysis was repeated using different parametric and semi-parametric distributions, with age corrected for. Lognormal, loglogistic and loggaussian distributions had lower Akaike information criterion (AIC) values, so pairwise comparisons between the variables in the survival models were computed to assess the best model to use.

Table S4.6 Pairwise comparisons between classification levels within the age-corrected survival model using different distributions

Pairwise comparisons between variables (age-corrected)	Distribution	P values (Bonferroni Holm correction)
Beckman 0-1	Weibull	1
Beckman 0-2	Weibull	1
Beckman 0-3	Weibull	<.0001
Beckman 1-2	Weibull	1
Beckman 1-3	Weibull	<.001
Beckman 2-3	Weibull	<.01
Beckman 0-1	Lognormal	1
Beckman 0-2	Lognormal	1
Beckman 0-3	Lognormal	<.0001
Beckman 1-2	Lognormal	1
Beckman 1-3	Lognormal	<.01
Beckman 2-3	Lognormal	<.05
Beckman 0-1	Loglogistic	1
Beckman 0-2	Loglogistic	.746
Beckman 0-3	Loglogistic	<.0001
Beckman 1-2	Loglogistic	1
Beckman 1-3	Loglogistic	<.001
Beckman 2-3	Loglogistic	<.001
Beckman 0-1	Loggaussian	1
Beckman 0-2	Loggaussian	1
Beckman 0-3	Loggaussian	<.0001
Beckman 1-2	Loggaussian	1
Beckman 1-3	Loggaussian	<.01
Beckman 2-3	Loggaussian	<.01
OCT 0-1	Weibull	.20
OCT 0-2	Weibull	<.001
OCT 1-2	Weibull	<.01
OCT 0-1	Lognormal	.082
OCT 0-2	Lognormal	<.001
OCT 1-2	Lognormal	<.05
OCT 0-1	Loglogistic	.062
OCT 0-2	Loglogistic	<.001
OCT 1-2	Loglogistic	.062
OCT 0-1	Loggaussian	.082
OCT 0-2	Loggaussian	<.001
OCT 1-2	Loggaussian	<.05

Despite having a higher AIC, there is no material difference between the p-values therefore it is appropriate for our analysis to use the Weibull distribution

Table S5.1 Bland-Altman statistics for AdaptDx and S-MAIA for cross centre comparison for iAMD

Test	Centre Location	n at baseline	n removed after screening of procedural errors (%)	n removed after screening of participant issues (%)	n removed after screening of unreliable data (%)	Final n	Bias (95% CI)	SD of differences	Lower LoA (95% CI)	Upper LoA (95% CI)	Interclass Correlation Coefficient (95% CI)	Variability Ratio
RIT (mins)	CS001	29	-	1 (6%)	-	28	-0.14 (-0.84, 0.56)	1.8	-3.68 (-4.89, -2.47)	3.46 (2.20, 4.72)	0.93 (0.86, 0.97)	0.38
	CS011	11	-	-	-	11	1.81 (-1.79, 5.41)	5.4	-8.69 (-15.05, -2.34)	12.32 (5.96, 18.67)	0.52 (-0.05, 0.84)	1.10
	CS015	12	-	-	1 (8%)	11	1.59 (-0.82, 4.00)	3.59	-5.44 (-9.70, -1.20)	8.63 (4.37, 12.88)	0.47 (-0.11, 0.82)	1.14
	CS030	12	-	1 (8%)	1 (8%)	10	-1.10 (-2.15, -0.04)	1.47	-3.98 (-5.84, -2.12)	1.79 (-0.08, 3.65)	0.94 (0.80, 0.99)	0.28
	Remaining (n14 centres)	103	15 (15%)	1 (1%)	44 (43%)	43	0.95 (-0.42, 2.32)	4.45	-7.78 (-10.42, -5.42)	9.68 (7.32, 12.03)	0.51 (0.25, 0.7)	1.13
MMAT (dB)	CS001	29	-	-	-	29	0.92 (-0.66, 2.49)	4.14	-7.20 (-9.92, -4.48)	9.03 (6.31, 11.76)	0.82 (0.66, 0.91)	0.62
	CS006	10	-	-	-	10	-0.42 (-1.57, 0.73)	1.6	-3.58 (-5.63, -1.54)	2.74 (0.70, 4.79)	0.75 (0.30, 0.93)	0.76
	CS011	11	-	-	-	11	-0.17 (-0.66, 0.32)	0.72	-1.6 (-2.46, -0.74)	1.25 (0.39, 2.11)	0.92 (0.73, 0.98)	0.42
	CS017	16	-	-	-	16	-0.62 (-1.32, 0.08)	1.31	-3.18 (-4.40, -1.96)	1.94 (0.73, 3.16)	0.88 (0.69, 0.96)	0.47
	CS024	11	1 (9%)	-	-	10	0.47 (-0.32, 1.27)	1.11	-1.71 (-3.12, -0.30)	2.65 (1.24, 4.06)	0.87 (0.58, 0.97)	0.51
	CS030	12	1 (8%)	-	-	11	-0.21 (-0.65, 0.23)	0.65	-1.49 (-2.26, -0.71)	1.07 (0.30, 1.84)	0.94 (0.81, 0.98)	0.35
	CS077	12	-	-	-	12	-0.46 (-1.13, 0.21)	1.05	-2.52 (-3.69, -1.34)	1.60 (0.43, 2.77)	0.69 (0.25, 0.9)	0.81
Remaining (n11 centres)	66	36 (55%)	-	1 (2%)	29	0.76 (-0.41, 1.92)	3.06	-5.24 (-7.25, -3.23)	6.75 (4.74, 8.76)	0.75 (0.54, 0.88)	0.74	
SMAT (dB)	CS001	29	-	1 (3%)	-	29	1.34 (0.24, 2.43)	2.87	-4.30 (-6.19, -2.41)	6.97 (5.08, 8.86)	0.82 (0.66, 0.91)	0.58

CS006	10	-	-	-	10	0.13 (-0.68, 0.94)	1.13	-2.08 (-3.51, -0.65)	2.34 (0.91, 3.77)	0.65 (0.12, 0.90)	0.97
CS011	11	1 (9%)	-	-	10	1.07 (-1.22, 3.36)	3.20	-5.19 (-9.24, -1.15)	7.33 (3.29, 11.38)	0.33 (-0.31, 0.78)	1.41
CS017	16	1 (6%)	-	-	15	-0.31 (-1.20, 0.59)	1.62	-3.48 (-5.04, -1.91)	2.86 (1.30, 4.43)	0.83 (0.59, 0.94)	0.61
CS020	20	6 (30%)	-	-	14	0.52 (-0.25, 1.29)	1.33	-2.09 (-3.43, -0.74)	3.13 (1.78, 4.47)	0.87 (0.66, 0.96)	0.50
CS030	12	1 (8%)	-	-	11	0.04 (-0.88, 0.95)	1.36	-2.63 (-4.24, -1.02)	2.70 (1.09, 4.31)	0.92 (0.74, 0.98)	0.44
Remaining (n12 centres)	69	26 (38%)	-	1 (1%)	42	0.02 (-0.76, 0.80)	2.50	-4.89 (-6.23, -3.54)	4.92 (3.58, 6.27)	0.84 (0.73, 0.91)	0.59

Table S5.2 Bland-Altman statistics for AdaptDx and MAIA for control participants

Test	N	Mean Baseline (\pm SD)	Mean FU (\pm SD)	Bias (95% CI)	SD of differences	Lower LoA (95% CI)	Upper LoA (95% CI)	Interclass Coefficient (95% CI)	Correlation (95% CI)	Variability Ratio
RIT (mins)	33	4.39 (1.41)	4.14 (0.97)	0.25 (-0.21, 0.71)	0.25	-2.29 (-3.08, -1.5)	2.78 (1.99, 3.58)	0.42 (0.10, 0.66)		1.27
RIT (10*log10)	33	6.20 (1.47)	6.05 (1.05)	0.15 (-0.31, 0.60)	1.29	-2.38 (-3.17, -1.59)	2.67 (1.88, 3.46)	0.50 (0.20, 0.72)		1.17
MMAT (dB)	51	25.28 (2.06)	25.58 (2.11)	-0.30 (-0.72, 0.12)	1.48	-3.20 (-3.91, -2.49)	2.60 (1.89, 3.32)	0.74 (0.6, 0.85)		0.76
S MAT (dB)	49	21.08 (2.46)	20.49 (2.33)	0.59 (-0.0, 1.2)	2.10	-3.53 (-4.57, -2.49)	4.71 (3.68, 5.75)	0.60 (0.38, 0.75)		0.98

Table S5.3 Bland-Altman statistics for AdaptDx and MAIA for early AMD participants

Test	N	Mean Baseline (\pm SD)	Mean FU (\pm SD)	Bias (95% CI)	SD difference of	Lower LoA (95% CI)	Upper LoA (95% CI)	Interclass Coefficient (95% CI)	Correlation (95% CI)	Variability Ratio
RIT (mins)	26	6.26 (5.08)	6.05 (4.32)	0.20 (-0.52, 0.92)	1.79	-3.30 (-4.56, -2.05)	3.72 (2.46, 4.97)	0.93 (0.85, 0.97)		0.39
RIT (10*log10)	26	7.38 (1.93)	7.33 (1.78)	0.05 (-0.42, 0.52)	1.17	-2.24 (-3.06, -1.42)	2.33 (1.52, 3.15)	0.81 (0.62, 0.91)		0.66
MMAT (dB)	28	23.56 (2.66)	22.94 (3.19)	0.62 (-0.08, 1.32)	1.80	-2.91 (-4.12, -1.7)	4.15 (2.95, 5.36)	0.80 (0.61, 0.9)		0.64
S MAT (dB)	26	19.30 (3.09)	18.62 (3.44)	0.68 (-0.09, 1.45)	1.90	-3.05 (-4.38, -1.72)	4.41 (3.08, 5.74)	0.82 (0.64, 0.91)		0.61

Table S5.4 Bland-Altman statistics for AdaptDx and MAIA for late AMD participants

Test	N	Mean Baseline (\pm SD)	Mean FU (\pm SD)	Bias (95% CI)	SD difference	of Lower LoA (95% CI)	Upper LoA (95% CI)	Interclass Correlation Coefficient (95% CI)	Variability Ratio
RIT (mins)	8	12.37 (11.25)	12.35 (11.16)	0.02 (-0.68, 0.72)	0.83	-1.61 (-0.37, -2.85)	1.65 (0.41, 2.89)	1.00 (0.99, 1.00)	0.07
RIT (10*log10)	8	9.45 (3.76)	9.55 (3.52)	-0.10 (-0.81, 0.61)	0.85	-1.77 (-3.04, -0.50)	1.56 (0.29, 2.83)	0.98 (0.9, 1.00)	0.23
MMAT (dB)	32	6.66 (6.79)	5.81 (6.89)	0.85 (-0.4, 2.10)	3.47	-5.95 (-8.12, -3.79)	7.65 (5.49, 9.82)	0.87 (0.75, 0.93)	0.52
S MAT (dB)	29	4.30 (5.89)	3.21 (4.66)	1.09 (-0.11, 2.28)	3.15	-5.08 (-7.15, -3.01)	7.25 (5.18, 9.32)	0.81 (0.64, 0.91)	0.62

Table S5.5 Bland-Altman statistics for mesopic point-wise threshold sensitivity, grouped by eccentricity for people with iAMD

Degrees of fixation	from	N points	Mean Visit 1 (\pm SD)	Mean Visit 2 (\pm SD)	Bias (95% CI)	\pm SD difference	Lower LoA (95% CI)	Upper LoA (95% CI)	Interclass Correlation Coefficient (95% CI)	Variability Ratio
1		4	23.46 (4.78)	23.15 (5.79)	0.31 (-0.21, 0.82)	2.95	-5.46 (-6.35, -4.58)	6.08 (5.2, 6.96)	0.85 (0.79, 0.89)	0.58
3		12	23.13 (4.08)	22.65 (5.18)	0.49 (0, 0.97)	2.76	-4.92 (-5.76, -4.09)	5.89 (5.06, 6.71)	0.82 (0.76, 0.87)	0.62
5		12	23.01 (4.46)	22.98 (5.19)	0.02 (-0.51, 0.56)	3.06	-5.98 (-6.9, -5.06)	6.02 (5.11, 6.94)	0.80 (0.73, 0.86)	0.67
7		4	23.01 (5.22)	22.94 (5.79)	0.06 (-0.41, 0.54)	2.72	-5.26 (-6.08, -4.44)	5.39 (4.57, 6.20)	0.88 (0.83, 0.91)	0.51

Table S5.6 Bland-Altman statistics for scotopic point-wise threshold sensitivity, grouped by eccentricity for people with iAMD

Degrees fixation	from	N points	Mean 1 (\pm SD)	Visit Mean (\pm SD)	Visit 2 Bias (95% CI)	\pm SD of difference	Lower LoA (95% CI)	Upper LoA (95% CI)	Interclass Coefficient (95% CI)	Correlation (95% CI)	Variability Ratio
1		4	19.19 (4.63)	18.72 (4.08)	0.47 (0.00, 0.93)	2.69	-4.81 (-5.60, -4.00)	5.74 (4.94, 6.54)	0.83 (0.77, 0.88)		0.60
3		12	18.64 (4.38)	18.11 (4.36)	0.53 (0.04, 1.02)	2.82	-5.01 (-5.84, -4.17)	6.06 (5.23, 6.90)	0.79 (0.71, 0.84)		0.68
5		12	18.52 (4.15)	18.20 (4.36)	0.32 (-0.11, 0.76)	2.53	-4.63 (-5.37, -3.88)	5.27 (4.53, 6.02)	0.82 (0.76, 0.87)		0.62
7		4	18.66 (4.53)	18.40 (4.78)	0.26 (-0.14, 0.66)	2.30	-4.24 (-4.92, -3.56)	4.76 (4.08, 5.44)	0.88 (0.83, 0.91)		0.51

Table S5.7. AUC (95% confidence intervals) statistics to show discrimination performance of the AdaptDx to separate healthy controls, people with early AMD, people with iAMD and people with late AMD

	Controls	Early AMD	Intermediate AMD
Early AMD	73% (59%-86%)	-	-
Intermediate AMD	71% (61%-80%)	55% (43%-66%)	-
Late AMD	82% (61%-100%)	70% (46%-94%)	63% (39%-88%)

Table S5.8. AUC (95% confidence intervals) statistics to show discrimination performance of the mesopic microperimetry to separate healthy controls, people with early AMD, people with iAMD and people with late AMD

	Controls	Early AMD	Intermediate AMD
Early AMD	70% (57%-82%)	-	-
Intermediate AMD	68% (60%-77%)	50% (38%-62%)	-
Late AMD	100% (99%-100%)	99% (97%, 100%)	97% (95%-100%)

Table S5.9. AUC (95% confidence intervals) statistics to show discrimination performance of the scotopic microperimetry to separate healthy controls, people with early AMD, people with iAMD and people with late AMD

	Controls	Early AMD	Intermediate AMD
Early AMD	66% (53%-79%)	-	-
Intermediate AMD	69% (60%-77%)	53% (40%-65%)	-
Late AMD	99% (96%-100%)	97% (92%-100%)	96% (91%-100%)

Table S5.10 AUC (95% confidence intervals) statistics to show discrimination performance of AdaptDx, mesopic and scotopic microperimetry to separate healthy controls from all participants with AMD and control participants from participants with iAMD who completed all three tests

	Controls versus all participants with AMD (%)	Controls versus participants with iAMD who completed all three tests* (%)
RIT (mins)	73 (67-79)	70 (60-80)
MMAT (dB)	76 (71-80)	61 (50-72)
SMAT (dB)	72 (67-77)	67 (56-78)

*31 controls and 81 iAMD participants completed all three tests

8.2 SUPPLEMENTAL FIGURES

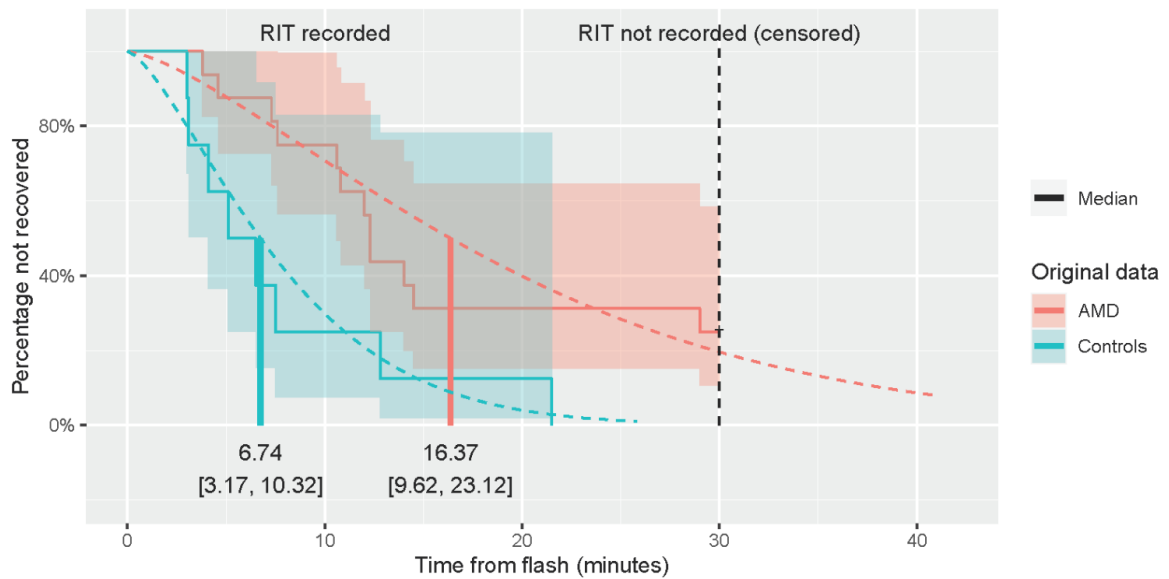


Figure S3.1 Survival curves of supplementary dataset RITs. The vertical dashed line acts as a marker, representing this capping limit of 30 minutes. Note that the empirical survival curve for AMD eyes does not reach 0, showing that the values beyond 30 minutes are censored. The time-to-event model predicts a median value beyond the capping limit (shown by the extended red dashed line).

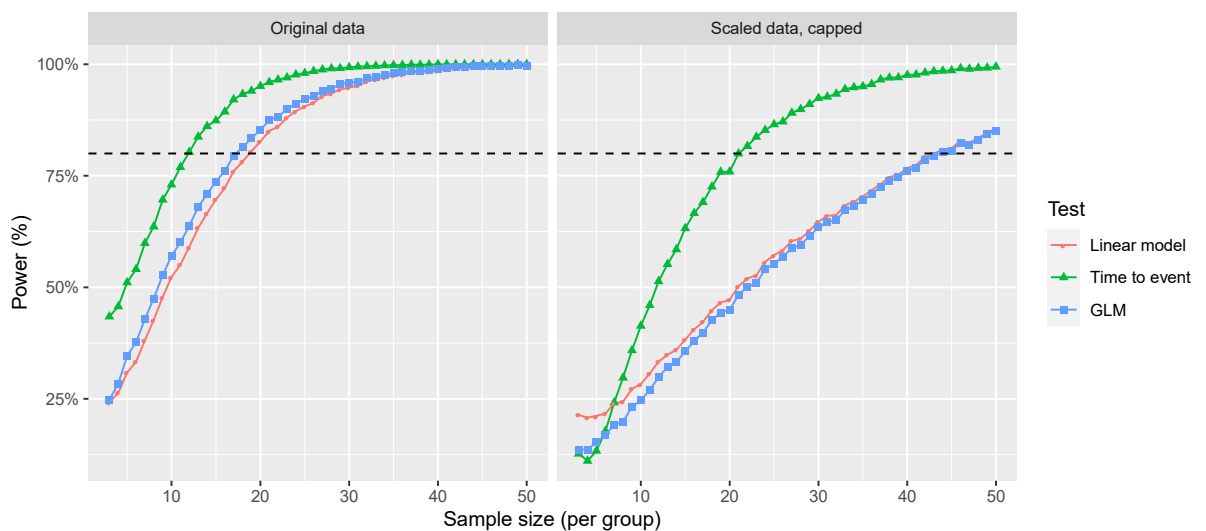


Figure S3.2 Power curves calculated using the p-values from the Wald test for all three models ($N = 10000$ bootstrap samples per sample size step).

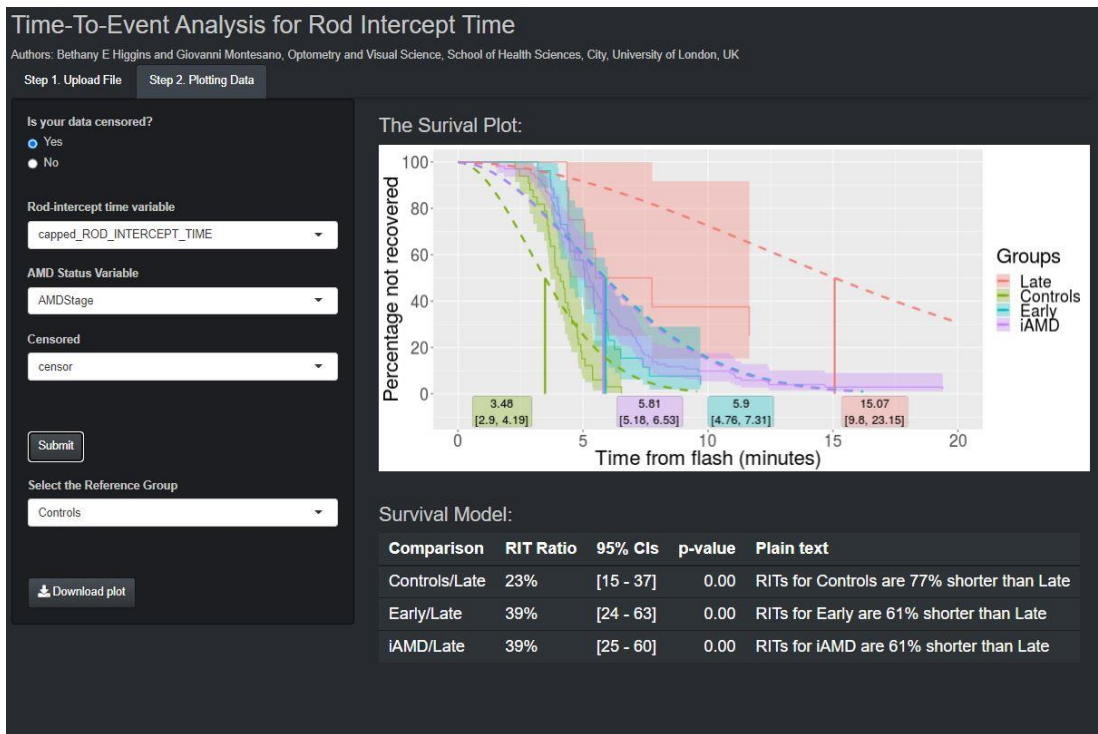


Figure S3.3 Screenshot of web app demonstrating the results page. On the left is the control panel to allow the user to choose the variables from the uploaded .csv file dataset. On the right is the survival plot of supplementary dataset sourced from data from the MACUSTAR study baseline visit, stratified by the Beckman classification. The plain text section below the plot allows for easy analysis of what the plot shows. Note that the empirical survival curve for late AMD eyes does not reach 0, showing that the values beyond 30 minutes are censored.

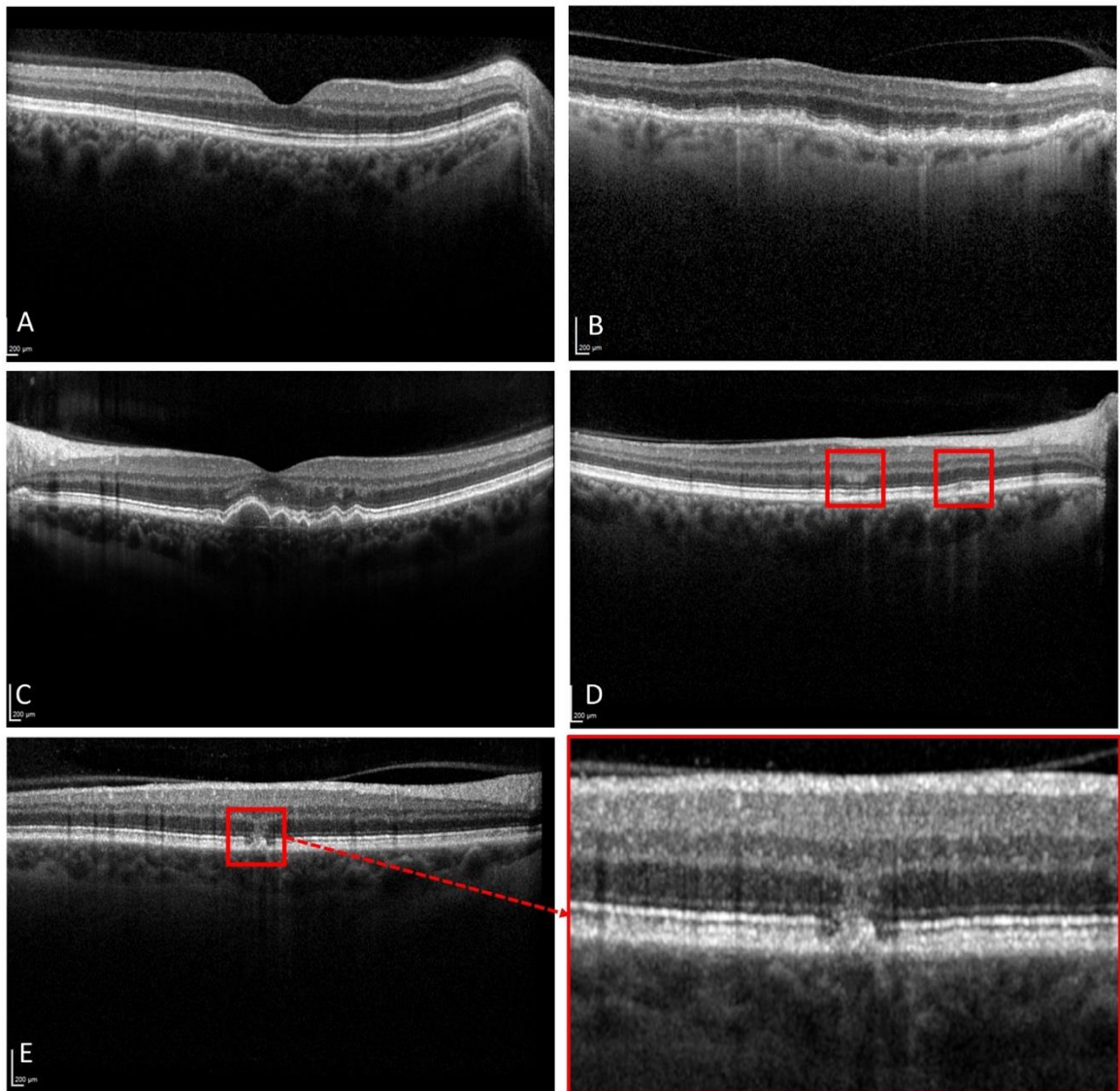


Figure S4.1 Representative OCT scans of study population. A: Scan from a healthy participant, all layers are discernible. B: SDD case. C: Intermediate AMD case with large drusen. D: RPE abnormality case. E: RPE abnormality case with magnified insert of abnormality. RPE abnormality was defined as the presence of lesions that altered the shape-structure of the RPE but could not be assigned to drusen and/or SDD. No cases of CNV or GA are given as these were excluded.

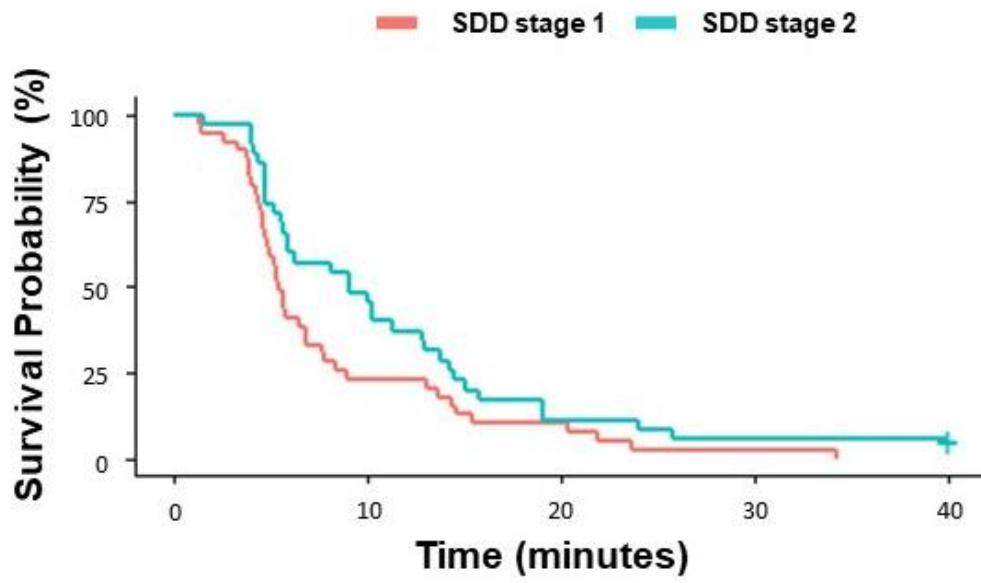


Figure S4.2. Kaplan-Meier curves illustrating the time taken for participant sensitivity to recover to a value of 5.0×10^{-3} scotopic cd/m^2 (3.0 log units of stimulus attenuation). This time taken is the RIT. Survival curves shown for people with stage 1 SDDS and people with stage 2 SDDS

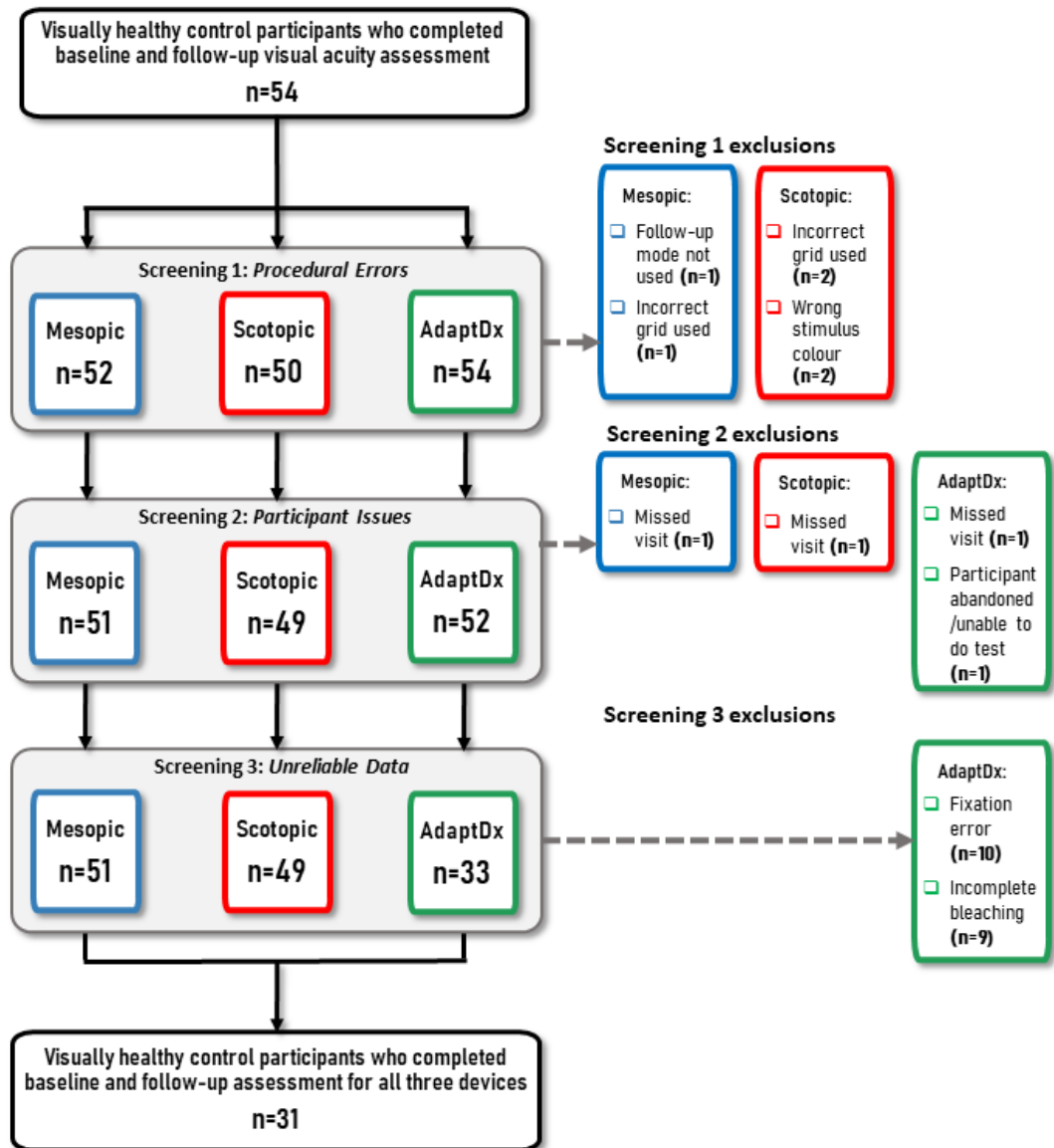


Figure S5.1. Flowchart of Control participant screening. During Screening Phase 1, the datasets corresponding to the three methods used in this study were assessed for procedural errors. During Screening Phase 2, the datasets were screened for unreliable data.

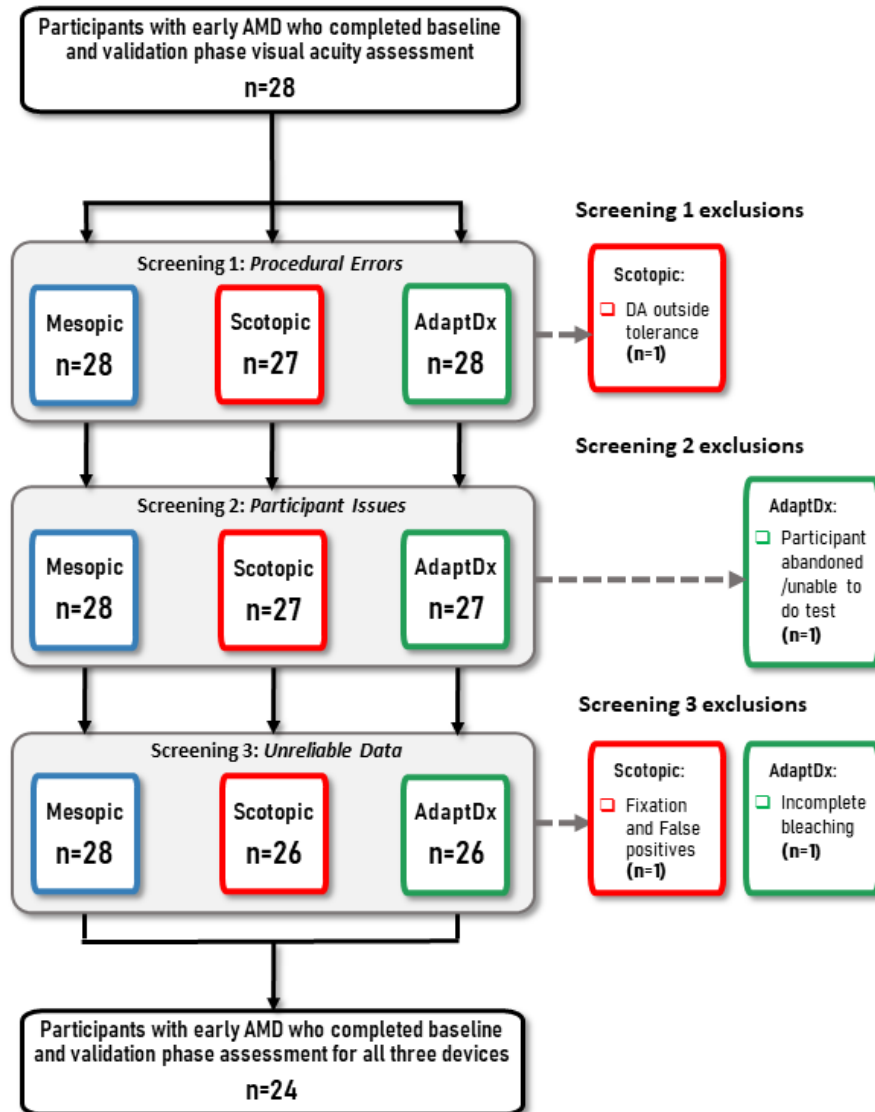


Figure S5.2. Flowchart of participant screening with early AMD. During Screening Phase 1, the datasets corresponding to the three methods used in this study were assessed for procedural errors. During Screening Phase 2, the datasets were screened for unreliable data.

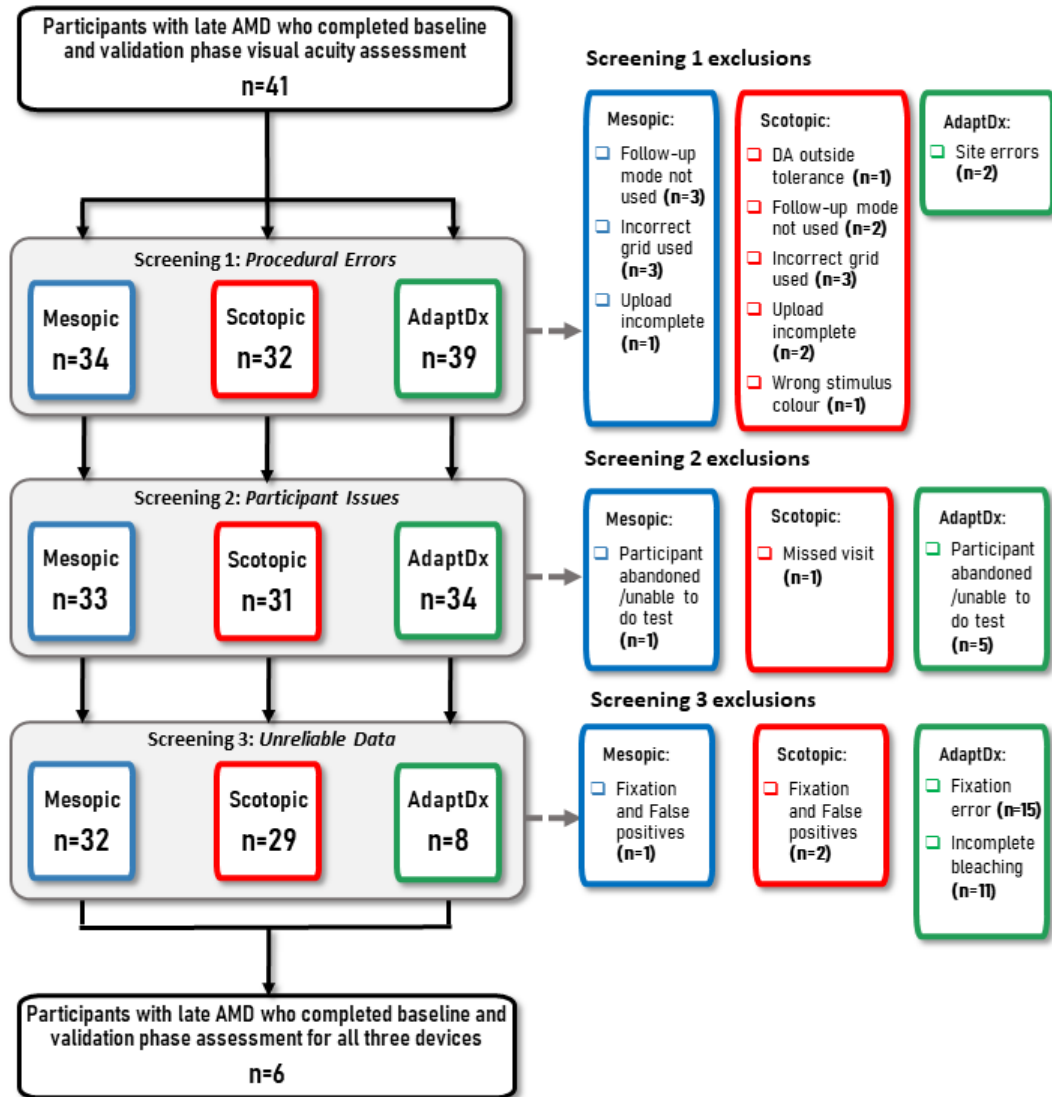


Figure S5.3. Flowchart of participant screening with late AMD. During Screening Phase 1, the datasets corresponding to the three methods used in this study were assessed for procedural errors. During Screening Phase 2, the datasets were screened for unreliable data.

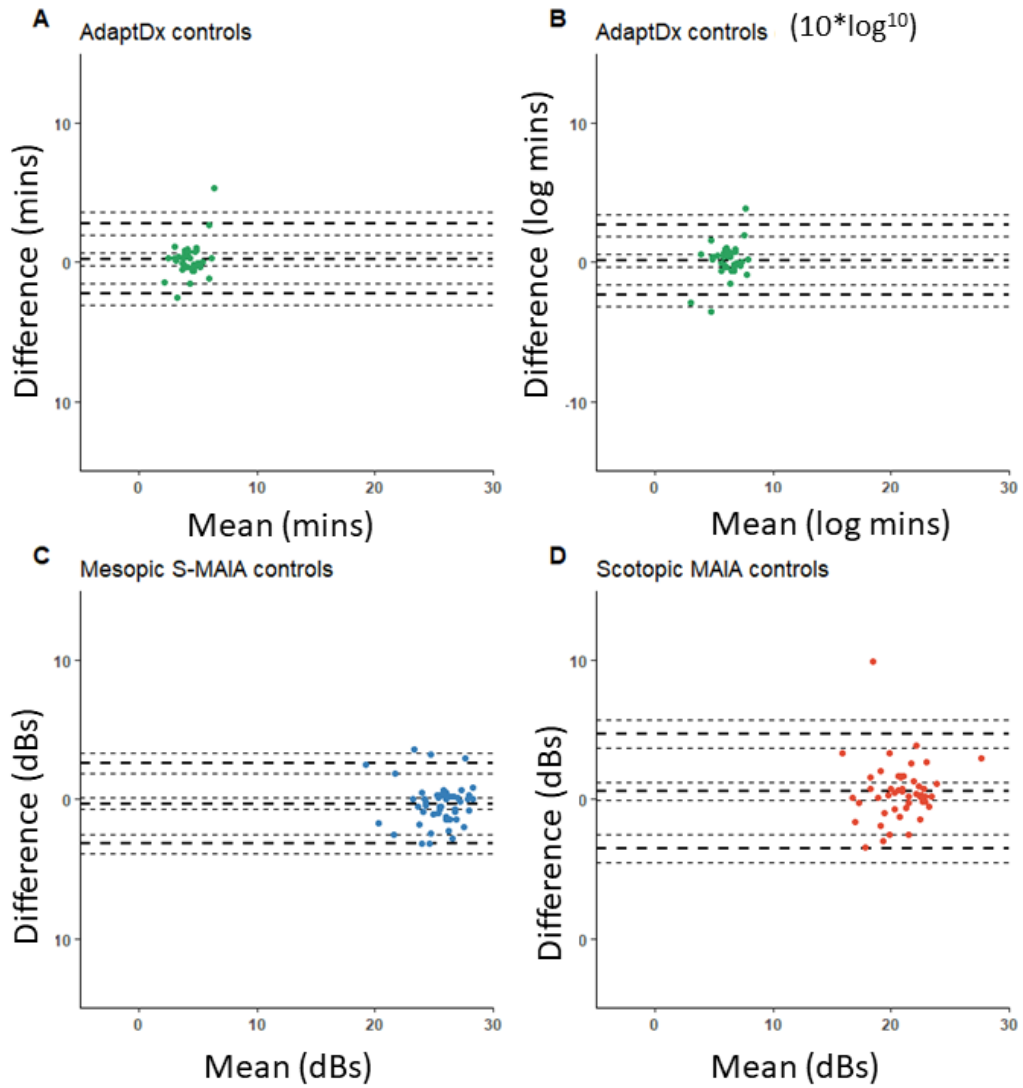


Figure S5.4 Bland-Altman plots to show the test-retest agreement for the three metrics for control participants. (Note RITv data [B] has been transformed by $10 \log_{10}$ to mimic the logged output of the S-MAIA for better comparison).

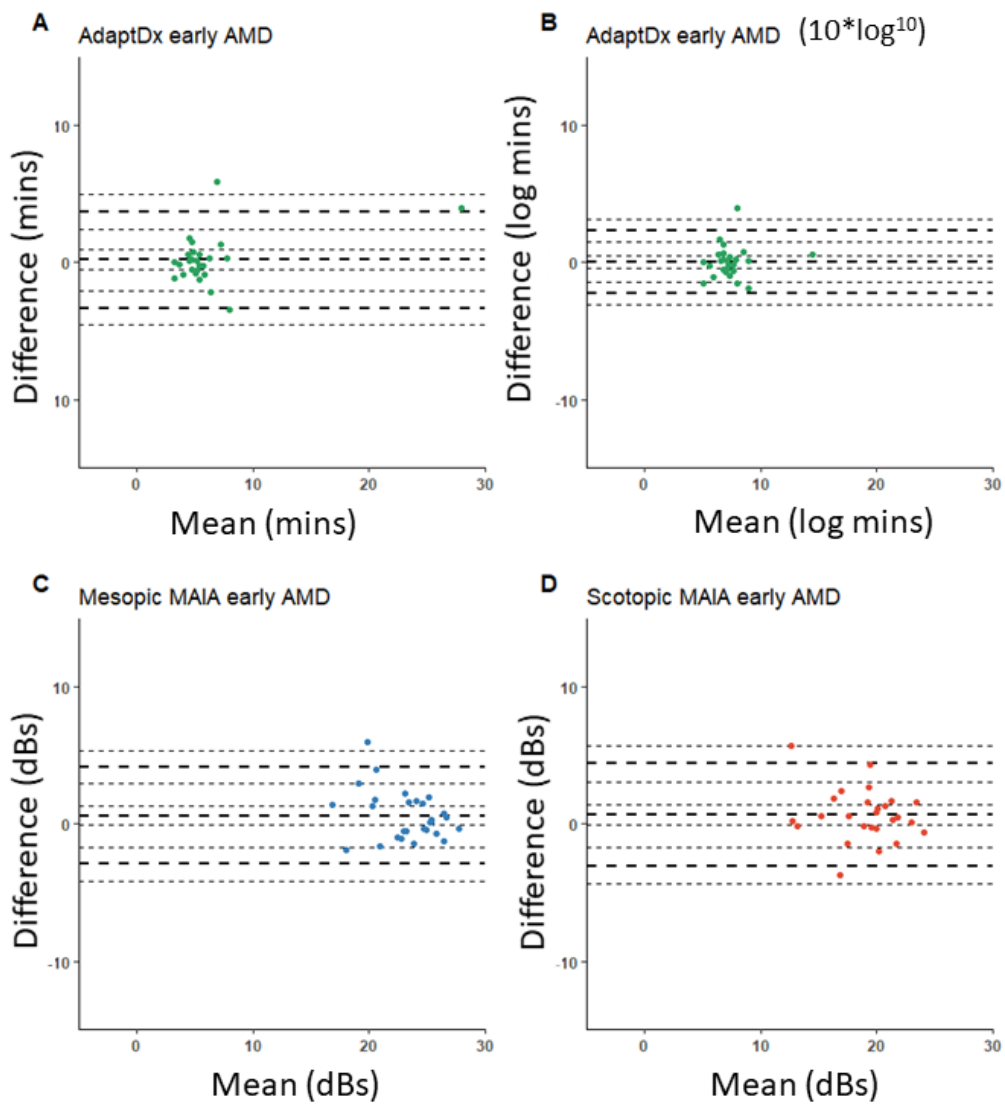


Figure S5.5 Bland-Altman plots to show the test-retest agreement for the three metrics for participants with early AMD. (Note RITv data [B] has been transformed by $10 \cdot \log^{10}$ to mimic the logged output of the S-MAIA for better comparison).

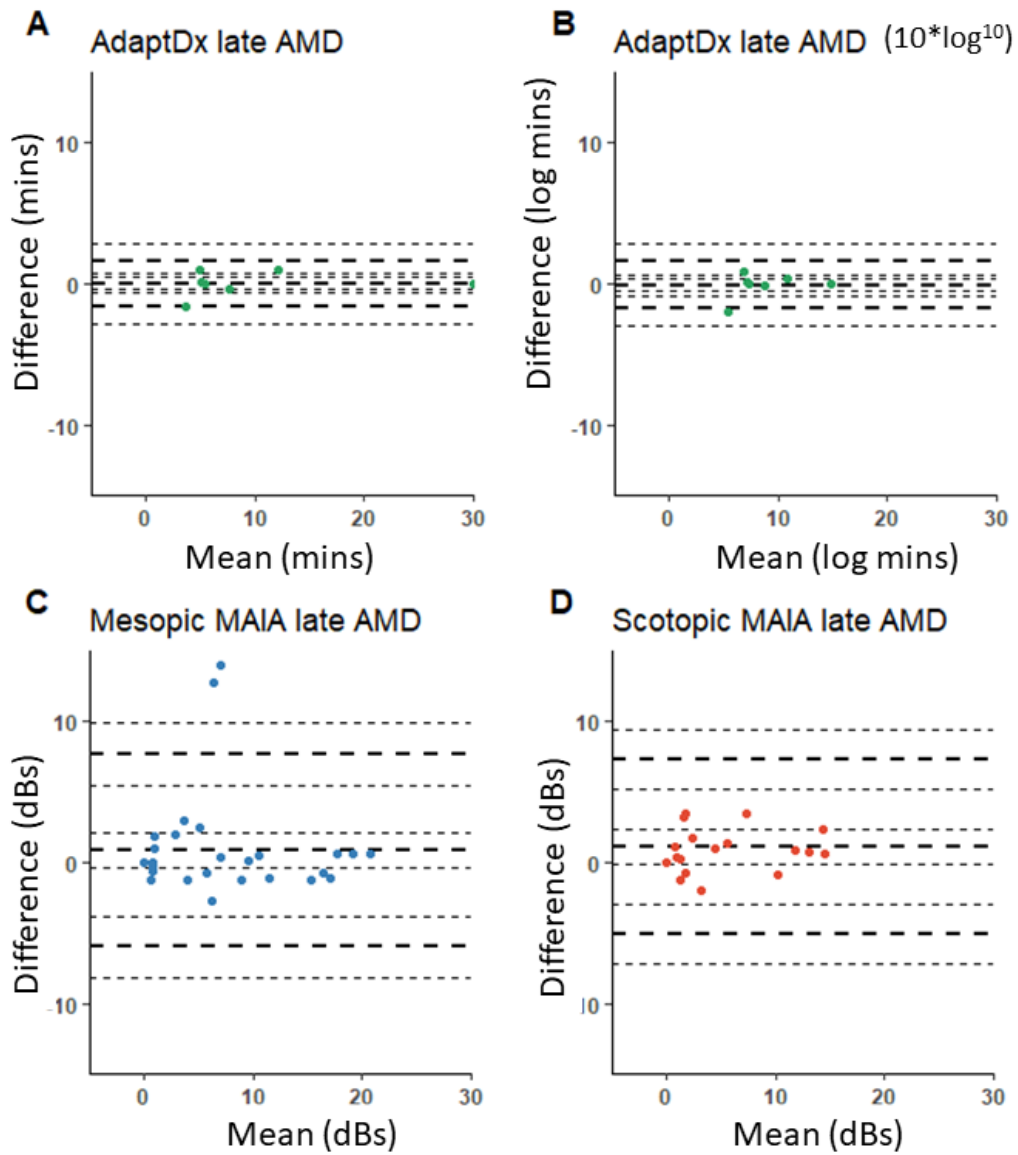


Figure S5.6 Bland-Altman plots to show the test-retest agreement for the three metrics for participants with late AMD. (Note RITv data [B] has been transformed by $10 \cdot \log^{10}$ to mimic the logged output of the S-MAIA for better comparison).

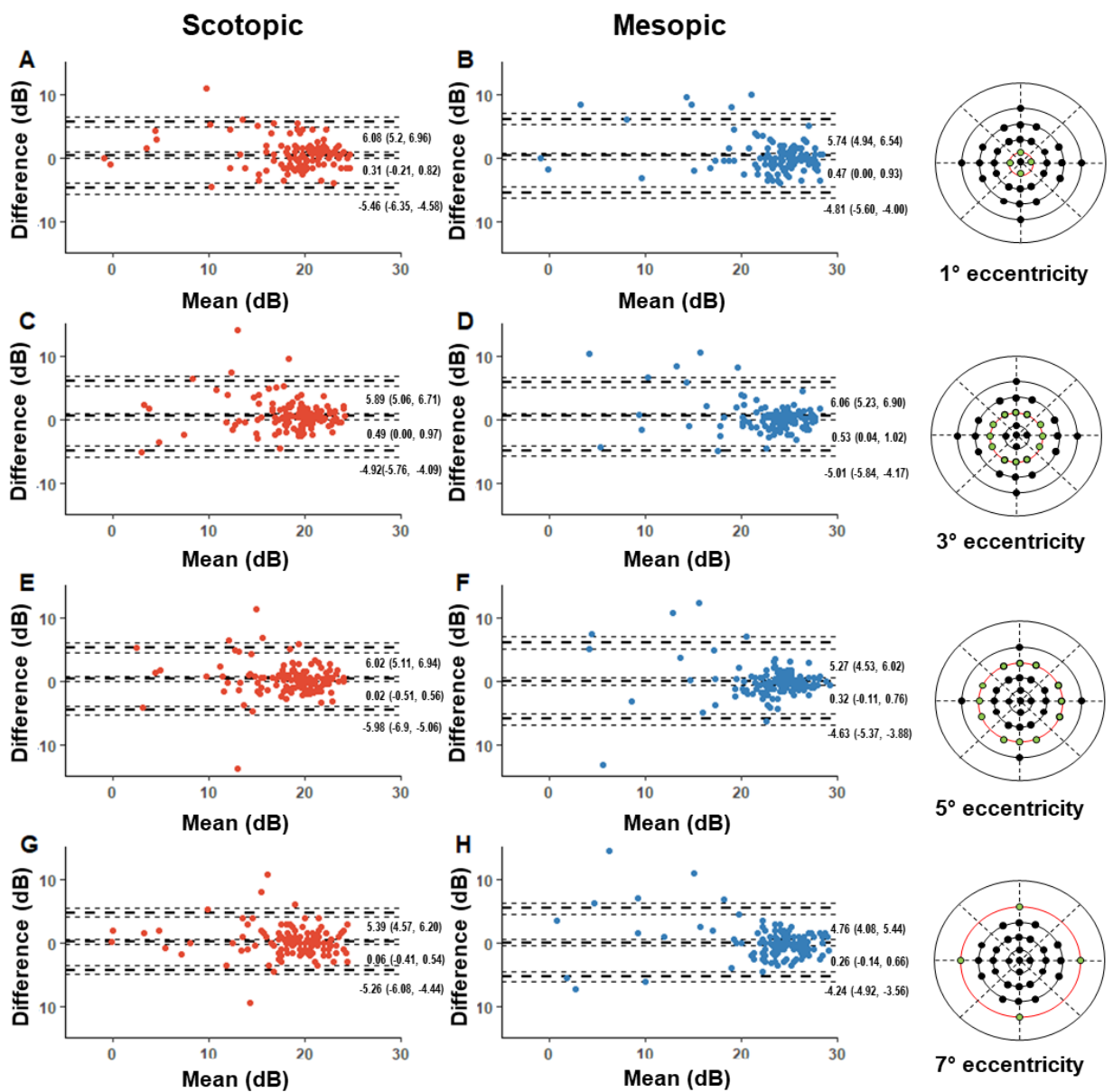


Figure S5.7 Bland Altman plots to show the test-retest agreement for mesopic and scotopic point-wise threshold sensitivity, grouped by eccentricity for people with iAMD. Bias, lower and upper limits of agreement are given (95% confidence intervals).

8.3 SUPPLEMENTAL METHODS

For this present analysis, data was included from participants aged ≥ 50 years with complete RMDA, CFP and SD-OCT data and had been classified both by the Beckman and SD-OCT-based grading system (See Supplemental Tables S4.1-S4.2; section 8.1). The full NICOLA study population had been graded according to pre-specified standardised protocols. Participants with no signs of retinal disease or any early AMD features were invited to attend a second appointment at additional imaging and battery of psychophysical tests were performed. Details on the imaging and grading procedure are provided in the next paragraphs. Exclusion criteria included presence of late stage (GA and/or exudative) AMD, diagnosis of any ocular disease, opaque ocular media, high refractive error ± 10 D and history of squint or amblyopia. While both eyes, if applicable, were imaged and graded, only one eye was selected for DA assessment (eye with worse VA) and this was the study eye assessed.

Imaging procedures were conducted under dilation. CFP was carried out with environment luminance 1.5 lux. Stereo optic disc and macular centred images were captured. CFP images were then uploaded to a centralised reading centre for secure grading and viewing via the Oculab interface; (Digital Healthcare Oculab, V3.7.98.0, Emis Health, Leeds, UK).

Thirty-degree volumetric SD-OCT images were taken on both eyes (61 B-scans [posterior pole] with pattern size $30^\circ \times 25^\circ$ distance between scans $118\mu\text{m}$ and 11 Automatic Real-time Tracking averaged frames), including the non-dilated eye. The device uses infrared Scanning Laser Ophthalmoscopy (SLO) to track eye movements during the acquisition of the image. As a result, all OCT maps can be overlaid with the infrared fundus picture. Heidelberg Eye Explorer (HEYEX) review software version 1.9.17.0 (Heidelberg Engineering, Heidelberg Germany) segmentation system was used and images were visually inspected and corrected if necessary. Room luminance was as above.

To detect and record the presence of AMD features on SD-OCT, the Heidelberg Eye Explorer HEYEX software was used. On OCT there is currently no widely accepted method of classifying drusen according to size or volume, therefore a simple feature-based scheme was used relying solely on the presence or absence of classical drusen, pigmentary irregularities and SDDs. For more details of the OCT grading, see Supplemental Table S4.2 and Supplemental Figure S4.1 (see section 8.1-8.2). OCT classical drusen were defined as dome-shaped lesions of hypo- or medium reflectivity located between the RPE and BM. The internal reflectivity of the largest drusen was recorded: homogenous (uniform internal reflectivity) or heterogenous (nonhomogeneous) as described by Khanifar et al. (2008) but this information was not used in this analysis. Clear deviation of the RPE was essential to distinguish drusen from SDD. Irregularities of the junctional components of the neurosensory retina and the inner surface of the RPE monolayer were observed and presence of RPE abnormalities were defined as of the presence of lesions that altered the shape-structure of the RPE but could not be assigned to drusen and/or SDD (See Supplemental Figure S4.1; section 8.2). Presence of SDDs were defined as granular hyper-reflective material lying between the RPE and the boundary between the

inside and outside sections of the photoreceptors (Zweifel et al., 2010). SDDs were graded as present, absent or questionable (those agreed upon as ‘questionable’ were ultimately graded as absent). A single SDD was deemed sufficient for grading of SDD presence, as per previous studies (Gabrielle et al., 2019; Zarubina et al., 2016).

Following this OCT assessment, both eyes (if eligible) were allocated into a three-level grading: no drusen or RPE abnormalities, drusen presence and both drusen and/or RPE abnormalities. Participants were also allocated into an additional two-level grading: participants with SDDs and participants without. SDDs were then further classified into severity stages using Zweifel et al. (2010) guidelines, see Supplemental Tables S3-S4 for details (section 8.1). See Table below for a comparison between the two classifications featured in this study.

Table comparing Beckman classification with the OCT classification (Ferris et al. 2013)

Stage Number	Beckman Classification	OCT Classification
0	No drusen or pigmentary changes	No drusen or RPE abnormalities
1	Only Drusen $\leq 63\mu\text{m}$ no AMD pigmentary abnormalities	Only Drusen, no RPE abnormalities
2	Medium drusen $>63\mu\text{m}$ and $\leq 125\mu\text{m}$, no AMD pigmentary abnormalities	Drusen and RPE abnormalities present
3	Large Drusen $>125\mu\text{m}$ and/or AMD pigmentary changes	-

Best-corrected distance VA and CS were tested using a retro-illuminated ETDRS chart and a Pelli-Robson chart, respectively. The eye with worse monocular VA (or right eye if both eyes had the same VA) was assigned the designated study eye. We assessed RMDA using the AdaptDx on the dilated study eye only (1% Tropicamide). The test took place in a room with lights off (luminance 0.01 lux) and the non-test eye was occluded. While the participant focussed on a red fixation light, the examiner used the infrared camera to position the eye to ensure the subsequent bleaching was administered correctly. Testing commenced with the study eye bleached using exposure to a flash (0.25 millisecond duration 58,000 scotopic $\text{cd}/\text{m}^2\text{s}$ equivalent to $\sim 83\%$ bleaching level for rods); this bleached a retinal location subtending 4° centred at 5° inferiorly in the vertical meridian, consequently projected superiorly to the fovea. This was also the location of the test target. Stimuli for the threshold measurement was a 2° diameter, 500nm circular target which began 15 seconds after the bleaching offset. The participant was instructed to retain focus on the fixation light and to press a hand-held button when a target first became visible in the bleached area. Log thresholds were expressed as sensitivity in dB as a function of time from bleaching and were estimated using a modified staircase

procedure (3 down/1 up). The procedure continued in intervals (30 seconds) with a break between each (15 seconds) until either the RIT was met, or the test protocol ended (40 minutes), whichever occurred first. The RIT was defined as the duration required for sensitivity to recover to a value of 5.0×10^{-3} scotopic cd/m^2 (3.0 log units of stimulus attenuation) (Jackson, Scott et al, 2014). In cases where the RIT was not met, a capped value of 40 minutes was assigned for analysis. The device records the percentage of threshold points which indicated a fixation error. In this study, as in previous reports (Binns et al., 2018), if fixation errors exceeded 30%, the test was deemed unreliable.